Peninsula Technikon

Department of Mechanical Engineering

Centre for Research in Applied Technology (CRATech)

# Experimental Sensitivity Analysis of Welding Parameters during Transition from Globular to Spray Metal Transfer in Gas Metal Arc Welding

Mark Ludick
NHD.Mech. Eng., B.Tech. M.E. (Peninsula Technikon, Rep. of South Africa)

*Under the supervision of*
Dr. Graeme Oliver, Ph.D

Submitted towards the degree of

Master of Technology in Mechanical Engineering

Peninsula Technikon

Cape Town 2001

Republic of South Africa

# DECLARATION

I, the undersigned, hereby declare that the work contained in this dissertation is my original work and has not previously in its entirety or part thereof been submitted at any tertiary institution towards a degree.

Signature: 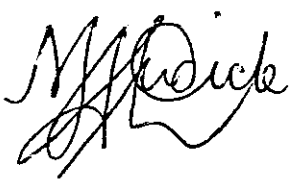

Date: 04/02/2002

# ACKNOWLEDGEMENT

The author wishes to thank the following persons and institutions for their invaluable contribution to the development of this document:

- Dr Graeme Oliver to whom the author would like to express his indebtedness for his encouragement, assistance and advice during the various stages of the manuscript and for correcting the document.

- The Japan International Cooperation Agency (JICA) and the Japan Welding Technology Center (JWTC) for giving me the opportunity to broaden my welding knowledge and to focus on research.

- The Laboratory for Welding and Cutting at the Mechanical Engineering department at Peninsula Technikon for providing me with the equipment to conduct experiments and tests.

- Michelle, who never doubted me, who always supported me and without whom I would not have succeeded in developing this document.

- To Louis and Magdalene for their strong values instilled in me, and who sacrificed so much for me.

- To Edward and Esmé who believed in me and accepted me as I am.

- Finally, to the staff at the Peninsula Technikon, Mechanical Engineering Department for their tolerance and assistance during the preparation of the document.

# ABSTRACT

Since the discovery of arc welding at the beginning of the century, metal transfer has been a topic of research interest. Metal transfer can, in fact be related to weld quality, because it affects the arc stability. Furthermore, it determines the weld spatter, penetration, deposition rate and welding position.

Gas Metal Arc Welding (also known as Metal Inert Gas- or MIG welding) is the most common method for arc welding steels and aluminum alloys. Approximately 40% of the production welding in the country is accomplished by this process in which the thermal phenomena and melting of the solid electrode are coupled to the plasma arc and the weld pool. Thus the thermo- fluid behaviour of the electrode and detaching drops can have significant effects on the subsequent weld quality and production rate. The knowledge of how metal transfer affects this arc welding process is important for welding control and process automation, as well as in the development of improved welding consumables.

Gas metal arc welding has a distinct feature, indicated by the results of Lesnewich [24], [23], that for most gases, there is a discrete metal droplet formation change between low and high current operations. Naturally the droplet size will have a significant influence on the properties of the welds.

In globular transfer which occurs at low current, the welding electrode melts and produces large droplets (usually larger in diameter than the electrode wire diameter). This mode of transfer is associated with high spatter levels and thus undesirable in terms of welding economics. An increase in welding current will, for most welding/ shielding gases, produce metal transfer with smaller droplets, which is termed spray transfer. This mode of transfer is associated with high voltage and amperage settings, thus producing high deposition rates limited to the flat/horizontal position. Due to the higher heat input, the spray transfer technique is limited to plate thicknesses greater than 6mm. To obtain an 'optimum balance' between globular and spray transfer will thus be beneficial for the welding of thin plates with high production rates, as well as providing an accurate boundary zone between these two modes of metal transfer for industrial and research purposes.

Based on the work performed by Haidar and Lowke [15], [24] with respect to the calculation of the transition current between globular- and spray metal transfer in MIG welding, the influence of different shielding gas mixtures on the transition current were studied. The effects of oxygen and carbon dioxide additions to argon shielding gas were studied to verify the vital importance of including the shielding gas effects on the transition current within the mathematical formulation of [24]. This research was done with the aid of Fortran programming, the Lasestrobe Camera System coupled to image capturing software and the results displayed using curve-fitting software.

# Contents

# Chapter 1

## Introduction to Gas Metal Arc Welding

### 1.1 Introduction

Any weld design must aim at ensuring the integrity of the weld and, effectively minimize the effects of welding defects. There are two major considerations: Firstly, the control of the dimensions and the thermal history of the molten metal in the weld pool. Secondly, the analysis of the geometrical constraints imposed by the system and its effect on the development of residual stresses during the welded cycle. Accordingly, a better understanding of the details of metal transfer is likely to lead to improvements in the quality and the efficiency of the welding process. Since the mode of metal transfer in Gas Metal Arc Welding occurs at different current values, the importance of the effects of shielding gas composition on the transition current from globular to spray metal transfer forms the main focus of this study.

Gas Metal Arc Welding (GMAW), also known as Metal Inert Gas- or MIG welding, is the most common method for arc welding steels and aluminum alloys. Approximately 40% of the production welding in the country is accomplished by this process in which the thermal phenomena and melting of the solid electrode are coupled to the plasma arc and the weld pool. Thus the thermo- fluid behaviour of the electrode and detaching drops can have significant effects on the subsequent weld quality and production rate. The knowledge of how metal transfer affects this arc welding process is important for welding control and process automation, as well as in the development of improved welding consumables.

In globular transfer, which occurs at low current, the welding electrode melts and produces large droplets (usually larger in diameter than the electrode wire diameter). This mode of transfer is associated with high spatter levels and thus undesirable in terms of welding economics, (i.e. grinding/cleaning costs, excessive electrode consumption, etc.). An increase in welding current will, for most shielding gases, produce metal transfer with smaller droplets, which is termed spray transfer. This mode of transfer is associated with high voltage and amperage settings, thus producing high deposition rates limited to the flat/horizontal position. Due to the higher heat input, the spray transfer technique is limited to plate thickness greater than 6mm. To obtain an 'optimum balance' between globular and spray transfer will thus be beneficial for the welding of thin plates with high production rates, as well as providing an accurate boundary zone between these two modes of metal transfer for industrial and research purposes.

### 1.2 The Importance and Effects of Metal Transfer on Weld Quality

Ever since arc welding was discovered at the beginning of the 20$^{th}$ century, metal transfer from the electrode to the weld pool has been an important topic of research interest [3]. As stated earlier, it was found that metal transfer can be related to weld quality and efficiency because it affects the arc stability. It also determines weld spatter, weld penetration, deposition rate and of course the welding position. Hence, the knowledge of how metal transfer affects the arc welding processes is vital for welding control and process automation, as well as in the development of improved

welding consumables [3]. It therefore affects the welding industry indirectly. The South African welding industry used to be a few years behind in the development and implementation of new and available technology. However, due to globalisation and the opening of our markets to international competition, welding supply companies are now bringing in the latest technology and making it available to local industry. Therefore, the research conducted in this study will assist in optimizing the GMA welding of thin metals due to optimal shielding gas selection for minimum current spray transfer, thus adding value to welding research, development and trends in South Africa. Ref. Chapter 1.5 for the latest trends in the welding industry.

## 1.3 Global Vision for the Welding Industry until the year 2020

Welding industries consist of the "users" of welding techniques as well as the companies, universities and other organizations that provide the equipment, materials, processes and support services for welding. All branches of the welding industry look to improve their operations by the year 2020. Therefore, on June 30 and July 1, 1998, at the National Institute of Standards and Technology in Gaithersburg, Md., a conference between 25 senior managers and respected experts from various segments of the welding community were held to formulate an ideal vision of the state of the industry in 20 years and the strategic goals to reach it [48]. This vision document is a pivotal step by the welding industry in meeting the needs of tomorrow's manufacturing and construction industries. Following is a summary of this document.

### 1.3.1 *Welding will be better integrated into the overall manufacturing process*:

As it is more completely integrated to the design and manufacturing cycles of products, welding will be accepted as crucial to improving the life-cycle costs, quality and reliability of manufactured goods. There are a number of "drivers" that will help determine this future favorable position of welding. The use of *information technology* will grow to help develop a "virtual manufacturing plant", in which technologies for design, fabrication and inspection are seamlessly integrated with welding technology where they are needed. Wise investments in capital goods and communication between the welding industry and its customers is also believed to be very effective methods for improving the competitiveness of welding. Likewise, the sharing of new information about welding operations within industry will ensure progress throughout the fabrication, manufacturing and construction industries.

### 1.3.2 *People issues may be the most important:*

Engineers employed in the welding field have been educated in a variety of disciplines, but rarely in welding. Workers who do the actual welding have usually learned their skills on the job – only occasionally through apprenticeships or formal welder training. Given the present-day image of welding, which does not yet reflect the recent progress made by the industry in machine processes and automation, it is not surprising that the percentage of workers who can weld and who can work in the manufacturing industries is on the decline. However, as in every field there is a crucial need for talented people. Manufacturers want to attract to welding who will help improve their products and their productivity. Industry has set a goal of investing in educational opportunities for people interested in welding, metallurgy and closely related disciplines. Early investments in training at all levels will generate a large return to industry.

***Quality, reliability and serviceability of welded joints will improve:***

This is a practical and an image issue. The industry must learn how to ensure that welds will have "zero defects", and establish practical methods that achieve that result.

### 1.3.3 *Materials of the future:*

This 'new age' materials will be designed to be weldable as part of the total integration of welding into the manufacturing cycle. Materials will also be energy efficient, environmentally benign, and "smart" with a computer component that will help with materials processing at any point in the life cycle of the component.

### 1.3.4 *Increased competition in global markets for materials fabrication:*

This will force industries to consider new manufacturing and distribution methods in order to attract customers worldwide. Numerous markets are emerging in developed and developing nations for the welding industry to exploit if it is alert to societal needs and has the appropriate technologies by participating in cooperative research programs with government and academia, however, the line between discovery and implementation must be reduced.

## 1.4 Strategic Goals to implement the vision for the welding industry by 2020

- ***Cost, productivity, markets, applications:*** Reduce the average cost of welding by one third, by providing better process selection guidance, increasing the use of automation and robots and lowering reject and repair rates; increase the welding by 25%.

- ***Process technology:*** Enhance the use of welding in manufacturing and construction operations by integrating welding with other manufacturing and construction disciplines at the engineering level and also at the operational level.

- ***Materials technology:*** Develop welding technology along with new materials so practical fabrication methods are available for all engineering applications.

- ***Quality technology:*** Through the modeling of systematic process selection and procedure development, and NDE technologies, assure that welding can be part of a sic-sigma quality environment.

- ***Education and training:*** Increase the knowledge base of all people employed in the welding industry, at every level, enabling them to make decisions that will result in utilization of the best welding technology for each application.

- ***Energy and environment:*** Reduce energy use by 50% through such productivity improvements as decreased pre- and post-heating operations; use of advanced, lower heat input welding processes; and avoidance of over welding.

This vision is of great importance to this research as it gives direction, not only to this project, but also to other welding research programmes. It ensures that the research undertaken will be relevant to the global welding industry.

## 1.5 Latest Trends in the South African Welding Industry

Trends in welding equipment are now moving towards inverter-type equipment and, in terms of processes, are moving towards gas metal arc welding (MIG/MAG) techniques. [19],[37] This is following the trend toward automated welding processes, and away from the manual metal arc (MMA) processes, which used to comprise well over fifty percent of the welding processes used in South Africa. The trend is to move towards welding processes, which give improvements in productivity and quality. These are requirements to enable our industry to be internationally competitive. The shift to MIG/MAG and flux core welding processes is being accompanies by improvements to the welding electrode wires which support these processes, with features such as reduced spatter and fume levels, and higher quality weld deposits. Therefore is this present study aimed at optimizing GMA welding by focussing on shielding gas composition to obtain the lowest globular to spray mode transition current for the welding of thin plates in the spray mode.

One of the main developments in the South African welding industry in the years to come will be in health and safety according to ISO 14000 specifications. This will be achieved through improvements in welding technology, equipment, consumables, process-control and workforce education. How the industry will develop over the forthcoming years depends on the economic growth, together with the specific requirements of our manufacturing industry. By optimizing the shielding gas mixture and consequently reducing the transition current for the welding of thin plates, energy wastage and pollution levels will decrease.

With the advent of inverter technology and the introduction of electronics into welding technology, robotic welding technology is advancing rapidly, [30] replacing the manually operated, electro-mechanically designs of the past. Additional advantages of robots are the repeatability, consistency and weld quality they produce. In a mass-production situation such as the automotive industry, where consistent quality and reliability is required, every part must be the same, and it can only be accomplished by machine. If the global markets are entered, expectations of robot usage is paramount, in order to achieve the same level of quality and reliability.

One of the main challenges facing the robotic-technology automotive industry is the accompanying technology to exploit the use of robots to the full, as well as highly skilled experts to provide the technology and run these machines. This accompanying technology will be realised through research and development. Globally, robots are used most widely in the automotive industry, which accounts for eighty percent of all robots used, including sub-suppliers to the vehicle manufacturers. Since the automotive industry involves the welding of thin metal sections/plates, the incorporation of the outputs from this present study with robotic technology will greatly benefit the automotive industry.

## 1.6 Problem Statement

The welding of sheet metal using the MIG welding method has its limitations, with regard to thin metal sections. [17]. MIG welding is a relatively high heat input process, which is why the heat transfer rate away from the weld pool becomes important. The surrounding material must be able to support and maintain the weld pool until it solidifies. Together with an acceptable bead profile of the final weld, visual and surface quality must also be within the specified requirements. (It should be noted that only visual and non-destructive requirements are normal in this field range.) Furthermore, heat input must be kept to a minimum. This implies a short-circuit- or globular transfer mode which, unfortunately are modes that are prone to spatter. Spray modes give high production rates and minimum spatter, but high heat inputs causing weld pool collapse due to an arc that is 'too hot.'

It is generally known that austenitic stainless steels have a thermal conductivity of one quarter that of the amount of carbon steels, while ferritic and martensitic stainless steels have about one third that of carbon steels. This implies that at the amperage used for carbon steels, more heat would be retained in the stainless steels, making it prone to weld pool collapse during welding [13],[17],[36],[43]. Thus, a compromise must be reached between heat input, travel speed, wire feed rate and bead shape, all of which are influenced by specific shielding gas compositions. Finding this ***balance*** between the globular and spray metal transfer modes implies a transition current where qualities of both zones will be present. In order for an acceptable weld that conforms to industrial standards with respect to strength, aesthetics, cost and production rates, the spray transfer mode is the mode most desired. Thus, if the spray mode can be obtained at a lower current setting (lower heat input), a thinner plate can be welded in this mode. Figure 1.1 schematically illustrates the transition current with respect to droplet transfer rate and size.

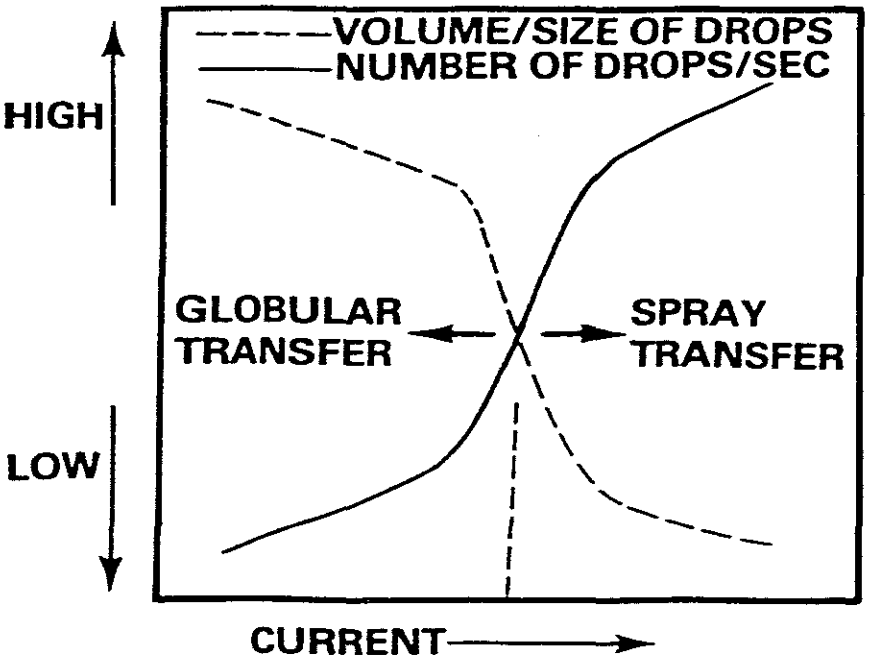


**Figure 1.1** Schematic illustration of Globular to Spray Transfer Transition Current in GMAW

Since the discovery of arc welding at the beginning of the century, metal transfer has been a topic of research interest. Metal transfer can, in fact be related to weld quality, because it affects the arc stability. Furthermore, it determines the weld spatter, penetration, deposition rate and welding position.

The welding of thin metal sheets, as described above, is just one of the problems encountered in the welding industry. [17] One company in particular is Consani Engineering, fabricators of steel containers for the local and international markets. Engineers in the welding field have been educated in a variety of disciplines, but rarely in the field of welding.

Although welding has become an indispensable manufacturing technology in our modern industries, the knowledge of welding and welding techniques, however, still lies with a select few scientists, engineers and welders with years of experience. Research in this multi-disciplinary area involves:

- Constitutive reaction of welded bodies, i.e. given to thermal, rate dependent, metallurgical and mechanical effects in constitutive modeling. When solved, these models produce results such as temperature distribution, metallurgical phase proportions, hydrogen diffusion, residual stress and strain and deformation. Some of these results, if not all, may be achieved, depending on the accuracy required.

- Solving for droplet formation using the Volume of Fluid method [12].

- Heat input modeling, i.e. the modeling of temperature physics for generation and control of energy sources for heat energy transfer to the weld bead for various welding processes. (Gas metal arc, tungsten inert gas, submerged arc, shielded metal arc, etc.)

- Heat output from the welded joint, i.e. this include heat exchange with the environment, cooling rates and chemical composition of a coolant. (heat treatment and/or quenching)

- Welding effects subject to the following: welding velocity, electromagnetism, frequency of and power supply, electrode construction, filler metal composition, electrode coating along with its initial temperature, electric arc pressure on weld pool, clamping and jig configurations as well as the sequence, strength and geometry of weld joint.

Most work in these areas of welding research fail to take into account the vital importance of the effects of shielding gas composition on drop formation and frequency of droplets.

Although previous experiments [11],[15],[23],[24] were either performed in pure argon shielding gas or argon based constituent, these experiments were conducted with one fixed shielding gas per experiment. The effect of varying the gas composition was not considered. Thus the influence of shielding gas permeability and other gas factors on droplet detachment, shape and size was not considered. Furthermore, constant gas flow rates were used by the different researchers whilst conducting their various experiments, instead of varying gas composition for the same experiments.

## 1.7 Related Literature

Welding research has taken great leaps forward since the turn of the 1900's especially in the last twenty years. Great advances in the mathematical modeling of welding, computational facilities and the coupling of material science into the constitutive modeling of welding, are some of the main factors contributing to this.

In the constitutive modeling of welding, previously developed welding benchmark problems, [1],[4],[5],[7],[29],[32] were formulated and solved where the welding heat sources/fluxes transferred from the electrode tip to the base/parent metal were spherical, ellipsoidal or double ellipsoidal Gaussian energy distributions. These energy distributions are imposed on the sphere and ellipse in all three dimensions and are considered a maximum immediately beneath the heat source and decay to the spherical or ellipsoidal boundaries. (Exponential functions following the Law of Decay)[32]. Nguyen et al (1999)[29], derived an analytical solution for a three-dimensional double ellipsoidal power density moving heat source in a semi-infinite body with conduction-only consideration. This solution has been obtained by integrating the instant point heat source throughout the volume of the ellipsoidal heat source. Validations were made by transient temperature measurements at various points in bead-on-plate weld specimens. This work was based upon research conducted by Goldak, et al (1985)[32], who first introduced the three-dimensional (3-D), double ellipsoidal moving heat source as a Gaussian model.

These heat sources, although adequate, have some delimitations/shortcomings when it comes to the control of the gas metal arc welding process, which include:

- The Balance of forces acting on the molten droplets. These forces include gravity, surface tension, magnetic pinch forces, plasma pressures and viscous drag forces.
- Thermal phenomena in the consumable welding electrode.
- Current density distribution in the molten droplet
- Flow of liquid in the droplet and weld pool
- Effects of shielding gas on transition current

Various researchers have investigated these problems either, approximately, and/or experimentally, and / or numerically [23]. Investigators who have included the above effects in the models of welding arcs include:

Spraragen and Lengyel (1943) [23],[37] reviewed the basic principles of an electric arc and summarised the development of the field of welding arc physics. They concluded that in the area of liquid metal transfer from the electrode to the weld pool, the electromagnetic pinch force, gravity, shielding gas drag force and surface tension are the major forces that act on the electrode tip.

Muller, Greene and Rothschild (1951) [23],[32] using high-speed cinematographic techniques, found that large spherical liquid metal droplets in a GMA arc decrease in size with increasing current. As the electrode feed rate was increased, however, a sudden decrease in droplet size occurred at what was termed the transition current. They also found that with inert gas shielding, the droplet composition remained constant during the metal transfer.

Ludwig (1957) [23] confirmed that the electromagnetic force is the major force among the chemical and physical forces that affect the formation and subsequent transfer of metal droplets.

Lesnewich (1958) [15],[23] investigated the physics of arc welding using shielded metal arc (SMA) and GMA welding in which the effects of welding process parameters such as current, voltage, electrode polarity, electrode extension and diameter on the electrode melting rate and metal transfer were studied. According to Lesnewich's work, in carbon steel welding with 1.2mm diameter electrodes, a transition in metal transfer occurred at approximately 250A.

The studies conducted by Lancaster (1986) [23],[32] provide very comprehensive reviews of metal transfer modes during arc welding. According to the International Institute of Welding (IIW), referenced in this work, metal transfer can be classified into three main groups: free-flight transfer, bridging transfer and slag protected transfer.

Liu and Siewert (1989) [23], who conducted an experimental study of droplet rates for various transfer modes to verify optimum operating parameters. They found that measurements of the arc current- and voltage fluctuations during short-circuiting transfer enable quantitative measurement of the transfer stability. They also found that the conditions of minimum fluctuation in droplet transfer rate correspond to the lowest spatter and least ripple effects. This research showed that voltages above and below the optimum for a given current result in a lower average rate and a greater fluctuation in droplet rate. It was also indicated that, for certain voltage-current combinations, the rate alternates between two values. This indicates that the transition between droplet transfer modes is not smooth, but discontinuous.

Nemchinsky (1994) [32], developed a steady state theory accounting for surface tension and magnetic pinch forces to derive the shape of the droplet attached to the electrode using a simple approximation for the current density distribution in the droplet. He was able to make predictions of the transition from globular to the spray transfer mode in fair agreement to experiments. This model, however, does not take account of the arc or make predictions as a function of time.

Simpson and Zhu (1995) [32], developed a one-dimensional model, accounting for the forces acting on the droplet but neglecting the arc. The model made the first prediction of drop shape as a function of time, including detachment of the drops.

Haidar and Lowke (1996)[15], developed a unified two-dimensional model for droplet formation of the gas metal arc welding process. Their model included the arc, welding wire (as an anode), and the parent metal (taken as cathode). A prediction was made of the formation of droplets as a function of time, accounting for the effects of surface tension, gravity, inertia and magnetic pinch forces. A calculation was made for current densities, electric potentials, temperatures, pressures and velocities in two

dimensions both in the arc, molten drop and solid electrode. The results of this model compared favourably with experimental results. This model was an attempt at solving the globular and spray modes as a dynamic analysis. The volume of fluid *(VOF)* method, developed by Hirt and Nichols [23], was used for the tracking of free surfaces. They found desired results for the droplet sizes within the transition current in that both large and small droplets were are present in this zone. However, in this model, wire feed rate and welding speed were held constant. In this research their predictions of metal droplet formation were based upon results obtained from experiments in pure argon using the following parameters: 1,6mm diameter mild steel welding electrode, feed rate at 10cm/sec, gas flow rate at 5 litres/min and a contact gap of 8mm.

Lowke (1996) [24] developed a theoretical formula based on the work by [15], for the transition current from the globular transfer mode to the spray transfer mode in MIG welding. In his study he indicates that the shielding gas composition/mixture will affect heat transfer between the arc and droplets and thus the temperature and surface tension of the droplets.

Fan and Kovacevic (1998) [11],[12] developed a mathematical model to describe the globular transfer in gas metal arc welding, the work being both theoretical and experimental in nature. Using the VOF method, the fluid flow and heat transfer phenomena during the impingement of a droplet on a solid substrate as well as arc striking, impingement of multiple droplets on the molten pool and solidification after the arc extinguishes were studied. In this study a He-Ne laser with the shadow-graphing technique was used to observe the metal transfer process. The welding was performed using direct current, electrode negative (polarity) with 1,2mm diameter mild steel electrodes in pure Argon shielding gas. Electrode extension was 16mm.

Ohring and Lugt (1999) [31] developed a numerical simulation of a transient three-dimensional GMA weld pool due to a moving arc. The addition of molten material was modelled by simulating an impacting liquid-metal spray on the weld pool, with evaporation and latent heat absorption for boiling being computed at the weld pool surface. This model included heat transfer, radiation, evaporation and viscous stress in the deformable free surface boundary conditions. However, in this model, the spray transfer mode was assumed and the effects of electromagnetic fields generated by the arc and shielding gas were neglected. The results of this study proved the relationship between the size and shape of the weld pool and time. This agreement exists despite a discrepancy regarding the reinforcement, which is largely due to the numerical inlet spray transfer model that was used.

A distinct feature of gas metal arc welding, indicated by the results of Lesnewich [15], is that, for most shielding gases, there is a discrete change in the frequency and size of the molten metal droplet formation, between low and high current operations. Naturally the droplet size will have a significant influence on the properties of the welds. Kim and Eagar [32] and Nemchinsky [32] researched the current energy distribution during the transition from globular to spray transfer modes within the molten droplet. It was found that for currents below the transition current, there is globular transfer and drop sizes are determined by the 'Static Force Balance Theory' (SFBT), developed by Greene et al [24]. In the SFBT, the droplet size is predicted from a balance of forces in the liquid from the self-magnetic field, gravity and surface tension. Furthermore the 'Pinch Instability Theory' (P.I.T.), developed by Lancaster and Allum [32], are used to determine droplet sizes in the spray transfer mode above

the transition current. The P.I.T. considers instabilities due to the magnetic pinch force acting on an infinite column of liquid metal. It should be noted, however, that the SFBT and P.I.T. take no account of heating in the wire by the arc or by ohmic and also are unable to predict the influence of wire feed rate and shielding gas composition.

Past research has shown the importance of various welding parameters on weld quality. The importance of shielding gas compositions have been mentioned as being important during metal transfer, but no in-depth research has been conducted in this sensitive field.
This study attempts to relate the permeability phenomena [2],[18] with shielding gas composition and the effect that it has on obtaining the transition to spray metal transfer in GMA welding at lower current levels (lower heat input).

## 1.8 Outline of study

Continuing from chapter 1, ***chapter 2*** gives an outline of the arc welding process classification followed by a description of the GMAW process and its history. This is followed by an overview of the different metal transfer modes in GMAW, schematically indicating the approximate current/voltage range of each mode.

In ***chapter 3***, the different phenomena influencing weld metal transfer are discussed with emphasis on shielding gas compositions and flowrates.

A mathematical formulation of the physical phenomenon in gas shielded arc welding is expressed in ***chapter 4*** starting from the continuity equations up to the development of the equations for transition current and approximate droplet size [24]. This chapter shows a Fortan code [28], [34] developed for the calculation of the transition current and drop size with initial outputs which will be compared with experimental results in chapter 6.

***Chapter 5*** describes the experimental set-up with a description of the equipment. A schematic layout explains the set-up of equipment for the experiments.

Experimental results and discussions follow in ***chapter 6,*** comparing it with past research of [15], [23], [24].

# Chapter 2

## GMAW – Description of Process

### 2.1 Process Classification

**Classification of Gas Shielded Arc Welding Processes by Shielding Gas and Wire**

The welding process using carbon dioxide, $CO_2$, gas is called $CO_2$ gas shielded arc welding and that process using an inert gas such as argon or helium is termed GMAW (gas metal arc welding) or MIG (metal inert gas) welding. The process utilizing mixed gas of argon and $CO_2$ is called MAG (Metal Active Gas) welding.

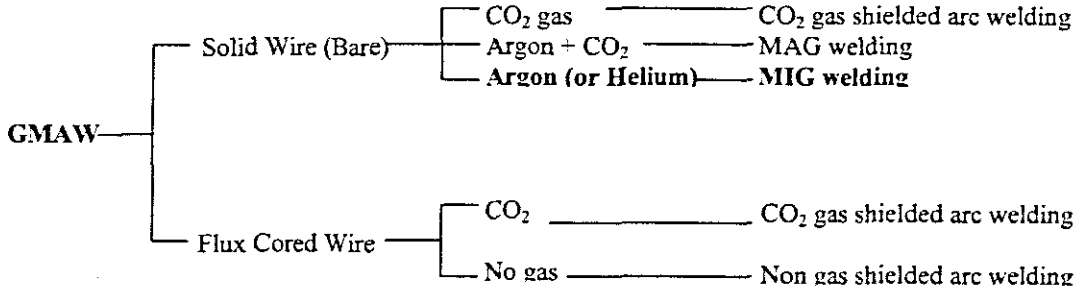


### 2.2 Process Description

Gas metal arc welding embraces a group of arc welding processes in which a continuous electrode is fed by powered rolls into the weld pool, with an electric arc between the tip of the wire and the weld pool. The wire is progressively melted with the same speed at which it is being fed. Both the arc and the weld pool are protected from atmospheric contamination by a shield of non-reactive gas which is delivered through a nozzle that is concentric with the welding wire guide tube.

The shielding gas may be Argon or Helium or mixtures, each of which has characteristic advantages and limitations.

GMA welding is most commonly employed as a semi-automatic process; however, it lends itself well to mechanized and automatic applications as well. Therefore, it finds itself well suited for robotic welding applications. In application it combines the advantages of continuity, speed, comparative freedom from distortion and the reliability of automatic welding with the versatility and controllability of manual welding.

The power supply utilized for GMA welding is referred to as a constant voltage or constant potential power source. That is, welding is performed using a preset value of voltage over a range of welding currents. GMA welding is generally performed using direct current, electrode positive (DC-EP). When this type of power source is combined with a wire feeder, the result is a welding process that can either be semi-automatic, mechanized or fully automatic. This reduces the amount of welder skill required to perform gas metal arc welding.

Figure 2.1(a) shows a typical gas metal arc welding setup and Figure 2.1(b) depicts the GMAW process.

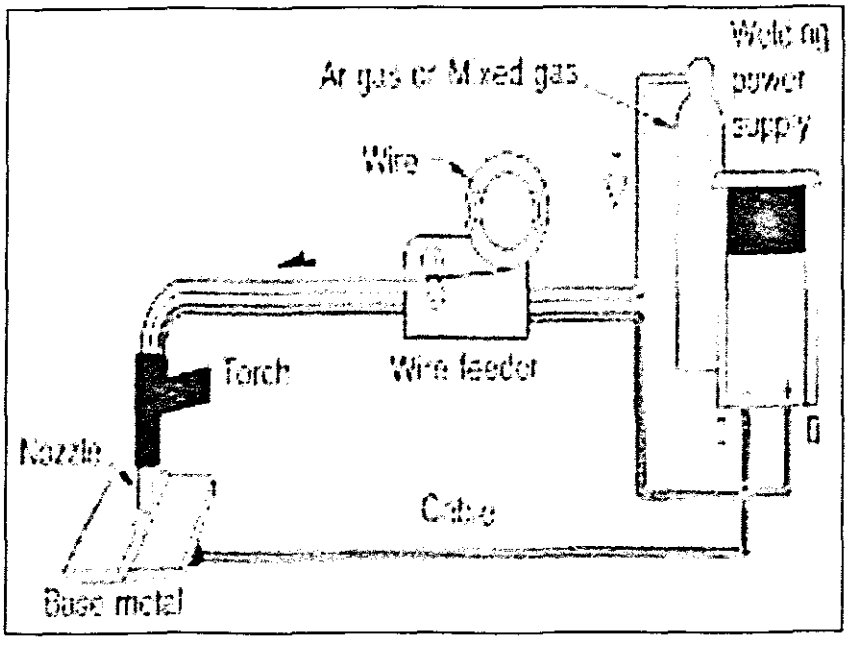


**Figure 2.1(a)** Typical GMAW Set-up. Reprinted from Operation Guide, $CO_2$MAG Semi-Automatic Welding Machine [44].

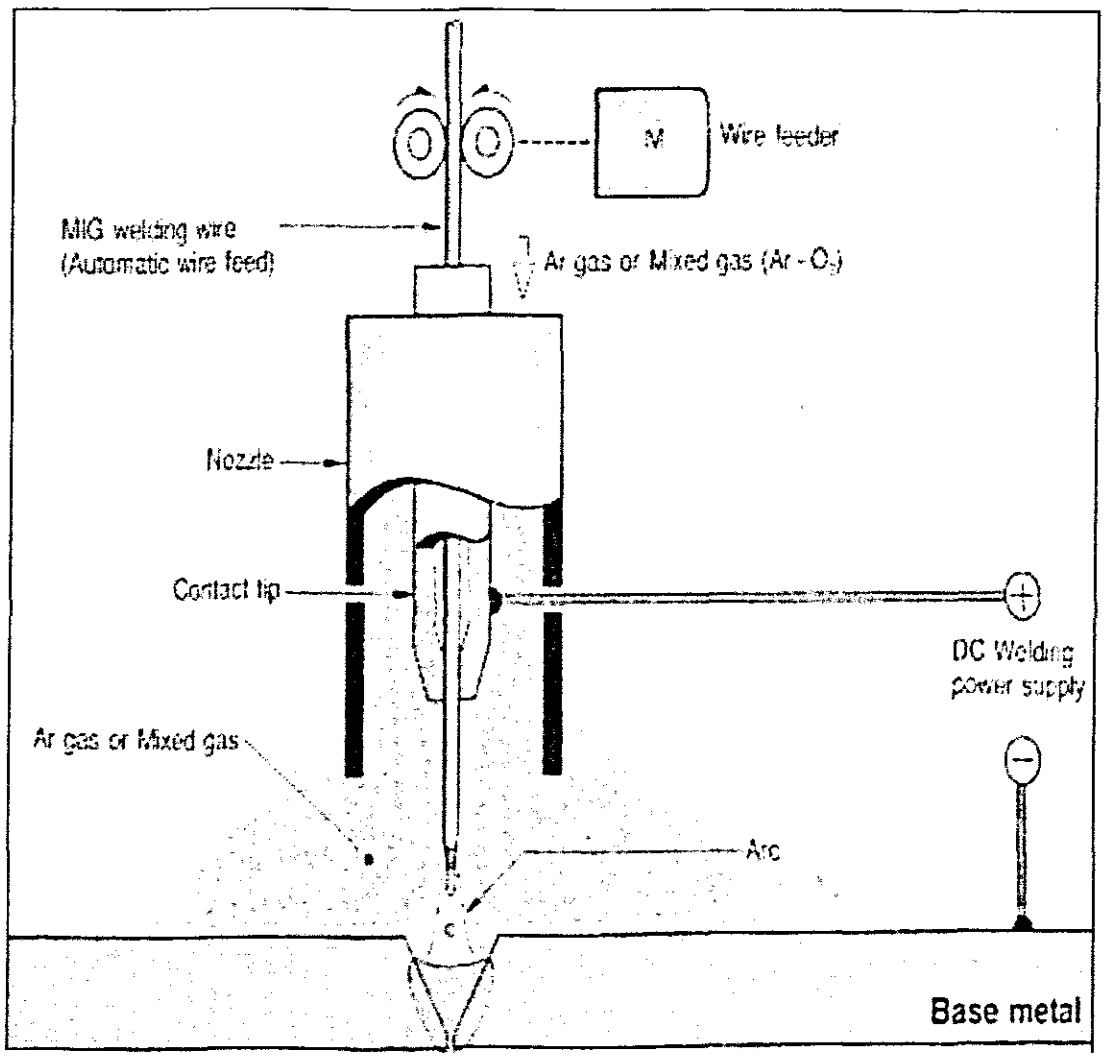


**Figure 2.1(b)** The GMAW Process. Reprinted from Operation Guide, $CO_2$MAG Semi-Automatic Welding Machine [44].

The versatility offered by the GMA/MIG welding process has resulted in its utilization in many industrial applications. It can be effectively used to join or overlay many types of ferrous and non-ferrous metals.

The use of gas shielding instead of some type of flux reduces the possibility of introducing hydrogen into the weld zone, so GMA welding can be used successfully in situations where the presence of hydrogen could cause problems.

One of the major advantages of this process is the fact that there is little or no cleaning following welding, which makes it such a well-suited process for automatic and robotic welding. Thus, the overall production efficiency is greatly improved and even further increased by the fact that the continuous roll of wire does not require changing as often as the individual electrodes used in processes such as shielded metal arc welding (SMAW).

## 2.3 History of the GMA Welding Process

GMA welding is a welding process that dates from about 1952. In the early Fifties, the benefits of Gas Tungsten Arc Welding (TIG) were being used on an increasing scale in commerce, but its limitations too, were becoming increasingly manifest. On the mechanical side it was a relatively simple matter to replace the non-consumable electrode of TIG welding with a continuously fed filler wire whilst maintaining the inert atmosphere provided by Argon or Helium. From the welding side and from the all-important aspect of economics, however, it was far from simple. In fact, it was not until the Sixties that the wide range of inter-related processes now making up the GMA welding 'family', were finally accorded general acceptance.

In 1952, equipment to weld Aluminium, stainless steel and some of the copper alloys became generally available to industry. Towards the end of the Fifties, the major problems associated with the application of GMA welding to the welding of mild- and medium carbon steels were solved. From that time the process began to be seriously considered by industry. Within a very short time, the real advantages that GMA welding had to offer resulted in its adoption and almost universal utilization.

However, three major difficulties had to be overcome. These were economic, electrical and metallurgical. Cost-wise, the price of Argon or Helium was too high to allow it to be used for the welding of the mild- and medium carbon steels that make up over ninety percent of the metals commonly fabricated by welding. The search for a less expensive gas brought about the use of carbon dioxide ($CO_2$), which was a fraction of the price of Argon.

The use of $CO_2$ posed its own problems such as excessive spatter at low current settings. Solutions to these problems were developed as technology delved deeper into the mechanics of GMA welding. Changes in power source characteristics, such as the change from a 'drooping' curve relationship between current and voltage to 'flat' curve, in which the voltage hardly varies irrespective of the current drawn, enabled new modes of welding to be developed. Shielding gas mixtures also influenced the welding process and changes to chemistry of the filler wire with deoxidizing agents led to the reduction in porosity and other weld defects.

In the last few years, especially with the current trends in welding industries, the trend has been away from the use of straight $CO_2$ as the shielding gas. Due to an increased demand for oxygen, more Argon has become available which in turn has caused its price to fall dramatically. When Argon is used in conjunction with other gases, the resulting mixed gases now enjoy a rapidly increasing popularity as the shielding medium for GMA welding of steel and other metals.

A great emphasis has always been put on the welding current and wire diameter to predict the occurrence of the transition between welding transfer modes and overall welding quality. However, one of the most important and constantly overlooked parameters in GMA welding is the effect of shielding gas composition on the transition zone. This has been indicated by the research conducted by Lowke [24], where it is mentioned that the theoretical transition current and approximate droplet diameter formula developed by the said author neglects the vital importance of gas mixtures in determining the current value at which transition occurs.

The need for research into the effects of shielding gas on transition current values will be crucial to align the theoretical approach of [24] with the practical requirements of the welding industry. Obtaining values for low transition currents from globular to spray transfer by optimizing the gas shield will lead to thinner metals to be welded in the spray mode without fear of weld pool collapse due to an arc that is 'too hot'.

## 2.4 Metal Transfer in GMAW

Molten metal are transferred in every arc welding operation, however the greatest concern about the transfer of molten metal should be paid for gas metal arc welding.

Metal transfer modes are generally divided into three (3) types. These are short circuit transfer, globular transfer and spray transfer including pulsed spray transfer.

Shape, size, direction of drops (axial or non-axial) and type of transfer are determined by a number of factors including: magnitude and type of welding current, current density, electrode composition and extension, power source characteristics and, as mentioned before, the mixture of the shielding gas.

### 2.4.1 *Short Circuit (DIP) Transfer*

Short circuit transfer occurs when the consumable electrode 'short circuits' (touches) the base metal many times a second and melts off into the weld pool. During welding this cycle can repeat itself between 20 and 250 times per second and will depend on inductance settings, consumable wire diameter and wire feed speed. This can occur between 60A and 230A, with lower deposition rates than the spray transfer method. During this mode of transfer, a fair amount of spatter is generated.

Figure 2.2 depicts the short-circuit metal transfer mode in Gas metal arc welding.

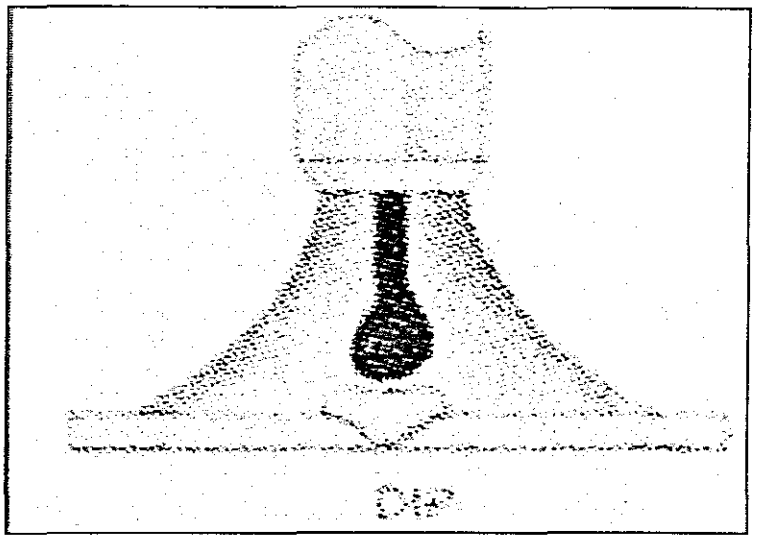

**Figure 2.2** Short Circuit Transfer. Reprinted from Trends in Welding Technologies. [38]

### 2.4.2 *Globular Transfer*

This metal transfer mode gets its name from the globs that are expelled off the end off the electrode. The globs are often larger in diameter than the unmelted electrode wire. This transfer mode was found to be common with pure $CO_2$ as a shielding gas and the welding parameters such as voltage set higher than the settings for short circuit transfer. Globular transfer is associated with high spatter levels and is undesirable in terms of welding economics. This mode of metal transfer is depicted in figure 2.3 below.

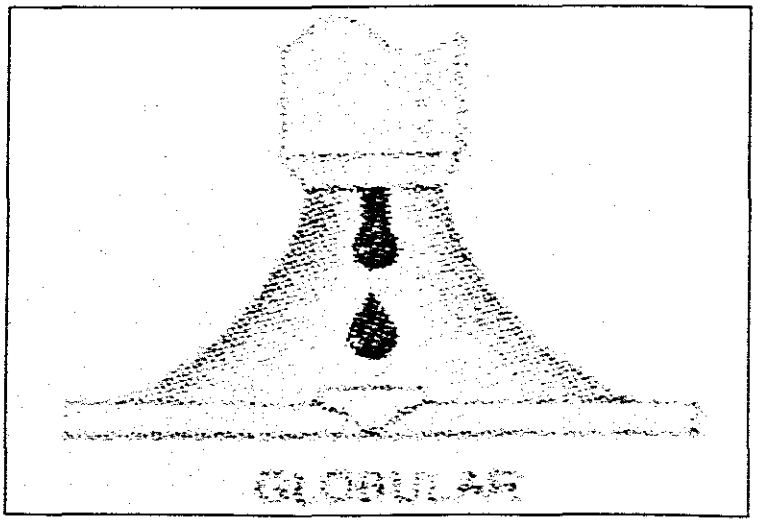

**Figure 2.3** Globular Transfer. Reprinted from Trends in Welding Technologies. [38]

### 2.4.3 *Spray Transfer*

Spray transfer refers to a stream of tiny molten droplets spraying across the arc, from the electrode wire to the base metal. This transfer mode is associated with high voltage and ampere, thus producing high metal deposition rates. This is limited to the flat or horizontal position. Due to the higher heat input, spray transfer is most suited to thicker metals (>6mm). High arc stability and minimal spatter make this a desirable mode of transfer for achieving a high level of productivity.

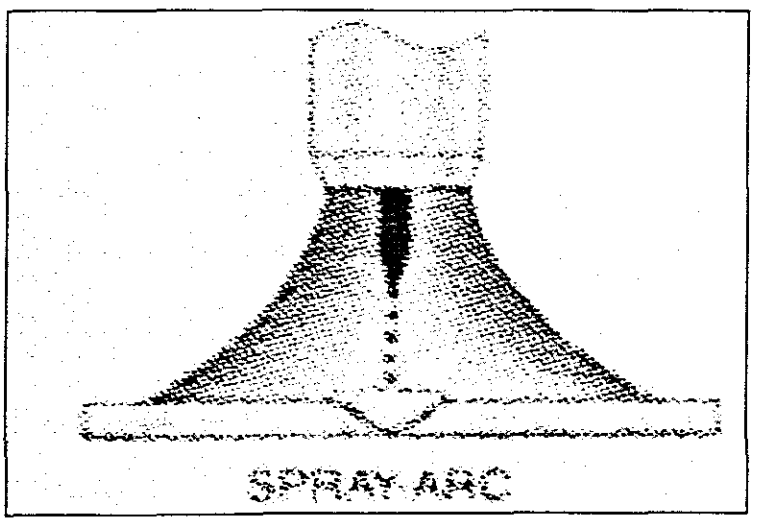

**Figure 2.4** Spray Transfer. Reprinted from Trends in Welding Technologies. [38]

### 2.4.4 *Pulsed Spray Transfer*

This method requires special welding equipment, which tend to be very expensive and not easily affordable to the smaller scale welding community. Generally most inverter-based power sources can provide the high response times required for this mode of transfer. Spray transfer mode is associated with high weld deposition rates and low spatter levels, but limited to the flat or horizontal welding positions. However, with pulsed spray transfer MIG welding, it has been found that it would provide an all position capability.

In pulsed spray transfer, the welding power source pulses the welding output with high peak currents, which are set at levels that will cause the transfer to go into a spray. The background current is set at a level that will maintain the arc but is too low for any metal transfer to occur. Because there are no metal transfer during the background current portion of the cycle, the weld puddle is able to freeze slightly. The faster freezing weld puddle allows the pulsed transfer to be used for sheet metal welding and for better control of 'out-of- position work'.

This mode of transfer relies on the type of shielding gas used. Spray and pulsed spray transfer are found to be more suited to argon-rich gas mixtures. Due to the cost involved with pulsed spray welding, the specific equipment required and the use of Argon rich gas mixtures, it is therefore vital to have an alternative approach to thin sheet metal welding. Low heat inputs are required to prevent 'melt-through' and weld pool collapse, tend to be in the globular transfer mode, and undesirable in terms of

welding economics. The spray transfer mode's heat input levels are too high for sheet metal welding, therefore should the transition between these two modes be explored as an alternative option for the welding of thin metals. The influence of the gas mixture greatly affects the transition currents and research in this unknown will definitely lessen the problems associated with the affordable welding of thin metals using the GMAW method.

### 2.4.5 *Surface Tension Transfer*

Surface tension transfer (STT) is a proprietary mode of metal transfer from The Lincoln Electric Co. [36]. This mode precisely controls the current during the welding cycle. It is a controlled short-circuiting transfer mode. Current generation inverter-based systems allow the power source to control arc dynamics. It is particularly effective for automated welding of thin-gauge steel. Joining of nickel alloys and open root welding are also accomplished with this transfer mode.

During welding using this mode, electrode current adjusts instantaneously to the heat requirements of the arc. It then decreases before the electrode first enters the weld pool, then increases to a pinch current that speeds up the transfer of the drop before reducing to a lower level to allow drop separation with minimal spatter. The current then returns to a high level to establish arc length and form the next droplet before reducing to a medium or background value. This control over the arc current eliminates the sometimes violent and explosive nature of short-circuit transfer.

Figure 2.5 below shows the various metal transfer modes and the approximate current ranges of each. In Appendix A, the complete IIW classification of metal transfer modes with examples can be found in table form and schematically illustrated.

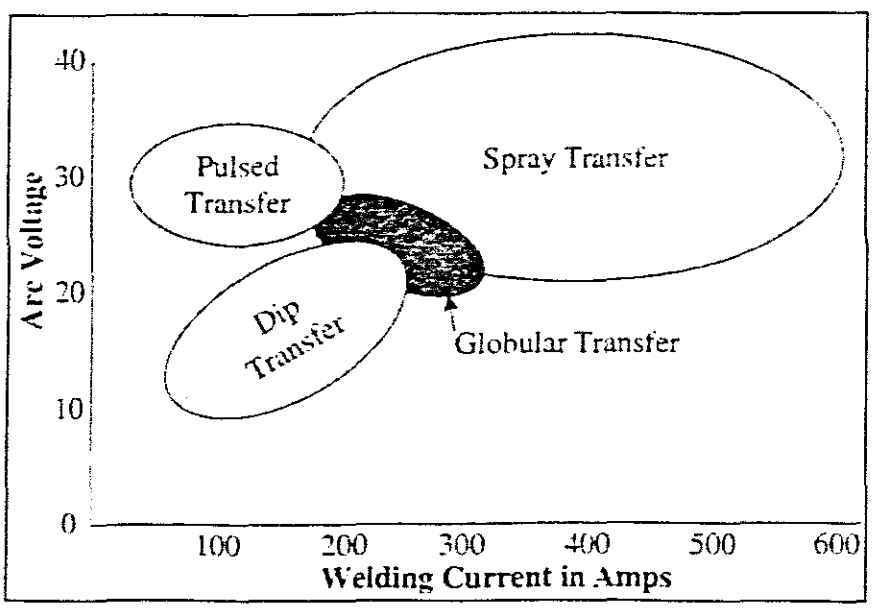


**Figure 2.5** Modes of Transfer in GMAW. Reprinted from MIG Welding Thin Stainless Steel Sheet. [17]

# Chapter 3

## Phenomena influencing weld metal transfer

### 3.1 Introduction

A stage of utmost importance during arc welding is the transfer of molten filler metal to the weld pool. In gas metal arc welding, the forces controlling this transfer from the filler wire are very complex, but in all cases the transfer occurs in the form of liquid metal droplets. The size of these droplets and the forces acting on them during their formation determines the mechanisms of metal transfer. Forces affecting metal transfer are *gravity, surface tension*, the *electromotive force (EMF)*, the *hydrodynamic forces*, *viscous drag forces* and forces due to *arc pressure*. The *filler metal feed rate* will also play an important role in the metal transfer process as well as the *shielding gas composition.*

The effects of the above forces and parameters are briefly discussed below:

#### 3.1.1 *Gravity*

The gravitational forces acts to pull the drop off the electrode against the surface tension forces when welding in the flat or horizontal position. Welding in the upright or overhead position will dictate the direction the electrode will point, thus affecting the effect that the gravitational force will have on the detaching droplet. The effect of gravity in the different welding positions will have an influence on the current setting, welding speed electrode feed rate and other related parameters.

#### 3.1.2 *Surface Tension*

The surface tension forces act in the surface of the molten droplet and compress the drop and, thereby effectively increasing the pressure inside the drop. The effective result being that it tends to make the drop adhere to the electrode. Thus, for the droplet to be detached from the wire, the surface tension force must first be overcome.

#### 3.1.3 *Hydrodynamic forces*

These forces act on the falling drop and results from the hydrodynamic properties of the plasma. It depends primarily on the jet velocity and the droplet size. That is the extent to which the droplet is accelerated by the jet stream. The MIG process involves 'free flight' of the liquid metal droplets, which break away from the filler metal electrode and propelled into the weld pool.

### 3.1.4 *EMF*

In MIG welding, one of the most important factors to consider in metal transfer is the pinch effect or 'squeeze' around the conductor due to the electromagnetic effects of the current. It is a radial force caused by the flow of current in the conductor or electrode. As shown in Figure 3.1(a) below, a droplet attached to the tip of an electrode is squeezed by the pinch effect to be transferred through the arc path. Figure 3.1(b) illustrates a short-circuited droplet is about to be squeezed to break the short-circuit and to recover the arc.

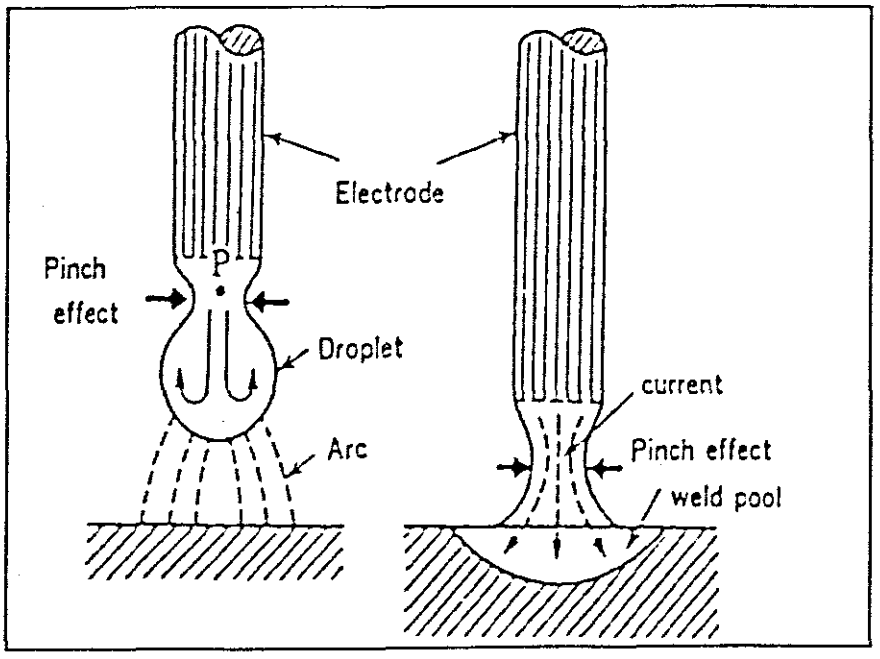


**Figure 3.1(a)** Squeezing of Droplet. **(b)** Squeezing of Short-Circuited Metal. Reprinted from Welding Processes and Power Source lecture notes. [51]

### 3.1.5 *Viscous Drag forces*

The viscous drag force of the plasma is due to the momentum transfer between the gas and the electrode. The constriction of the arc region near the wire tip can result in very high velocities (to the order of 500m/s) in the arc plasma. The resulting gas flow in the direction from the wire to the work piece results in this extra detaching force acting on the drop.

### 3.1.6 *Arc Pressure forces*

The pressure upwards on the drop due to the arc causes a supporting effect tending to oppose the viscous drag forces by slowing the droplet velocity down and/or adhering the drop to the wire.

### 3.1.7 *Electrode Feed Rate*

It is sometimes possible to observe a transition in the metal transfer processes as the wire electrode feed rate is changed. At low feed rates (and low currents) the liquid drop grows until it is detached under gravity, but at a rapid rate of feed the droplets are pulled off by electromotive forces. There is a sharp increase in current, and correspondingly a sharp decrease in droplet size, when the mechanism changes in the transition region. If the current (and corresponding feed rate) are raised too far, then the high droplet velocity leads to defective welds associated with extensive spatter.

### 3.1.8 *Shielding Gas*

A variety of shielding gases has been refined to suit different welding or cutting applications. In addition to the general shielding of the arc and the weld pool, the shielding gas performs a number of important functions:

- It forms the arc plasma
- It stabilises the arc roots on the material surface
- It ensures smooth transfer of molten droplets from the wire to the weld pool.

This means that the primary purpose of the torch shielding gas is to protect the electrode, the molten weld metal and the weld pool from exposure to contamination, oxygen and water that are present in the atmosphere. The shielding gas is directed by the torch to the arc and weld pool.

## 3.2 Shielding Gas – Description, composition and importance in welding

The shielding gas will have a substantial effect on the stability of the arc and metal transfer and the behaviour of the weld pool, in particular its penetration.
In South Africa, the common MIG shielding gases are Argon and Carbon Dioxide. Mixtures of these gases, as well as a 1% or 2% addition of Oxygen are common when welding carbon- and low alloy steels. Additions of other gases such as helium, oxygen, hydrogen and nitrogen afford certain qualities to shielding gases used for certain materials

### 3.2.1 *Argon*

The most commonly used shielding gas is argon (Ar). It is a heavier than air monatomic gas with an atomic weight of 40. Argon's density is 1.7837gm/l at standard temperature and pressure (STP). The gas is readily available in several grades, including a "high purity grade" refined to a minimum purity of 99.998%, or a "welding grade" refined to a minimum purity of 99.995%. (The purity of the gas, i.e. high purity, welding grade, etc. has not been established as a standard and therefore the purity percentage specified for the different grades may vary slightly between manufacturers).

Welding grade argon is satisfactory for most welding applications. It is a chemically inert, colorless, odorless, tasteless nontoxic gas. It is obtained from the atmosphere by the separation of liquefied air.
The chief factor influencing shielding effectiveness is the gas density. Argon is approximately 1.3 times as heavy as air and ten times heavier than helium. After

exiting the torch gas nozzle/cup, argon tends to form a blanket over the weld area.

Although argon itself is chemically inert, it is readily ionized to form a plasma. Impurities such as moisture and oxygen can cause variable arc behaviour and a reduction in weld metal properties. This is especially true in reactive metals such as titanium and magnesium. Due to argon ionizing, it stabilizes the arc, but is a poor heat conductor and leads to high surface tensions.
The reduced penetration of an argon-shielded arc is particularly advantageous when manual welding thin material, because the tendency for excessive melt-through is lessened. The reduced penetration characteristic is advantageous in vertical and overhead welding since the tendency for the base metal to sag or run is decreased.

Argon is used for welding a wide range of materials including mild steel, stainless steels, aluminium, copper, nickel alloys and the reactive metals, titanium and magnesium. Argon is used more extensively for shielding because of the following advantages: easier arc initiation, better weld pool control, smoother and quieter arc action, lower cost and greater availability, better cross draft resistance (due to density), lower flow rates for shielding, reduced penetration when welding thin materials.

### 3.2.2 *Carbon Dioxide*

Carbon dioxide ($CO_2$) is used only for GMA welding of steel. The gas differs from other gases normally used in that it is a compound of carbon and oxygen. In the welding arc the carbon dioxide dissociates in the arc, thus forming a carbon monoxide and free oxygen. This may lead to carbon contamination. If the arc temperature increases sufficiently the free oxygen will ionise. However, there is insufficient free oxygen to maintain a proper arc column. Dissociation means that the welding atmosphere is highly oxidizing, even though the carbon monoxide restricts the effectiveness of the free oxygen.

The most common metal transfer modes encountered in carbon dioxide shielding is short-circuit and globular transfer modes. True spray transfer does not occur and the free flight transfer that occurs is globular or repelled.

The poor process tolerance is balanced by the relatively high heat input of the gas and this, combined with the high oxidizing potential, may assist in welding on coated steels. The gas mixtures have been designed to obtain the best characteristics of each gas and improve arc stability, metal flow, sidewall fusion and wetability. It is important to note that the above effects will influence the properties of the welded joint. For example, improved wetting can improve the fatigue life of a joint by increasing the contact angle of the weld bead to the base metal.

### 3.2.3 *Helium*

Helium is one of the lightest monatomic gases with an atomic weight of four. The density of helium is approximately 0.1785gm/l at STP. It is significantly more expensive than argon and is available in a welding grade of 99.95% purity, or a high-purity grade of 99.995% Helium is also a chemically inert, colorless, odorless and tasteless gas. It is a mined resource obtained by the separation of natural gas. Helium,

because it is lighter than air, tends to rise around the gas nozzle/cup. Thus to produce equivalent shielding effectiveness, the flow of helium must be two to three times that of argon.

The higher ionization potential of helium, approximately 25eV compared to 16eV for argon, produces a significantly higher arc voltage. For given values of welding current and arc length, helium transfers more heat into the work than argon. Since the arc formed in helium is considerably hotter than with argon, and because it has a higher thermal conductivity, it can often promote higher welding speeds and improve the weld bead penetration profile (deeper penetration and a flatter surface profile). The greater heating power of helium can be advantageous for joining thick metals of high thermal conductivity and for high speed mechanized applications.

Although helium offers definite advantages for some applications, it produces less stable arcs and arc starting characteristics than argon. Helium requires higher shielding flow rates and the hotter arc produced by helium makes it unsuitable for the welding of thin metals. Mixtures of helium and argon are useful when a balance between the characteristics of the two is required. Helium additions to shielding gases are limited to gas tungsten arc welding (GTAW) processes, although tests have been conducted with GMAW.

### 3.2.4 *Oxygen*

In GMA welding, oxygen ($O_2$) is often deliberately introduced through the shielding gas to increase the arc stability and bead morphology. It reduces the surface tension of the droplet and causes a fine spray transfer. However, this is accomplished at the expense of an increased content in the weld metal and intensified losses of alloying elements.

An interesting effect of oxygen on the weld metal hydrogen content is that the hydrogen level is significantly higher in the presence of oxygen. This is probably due to the formation of a thin protective layer of slag on the top of the bead, which kinetically suppresses the desorption of hydrogen during cooling. Oxygen is present as non-metallic inclusions in deposited metals, and has a bad effect on impact values.

### 3.2.5 *Nitrogen*

Since the total nitrogen level in most welding consumables and shielding gases is quite low, the main source of nitrogen contamination is air infiltrated in the arc column due to insufficient shielding for the molten pool. For this reason weld metal nitrogen content is very sensitive to variations in the operational conditions, such as arc length, shielding gas nitrogen content, gas flow rate, etc.

Nitrogen additions results in improvements of mechanical properties such as tensile strength and hardness, but will decrease impact values. Furthermore, additions of nitrogen help the formation of an austenite structure but excessive nitrogen content can cause porosity of steel because of gas evolution during solidification as well as embrittlement due to the precipitation of nitrides. Nitrogen additions are especially necessary to keep austenite-ferrite proportions when welding duplex or super duplex stainless steels.

### 3.2.6 *Hydrogen*

Hydrogen is the lightest and most abundant of all the elements. It is a flammable colourless, odorless tasteless non-toxic gas with a density of approximately 0.08988g/l at STP. Several grades are also available.

Argon-hydrogen mixtures are employed in special cases, such as mechanized welding of light gauge stainless steel and nickel based alloys, where the hydrogen does not cause metallurgical defects such as porosity and hydrogen induced cracking. Excessive hydrogen in argon will cause porosity. Increased welding speeds can be achieved in almost direct proportion to the amount of hydrogen added to argon because of the increased arc voltage and thermal conductivity. However, the amount of hydrogen that can be added varies with the type of material, thickness and joint design. Hydrogen can be added to argon or helium to increase the temperature of the arc and to provide a slightly reducing atmosphere.

The higher heat input is derived from the dissociation of the hydrogen in the arc to form monatomic hydrogen, which then recombines to the molecular form in the cooler regions of the arc and at the surface of the workpiece. The arc voltage of a hydrogen mixture is correspondingly higher compared with pure argon or helium, although the arc length and the welding current level will determine the actual voltage.

The arc itself in argon-hydrogen mixtures improves the weld bead penetration, i.e., it produces a greater depth-to-width ratio, and enables higher welding speeds to be attained. Additionally, the reducing atmosphere produces a cleaner weld bead surface and, in multi-pass welds, reduces the risk of oxide/slag buildup.

It should be noted, however, that the use of hydrogen may cause cracking in carbon and alloy steels. It causes porosity in ferritic steels, aluminium, copper, and in multi-pass welds in nickel and austenitic stainless steels. As mentioned before, argon-hydrogen gas mixtures are normally limited to stainless steel, nickel-copper and nickel based alloys.

It needs also to be stressed that all hydrogen mixtures are potentially hazardous and may require special procedures and special equipment.

The datasheet [45] in Appendix B gives recommended shielding gas selections for the various metal transfer modes in GMA welding.

## 3.3 Shielding gas flow rates

Shielding gas flow rates are based on gas nozzle/cup size, weld pool size and air movement. In general, the flow rate increases in proportion to the cross-sectional area at the gas nozzle/cup. The gas nozzle diameter is selected to match the size of the weld pool and the reactivity of the metal to be welded. The minimum flow rate is determined by the need for a stiff stream of shielding gas to overcome the heating effects of the arc and local cross drafts. An excessive flow rate may cause turbulence in the gas stream, which may aspirate atmospheric contamination into the weld pool. Turbulence in the gas flow system can cause instabilities in the welding arc. Sharp

bends, sharp edges and massive volume changes in the gas supply system may also cause turbulence in the gas flow. As a rule of thumb, a 5:1 reduction ratio between the inner diameter of the supply line and the inner diameter of the torch hose will assure laminar (non-turbulent) flow.

Choosing the proper shielding gas mixture and gas flow rate can therefore help ensure flawless GMA and GTA welding. Research results have shown that great discrepancies exist between theoretical results and actual experimental data. In order to bring theoretical research closer to the actual industrial problems with respect to the welding of thin metals, the study of the influence of shielding gas composition on the globular-spray transition zone will be of great advantage to the welding industry. As mentioned before, in chapter one, the pulsed spray transfer mode overcome some of these problems, but the necessary equipment is well beyond the financial reach of most welding companies. The other alternative is then to look at the optimization of the globular-spray transition mode for maximum utility of the benefits both modes offer, but without the adverse effects associated with each mode.

Since 1899 when Dr. Hugo Zerner patented a method of welding metal under a protective gas shield, to keep atmospheric contamination away, many years of further developments and research were required to bring shielding gas processes to the standard that it is today. Further research into this phenomenon of welding will definitely be required to bring GMA welding in line with the global vision of the welding industry.

# Chapter 4

## Mathematical Formulation of Physical Phenomenon

### 4.1 Introduction

In Figure 4.1, when the pendant drop is assumed to be axisymmetric, and the material properties are assumed to be constant, the motion of an incompressible fluid within the drop is governed by the continuity and momentum equations [7],[10],[15]: These dynamic differential equations governing the arc and electrodes include:

- ***Mass continuity equation***

$$\frac{\partial \rho}{\partial t}+\frac{1}{r}\frac{\partial}{\partial r}(r\rho v_r)+\frac{\partial}{\partial z}(\rho v_z)=0$$

- ***Energy equation***

$$\frac{\partial \rho h}{\partial t}+\frac{1}{r}\frac{\partial}{\partial r}(r\rho v_r h)+\frac{\partial}{\partial z}(\rho v_z h)=\frac{1}{r}\frac{\partial}{\partial r}\left(\frac{rk}{c_p}\frac{\partial h}{\partial r}\right)+\frac{\partial}{\partial z}\left(\frac{k}{c_p}\frac{\partial h}{\partial z}\right)+\frac{j_r^2+j_z^2}{\sigma}-U$$

- ***Radial momentum equation***

$$\frac{\partial \rho v_r}{\partial t}+\frac{1}{r}\frac{\partial}{\partial r}(r\rho v_r^2)+\frac{\partial}{\partial z}(\rho v_r v_z)=-\frac{\partial P}{\partial r}-j_z B_\theta+\frac{1}{r}\frac{\partial}{\partial r}\left(2r\eta\frac{\partial v_r}{\partial r}\right)+\frac{\partial}{\partial z}\left(\eta\frac{\partial v_r}{\partial z}+\eta\frac{\partial v_z}{\partial r}\right)-2\eta\frac{v_r}{r^2}$$

- ***Axial momentum equation***

$$\frac{\partial \rho v_z}{\partial t}+\frac{1}{r}\frac{\partial}{\partial r}(r\rho v_r v_z)+\frac{\partial}{\partial z}(\rho v_z^2)=-\frac{\partial P}{\partial z}+j_r B_\theta+\frac{\partial}{\partial z}\left(2\eta\frac{\partial v_z}{\partial z}\right)+\frac{1}{r}\frac{\partial}{\partial r}\left(r\eta\frac{\partial v_r}{\partial z}+r\eta\frac{\partial v_z}{\partial r}\right)+\rho g$$

- ***Current continuity equation***

$$\frac{1}{r}\frac{\partial}{\partial r}\left(r\sigma\frac{\partial}{\partial r}V\right)+\frac{\partial}{\partial z}\left(\sigma\frac{\partial}{\partial z}V\right)=0$$

- ***Ohm's law***

The current density is derived as the derivative of the voltage:

$$j_r=-\sigma\frac{\partial V}{\partial r} \quad \text{and} \quad j_z=-\sigma\frac{\partial V}{\partial z}$$

- ***Maxwell's equation***

As the magnetic field is generated by the welding current in the $z$ - direction (ref. Fig. 4.1), the magnetic flux density $B_\theta$ can be described as $B_\theta=\mu_0/r\int_0^r j_z r\,dr$, yielding Maxwell's equation:

$\frac{1}{r}\frac{\partial}{\partial r}(rB_\theta)=\mu_0 j_z$ where $\mu_0=4\pi10^{-7}\ H.m^{-1}$ is the permeability of free space.

The basic variables describing the physical conditions of the arc and electrodes defined in the equations include the pressure $P$, temperature $T$, radial and axial velocities $v_r$ and $v_z$, electric potential $V$, radial and axial current densities $j_r$ and $j_z$ magnetic flux density $B_\theta$.

The input material functions required for the arc plasma as well as for the solid and liquid electrode materials are the density $\rho$, viscosity $\eta$, specific heat $c_p$, thermal and electrical conductivities $k$ and $\sigma$ as well as the enthalpy $h$.

In addition, the radiation loss per unit volume $U$ for the plasma and the surface tension $\gamma$ for the liquid metal surface are required.

Assumptions and boundary conditions include the initial shape of the pendant drop, the velocity within the molten drop and the current density distribution on the drop surface. The initial drop shape is a hemisphere to ensure numerical stability, and the free slip condition is enforced along the $z$ - axis. The initial velocity within the drop is assumed to be the same as the wire feed rate.

In the arc region, the plasma is assumed to be in local thermodynamic equilibrium (L.T.E.) and laminar flow is assumed.

An important boundary condition is the current density distribution on the drop surface, which determines the distribution of the voltage and current density within the drop, and thus influences the electromagnetic force. Estimation of the actual current density on the drop surface is very difficult due to the involvement of the arc.

The effect of shielding gas composition will influence the current density distribution on the drop surface. Due to the fact that *permeability* is the property of materials that measures its ability to permit the establishment of magnetic lines of force [2],[18] the shielding gas surrounding the pendant droplet will have a relative permeability $\mu_r$ depending on its composition yielding the absolute permeability $\mu = \mu_r \mu_0$ of the gas. Non-magnetic materials (e.g. air, glass, copper and aluminium) are characterized by its $\mu_r$, which is approximately unity. Diamagnetic materials have a lower permeability than air ($\mu_r$ is a fraction). Paramagnetic materials have a slightly higher permeability than air ($\mu_r$ is 1 to 10). However, magnetic materials (e.g. iron, steel, cobalt, nickel, etc.) termed ferromagnetic materials are characterized by high permeability values ($\mu_r$ ranges from 100 to 100 000). Calculations by [15], [23], [24] neglect this phenomena and assumes $\mu_r$ as unity. It is conjectured by [7] that the current density increases along the $z$ - axis because the electrical resistance is reduced as the molten drop elongates and approaches the workpiece. The reasonability of this assertion is because the current density is higher in the lower part of the drop than in the upper part due to the higher temperature at the centre of the arc. It is thus assumed that the current density on the drop surface is uniform and can be linear on the drop surface along the $z$ - axis.

For the development of the current formulation from globular to spray transfer modes, developed by [15] and [24], a liquid hemisphere at the end of a solid cylindrical electrode was considered, as shown below. The sphere was considered because it gives the simplest possible model. A mentioned before, hemisphere is considered, because for all spheres of different radii passing through AC in the figure below, it is a hemisphere with AC as diameter which has the minimum radius and thus maximum curvature and surface tension pressure to support a drop.

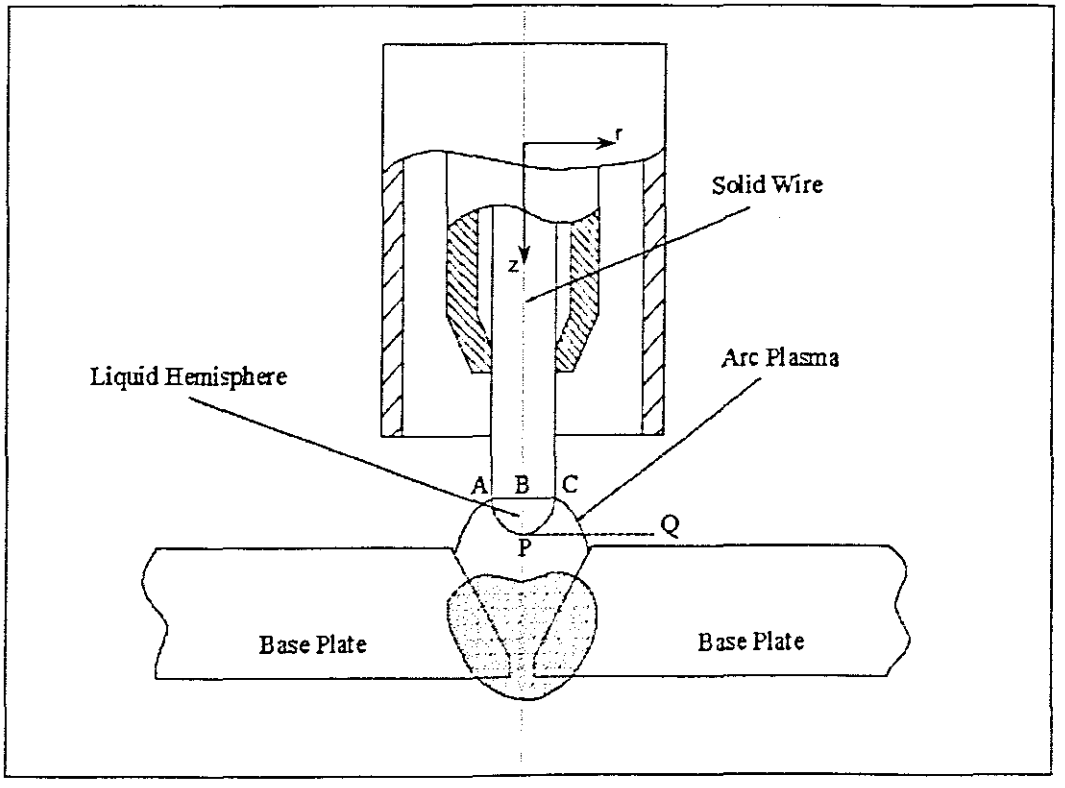


**Fig. 4.1** Physical model for GMA Welding

At low current, magnetic pinch forces are negligible and drop behaviour are dominated by a balance of surface tension forces and gravity. With an increase in current, however, magnetic pinch forces disturb the hemispherical surface and a mode change is introduced.

This simple model gives an analytic relationship and a clear insight into the dominant physical forces that are operating at the critical current for the transition from globular to spray transfer mode.

### 4.2 *Gravity and Surface Tension*

When the curvature of the drop surface is calculated, the pressure on the free surface is determined by the surface tension and radius of curvature.

The effect of the surface tension acting in the surface of the liquid hemisphere in Fig. 4.1 is to compress the drop and effectively increase the pressure inside of the drop by $P_s$, where:

$$P_s = \gamma\left(\frac{1}{R_1}+\frac{1}{R_2}\right); \qquad 4.1$$

$\gamma$ is the surface tension coefficient. $R_1$ and $R_2$ are principal radii of curvature of the surface. For a hemisphere $R = R_1 = R_2$ so that

$$P_s = {}^{2\gamma}/_{R} \qquad 4.2$$

$R$ is now the radius of the hemisphere and equals AB and BC in Fig. 4.1. The effect of this force is to tend to hold the drop onto the wire.

For very low currents, which is the globular transfer mode, The effect of magnetic pinch forces will be negligible, and we consider just the effect of surface tension and gravity. For normal welding (flat or horizontal position), gravity will exert a pressure downwards on the surface of the liquid hemisphere, tending to pull it off of the wire. Gravity will thus cause an increase in pressure equal to $\rho gR$ from point B to point P in Fig. 4.1. It is thus evident that gravity acts to reduce the effective pressure due to surface tension, which tends to make the drop adhere to the wire.

### 4.3 *Magnetic Pinch Force*

The axial current within the liquid drop induces an azimuthal magnetic field with the dominant effect of exerting a squeezing or pinch force radially. This squeezing force is balanced by a radial pressure gradient within the drop. While the magnetic pinch force is primarily radial, it has the effect of increasing the pressure at P in Fig. 4.1, which produces an axial force tending to extrude liquid away from the solid wire, and thus detach drops. It is possible to derive the pinch pressure at P accurately from Maxwell's equations, assuming that all the current enters the solid wire through the hemispherical drop.

It is assumed that the axial current density j through the cross section AC of Figure 4.1 is uniform. The self-magnetic field $B$, induced by this current density is given by:

$$\frac{1}{r}\frac{\partial}{\partial r}(rB) = \mu j \qquad 4.3$$

which is Maxwell's equation; $r$ is the radial distance from the axis of the cylinder of current and $\mu = 4\pi 10^{-7}\ N/A^2$ is the absolute permeability of free space.

Upon integration this equation gives

$$B = \mu jr/2 \quad , \qquad 4.4$$

using the fact that the magnetic field is zero at the axis of the wire. The radial magnetic pinch force (electromagnetic force) exerted by this magnetic field is given by $j \times B$, where $j$ and $B$ represent the vectors of the current density and of the magnetic flux density respectively

The radial momentum equation, within the liquid drop is:

$$\partial P_m / \partial r = -j \times B \, , \qquad 4.5$$

because for zero flow in the liquid, terms involving inertial and viscous forces are zero; $P_m$ is the magnetic pinch pressure. An expression for the radial variation of this pressure along AB can be obtained by integrating Equation 4.5 over the total radius $R$ of the cylinder, using the previously derived expression for $B$. Hence

$$P_m = \frac{\mu I^2}{4\pi^2 R^2}\left[1 - \left(\frac{r}{R}\right)^2\right] \qquad 4.6$$

It is assumed that $P_m = 0$ at $r = R$ and that the total current $I = \pi R^2 j$. Thus, the magnetic pressure will be a maximum at the centre of the cylinder, i.e. at point B in Figure 4.1, where $r = 0$ and where, from Equation 4.6, $P_m$ will equal $\mu I^2 / 4\pi^2 R^2$. The axial momentum equation can now be applied along BP to find the pressure at P.

$$\partial P_m / \partial Z = jr \times B + \rho g \qquad 4.7$$

where $j \times r$ is the radial current density. Along the axis of the drop, $j \times r = 0$ and also $B = 0$, so that the pressure at P equals the pressure at B of $\mu I^2 / 4\pi^2 R^2$, plus the gravitational contribution $\rho g R$.

### *4.4 The Threshold Current for transition to spray transfer*

It is assumed in the present arc model that the arc envelopes the hemispherical drop at the end of the wire as per Fig. 4.1, but that the arc has a much larger radius away from the liquid drop. Along line PQ, in the arc region, the current density will be much lower than along the line BC in the liquid. Thus the magnetic pinch pressure at P in the arc, obtained by integrating equation 4.3, will be much less than the pressure at P inside the liquid. There is a magnetic pressure in the liquid from the magnetic field of $p_m = \mu I^2 / 4\pi^2 R^2$. This reduces the net pressure of $2\gamma / R - \rho g R$ which holds the drop to the wire. It is thus evident that the effect of the self-magnetic field is to produce a nett axial pressure tending to detach the hemispherical drop from the wire.

This is given when the magnetic pressure is just equal to the net pressure holding the drop to the wire. Considering the extreme case where there is a negligible contribution

from the arc pressure in supporting the drop, the ***critical current for transition from globular to spray transfer modes*** is given by

$$\mu I^2 / 4\pi^2 R^2 = 2\gamma / R - \rho g R$$

which gives

$$I = \left( 2\pi / \mu^{1/2} \right) \left( 2\gamma R - \rho g R^3 \right)^{1/2} \qquad 4.8$$

This equation is the fundamental one when deciding on a particular current to use for a welding process as it is the least current at which the drop will detach. For currents above this critical current the magnetic pressure will result in the drop being broken up into a spray. As can be seen from the equation this current is determined only by the permeability, $\mu$, the surface tension of the molten metal, $\gamma$, the density of the molten metal, ρ, and the radius of the liquid hemisphere.

For an understanding of the pressure variations from P to A in Fig. 4.1, consider the following:

Let the pressure outside of the drop at P be $P_{PO}$. This pressure is increased on crossing the liquid surface by $2\gamma/R$ reduced along the line from P to B by $\rho g R$, and further reduced along the line from B to A by $\mu I^2/4\pi^2 R^2$. The transition current of Equation 4.8 is obtained by requiring that the difference in the pressure at A inside the drop, and the pressure $P_{AO}$ at A outside of the drop be not less than zero; i.e. if we assume that $P_{PO} = P_{AO}$, we require that $2\gamma/R - \rho g R - \mu I^2/4\pi^2 R^2$ be greater than zero. If this quantity is less than zero, the radius of curvature of the surface at A will become negative, producing a neck in the drop. This radius of curvature of the surface at P will also increase, producing an elongation.

Once such an elongation has developed, the attachment point of the arc current will tend to concentrate on the elongation and the current density in this region will become larger. The magnetic pinch pressure will then further increase in the elongation, and as a consequence, there will be a runaway effect that will produce a small drop. The effect of gravity from the increased mass in the elongation also increases the pressure difference due to gravity, also enhancing the runaway effect. The effect of the magnetic pinch fore is a maximum at the centre of the elongation because of the factor $\left[1 - (r/R)^2\right]$ in Equation 4.6.

When an elongation is first formed at P, the radius of curvature of this region will become smaller than the radius of the hemisphere. Thus the surface tension forces will increase at P, but the surface tension pressure varies as $1/R$ compared to $1/R^2$ for the magnetic pressure, so that beyond the critical current, liquid motion is unstable and will proceed to the formation of a small drop.

By equating the surface tension pressure to magnetic pressure, an ***estimated droplet size*** can be obtained, giving

$$R_d = \mu I^2 / 8\pi^2 \gamma \qquad 4.9$$

It can be seen that for overhead welding, the sign of the term in $\rho g$ in Equation 4.8 will be reversed as the electrode is then pointing upwards. The transition current will then be larger because a larger magnetic pinch pressure is need to oppose the force of gravity, as well as the surface tension forces which tend to hold the droplet onto the wire.
In consideration of the above formulation, a small FORTRAN program was developed to calculate the transition current and droplet diameter for a range of solid wire MIG electrodes for different materials. Refer to Appendix C for the listing. Input data for the program includes material properties of the solid wire electrodes.

The results, for mild steel, obtained from the developed Fortran program are presented in Table 4.1 below. The results include the transition current and droplet diameter. The material considered for the experiments is mild steel and thereafter-future projects will include stainless steels and other metals that can be welded using the GMAW process.

It should be noted that these transition current results, obtained from the mathematical formulations of Haidar and Lowke [15] are independent of voltage setting, wire feed rate, shielding gas effects and welding speed. However, it correlates well with experimental results obtained by Simpson *et al* and Lesnewich for 1.2mm and 1.6mm diameter mild steel wire as noted in [15].

| MIG Wire Diameter (mm) | Transition Welding Current (Ampere) | Droplet Diameter at Transition (mm) |
|---|---|---|
| 0.8 | 237.8 | 0.785 |
| 0.9 | 251.6 | 0.879 |
| 1.0 | 264.5 | 0.971 |
| 1.1 | 276.5 | 1.06 |
| 1.2 | 287.8 | 1.15 |
| 1.3 | 298.5 | 1.24 |
| 1.4 | 308.5 | 1.32 |
| 1.5 | 317.9 | 1.40 |
| 1.6 | 326.7 | 1.48 |
| | | |

**Table 4.1** Fortran results for GMAW Transition Current and Droplet Diameter for mild steel

From Table 4.1, it can be seen that the droplet diameter is approximately equal to the wire diameter (slightly smaller), giving fair agreement to the developed theory for the transition zone between globular and spray transfer.

In chapter 6, the experimental results for transition current and droplet diameter for mild steel will be compared to the results in Table 4.1 and discussed. It will be shown that the effect of the shielding gas, which is neglected in the model, is significant. As will be shown (Table 6.13) differences of between 9 and 36% with the model.

It is envisaged that these results, together with the experiments that will be conducted with different shielding gases (ref. Chapter 6) will assist in the development of a comprehensive database to establish the relationship between transition current, electrode feed rate, welding speed and shielding gas composition. The completed database will serve as a guide to industry and researchers to pinpoint the transition zone and to select optimum welding parameters for good quality welds, especially for the welding of thin material in the spray metal transfer mode by optimum parameter selection.

The results of Haidar and Lowke [15] were obtained for arcs operating in pure Argon only, at various current settings, using the same diameter mild steel electrodes at constant feed rate for all experiments. As mentioned before, these results fail to give a holistic view of the effects of shielding gas mixture, voltage setting, wire diameter and feed rate on the transition current for different materials.

In chapter 5 the experimental set-up and procedures for the verification experiments will be outlined together with descriptions of the equipment involved.

# Chapter 5

## Experimental Set-Up and Procedure

### 5.1 Equipment Requirements

The experimental set-up used to obtain the results study included the following:

a) Migatronic BDH 400, inverter based Welding Machine

b) Migatronic InfoWeld PC-Software

c) Laser-Strobe Camera System

d) Windows based PixelView/TVMAX software package

e) Linear Tractor

f) Fixed GMA/MIG Torch Holder

Welding consumables include:

g) 300 x 100mm various thickness mild steel plates

h) 1mm MIG wire

i) Available Shielding gases that will be used include the following: Pure Argon, 99%Argon+1%Oxygen, 98%Argon+2%Oxygen and 98%Argon+2%Carbon Dioxide

### 5.2 Experimental Set-up

The schematic diagram shown in Figure 5.1 depicts the physical set-up shown in Figure 5.2 and Figure. 5.3

When the weld is performed, the plate to be welded moves on the tractor underneath the fixed BDH400 welding torch. The laser strobe sends laser radiation pulses into the weld arc, which is picked up by the high-speed camera and relayed, back to the laser strobe CPU. The image is then displayed on the screen.

During welding operations, the InfoWeld package documents and controls the welding operations of the BDH400 welding machine.

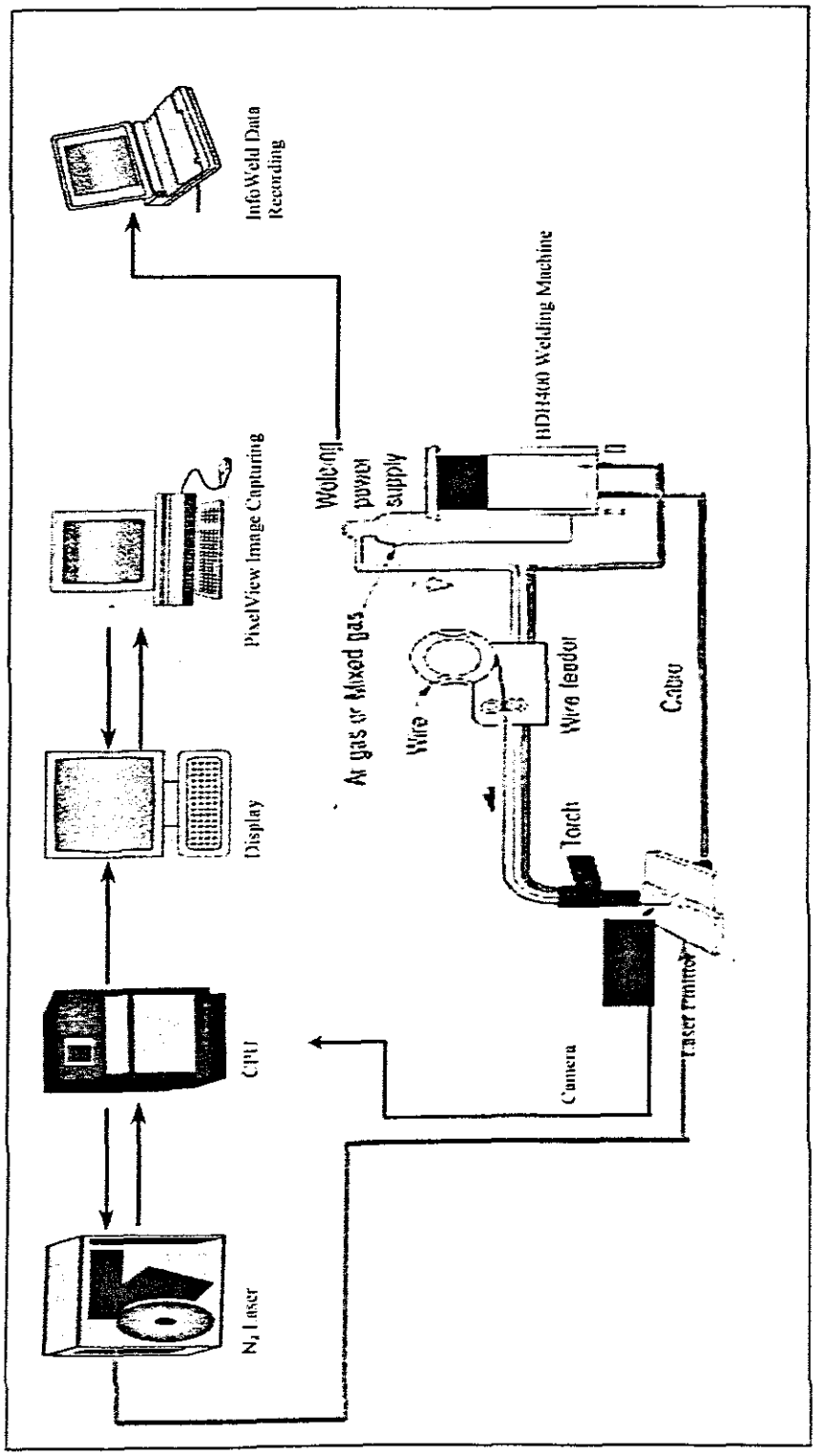


Figure 5.1 Schematic Layout of Welding Set-up

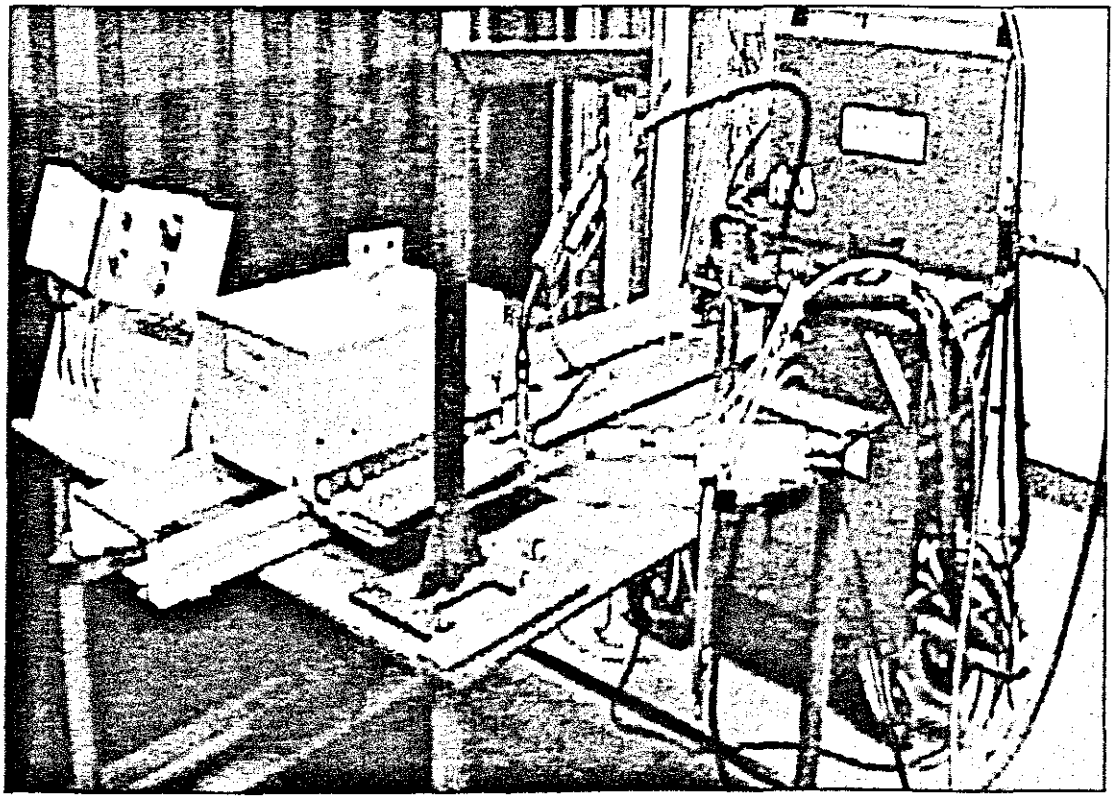

Fig. 5.2 Welding Set-up showing the Welding Torch, Linear Tractor, Laser Emitter and Camera, with the BDH400 welding machine in the background.

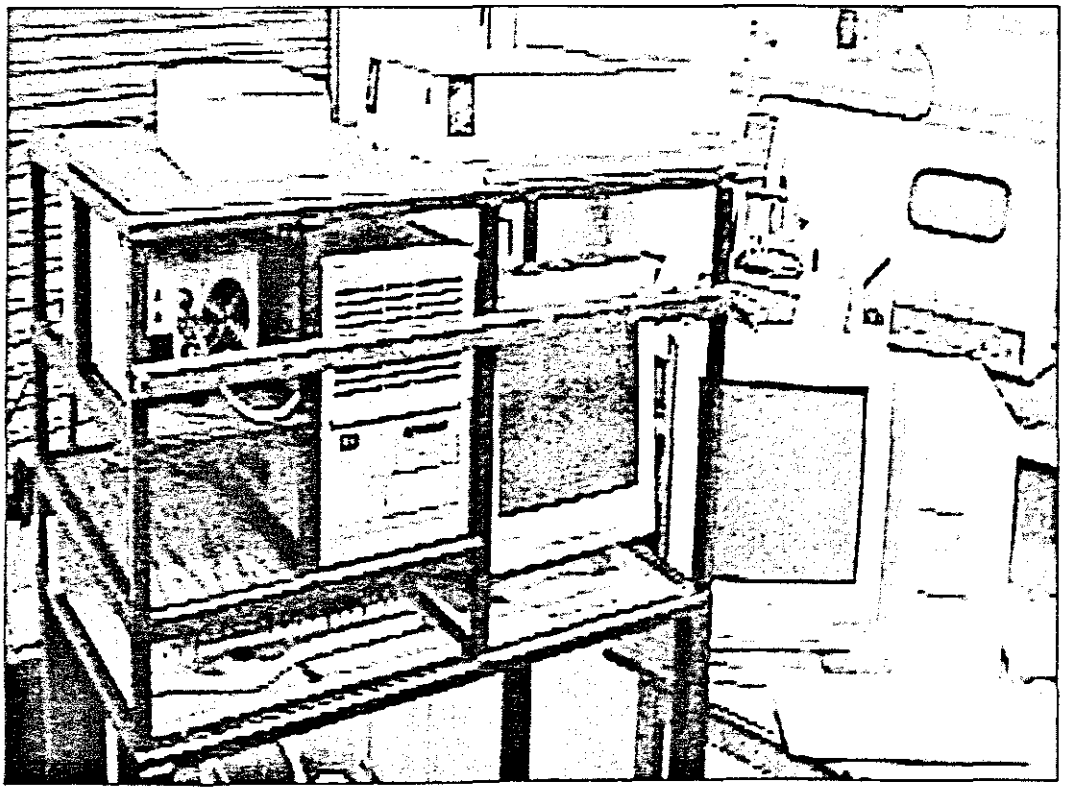

Fig. 5.3 LaserStrobe Camera System with $N_2$ Laser, CPU and Displays

## 5.3 Description of Equipment

### 5.3.1 The Migatronic BDH 400 welding machine

This is an inverter-based machine for MMA; TIG and MIG/MAG electrode welding equipped with a separate feed unit. The advantages of this machine are as follows:

- programmable welding properties and improved welding characteristics
- a reduction in power loss
- increased duty cycle
- reduced weight and size

The inverter, like all other components in the machine, is controlled by a central microprocessor, which makes it possible to achieve advanced welding control combined with straightforward operation and ease of use.

The design of the BDH is based to a large extent on modules, which have two advantages:

- great flexibility, enabling users to design the machine they need to meet their specific requirements.
- Ease of service, since repairs can be carried out simply replacing defective modules.

As mentioned before, the BDH is an ***inverter-based*** machine. That is, the power source (power module) is constructed in accordance with the switch-mode principle. The power module switches at 100kHz, which makes it one of the fastest inverters on the market to date. The principle involved is illustrated in Figure 5.4 below.

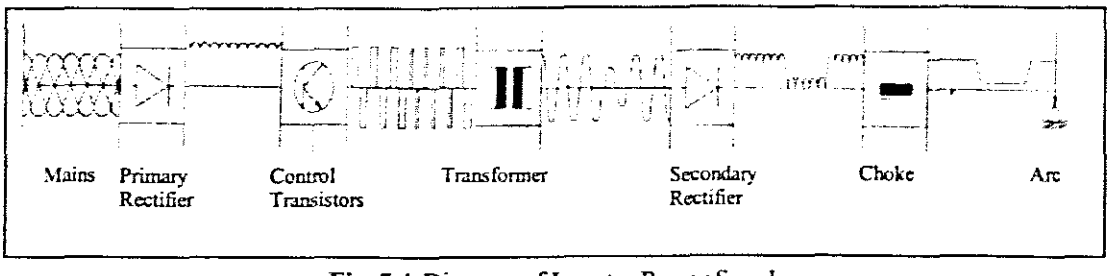


**Fig. 5.4** Diagram of Inverter Power Supply

The microprocessor is placed in the ***electronic box***, and forms part of a regulating loop in which measurement s of welding current and voltage are carried out. The current and voltage references are generated to the inverter based on these measurements, with a frequency of 10kHz. In addition to the regulation of welding current and welding voltage, the microprocessor deals with all control and collection of data from modules in the welding machine. It also provides communication with the user via the front of the electronic box and operation using either the torch or remote control.

The ***wire feed*** system is used in Mig/Mag welding, and can be situated as a separate feed unit (STB and Triple) on the machine. The wire feed unit can be fitted with either two or four –wheel drive. Four wheel drive is recommended for many or fluxcored wire used. It also important to use wire feed rolls that fit the dimensions of the wire,

and that the liners used in the torch hose are of the correct diameter and material to suit the type of welding wire in question.

The ***HF module*** consists of a HF box and a coil. The HF module is used to initiate the arc during TIG welding.

The ***water module*** consists of a water tank, a water cooler, a water pump, a filter and a flow control. The flow control system indicates a water cooling error if the cooling water flow is either insufficient or absent altogether.

### 5.3.2 The Migatronic InfoWeld PC-software

The Migatronic InfoWeld PC-software is designed to enhance the operation of Commander BDH400 welding machine in the areas of documentation and control of welding jobs. The only special hardware needed to run the system is the fibre optical cable supplied with the software.

#### 5.3.2.1 Main Features

The main part of the system concerns documentation and control of welding jobs. Documentation is recorded for individual seams in the form of:

- Curves for the main parameters
- The setting of the welding machine and
- Accumulated statistics and mean values.

The documentation for seams are logically grouped into jobs defined by the user. Each job can contain up to ten machine settings and an unlimited number of seam recordings. A simple form of job control is provided by the ability to define in advance what welding machine settings must be used while making recordings with the job.

The use of the job can be further restricted by having the PC control, the Amp setting of the welding machine. The Amp control is defined as a curve, that the welding machine is forced into following while welding.

The documentation recorded can be reviewed on the screen of the PC or printed on paper. The documentation collected in a job is first stored on the hard disk of the PC, but can later be transferred to diskettes or other types of back-up units.

Two subprograms will let the user monitor the settings of the welding machine. One displays the complete setting of the machine on a single screen, and the other gives a graphical overview of the main parameters.
The control box of every BDH shipped keeps a log of how the welding machine has performed throughout its entire lifetime. These statistics of use and errors can be transferred to the PC for viewing and printing.

### 5.3.2.2 Hardware of the PC system

The program is MS-DOS based and runs on standard PC hardware. The only requirement is that the video adapter must be capable of displaying graphics in the VGA mode.
The recommended minimum configuration is a system based on a 16MHz processor with 640Kbyte hard disk. The performance will benefit from a faster and bigger system.

### 5.3.3 LaserStrobe Camera System

LaserStrobe gives unique insight into high-temperature/high-luminosity industrial processes. When used in thermal spray processes, details of the molten spray, flow characteristics of the feed material, and coating build up on the substrate can be seen without the plasma or arc affecting the image quality. Detailed images are produced in real time unlike high frame rate video camera systems.

LaserStrobe's lightweight camera sensor is sensitive only to the laser illumination provided by the LaserStrobe system. The high-resolution camera provides very fine detail of the field of interest being viewed. In depth cause and effect studies of a process and its parameters is possible in real-time. Using the variable shutter feature, the operator has full exposure control to see some, or none, of the process incandescence, allowing the study of plasma characteristics or flame behaviour.

The software-driven camera controller allows on-board image processing and particle image velocity measurements. A convenient pseudo colour feature allows details of the image to be revealed, normally hidden by grey-scale systems. The camera system can be internally or externally triggered, allowing programmable capture of important timing windows during the entire viewing process. The system has multiple output ports for the imagery: SVGA, s-video, and RS-170. The camera system also features nanosecond electronic shuttering eliminating motion-induced blur when viewing ballistics or other high-speed events.

In the early 1980's Control Vision designed the LaserStrobe for viewing electric arc welding. Since patenting and commercialising the technology in 1986, LaserStrobe has attained wide acceptance within both the welding and thermal spray research and development communities, world-wide.

The LaserStrobe uses an intense laser pulse to create the video image while ignoring the brightness coming from the process (such as the plasma in plasma spray). The sensor is essentially blind to the radiation coming from the process. The five-nanosecond laser pulse also freezes powder particles in flight. In order to perform velocity measurements, two lasers are used to create double-exposed images of the particles. Measuring the distance that the particles have travelled and knowing the time between laser pulses, velocity is obtained.

The LaserStrobe system incorporates a specialised camera head, one or two compact pulsed nitrogen lasers, for illumination, and a computerised controller unit. A LaserStrobe system includes everything needed to operate the equipment and make video; essentially LaserStrobe is a "turn-key" arrangement. All systems include an

optics package with each camera head. This optics package provides users with a variety of magnifications and close-up optics with varying stand-off distances to accommodate research needs. Every nitrogen laser includes a fibre optic cable, which is used to deliver the laser illumination to the specific welding arc area being viewed.

### 5.3.4 PIXELVIEW / Zoltrix TV MAX software packages

The PixelView package is used for motion video as well as still image capturing of the welding process. From these images, measurements such as droplet size, deposition rate, mode of metal transfer and effects of shielding gas compositions on metal transfer can be obtained or viewed.

### 5.3.5 Linear Tractor

The straight-line cutter/ linear tractor used for the experiments was designed and built by [9], towards a BTech. Degree in Mechanical Engineering in 1998.

The linear tractor travels on a 1.6m long twin guide-rail track. It is a heavy-duty design with a 4mm thick carriage housing to protect the internal parts from spatter and excessive heat from the welding or cutting operation. Propulsion is provided by a 0.37kW, 38Nm worm geared motor, known as a spiroplan gear unit. This is a high torque drive unit designed to provide quiet operation and minimum wear components.

The forward/reverse control unit is a compact frequency inverter type U120 micro inverter of Mitsubishi Electric. The inverter provides variable speed in alternating current (ac) motors by providing the variable voltage and frequency needed to achieve variable speed. The geared motor operates at the design speed of 50Hz. If the frequency decreases, the speed will decrease without the torque decreasing. The acceleration and deceleration time can also be varied through the inverter.

The reason for the usage of this linear tractor is due to its robust heat and spatter resistant features. Machine features also include:
- A built-in keypad for simple direct input/operation
- Forward/reverse selection with simple contacts
- Torque boost for difficult to start loads, (the tractor transports the 300 × 100 × 12 mild steel plates).
- Adjustable stall prevention
- Built-in thermal overload for the motor
- Built-in dc injection braking for positive load stopping at the end of a weld run.

For these experiments, the torch holder was replaced with a horizontal 400 × 150mm specimen table for continuous/automatic welding with a fixed stationary welding torch from the BDH400 welding machine. The specimen table was designed to bolt directly to the existing 11mm diameter holes attaching the bearing supports to the carriage housing. Figure 5.5 below depicts the tractor with the specimen table attached.

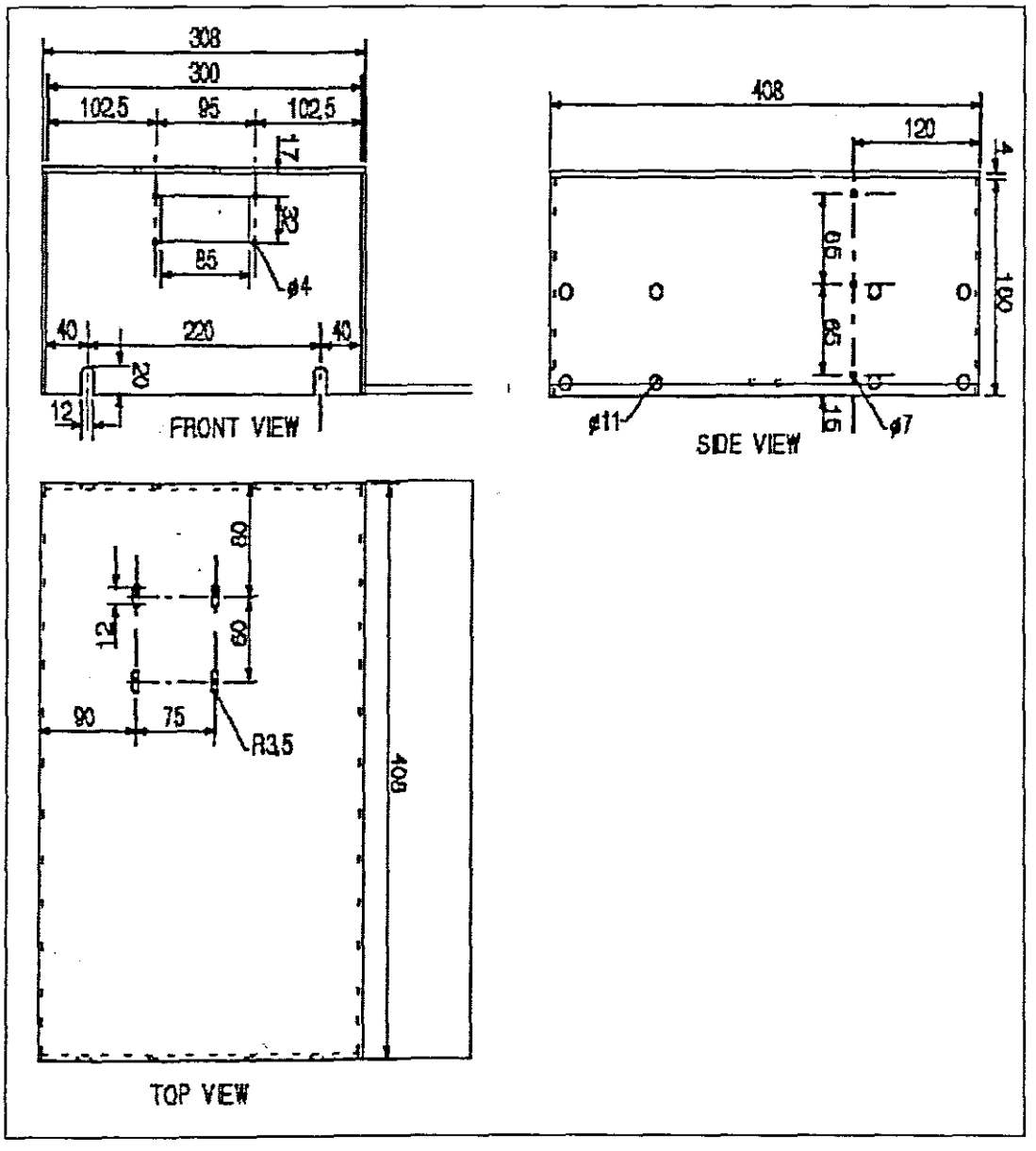


Fig. 5.5 Linear Tractor Carriage Housing Modification

## 5.4 Experimental Procedure

For the first set of experiments, bead-on-plate welds were prepared on mild steel 300× 100× 12mm, using Spec. Argon as a shielding gas. A 1mm diameter ER70S-6 electrode was used. Welding parameters were varied between 150 and 280A and 25V to 30V. The contact distance between the shielding gas cup and the workpiece was set at 18mm. At each combination of current and voltage, the welding arc and droplet transfer was recorded using the equipment as per experimental set-up.

A second set of experiments was made using 99%Ar-1%$O_2$ shielding gas. The same range of parameters as those for the first experiments was used. This was followed by a third set of experiments using 98%Ar-2%$O_2$ shielding gas. These sets of experiments were conducted to ascertain the effects of additions of oxygen to argon shielding gases on the transition current from the globular- to the spray transfer mode.

A fourth set of experiments was conducted using the same parameters as for the previous sets, but using 98%Ar-2%$CO_2$ shielding gas instead. This was done to study the effects that carbon dioxide additions to argon have on the transition current.

The results of the above are presented graphically and in table format and analysed in chapter 6.

# Chapter 6

## Experimental Results and Analysis

---

### 6.1 Modeling of Data

The curve fitting and plotting of the data in Table 6.1 was done using the **'WFit'** and **'WPlot'** programs. The 'WFit' (Non-linear Curve Fitter) program uses Marquardt's algorithm to find values of parameters that make an equation fit a set of data points in a least squares sense. 'WPlot' is used to plot the fit.

### 6.1.1 The Marquardt Algorithm for Numerical Computing

The Levenberg-Marquardt method (also known as the Marquardt method) of numerical computing is an efficient, elegant and practical method related to an earlier suggestion of Levenberg, for varying smoothly between the extremes of the inverse Hessian method and steepest descend method [50]. The Marquardt method works very well in practice and has become the standard of non-linear least squares routines. This algorithm is based on an elementary but important insight, i.e. The components of the Hessian matrix, even if they are not usable in any precise fashion, give some indication about the order of magnitude scale of the problem. The basic approach of this algorithm can be summarized as follows:

1. Choose or design a merit function that measures the agreement between the data and the model with a particular choice of parameters.
2. The parameters of the model are then adjusted to achieve a minimum in the merit function, yielding 'best-fit parameters'.
3. The fitting procedure then provides an error estimation on the parameters
4. A statistical measure or test of the 'goodness of fit' (i.e. assess whether the model is appropriate or not) is then carried out.
5. When point 4 suggests that the model is an unlikely match to the data then points 1-3 needs revising.

The Levenberg-Marquardt algorithm can be implemented as a model-trust region method for minimization applied to the special case of a least squares function.

The equation used to fit the data can be non-linear with respect to the parameters. The algorithm requires an initial estimate of the value of each parameter; it then uses an iterative process to find new values of the parameters that give a better fit. Commands are used to read the data from a file (or keyboard), specify the number of parameters, specify initial estimates of the parameters, specify the equation that is to be fit to the data, find the best fit and plot the fit.

'WPlot' is a 32-bit Windows program that plots two- and three-dimensional plots with linear or log axes with automatic or manual scaling. Up to 250 sets of data can be plotted on the same two-dimensional using either one or two vertical axis. There can be up to 131072 data points per data set. Each data set can be plotted as a line plot, a smooth curve plot, a scatter plot, a step plot or a histogram. Multiple data sets can also

be plotted as a three-dimensional plot. Data can be fit by a smooth curve, least squares polynomial or exponential. 'WPlot' can be controlled from a graphic user interface (GUI) or a command. Two-dimensional plots can also have cumulative normal probability axes, error bars and descending as well as ascending axes. The 'WFit' program was originally written for DOS. It was compiled as a windows program so that it could use the 'WPlot' program to do the plotting, but it does however, not have a true Windows menu interface, as is found with the 'WPlot' program.

## 6.2 Experimental Results

Table 6.1 below depicts the experimental results obtained for mild steel welded with **Pure Argon shielding gas**. All calculations are based upon the properties for mild steel as indicated in Appendix D. With the InfoWeld software, the wire speed, actual corrected voltages and machine voltages were obtained. The Laserstrobe was used to obtain the droplet frequency and PixelView/TVMAX imaging for the droplet diameter as per Appendix E1.

| Exp. No | Wire Speed m/min | Welding Current A | Corrected Voltage V | Machine Voltage V | Droplet Freq. Hz | Drop ϕ Diameter mm | Welding Speed mm/s |
|---|---|---|---|---|---|---|---|
| 1 | 10,0 | 187 | 24,3 | 25 | 2,69 | 2,335 | 4 |
| 2 | 10,5 | 189 | 24,3 | 25 | 2,71 | 2,313 | 4 |
| 3 | 11,0 | 194 | 24,6 | 25 | 2,74 | 2,234 | 4 |
| 4 | 11,5 | 198 | 24,9 | 25 | 2,76 | 2,152 | 4 |
| 5 | 12,0 | 202 | 24,2 | 25 | 2,90 | 2,187 | 4 |
| 6 | 12,5 | 203 | 24,5 | 25 | 3,04 | 2,251 | 4 |
| 7 | 13,0 | 205 | 24,1 | 25 | 3,73 | 2,091 | 4 |
| 8 | 13,5 | 206 | 24,4 | 25 | 3,90 | 2,433 | 4 |
| 9 | 14,0 | 212 | 24,1 | 25 | 4,17 | 2,136 | 4 |
| 10 | 14,5 | 217 | 24,2 | 25 | 4,36 | 1,422 | 4 |
| 11 | 15,0 | 216 | 24,0 | 25 | 4,24 | 1,706 | 4 |
| 12 | 15,5 | 220 | 23,9 | 25 | 4,09 | 1,489 | 4 |
| 13 | 16,0 | 221 | 23,9 | 25 | 3,90 | 1,256 | 4 |
| 14 | 16,5 | 222 | 23,9 | 25 | 3,85 | 1,121 | 4 |
| 15 | 16,6 | 224 | 24,2 | 25 | 17,5 | 1,001 | 4 |
| 16 | 16,7 | 226 | 24,3 | 25 | 27,30 | 1,00 | 4 |
| 17 | 16,8 | 227 | 24,3 | 25 | 54,00 | 0,973 | 4 |
| 18 | 16,9 | 230 | 24,5 | 25 | 79,34 | 0,955 | 4 |
| 19 | 17,0 | 229 | 24,4 | 25 | 84,80 | 0,870 | 4 |
| 20 | 17,0 | 228 | 24,0 | 25 | 83,57 | 0,889 | 4 |
| 21 | 17,5 | 231 | 23,9 | 25 | 85,45 | 0,767 | 4 |
| 22 | 18,0 | 237 | 23,9 | 25 | 85,69 | 0,683 | 4 |
| 23 | 18,5 | 234 | 24,1 | 25 | 85,96 | 0,567 | 4 |
| 24 | 19,0 | 238 | 24,1 | 25 | 86,70 | 0,731 | 4 |
| 25 | 20,0 | 245 | 24,1 | 25 | 87,74 | 0,723 | 4 |
| 26 | 22,0 | 258 | 24,0 | 25 | 86,76 | 0,731 | 4 |
| 27 | 22,0 | 260 | 24,3 | 25 | 87,74 | 0,730 | 4 |
| 28 | 24,0 | 265 | 24,4 | 25 | 87,93 | 0,654 | 4 |

**Table 6.1** Experimental Results for Argon shielding gas on mild steel

Using the WPlot program, the following graphs for welding current vs. droplet frequency and welding current vs. droplet diameter were plotted. These graphs, when plotted on the same horizontal current axis, yielded an intersection which represents the globular-to-spray metal transfer transition point for a 1mm diameter mild steel electrode welded with Argon shielding gas. Refer to Figures 6.1 to 6.3.

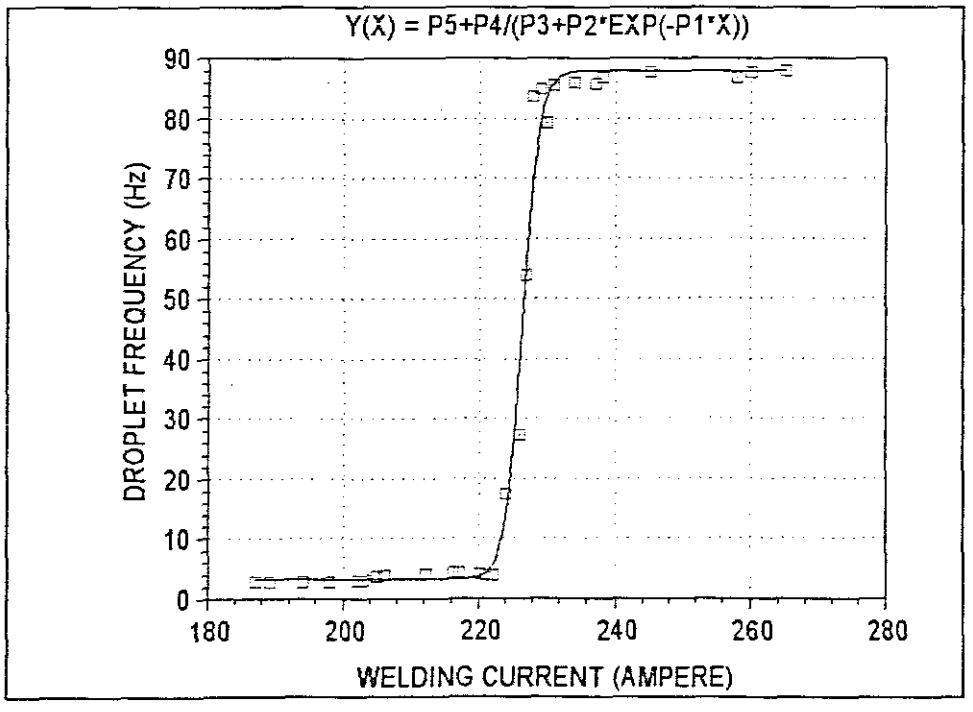


**Fig. 6.1** Welding Current vs. Droplet Frequency

| | |
|---|---|
| Coefficient of Determination | 0.99124 |
| Residual Variance | |
| Number of Iterations | 127 |
| | |
| **Parameters** | **Values** |
| P1 | 0.810691 |
| P2 | 7.70455E+78 |
| P3 | 0.148956 |
| P4 | 12.619 |
| P5 | 3.20191 |

**Table 6.2** WFit Output Data for Figure 6.1

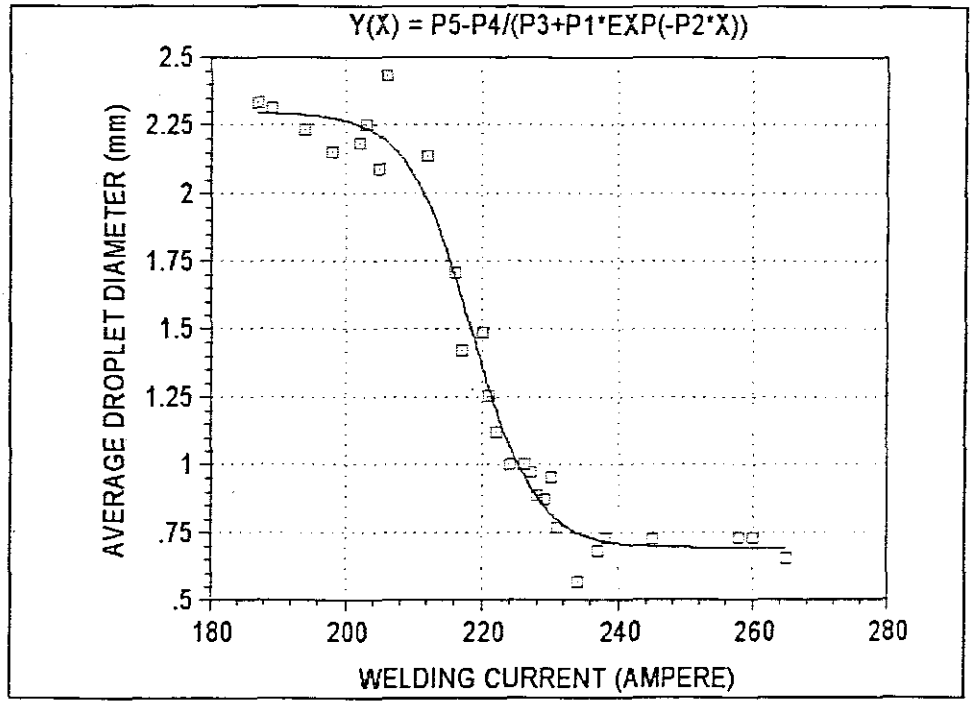


**Fig 6.2** Welding Current vs. Average Droplet Diameter

| | |
|---|---|
| Coefficient of Determination | 0.989243 |
| Residual Variance | |
| Number of Iterations | 142 |
| | |
| **Parameters** | **Values** |
| P1 | 8.62896E+19 |
| P2 | 0.213368 |
| P3 | 0.494412 |
| P4 | 0.7931 |
| P5 | 2.29584 |

**Table 6.3** WFit Output Data for Figure 6.2

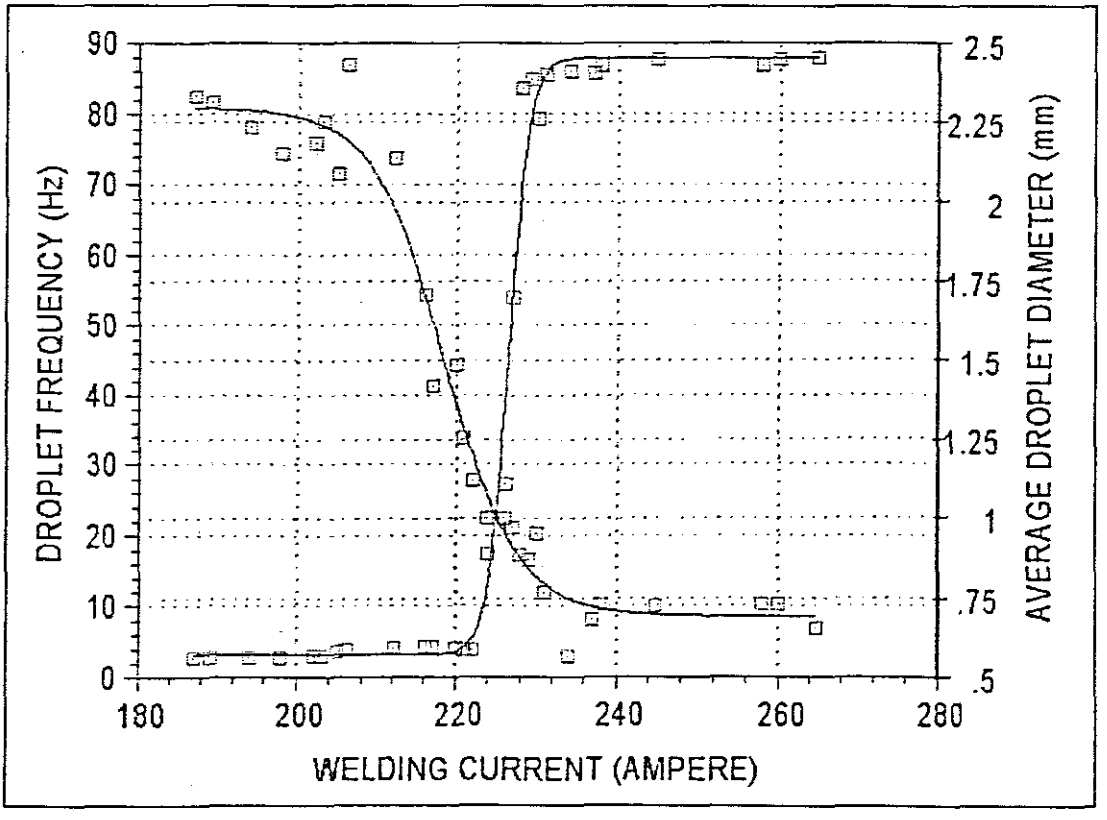


**Fig 6.3** Welding Current vs. Droplet Frequency and Average Droplet Diameter

Table 6.4 below depicts experimental values obtained for mild steel GMA welded with a 99%Argon-1%Oxygen shielding gas.

| Exp. No | Wire Speed m/min | Welding Current A | Corrected Voltage V | Machine Voltage V | Droplet Freq. Hz | Droplet Diameter mm | Welding Speed mm/s |
|---|---|---|---|---|---|---|---|
| 1 | 10 | 176 | 23.7 | 25 | 2.06 | 1.405 | 4 |
| 2 | 11 | 185 | 23.6 | 25 | 3.06 | 1.388 | 4 |
| 3 | 11.5 | 191 | 23.6 | 25 | 3.96 | 1.370 | 4 |
| 4 | 12 | 194 | 23.5 | 25 | 4.96 | 1.301 | 4 |
| 5 | 12.5 | 198 | 23.5 | 25 | 4.86 | 1.225 | 4 |
| 6 | 13 | 201 | 23.5 | 25 | 6.46 | 1.080 | 4 |
| 7 | 13.5 | 205 | 23.5 | 25 | 6.46 | 1.059 | 4 |
| 8 | 14 | 207 | 23.4 | 25 | 7.56 | 1.047 | 4 |
| 9 | 14.5 | 213 | 23.3 | 25 | 8.66 | 1.018 | 4 |
| 10 | 15 | 219 | 23.4 | 25 | 9.66 | 1.040 | 4 |
| 11 | 15.5 | 222 | 23.3 | 25 | 10.36 | 1.037 | 4 |
| 12 | 16 | 227 | 23.3 | 25 | 14.86 | 1.035 | 4 |
| 13 | 16.5 | 231 | 23.3 | 25 | 18.36 | 1.005 | 4 |
| 14 | 17 | 231 | 23.2 | 25 | 21.76 | 1.005 | 4 |
| 15 | 17.5 | 235 | 23.2 | 25 | 27.86 | 1.000 | 4 |
| 16 | 18 | 240 | 23.2 | 25 | 58.46 | 1.003 | 4 |
| 17 | 18.5 | 242 | 23.1 | 25 | 57.16 | 0.993 | 4 |
| 18 | 19 | 247 | 23.1 | 25 | 57.56 | 0.988 | 4 |
| 19 | 19.5 | 251 | 23.1 | 25 | 57.16 | 0.988 | 4 |
| 20 | 20 | 254 | 23.2 | 25 | 57.76 | 0.975 | 4 |

**Table 6.4** Experimental Results for Ar99%-$O_2$1% shielding gas on mild steel

The resulting WFit and WPlot results are shown below in Figures 6.4 – 6.6. The images from the AVI files are found in Appendix E2.

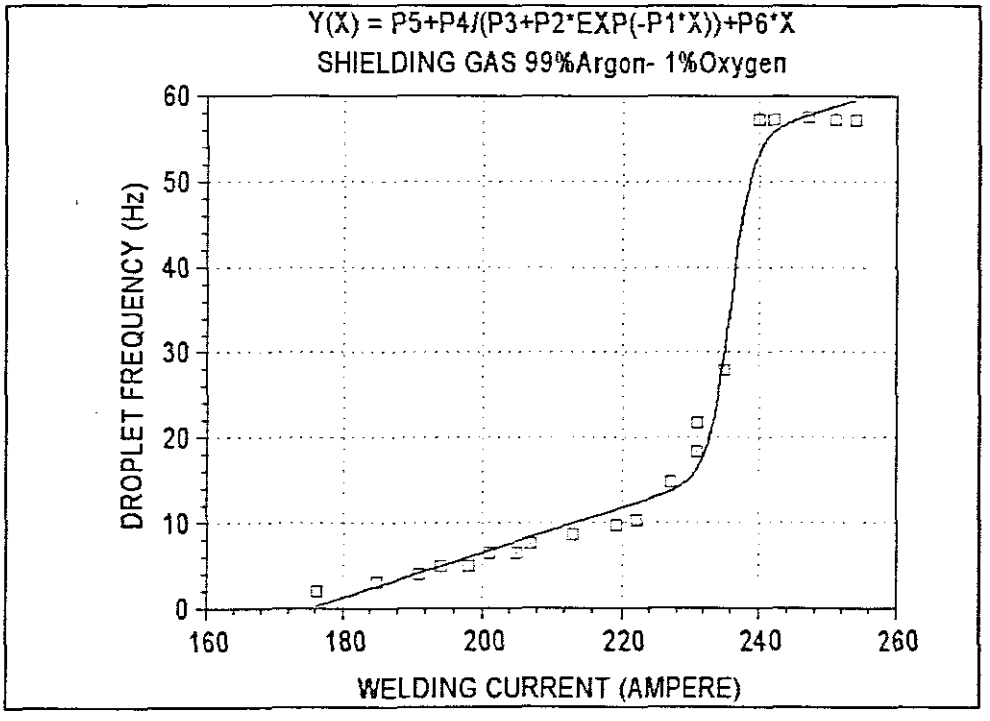


**Table 6.4** Welding Current vs. Droplet Frequency

| | |
|---|---|
| Coefficient of Determination | 0.99114 |
| Residual Variance | 5.7776 |
| Number of Iterations | 26 |
| | |
| **Parameters** | **Values** |
| P1 | 0.63952 |
| P2 | -5.4965E+63 |
| P3 | -0.017634 |
| P4 | -0.68581 |
| P5 | -45.958 |
| P6 | 0.26252 |

**Table 6.5** WFit Output Data for Figure 6.4

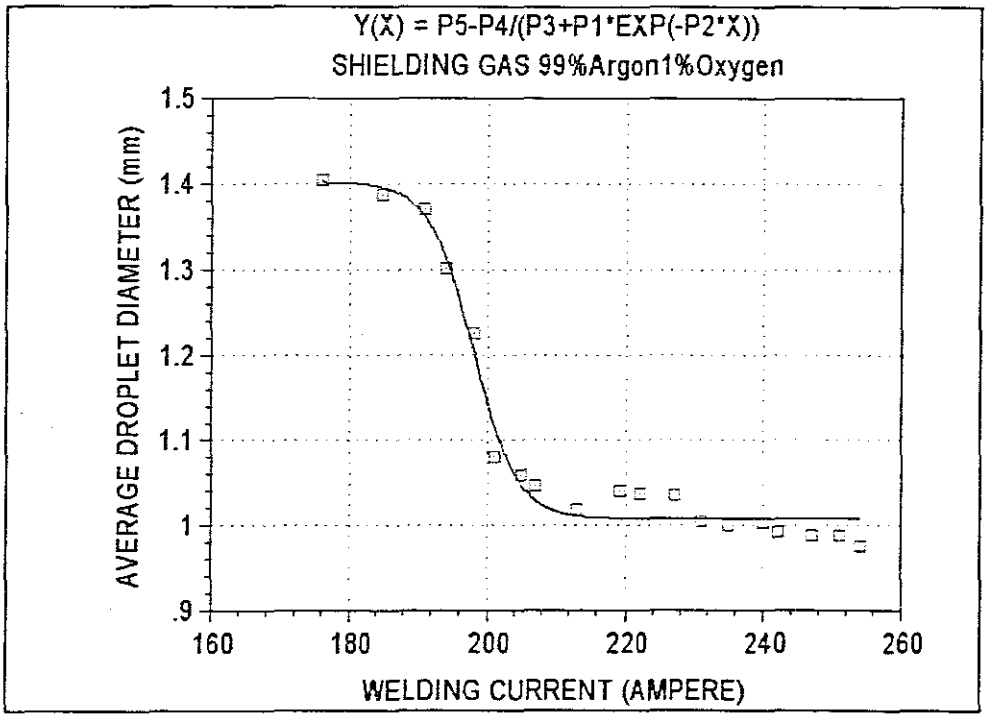


**Fig. 6.5** Welding Current vs. Average Droplet Diameter

| | |
|---|---|
| Coefficient of Determination | 0.98234 |
| Residual Variance | 0.00049206 |
| Number of Iterations | 139 |
| | |
| **Parameters** | **Values** |
| P1 | 5.1329E+26 |
| P2 | 0.31186 |
| P3 | 0.81786 |
| P4 | 0.32274 |
| P5 | 1.4026 |

**Table 6.6** WFit Output Data for Figure 6.5

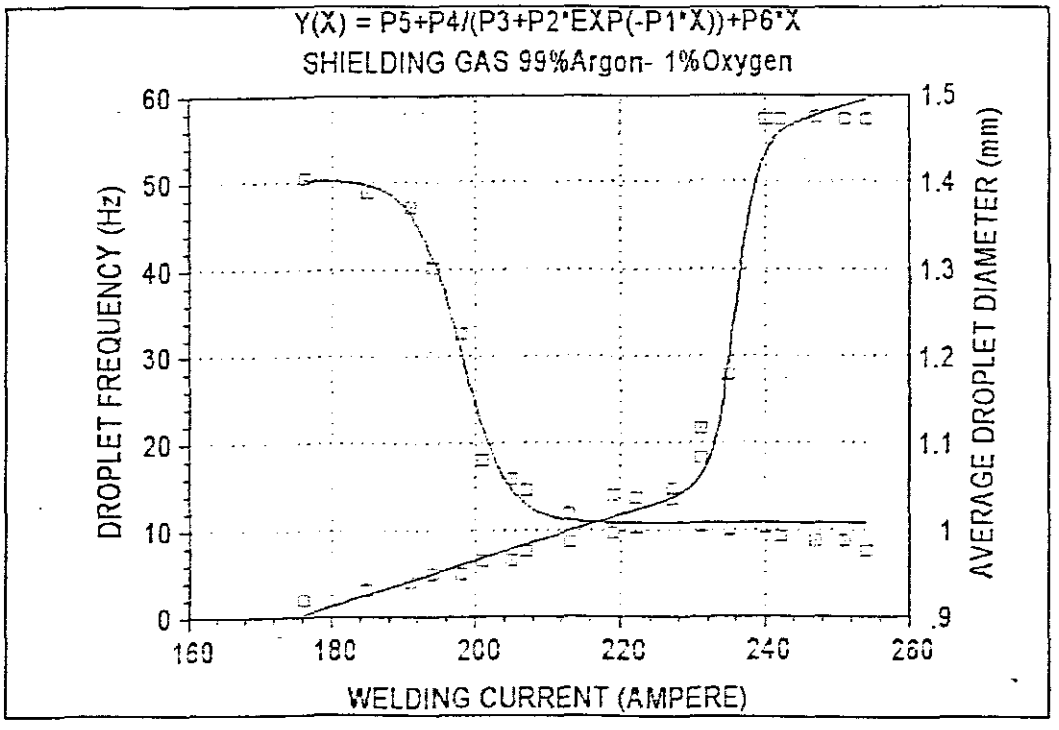


**Fig. 6.6** Welding Current vs. Droplet Frequency and Average Droplet Diameter

Table 6.7 below depicts experimental values obtained for mild steel GMA welded with a 98%Argon-2%Oxygen shielding gas.

| Exp. No | Wire Speed m/min | Welding Current A | Corrected Voltage V | Machine Voltage V | Droplet Freq. Hz | Droplet Diameter mm | Welding Speed mm/s |
|---|---|---|---|---|---|---|---|
| 1 | 5 | 124 | 24.1 | 25 | 2.00 | 1.662 | 4 |
| 2 | 6 | 132 | 24.0 | 25 | 3.52 | 1.653 | 4 |
| 3 | 7 | 150 | 24.2 | 25 | 6.79 | 1.670 | 4 |
| 4 | 7.5 | 156 | 23.8 | 25 | 7.00 | 1.645 | 4 |
| 5 | 8 | 174 | 23.9 | 25 | 43.90 | 1.640 | 4 |
| 6 | 8.5 | 182 | 23.7 | 25 | 50.90 | 1.240 | 4 |
| 7 | 9 | 185 | 23.6 | 25 | 57.91 | 1.425 | 4 |
| 8 | 10 | 181 | 23.9 | 25 | 58.90 | 1.500 | 4 |
| 9 | 11 | 186 | 23.3 | 25 | 58.94 | 1.175 | 4 |
| 10 | 11.5 | 199 | 23.7 | 25 | 86.90 | 1.212 | 4 |
| 11 | 12 | 200 | 23.5 | 25 | 88.50 | 1.210 | 4 |
| 12 | 12.5 | 211 | 23.4 | 25 | 98.80 | 1.198 | 4 |
| 13 | 13 | 212 | 23.3 | 25 | 108.70 | 1.154 | 4 |
| 14 | 14 | 214 | 23.4 | 25 | 112.80 | 1.129 | 4 |
| 15 | 15 | 218 | 23.3 | 25 | 115.00 | 1.016 | 4 |
| 16 | 16 | 220 | 23.2 | 25 | 119.08 | 1.075 | 4 |
| 17 | 17 | 220 | 23.3 | 25 | 122.30 | 1.069 | 4 |
| 18 | 18 | 241 | 23.3 | 25 | 131.33 | 0.746 | 4 |
| 19 | 19 | 248 | 23.3 | 25 | 131.92 | 0.870 | 4 |
| 20 | 20 | 257 | 23.1 | 25 | 133.19 | 0.888 | 4 |
| 21 | 22 | 265 | 23.0 | 25 | 135.20 | 0.776 | 4 |
| 22 | 24 | 269 | 23.1 | 25 | 135.50 | 0.772 | 4 |

**Table 6.7** Experimental Results for 98%Ar-2%$O_2$ shielding gas on mild steel

The resulting WFit and WPlot results are shown below in Figures 6.7 – 6.9. The images from the AVI files are found in Appendix E3.

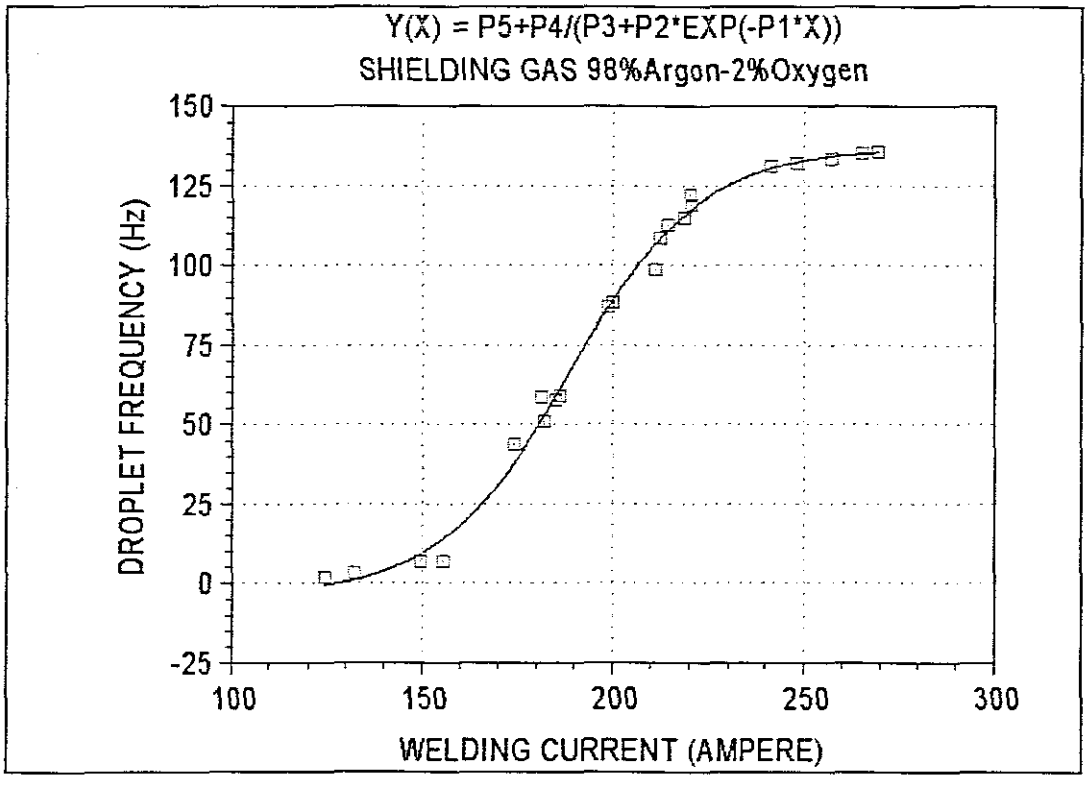


**Fig. 6.7** Welding Current vs. Droplet Frequency

| | |
|---|---|
| Coefficient of Determination | 0.99412 |
| Residual Variance | 16.334 |
| Number of Iterations | 2 |
| | |
| **Parameters** | **Values** |
| P1 | 0.058659 |
| P2 | 64458 |
| P3 | 1.0132 |
| P4 | 142.17 |
| P5 | -3.6463 |

**Table 6.8** WFit Output Data for Figure 6.7

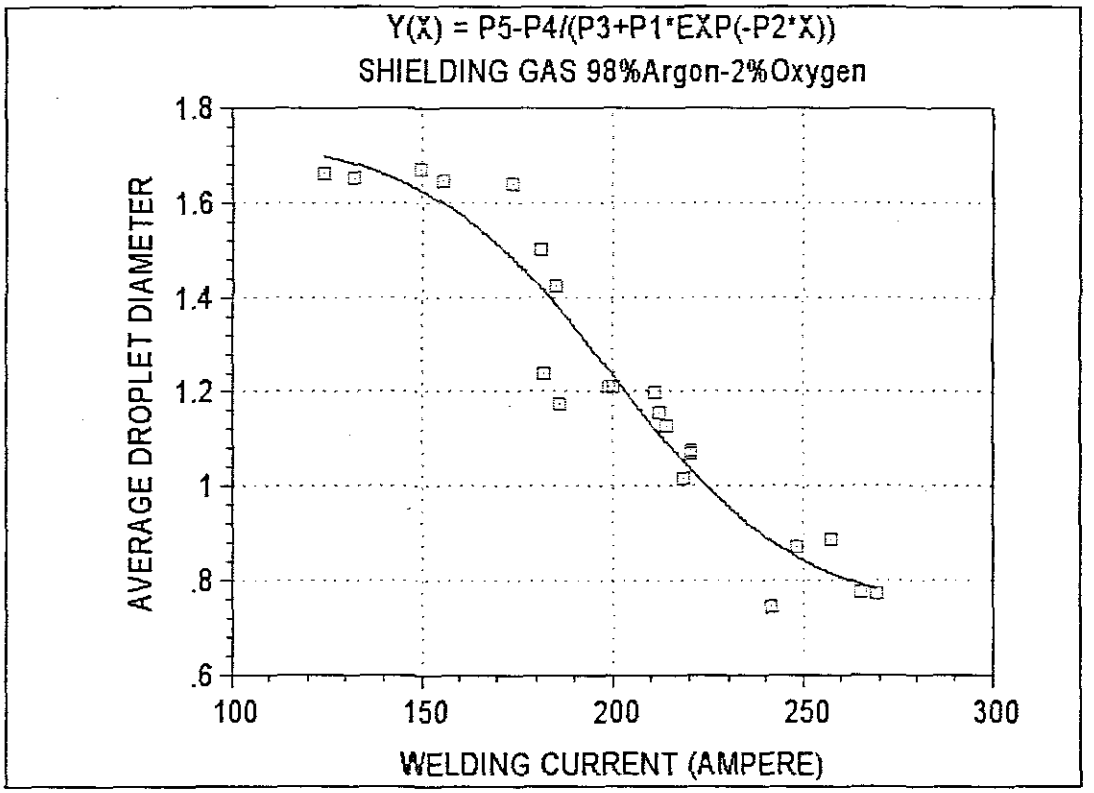


**Fig. 6.8** Welding Current vs. Average Droplet Diameter

| | |
|---|---|
| Coefficient of Determination | 0.92593 |
| Residual Variance | 0.0087956 |
| Number of Iterations | 2 |
| | |
| **Parameters** | **Values** |
| P1 | 7050.3 |
| P2 | 0.040699 |
| P3 | 2.0779 |
| P4 | 2.1191 |
| P5 | 1.7448 |

**Table 6.9** WFit Output Data for Figure 6.8

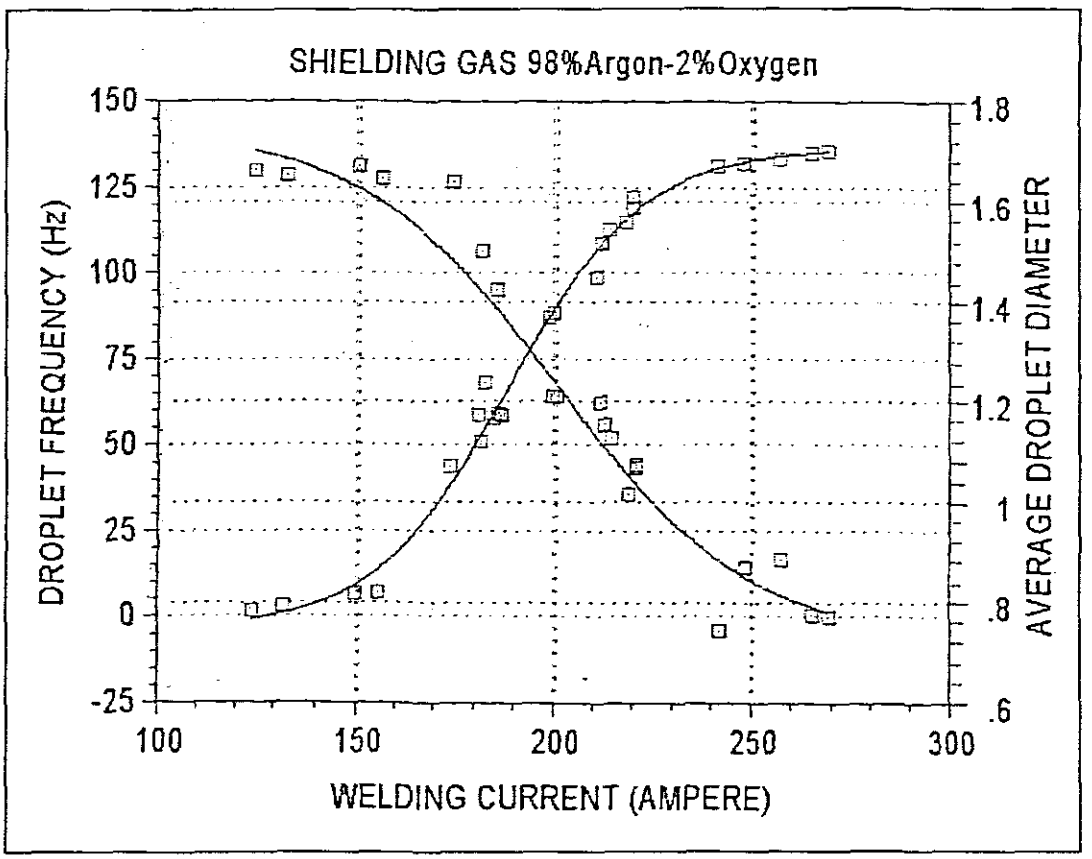


**Fig. 6.9** Welding Current vs. Droplet Frequency and Average Droplet Diameter

Table 6.10 below depicts the experimental results obtained for mild steel welded with 98%Ar-2%$CO_2$ shielding gas.

| Exp. No | Wire Speed m/min | Welding Current A | Corrected Voltage V | Machine Voltage V | Droplet Freq. Hz | Drop ϕ Diameter mm | Welding Speed mm/s |
|---|---|---|---|---|---|---|---|
| 1 | 10.0 | 197 | 24.4 | 25 | 2.59 | 2.402 | 4 |
| 2 | 10.5 | 199 | 24.8 | 25 | 2.69 | 2.370 | 4 |
| 3 | 11.0 | 205 | 24.5 | 25 | 2.69 | 2.325 | 4 |
| 4 | 11.5 | 208 | 24.3 | 25 | 2.70 | 2.249 | 4 |
| 5 | 12.0 | 211 | 24.6 | 25 | 2.78 | 2.197 | 4 |
| 6 | 12.5 | 213 | 24.2 | 25 | 2.71 | 2.150 | 4 |
| 7 | 13.0 | 215 | 24.1 | 25 | 2.93 | 2.010 | 4 |
| 8 | 13.5 | 218 | 24.1 | 25 | 2.99 | 2.001 | 4 |
| 9 | 14.0 | 220 | 24.3 | 25 | 3.68 | 1.948 | 4 |
| 10 | 14.5 | 225 | 24.0 | 25 | 3.73 | 1.849 | 4 |
| 11 | 15.0 | 226 | 24.1 | 25 | 4.01 | 1.752 | 4 |
| 12 | 15.5 | 230 | 23.9 | 25 | 3.85 | 1.750 | 4 |
| 13 | 16.0 | 231 | 23.9 | 25 | 3.79 | 1.741 | 4 |
| 14 | 16.5 | 233 | 23.7 | 25 | 12.77 | 1.660 | 4 |
| 15 | 17.0 | 236 | 23.8 | 25 | 14.05 | 1.550 | 4 |
| 16 | 17.5 | 239 | 23.6 | 25 | 13.89 | 1.501 | 4 |
| 17 | 18.0 | 241 | 23.2 | 25 | 14.88 | 1.455 | 4 |
| 18 | 18.5 | 240 | 23.0 | 25 | 19.78 | 1.500 | 4 |
| 19 | 19.0 | 244 | 23.3 | 25 | 27.71 | 1.405 | 4 |
| 20 | 19.5 | 249 | 22.9 | 25 | 31.00 | 1.351 | 4 |
| 21 | 20.0 | 251 | 23.5 | 25 | 33.80 | 1.259 | 4 |
| 22 | 20.5 | 254 | 23.2 | 25 | 34.59 | 1.250 | 4 |
| 23 | 21.0 | 256 | 23.2 | 25 | 36.30 | 1.105 | 4 |
| 24 | 22.0 | 260 | 23.2 | 25 | 40.91 | 1.075 | 4 |
| 25 | 23.0 | 272 | 23.4 | 25 | 43.01 | 0.998 | 4 |
| 26 | 24.0 | 275 | 23.0 | 25 | 44.32 | 0.980 | 4 |

**Table 6.10** Experimental Results for 98%Ar-2%$CO_2$ shielding gas on mild steel

The resulting WFit and WPlot results are shown below in Figures 6.10 – 6.12. The images from the AVI files are found in Appendix E4.

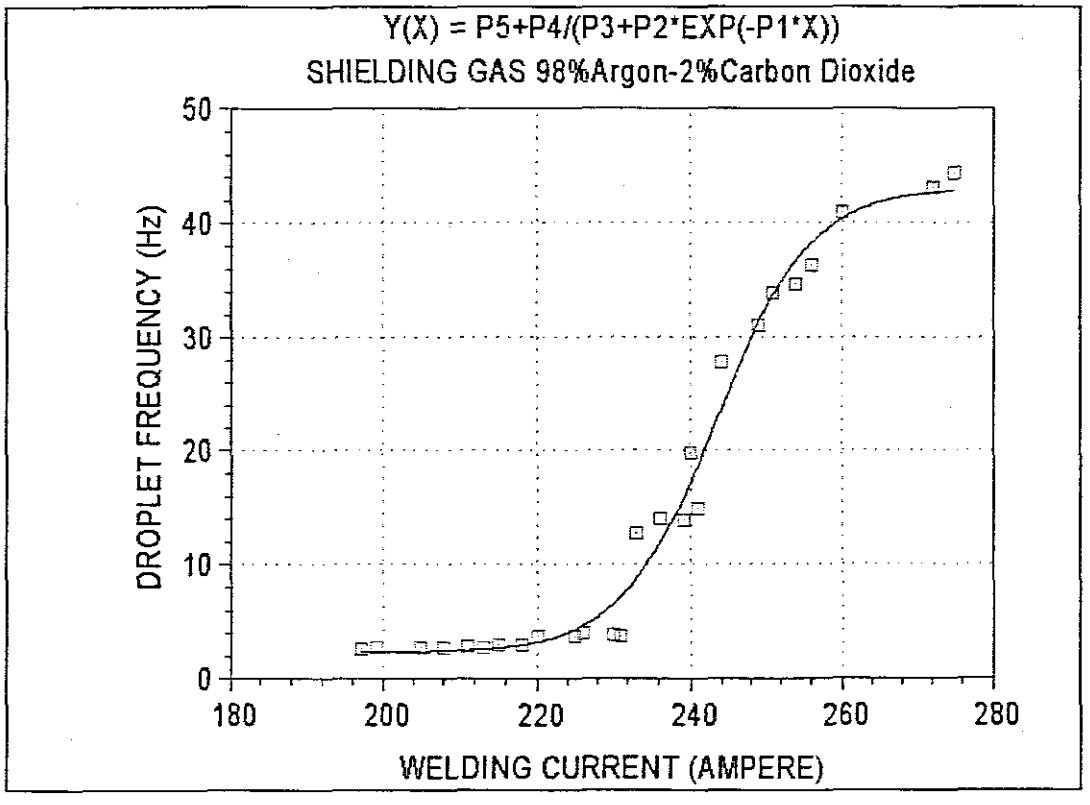


**Fig. 6.10** Welding Current vs. Average Droplet Diameter

| | |
|---|---|
| Coefficient of Determination | 0.98363 |
| Residual Variance | 4.4946 |
| Number of Iterations | 144 |
| | |
| **Parameters** | **Values** |
| P1 | 0.15928 |
| P2 | 7.8722E+16 |
| P3 | 1.1467 |
| P4 | 46.783 |
| P5 | 2.2703 |

**Table 6.11** WFit Output Data for Figure 6.10

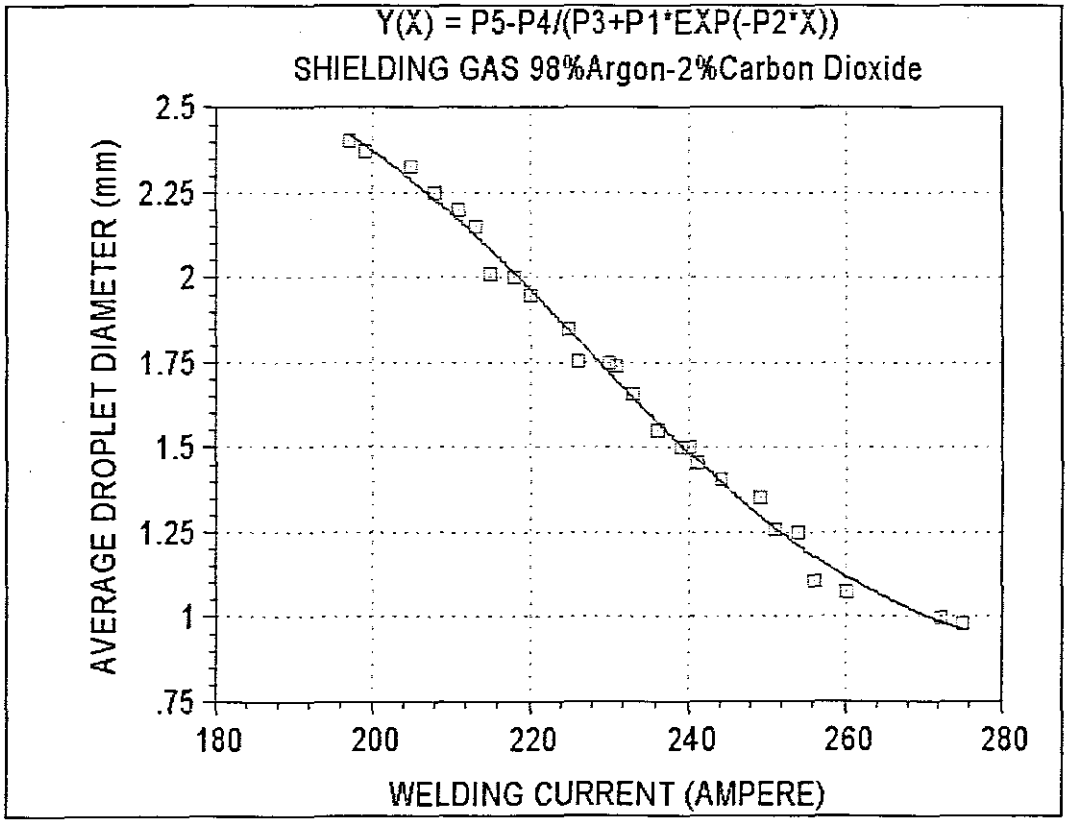


**Fig. 6.11** Welding Current vs. Average Droplet Diameter

| | |
|---|---|
| Coefficient of Determination | 0.99380 |
| Residual Variance | 0.0014417 |
| Number of Iterations | 4 |
| | |
| **Parameters** | **Values** |
| P1 | 71550 |
| P2 | 0.049076 |
| P3 | 1.023 |
| P4 | 2.0474 |
| P5 | 2.7869 |

**Table 6.12** WFit Output Data for Figure 6.11

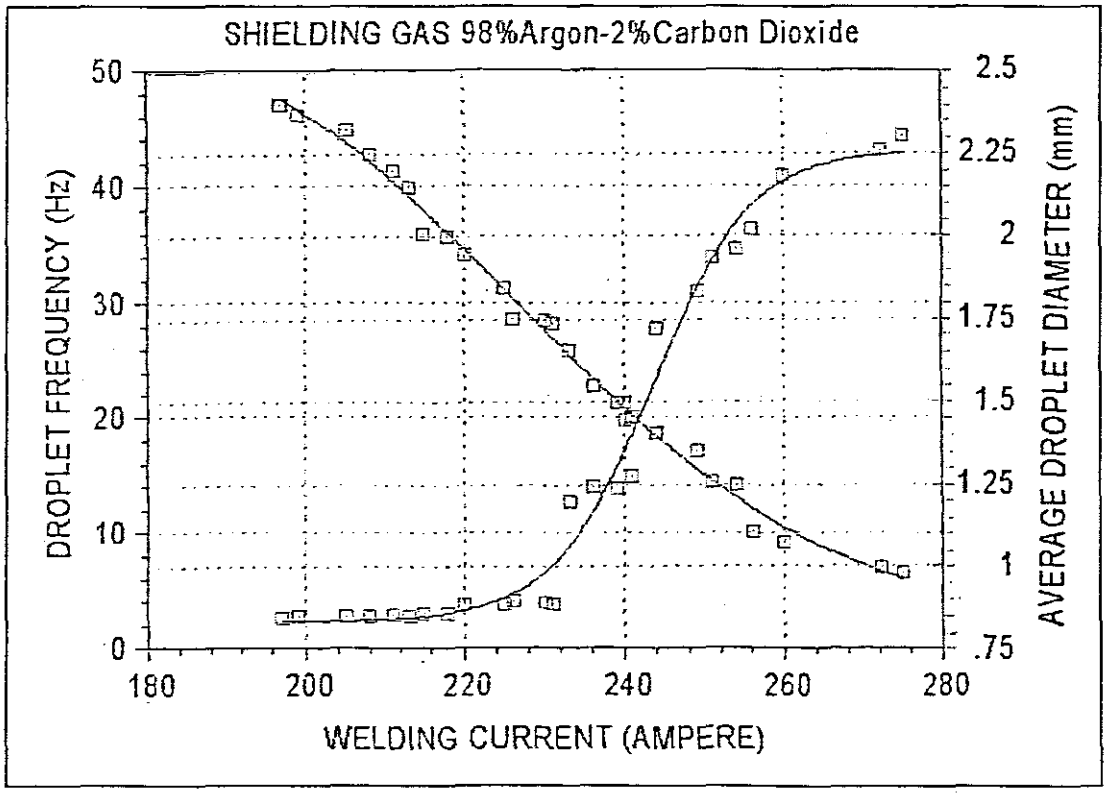


**Fig. 6.12** Welding Current vs. Droplet Frequency and Average Droplet Diameter

## 6.3 DISCUSSION

A useful parameter to characterize any welding process is the droplet-transfer rate. Not only does it provide information on the stability of the process, it also indicates the rate of transfer, the size of the molten droplet being transferred and the behaviour between transfer modes. Lesnewich [23] performed studies at a constant arc length with varying arc current, electrode type and diameter without considering effects of shielding gas on the process variables. His studies were conducted with only pure argon shielding gas. Fig. 6.10 below is a plot, which includes data of Lesnewich and Ludwig [23], and the graphical results of this present study show significant correlation with the graphical curvature of Lesnewich. Ref. Figs. 6.1 – 6.8.

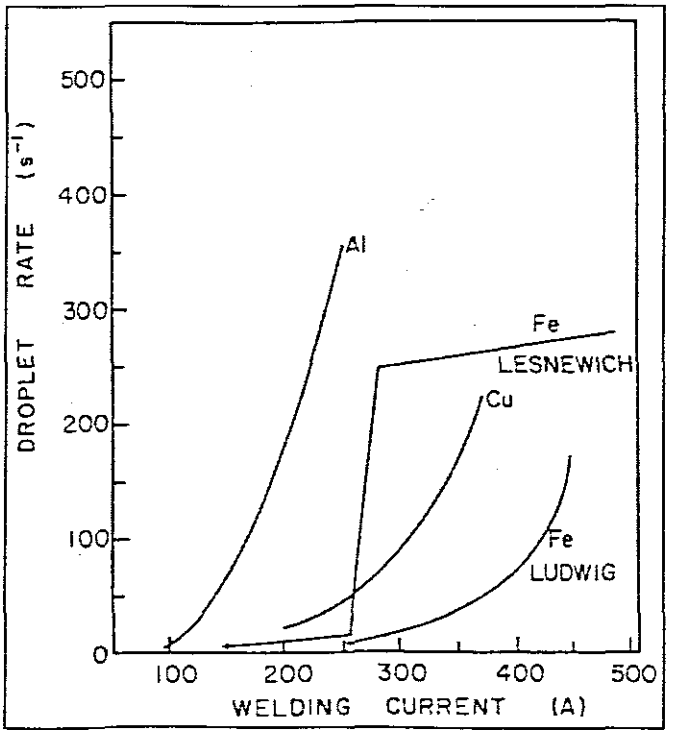


**Fig. 6.13** Transition in droplet transfer rate as a function of welding current

As mentioned previously in Chapter 2, the GMA welding shielding gas may contain argon (Ar), carbon dioxide ($CO_2$), oxygen ($O_2$), helium (He) and hydrogen ($H_2$). Argon, because of its good ionization potential and excellent shielding properties, is commonly used as a base vector.

### 6.3.1 Pure Argon Shielding

Welding with pure Argon shielding gas and a welding voltage of 25V, it is evident from Table 6.1 and Figure 6.1 that the droplet frequency remained near constant between 2,69Hz and 4,36Hz for welding currents up to 220A, with a sudden increase in frequency up to 86Hz. Thereafter the droplet frequency stabilized indicative of the complete transition from the globular to the spray transfer mode. The droplet frequency increase (i.e. transition zone) spanned a current range of approximately 16A (from 220A to 236A).

At the same time the droplet diameter decreased from approximately 2,335mm to 0,654mm as per Table 6.1 and figure 6.2. The sudden decrease in droplet size started at approximately 217A up to 229A (Table 6.1). The final droplet diameter of 0,654mm is well below the wire diameter of 1mm indicating complete spray metal transfer taking place.

For pure Ar shielding, Figure 6.3 indicates a transition current of 226A and average droplet diameter of 1mm, which correlates well with [13], [23], [47].

### 6.3.2 Additions of Oxygen to Argon

In the first set of experiments, the shielding gas used was pure Ar and thereafter Ar/$O_2$ mixtures were used. 1% and 2% $O_2$ was added to Ar respectively to determine the effect on the transition current relative to the transition current obtained with pure Ar shielding.

For an addition of 1% $O_2$, it can be seen in Figure 6.4 and Table 6.4 that the droplet frequency increases gradually from 2,06Hz to 10,36 Hz before a sudden frequency increase occurs. This gradual frequency increase occurred between 176A and 220A. The sudden increase in droplet frequency spanned a current range between 227A and 240A. Whereas the droplet frequency remained near stable before a sudden increase in droplet frequency for pure argon gas, the addition of oxygen to the argon resulted in a more gradual onset to the transition zone as well as exiting the transition zone into the spray transfer zone. Figure 6.5 and Table 6.4 shows the droplet diameter decreasing gradually from 1.405mm to 1.370mm with a sudden decrease to 0.993mm occurring within a current range of 191A to 240A. Thereafter it stabilized at approximately 0,988A. Figure 6.6 gives a transition current of 217A, which is less than the 226A for pure Ar shielding gas.

The results for an addition of 2% $O_2$ can be found in Table 6.7 and Figures 6.7 and 6.8. The droplet frequency increased more gradually from 2Hz to 7Hz within the current range of 124A to 156A. Thereafter a sharper increase in droplet frequency occurred to 131.33Hz at 240A. The frequency stabilized at approximately 133Hz to 135Hz for further current increases. In comparison, the 98Ar-2%$O_2$ gas allows for a higher droplet frequency to be attained than with the pure argon gas. (135.5Hz vs. 87.93Hz from Tables 6.1 and 6.7). The corresponding decrease in droplet diameter shows the expected experimental scatter with a gradual average decrease as indicated in Figure 6.8. Table 6.7 shows droplet diameters in the globular zone to be 1,662mm decreasing to 0,772mm in the spray zone in a current range from 124A to 269A.

The results indicate a lower transition current value as the $O_2$ % increased (194A as per Figure 6.9). This value is substantially lower than the transition current for pure Ar shielding. This is an indication that Ar/$O_2$ mixtures are limited mainly to the spray transfer mode and that the lowering of the transition current allows the spray mode to be utilized on thinner materials. From the images in Appendix E2 – E3, it is evident that the droplets detach more readily and with a higher fluidity than with pure Ar shielding, indicating a lowering of the surface tension of the droplets. This also limits these mixtures for use with the spray transfer mode. Penetration depth and surface wetting improved due to the fluidity of the droplets making this shielding gas mixture even more attractive for use with the welding of thin materials. This means that the

heat input and travel-speed increase at a lower current value due to the fact that oxygen is an active gas, which dissociates in the arc intensifying the arc plasma. From the AVI files it was observed that a more stable arc and droplet transfer was obtained. Ref. Appendix E1 – E3. Weld spatter also reduced and undercutting was virtually eliminated compared with welds conducted with pure argon shielding. This is ascribed to better fusion-line wetting. However, it should be borne in mind that excessive additions of oxygen will lead to oxidation and weld metal embrittlement.

### 6.3.3 Additions of Carbon Dioxide to Argon

The second set of experiments was conducted with $Ar/CO_2$ shielding gases. A 2% addition of $CO_2$ to Ar was used. From Table 6.10 and Figure 6.10, it is can be seen that the droplet frequency gradually increases from 2.59 Hz to 4.01Hz with the expected experimental scatter, thereafter increasing suddenly to 40.91Hz with a gradual further increase to 44.32Hz. This sudden frequency increase occurs within a current band ranging from 226A to 260A. The frequency range for this particular gas mixture was low (2.59Hz to 44.32Hz) compared with the range for a 2% $O_2$ addition to Ar (2Hz to 135.50Hz as per Table 6.7).

Figure 6.11 shows a gradual decrease in the average droplet diameter from 2.402mm down to 0.980mm. During the entire current range, no sudden droplet decrease occurred as normally expected in the globular- to spray metal transfer transition zone as observed with the other gas mixtures tested. It is also evident that the final droplet sizes of 0.998mm and 0.980 was very close to the 1mm electrode/wire size, indicating relatively large droplets still detaching at high current levels. The images in Appendix E4 show the droplet sizes at various current levels.

Figure 6.11, shows a transition current value of 242A thus indicating that the transition current increased with the addition of $CO_2$ in the shielding gas, as compared to 226A for pure Argon as per Figure 6.3 and 194A for 98%Ar+2%$O_2$ as per Figure 6.9. These results further prove the tendency of $CO_2$ to allow metal transfer only in the globular mode. This means that the spray mode would be obtained at a higher current setting, making it undesirable for usage with the welding of thin materials.

The penetration was observed to be higher than that of $Ar/O_2$ shielding and higher spatter levels than with $Ar/O_2$ mixtures was observed. It was also observed that the current flow tend to become non-axial compared to current flows with Ar or $Ar/CO_2$ mixtures. This is ascribed to the fact that $CO_2$ is not chemically inert. When subjected to high arc temperatures, its molecules dissociate at the top of the arc to form carbon monoxide and oxygen (i.e. $CO_2 \rightarrow CO + O$), which results in a high vapour pressure that lifts the droplet up causing an unstable arc and weld spatter.

Comparing the transition current of 264,5A in Table 4.1 obtained for 1mm mild steel electrodes from the formulation of [24] to the experimental results for a 1mm electrode of this study, Table 6.13 below indicates significant differences in the transition current values.

| Transition Current Obtained From: | Value |
|---|---|
| Mathematical Formulation of [24] | 264.5A |
| Experiments - Pure Argon Shielding Gas | 226A |
| Experiments – 99%Ar-1%$O_2$ Shielding Gas | 217A |
| Experiments – 98%Ar-2%$O_2$ Shielding Gas | 194A |
| Experiments – 98%Ar-2%$CO_2$ Shielding Gas | 242A |

**Table 6.13** Comparison of numerical transition current result with experimental results for 1mm electrode

## 6.4 Conclusions

- Shielding gas composition and properties is of paramount importance in determining the transition current between globular and spray metal transfer in GMA welding, as well as controlling the amount of spatter generated during welding. Different gas mixtures yielding different gas properties will affect the heat transfer between the arc and the droplets and thus the temperature and surface tension coefficient of the droplets will be influenced. The change in permeability due to gas composition will also influence the self-magnetic field as described in Chapter 4.

- The present study yields quite different results from the numerical results of Lowke [24], who neglected the effects of shielding gas composition on the transition current, as is apparent in Table 6.13. As can also be seen in Table 6.13 different shielding gases result in experimentally significant variations in the transition current. For 100% argon the transition current for 1mm mild steel electrodes is reduced from 226.5A to 194A for a 98%Ar-2%$O_2$ combination. This is also true for other compositions used in the experiments. There is in fact a systematic effect for particular gas additions to the shielding gas composition specifically the addition of oxygen lowers the transition current and the addition of carbon dioxide raises the transition current. This would indicate that the shielding gas composition plays a role in determining the transition current. This indicates that the effect of shielding gas composition has to be included in modelling this phenomenon. Since this phenomenon is neglected by Lowke [24] one would have to conclude that the model is not sufficiently developed. The value obtained from the model also typically overestimates the observed value as can be seen in Table 6.13.Continuation of the research will be undertaken by the author in order to build up an extensive database for future research and industrial purposes.

- For certain shielding gas mixtures/combinations the droplet frequency rate and droplet diameter become erratic, indicating that for these gases, the metal transfer modes is not smooth, but discontinuous.

- Oxygen additions to argon shielding gas tend to reduce the transition current whereas additions of carbon dioxide raise the value of the transition current.

- For thin plate welding, process stability and quality weldments are extremely dependent on the careful selection and/or adjustment of welding parameters. Weld penetration depth (i.e. material thickness) and profile is another consideration and

is affected by the shielding gas mixture. Wide 'bowl' shaped penetration profiles are more suited to joints on thick material than narrow 'wine glass' profiles that are susceptible to fusion defects.

- The experiments were conducted at constant voltage, but it is predicted that varied welding voltage together with shielding gas mixtures will have a profound effect on the transition current. The compilation of a transition current database for industry will require the study of this parameters influencing weld metal transfer as well as electrode feed rate, welding speed and electrode material composition.

Shielding gas selection is not related only to transfer modes but contributes to the effectiveness of shielding from air contamination, weld joint contamination and emission of fumes.

# Bibliography


1. ALLUM, C. J. 1985: Metal transfer in arc welding as a varicose instability: I. Varicose instabilities in a current-carrying liquid cylinder with surface charge. Journal of Physics Review D: Applied Physics, Vol. 18 pp. 1431-1446

2. BOCTOR, S. A. 1987: Electric Circuit Analysis. London, Prentice-Hall International

3. BRANDI, S.; TANIGUCHI, C.; LIU, S. 1991: Analysis of Metal Transfer in Shielded Metal Arc Welding. Welding Research Supplement to Welding Journal, (October issue) pp.261-270

4. BRANDON, D.; KAPLAN, W. D. 1997: Joining Processes, An Introduction. New York: John Wiley & Sons

5. CAO, Z. N.; DONG, P. 1998: Modeling of GMA Weld Pools with Consideration of Droplet Impact. Journal of Engineering Materials and Technology, ASME, Vol. 120 pp. 313-320

6. CERJAK, H.; BUCHMAYR, B. 1996: Mathematical Modeling – A Tool for Advanced Welding and Joining Technology?. Nagoya, Proc. Of the 6th International Symposium, JWS pp. 367-374

7. CHOI, S. K.; YOO, C. D.; KIM, Y. S. 1998: Dynamic Simulation of Metal Transfer in GMAW, Part 1: Globular and Spray Transfer Modes. Welding Research Supplement to Welding Journal, (January issue) pp38s-44s

8. CHOO, R. T. C.; SZEKELY, J.; WESTHOFF, R. C. 1990: Modeling of High Current Arcs with Emphasis on Free Surface Phenomena in the Weld Pool. Welding Journal, AWS, Vol. 69 pp. 346-361

9. CLIFFORD, T.; 1998: Design of a Straight-Line Cutter and the Simulation of Plasma Arc Cutting, BTech Thesis, Peninsula Technikon

10. EASTERLING, K. 1983: Introduction to the Physical Metallurgy of Welding. London: Butterworth

11. FAN, H. G.; KOVACEVIC, R. 1999: Droplet Formation, Detachment, and Impingement on the Molten Pool in Gas Metal Arc Welding. Metallurgical and Materials Transactions B. Volume 30B (August issue) pp791-801

12. FAN, H. G.; KOVACEVIC, R. 1998: Dynamic analysis of globular metal transfer in gas metal arc welding – a comparison of numerical and experimental results. Journal of Physics Review D: Applied Physics, Vol. 31 pp. 2929-2941

13. FAREED, S. 1999: Fundamentals of Gas Metal Arc Welding. Mechanical Technology, (April issue) pp. 13-15

14. GRONG, O. 1994: Metallurgical Modelling of Welding. London, The Institute of Materials

15. HAIDAR, J.; LOWKE, J. J. 1996: Predictions of Metal Droplet Formation in Arc Welding. Journal of Physics Review D: Applied Physics, Vol. 29 pp. 2952-2960

16. HEALEY, J. 1996: The Role of Inverters in the Welding Industry. SA Mechanical Engineer, (March issue) pp. 25-26

17. HENDERSON, J. 1998: MIG Welding Thin Stainless Steel Sheet. Mechanical Technology, (August issue) pp. 8-9

18. HUGHES, E. (Revised by McKenzie Smith, I.) 1987: Electrical Technology Longman Scientific and Technical, UK.

19. IRVING, B. 1999: Shielding Gases are the key to Innovations in Welding, Welding journal (January issue) pp.37-41

20. JACOBSEN, N. 1992: Monopulse investigation of drop detachment in pulsed gas metal arc welding. Journal of Physics Review D: Applied Physics, Vol. 25 pp. 783-797

21. KIM, Y., EAGAR, T. 1993: Metal Transfer in Pulsed Current Gas Metal Arc Welding. Welding Research Supplement to the Welding Journal, (July issue) pp279-287s

22. KOU, S. 1987: Welding Metallurgy. New York, John Wiley & Sons

23. LIU, S., SIEWERT, T. 1989: Metal Transfer in Gas Metal Arc Welding: Droplet Rate. Welding Research Supplement to the Welding Journal, (February issue) pp. 52s-58s

24. LOWKE, J. J. 1996: Simple Model for the Transition Current from Globular to Spray Transfer in Gas Metal Arc Welding. Nagoya, Proc. Of 6th International Symposium, JWS pp. 613-619

25. MARIAS, J. J. & ASSOCIATES; LIW (Metallurgical Engineering) 1990: Welding Design for Mechanical and Metallurgical Designers, Part 2.

26. MATSUMOTO, T. 1986: On Welding Materials. Technical Services, Nippon Steel Welding Products & Engineering Co. Ltd. Japan

27. MATSUTANI, T.; OHJI, T.; HIRATA, Y. 1996: A Mathematical Modeling of Circumferential GTA Welding of Pipes. Nagoya, Proc. of 6th International Symposium, JWS pp. 619-624

28. MONRO, D. M. 1989: A Crash Course in Fortran 77. London, Prentice-Hall International

29. NGUYEN, N., OHTA, A., MATSUOKA, K., SUZUKI, N., MAEDA, Y. 1999: Analytical Solutions for Transient Temperature of Semi-Infinite Body Subjected to 3-D Moving Heat Sources. Welding Research Supplement to the Welding Journal, (August issue) pp. 265s-274s

30. NOIK, R. 1999: Robotic Welding Technology is Advancing. Engineering News, (8-14 October issue) pp.21-22

31. OHRING, S., LUGT, H. 1999: Numerical Simulation of a Time-Dependent 3-D GMA Weld Pool Due to a Moving Arc. Welding Research Supplement to the Welding Journal, (December issue) pp.416s-424s

32. PHILANDER, O. 1998: Mathematical Modeling of Welding: Sensitivity of Residual Stresses and Thermal Dilatations on Welding Parameters. MTech. Thesis, Peninsula Technikon

33. PISTORIUS, P., LIU, S. 1997: Changes in Metal Transfer Behaviour during Shielded Metal Arc Welding. Welding Research Supplement to the Welding Journal, (August issue) pp.305s-315s

34. PRESS, W. H.; FLANNERY, B. P.; TEUKOLSKY, S. A.; VETTERLING, W. T. 1989: Numerical Recipes – The Art of Scientific Computing (Fortran Version). Cambridge, Cambridge University Press

35. RICHARDSON, I., BUCKNALL, P., STARES, I. 1994: The Influence of Power Source Dynamics on Wire Melting Rate in Pulsed GMA Welding. Welding Research Supplement to the Welding journal, (February issue) pp.32s-37s

36. SADLER, H. 1999: A Look at the Fundamentals of Gas Metal Arc Welding. Welding Journal (May issue), pp.45-50

37. SPRARAGEN, W., LENGYEL, B. 1943: Physics of the Arc and the Transfer of Metal in Arc Welding. Welding Journal, Volume 22 (January issue) pp2s-42s

38. WOODS, T. 1996: Trends in Welding Technologies. SA Mechanical Engineer, March (issue) pp.27-30

39. YOUNG, B. 1995: Shielding and Purging Gases: Making the Right Selection. Welding Journal pp. 47-49

40. AFROX LTD. 1986: Argoshield Shielding Gases Catalogue. Johannesburg

41. AMERICAN SOCIETY FOR METALS, 1983: Welding, Brazing and Soldering. Ohio, Metals Handbook, Ninth Edition, Vol. 6

42. AVESTA WELDING. Handbook for the Welding of Stainless Steels. Avesta, Sweden

43. COLUMBUS STAINLESS, 1998: POCKET GUIDE – Stainless Steel & 3CR12. Technical Services, Columbus Stainless, Middelburg

44. DAIHEN CORPORATION. 1986: Operation Guide, $CO_2$MAG Semi-Automatic Welding Machine. Osaka, (Available from Afrox, Brits, South Africa)

45. ELECTRIC WELDING MACHINE COMMITTEE 1978: Practice and Experimentation for Semi-automatic Gas Shielded Arc Welding and Handling of Instruments. Nagoya, Nagoya International Training Centre & JICA

46. FEDGAS, 1986: MIG Welding and Shielding Gases for the MAG Process. Alberton

47. Solid Wire MIG Welding. 1996: http://www.twi.co.uk/bestprac/jobknol/jk4.html

48. Vision for Welding. 2000: http://www.aws.org/frontpage.html#vision

49. WELDING WORKBOOK, December 1998: Basic Welding Equations and Formulas – How to Estimate Weld Bead Sizes., Datasheet no. 106a&b (December issue) pp. 52-54

50. PRESS, W. H.; TEUKOLSKY, S. A.; VETTERLING, W. T.; FLANNERY, B. P. 1992: Numerical Recipes in C – The Art of Scientific Computing Second Edition, Cambridge, Cambridge University Press

51. JAPAN WELDING TECHNOLOGY CENTER, 1996: Welding Processes and Power Sources Lecture notes

# Appendix A

## Metal Transfer Classification

The following is a tabulated and schematic representation of the International Institute of Welding (IIW) classifications of metal transfer modes in arc welding [23].

Comparing these schematics with the photo frames in Appendix E, it is evident that the globular- and spray transfer modes were obtained.

Table 1—International Institute of Welding Classifications of Metal Transfer

| | Designation of Transfer Type | Welding Process (examples) |
|---|---|---|
| 1. | Free-flight transfer | |
| 1.1 | Globular | |
| 1.1.1 | Drop | Low-current GMA |
| 1.1.2 | Repelled | $CO_2$ shielded GMA |
| 1.2 | Spray | |
| 1.2.1 | Projected | Intermediate-current GMA |
| 1.2.2 | Streaming | Medium-current GMA |
| 1.2.3 | Rotating | High-current GMA |
| 1.3 | Explosive | SMA (covered electrodes) |
| 2. | Bridging transfer | |
| 2.1 | Short-circuiting | Short-circuiting GMA |
| 2.2 | Bridging without interruption | Welding with filler metal addition |
| 3. | Slag-protected transfer | |
| 3.1 | Flux-wall guided | SAW |
| 3.2 | Other modes | SMA, cored wire, electroslag |

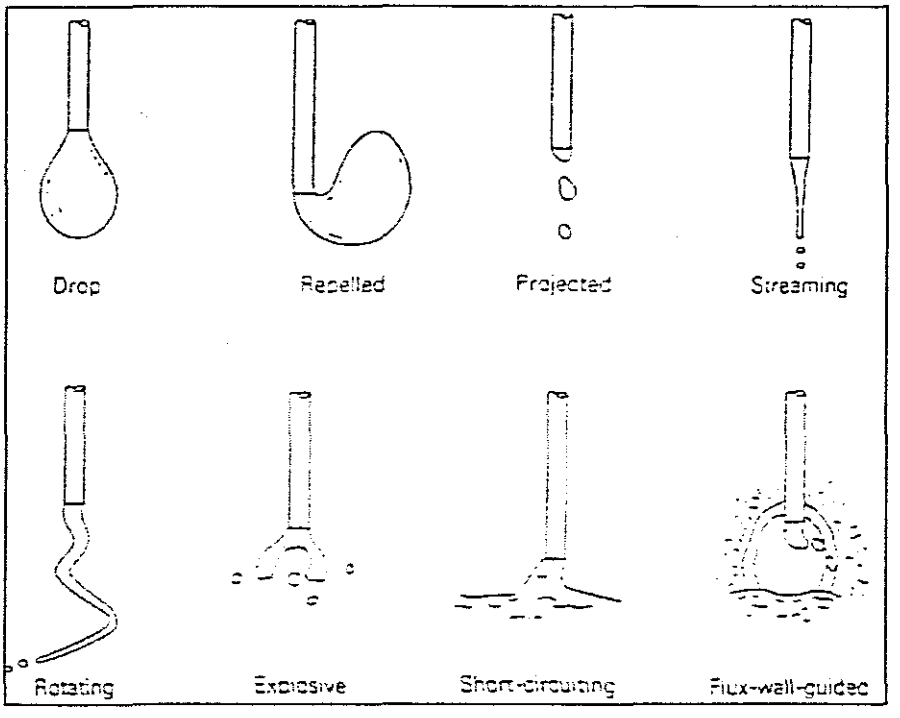

# Appendix B

## Gas Selection Guide

---

The following datasheets depicts the GMAW shielding gas selection for the various modes of transfer, as well as the gas composition and advantage(-s).

**WELDING WORKBOOK** Datasheet 228a

*Practical information for welders and others involved in welding and its allied processes.*

# Gas Selection for Gas Metal Arc Welding

| Metal Type | Thickness | Transfer Mode | Recommended Shielding Gas | Advantages/Description |
|---|---|---|---|---|
| Carbon Steel | Up to 14 gauge | Short Circuit | Argon + $CO_2$<br>Argon + $CO_2$ + $O_2$ | Good penetration and distortion control to reduce potential melt-through. |
| | 14 gauge—¼ in. | Short Circuit | Argon + 8 to 25% $CO_2$<br>Argon + He + $CO_2$ | Higher deposition rates without melt-through. Minimum distortion and spatter. Good weld control for out-of-position welding. |
| | More than ¼ in. | Short Circuit | Carbon Dioxide.<br>Argon + 15 to 25% $CO_2$ | High welding speeds. Good penetration and pool control. Applicable for out-of-position welds. |
| | | Short Circuit Globular | Argon + 25% $CO_2$ | Suitable for high current and high-speed welding. |
| | | Short Circuit | Argon + 50% $CO_2$ | Deep penetration; low spatter; high travel speeds. Good out-of position welding. |
| | | Short Circuit Globular (buried arc) | Carbon Dioxide | Deep penetration and fastest travel speeds but with higher melt-through potential. High-current mechanized welding. |
| | | Spray Transfer | Argon +1 to 8% $O_2$ | Good arc stability; produces a more fluid weld pool as $O_2$ increases; good coalescence and bead contour. Good weld appearance and weld pool control. |
| | | Spray Transfer | Argon + 5 to 20% $CO_2$ | Fluid weld pool and oxidizing to weld metal causes higher amounts of slag and scale as $CO_2$ increases. Good arc stability, weld soundness and increasing width of fusion. |
| | | Short Circuit Spray Transfer | Argon + $CO_2$ + $O_2$<br>Argon + He + $CO_2$<br>Helium + Ar + $CO_2$ | Applicable to both short circuiting and spray transfer modes. Has wide welding current range and good arc performance. Weld pool has good control, which results in improved weld contour. |
| | | High Current Density Rotational | Argon + He + $CO_2$ + $O_2$<br>Argon + $CO_2$ + $O_2$ | Used for high deposition rate welding where 15 to 30 lb/h (7 to 14 kg/h) is typical. Special welding equipment and techniques are sometimes required to achieve these deposition levels. |
| | More than 14 gauge | Pulsed Spray | Argon + 2 to 8% $O_2$<br>Argon + 5 to 20% $CO_2$<br>Argon + $CO_2$ + $O_2$<br>Argon + He + $CO_2$ | Used for both light-gauge and heavy out-of-position weldments. Achieves good pulse spray stability over a wide range of arc characteristics and deposition ranges. |

Excerpted from C5.10-94, *Recommended Practices for Shielding Gases for Welding and Plasma Arc Cutting*

Datasheet 228b

# Gas Selection for Gas Metal Arc Welding

| Metal Type | Thickness | Transfer Mode | Recommended Shielding Gas | Advantages/Description |
|---|---|---|---|---|
| Low- and High-Alloy Steel | Up to ⅜ in. | Short Circuit | Argon + 8 to 20% $CO_2$<br>Helium + Ar + $CO_2$<br>Argon + $CO_2$ + $O_2$ | Good coalescence and bead contour. Good mechanical properties |
| | | Short Circuit Globular | Argon + 20 to 50% $CO_2$ | High welding speeds. Good penetration and weld pool control. Applicable for out-of-position welds. Suitable for high-current and high-speed welding. |
| | More than ⅜ in. | Spray Transfer (High Current Density & Rotational) | Argon + 2% $O_2$<br>Argon + 5 to 10% $CO_2$<br>Argon + $CO_2$ + $O_2$<br>Argon + He + $CO_2$ + $O_2$ | Reduces undercutting. Higher deposition rates and improved bead wetting. Deep penetration and good mechanical properties. |
| | | Pulsed Spray | Argon + 2% $O_2$<br>Argon + 5% $CO_2$<br>Argon + $CO_2$ + $O_2$<br>Argon + He + $CO_2$ | Used for both light-gauge and heavy out-of-position weldments. Achieves good pulse spray stability over a wide range of arc characteristics and deposition ranges. |
| Steel, Stainless, Nickel, Nickel Alloys | Up to 14 gauge | Short Circuit | Argon + 2 to 5% $O_2$ | Good control of melt-through and distortion. Used also for spray arc welding. Weld pool fluidity sometimes sluggish, depending on the base alloy. |
| Steel, Stainless, Nickel, Nickel Alloy | More than 14 gauge | Short Circuit | Helium + 7.5 Ar + 2.5 $CO_2$<br>Argon+ 2 to 5% $CO_2$<br>Argon + He + $CO_2$<br>Helium + Ar + $CO_2$ | Low $CO_2$ percentages in He mix minimizes carbon pickup, which can cause intergranular corrosion with some alloys. Helium improves wetting action and contour. $CO_2$ percentages above 5% should be used with caution on some alloys. Applicable for all position welding. |
| | | Spray Transfer | Argon + 1 to 2% $O_2$<br>Argon + He + $CO_2$<br>Helium + Ar + $CO_2$ | Good arc stability. Produces a fluid but controllable weld pool; good coalescence and bead contour. Minimizes undercutting on heavier thickness. |
| Stainless Steel | More than 14 gauge | Pulsed Spray | Argon + 1 to 2% $O_2$<br>Argon + He + $CO_2$<br>Helium + Ar + $CO_2$<br>Argon + $CO_2$ + $H_2$ | Used for both light-gauge and heavy out-of-position weldments. Achieves good pulse spray stability over a wide range of arc characteristics and deposition ranges. |
| Aluminum | Up to ½ in. | Spray Transfer Pulsed Spray | Argon | Best metal transfer, arc stability and plate cleaning. Little or no spatter. Remove oxides when used with DCEP (Reverse polarity). |
| | More than ½ in. | Spray Transfer Pulsed Spray | Helium + 20 to 50 % Argon<br>Argon + Helium | High heat input. Produces fluid weld pool, flat bead contour and deep penetration. Minimizes porosity. |

# Appendix C

The Fortran program below was developed from the mathematical formulation of [24], with the addition of the relative permeability of the shielding gas.

Calculation of the Transition Current from Globular to Spray Transfer in MIG Welding
Developed by: Mark Ludick
Centre for Research in Applied Technology

```
      PROGRAM MTECH
! TRANSITION CURRENT SENSITIVITY
   PRINT*,"TYPE OF MATERIAL = MILD STEEL"
      GAM=1.2
      RHO=7.0E3
      PI=22/7
      PERM=4E-7*PI
      RPERM=1
      GRAV=9.81
      PRINT*,"SURFACE TENSION COEFFICIENT (N/m)",GAM
      PRINT*,"MILD STEEL DENSITY @ BOILING POINT (kg/m3)",RHO
      PRINT*,"PERMEABILITY (N/A2)",PERM
      PRINT*,"SHIELDING GAS RELATIVE PERMEABILITY",RPERM
      WRITE(*,30)
30    FORMAT(1X,"DIAMETER",5X,"TRANS. AMP",5X,"DROP DIA")
      do R=0.8E-3,1.6E-3,0.1E-3
       A=2*PI
       B=PERM*RPERM
       C=B**0.5
       D=A/C
       E=2*GAM*R
       F=RHO*GRAV*R**3
       G=E-F
       H=G**0.5
       AMP=D*H
       O=PERM*AMP**2.0
       P=8*GAM*PI**2.0
       Q=H/O
       WRITE(*,20) R*1000,AMP,Q
20     FORMAT(1X,F5.1,10X,F5.1,3X,E13.3)
      end do
      END
```

# Appendix D

All values of material properties for mild steel as shown in the table below, were obtained from [11],[24].

| | | **Mild Steel** |
|---|---|---|
| Melting point | $^{o}C$ | $1620^{0}$C |
| Material Density | $\rho$ | 7300 kg/m$^3$ |
| Surface Tension coefficient | $\gamma$ | 1.2 |
| Viscosity | $\upsilon$ | 0.006 kg/m.s |
| Heat Capacity | $C_p$ | 0.753 J/kg.K |
| Thermal Expansion coeff | $\beta_T$ | $10^{-4}$ K$^{-1}$ |
| Electrical Conductivity | $\sigma_e$ | 7.7E-5 $\Omega^{-1}$m$^{-1}$ |
| Magnetic | | Yes |

# Appendix E1

**Laserstrobe Images of MIG Welding with Pure Argon Shielding Gas**

The table below represents the mean droplet diameters obtained from the welding images of a 1mm mild steel electrode with pure Argon shielding. A minimum of 4 images per weld run was used to calculate the mean droplet diameter.

| Weld No. | Wire Feed Rate | Mean droplet diameter |
|---|---|---|
| 1 | 10 | **2.335** |
| 2 | 10.5 | **2.313** |
| 3 | 11 | **2.234** |
| 4 | 11.5 | **2.152** |
| 5 | 12 | **2.187** |
| 6 | 12.5 | **2.251** |
| 7 | 13 | **2.091** |
| 8 | 13.5 | **2.433** |
| 9 | 14 | **2.136** |
| 10 | 14.5 | **1.422** |
| 11 | 15 | **1.706** |
| 12 | 15.5 | **1.489** |
| 13 | 16 | **1.256** |
| 14 | 16.5 | **1.121** |
| 15 | 16.6 | **1.001** |
| 16 | 16.7 | **1.00** |
| 17 | 16.9 | **0.973** |
| 18 | 16.9 | **0.955** |
| 19 | 17 | **0.870** |
| 20 | 17 | **0.889** |
| 21 | 17.5 | **0.767** |
| 22 | 18 | **0.683** |
| 23 | 18.5 | **0.567** |
| 24 | 19 | **0.731** |
| 25 | 20 | **0.723** |
| 26 | 22 | **0.731** |
| 27 | 22 | **0.730** |
| 28 | 24 | **0.654** |

Welding current **187A**, wire speed **10m/min**

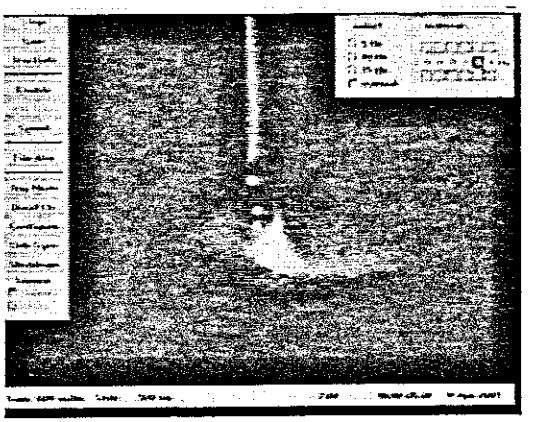

| | Photo | Actual |
|---|---|---|
| Droplet ∅ | 7,00 | **2,26** |
| Wire ∅ | 3,10 | 1,00 |

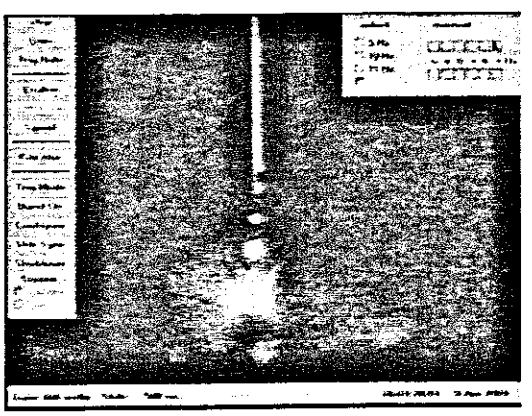

| | Photo | Actual |
|---|---|---|
| Droplet ∅ | 6,82 | **2,37** |
| Wire ∅ | 2,88 | 1,00 |

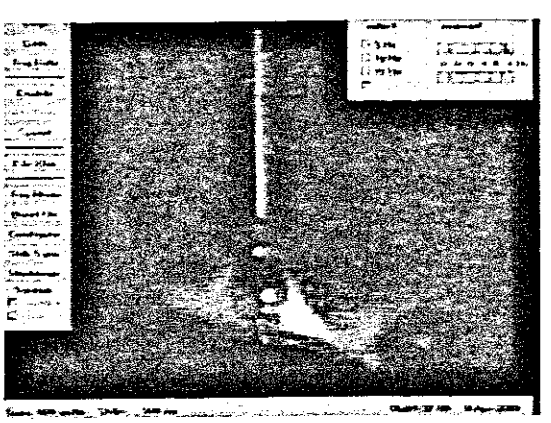

| | Photo | Actual |
|---|---|---|
| Droplet ∅ | 8,00 | **2,52** |
| Wire ∅ | 3,18 | 1,00 |

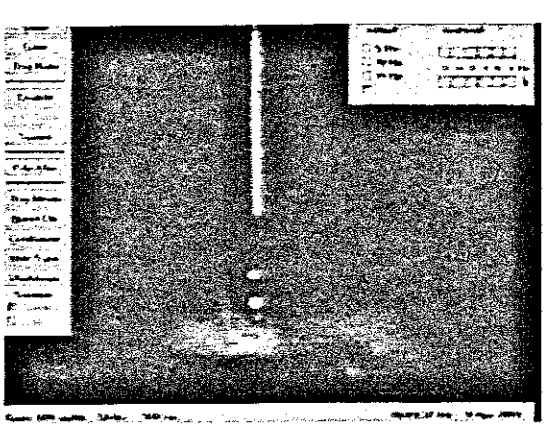

| | Photo | Actual |
|---|---|---|
| Droplet ∅ | 6,18 | **2,19** |
| Wire ∅ | 2,82 | 1,00 |

| **Average Droplet ∅** | **2,335** |
|---|---|

Welding current **189A**, wire speed **10.5m/min**

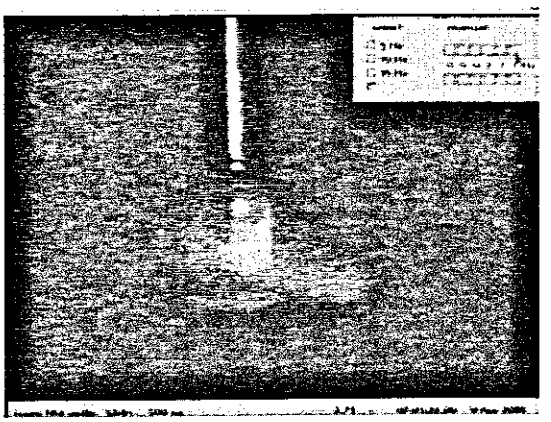

| | Photo | Actual |
|---|---|---|
| Droplet ∅ | 8,60 | **2,263** |
| Wire ∅ | 3,80 | 1,00 |

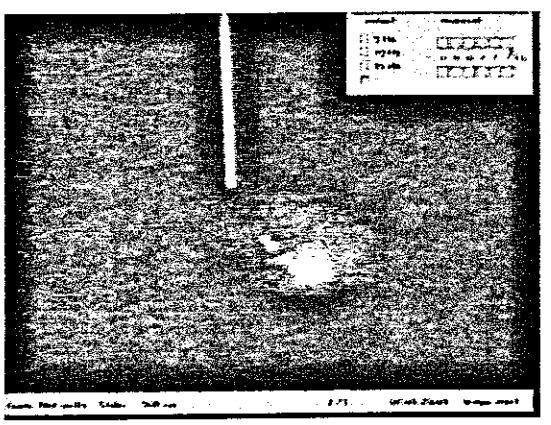

| | Photo | Actual |
|---|---|---|
| Droplet ∅ | 9,10 | **2,364** |
| Wire ∅ | 3,85 | 1,00 |

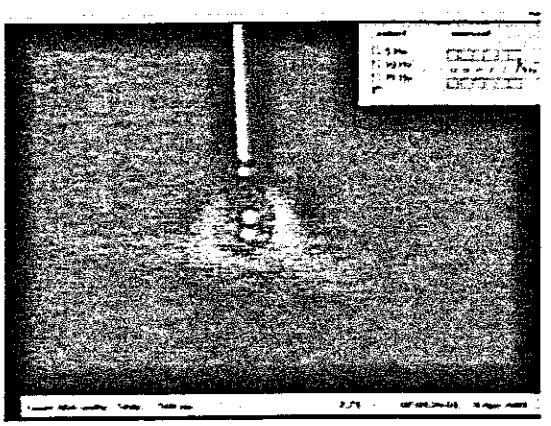

| | Photo | Actual |
|---|---|---|
| Droplet ∅ | 9,00 | **2,31** |
| Wire ∅ | 3,90 | 1,00 |

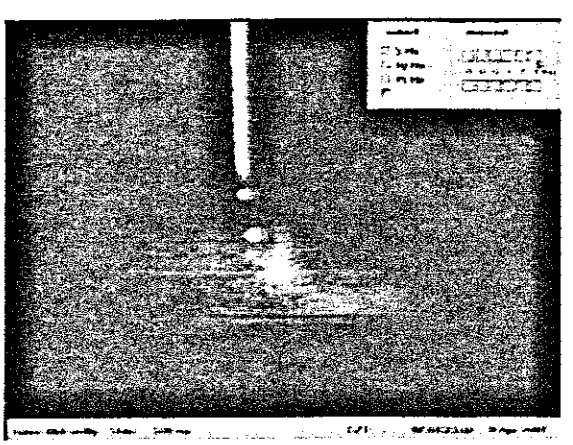

| | Photo | Actual |
|---|---|---|
| Droplet ∅ | 8,10 | **2,314** |
| Wire ∅ | 3,50 | 1,00 |

Welding current **194A**, wire speed **11m/min**

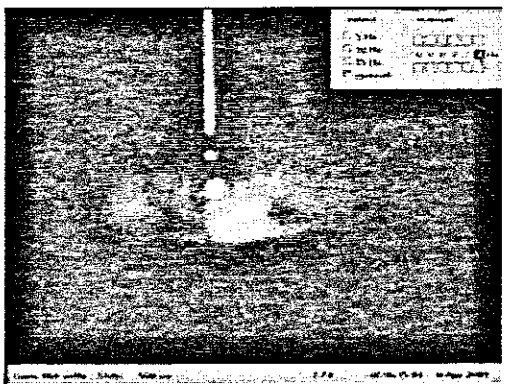

| | Photo | Actual |
|---|---|---|
| Droplet ∅ | 7,00 | **2,222** |
| Wire ∅ | 3,15 | 1,00 |

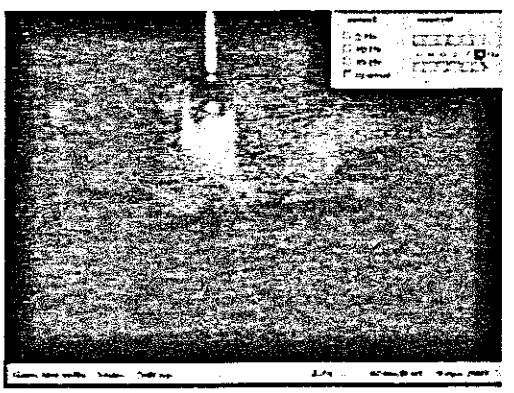

| | Photo | Actual |
|---|---|---|
| Droplet ∅ | 6,80 | **2,159** |
| Wire ∅ | 3,15 | 1,00 |

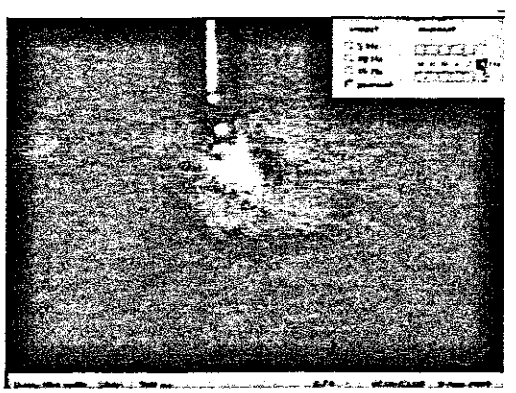

| | Photo | Actual |
|---|---|---|
| Droplet ∅ | 7,20 | **2,278** |
| Wire ∅ | 3,16 | 1,00 |

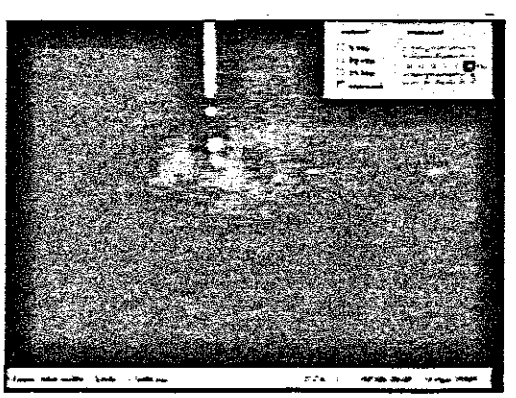

| | Photo | Actual |
|---|---|---|
| Droplet ∅ | 7,20 | **2,278** |
| Wire ∅ | 3,16 | 1,00 |

Welding current **198A**, wire speed **11.5m/min**

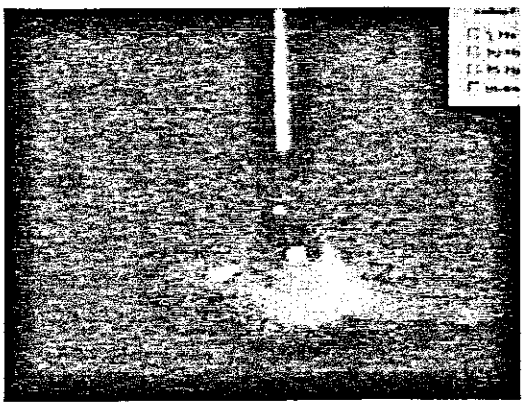

| | Photo | Actual |
|---|---|---|
| Droplet ∅ | 10,40 | **2,256** |
| Wire ∅ | 4,61 | 1,00 |

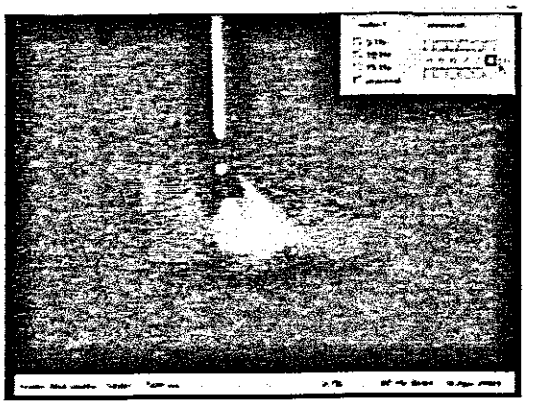

| | Photo | Actual |
|---|---|---|
| Droplet ∅ | 8,62 | **2,102** |
| Wire ∅ | 4,10 | 1,00 |

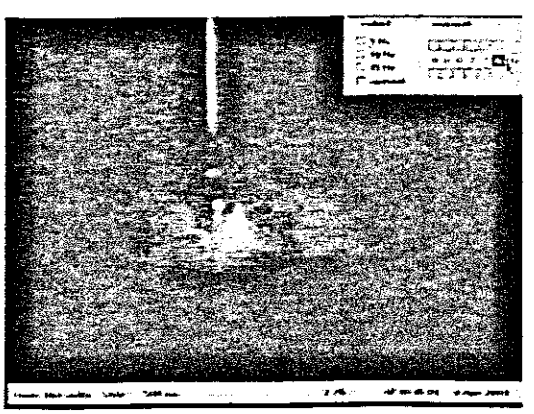

| | Photo | Actual |
|---|---|---|
| Droplet ∅ | 8,60 | **2,15** |
| Wire ∅ | 4,00 | 1,00 |

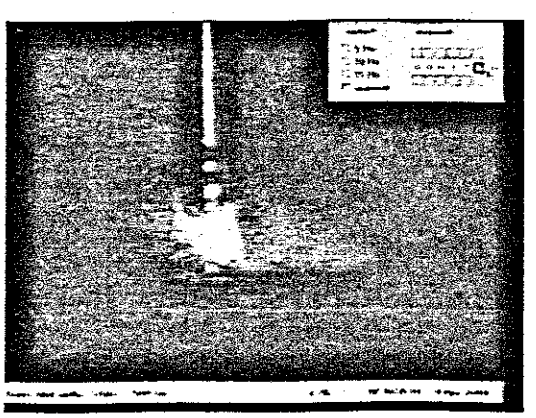

| | Photo | Actual |
|---|---|---|
| Droplet ∅ | 8,60 | **2,098** |
| Wire ∅ | 4,10 | 1,00 |

Welding current **202A**, wire speed **12m/min**

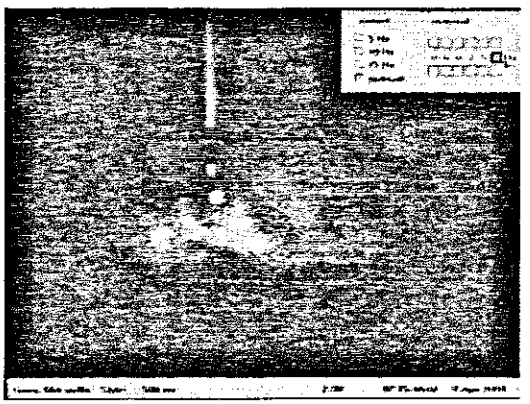

| | Photo | Actual |
|---|---|---|
| Droplet ∅ | 6,98 | **2,252** |
| Wire ∅ | 3,10 | 1,00 |

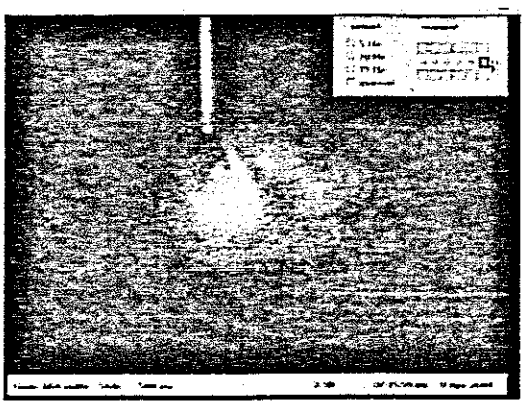

| | Photo | Actual |
|---|---|---|
| Droplet ∅ | 6,60 | **2,20** |
| Wire ∅ | 3,00 | 1,00 |

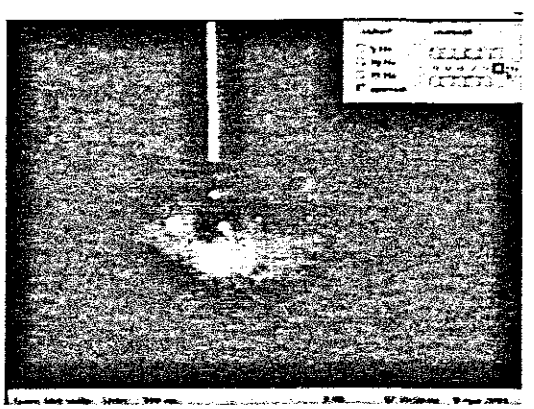

| | Photo | Actual |
|---|---|---|
| Droplet ∅ | 6,70 | **2,154** |
| Wire ∅ | 3,11 | 1,00 |

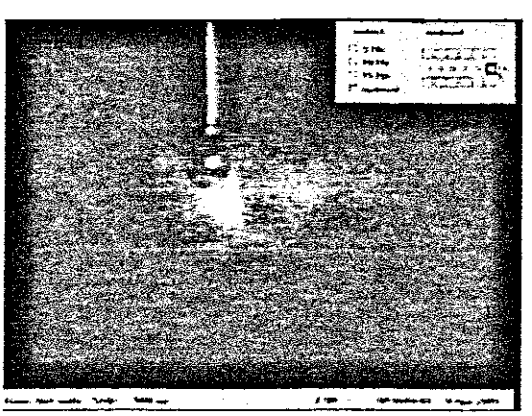

| | Photo | Actual |
|---|---|---|
| Droplet ∅ | 6,60 | **2,143** |
| Wire ∅ | 3,08 | 1,00 |

Welding current **203A**, wire speed **12.5m/min**

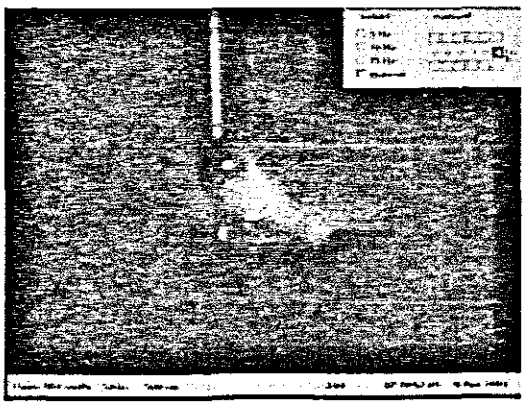

| | Photo | Actual |
|---|---|---|
| Droplet Ø | 7,72 | **2,238** |
| Wire Ø | 3,45 | 1,00 |

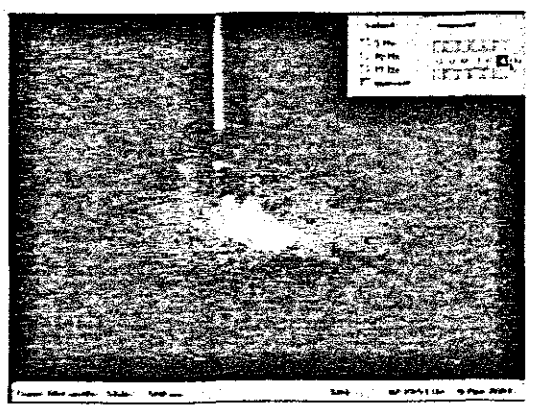

| | Photo | Actual |
|---|---|---|
| Droplet Ø | 7,73 | **2,247** |
| Wire Ø | 3,44 | 1,00 |

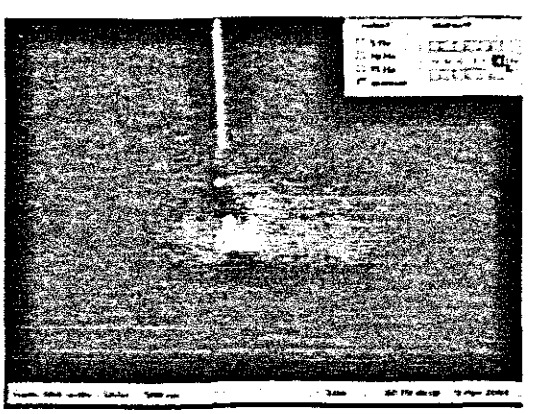

| | Photo | Actual |
|---|---|---|
| Droplet Ø | 7,70 | **2,245** |
| Wire Ø | 3,43 | 1,00 |

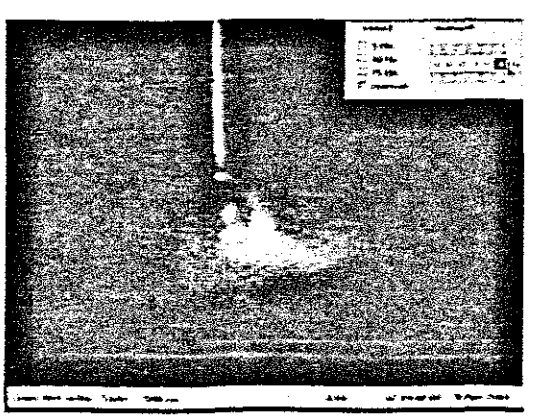

| | Photo | Actual |
|---|---|---|
| Droplet Ø | 7,80 | **2,274** |
| Wire Ø | 3,43 | 1,00 |

Welding current **205A**, wire speed **13m/min**

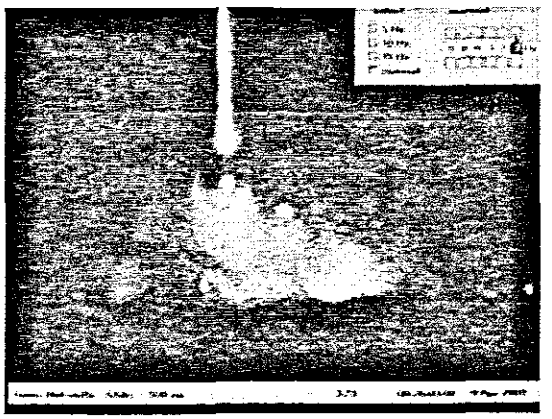

| | Photo | Actual |
|---|---|---|
| Droplet ∅ | 7,40 | **2,027** |
| Wire ∅ | 3,65 | 1,00 |

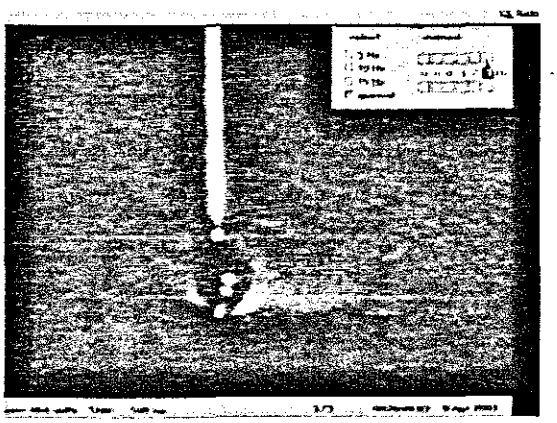

| | Photo | Actual |
|---|---|---|
| Droplet ∅ | 7,52 | **2,118** |
| Wire ∅ | 3,55 | 1,00 |

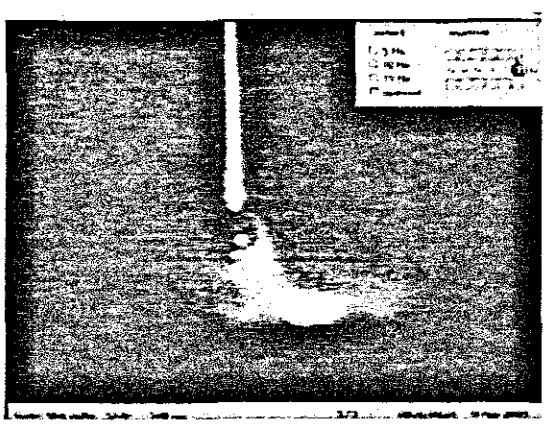

| | Photo | Actual |
|---|---|---|
| Droplet ∅ | 7,50 | **2,016** |
| Wire ∅ | 3,72 | 1,00 |

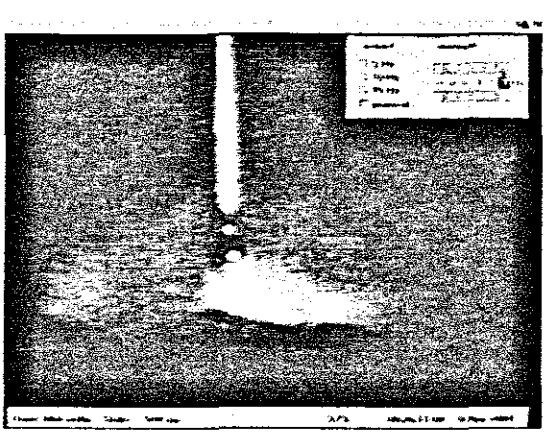

| | Photo | Actual |
|---|---|---|
| Droplet ∅ | 6,00 | **2,201** |
| Wire ∅ | 2,72 | 1,00 |

Welding current **206A**, wire speed **13.5m/min**

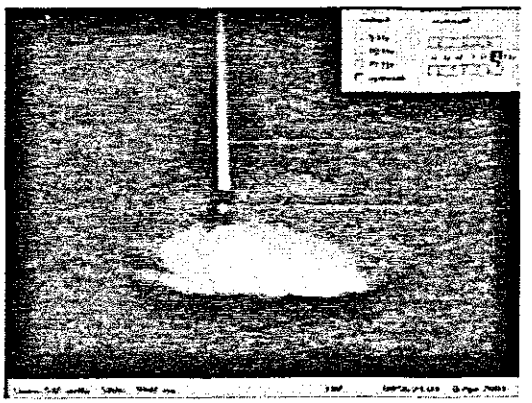

| | Photo | Actual |
|---|---|---|
| Droplet ∅ | 6,96 | **2,40** |
| Wire ∅ | 2,90 | 1,00 |

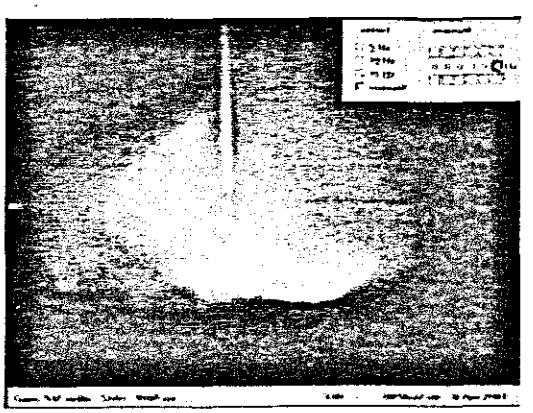

| | Photo | Actual |
|---|---|---|
| Droplet ∅ | 6,00 | **2,40** |
| Wire ∅ | 2,50 | 1,00 |

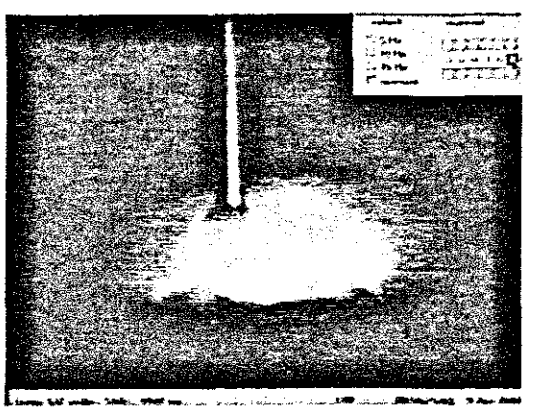

| | Photo | Actual |
|---|---|---|
| Droplet ∅ | 6,80 | **2,509** |
| Wire ∅ | 2,71 | 1,00 |

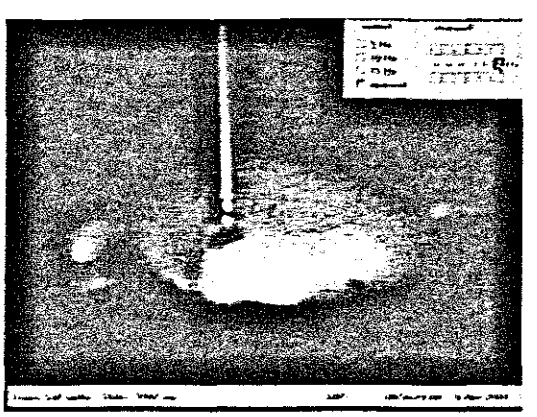

| | Photo | Actual |
|---|---|---|
| Droplet ∅ | 6,30 | **2,423** |
| Wire ∅ | 2,60 | 1,00 |

Welding current **212A**, wire speed **14m/min**

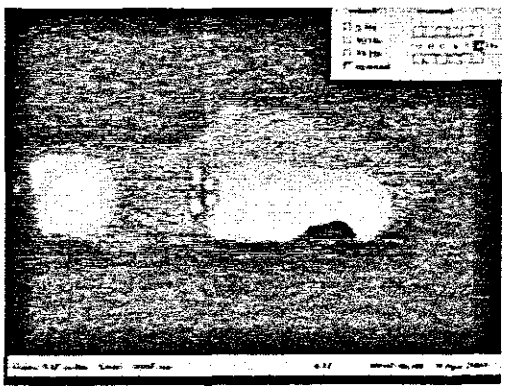

| | Photo | Actual |
|---|---|---|
| Droplet ∅ | 5,00 | **2,119** |
| Wire ∅ | 2,36 | 1,00 |

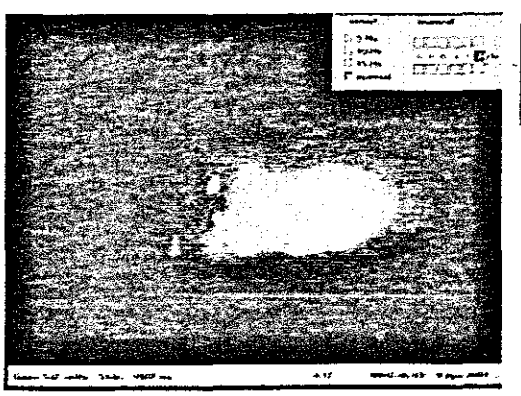

| | Photo | Actual |
|---|---|---|
| Droplet ∅ | 4,00 | -- |
| Wire ∅ | -- | 1,00 |

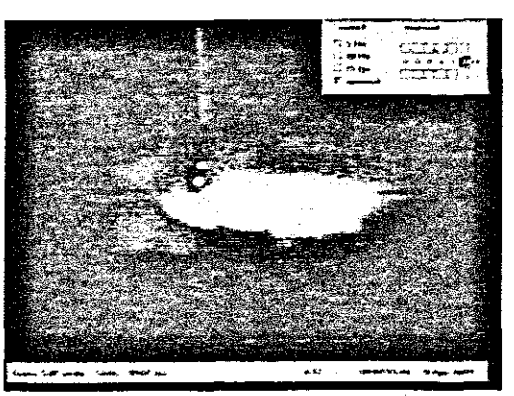

| | Photo | Actual |
|---|---|---|
| Droplet ∅ | 4,58 | **2,082** |
| Wire ∅ | 2,20 | 1,00 |

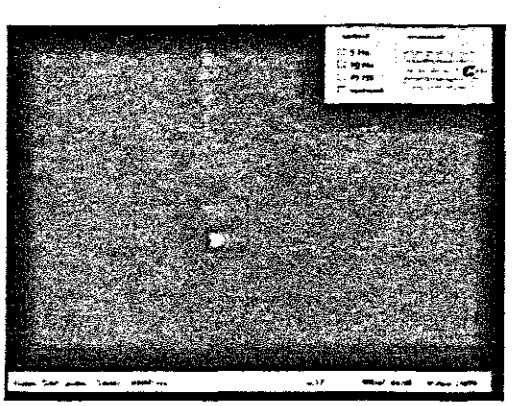

| | Photo | Actual |
|---|---|---|
| Droplet ∅ | 4,90 | **2,207** |
| Wire ∅ | 2,22 | 1,00 |

Welding current **217A**, wire speed **14.5m/min**

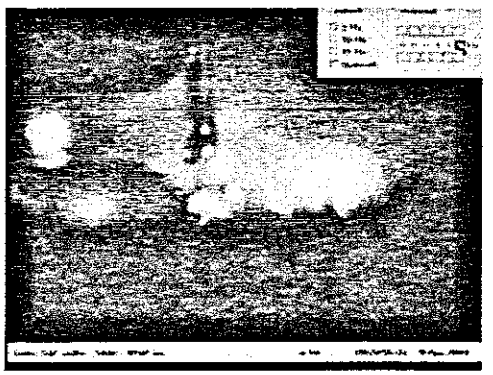

| | Photo | Actual |
|---|---|---|
| Droplet ∅ | 6,10 | **1,525** |
| Wire ∅ | 4,00 | 1,00 |

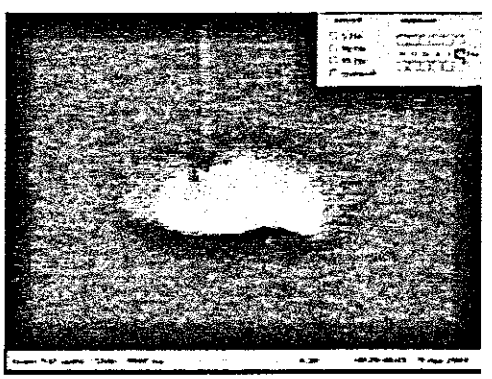

| | Photo | Actual |
|---|---|---|
| Droplet ∅ | 4,40 | **1,222** |
| Wire ∅ | 3,60 | 1,00 |

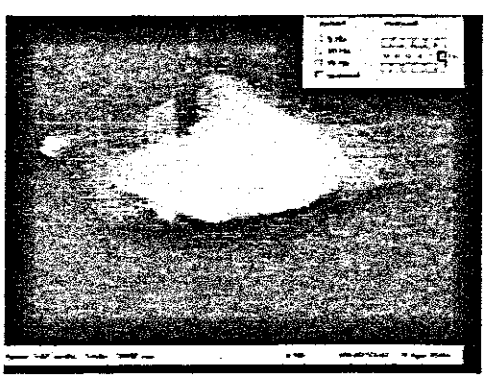

| | Photo | Actual |
|---|---|---|
| Droplet ∅ | 5,50 | **1,467** |
| Wire ∅ | 3,75 | 1,00 |

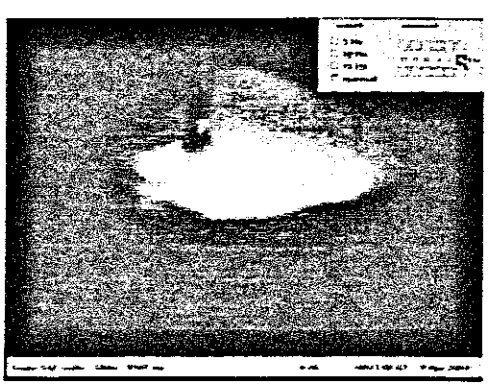

| | Photo | Actual |
|---|---|---|
| Droplet ∅ | 5,90 | **1,475** |
| Wire ∅ | 4,00 | 1,00 |

Welding current **216A**, wire speed **15m/min**

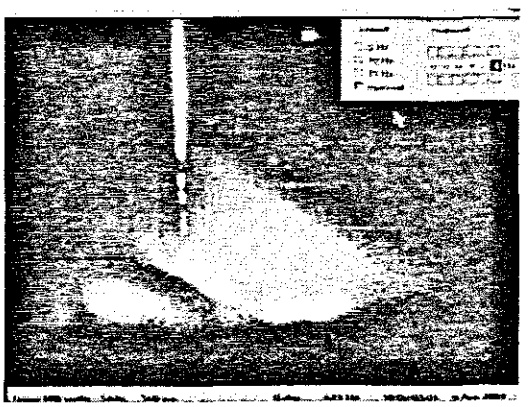

| | Photo | Actual |
|---|---|---|
| Droplet ∅ | 5,20 | **1,730** |
| Wire ∅ | 3,00 | 1,00 |

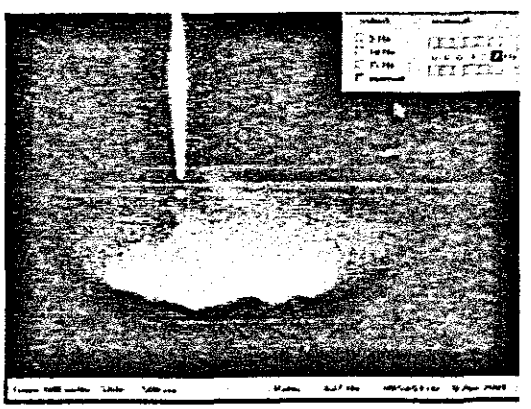

| | Photo | Actual |
|---|---|---|
| Droplet ∅ | 5,10 | **1,70** |
| Wire ∅ | 3,00 | 1,00 |

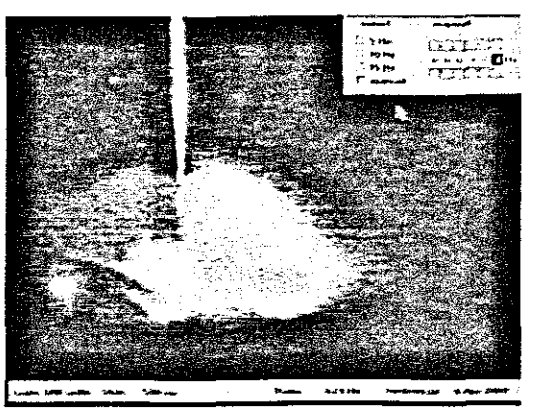

| | Photo | Actual |
|---|---|---|
| Droplet ∅ | 5,10 | **1,70** |
| Wire ∅ | 3,00 | 1,00 |

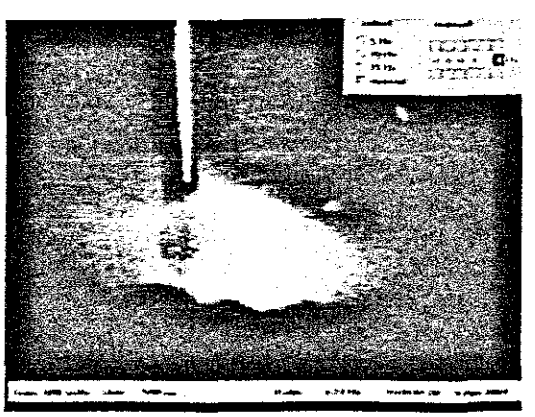

| | Photo | Actual |
|---|---|---|
| Droplet ∅ | 7,50 | **1,697** |
| Wire ∅ | 4,42 | 1,00 |

Welding current **220A**, wire speed **15.5m/min**

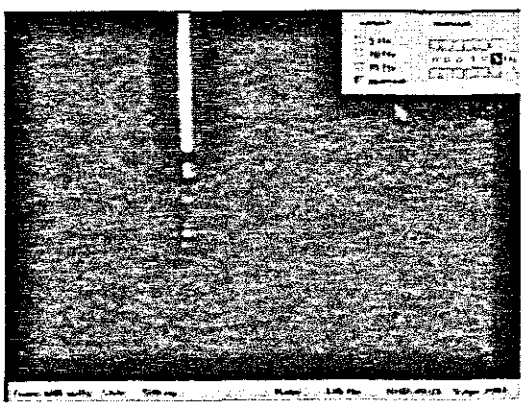

| | Photo | Actual |
|---|---|---|
| Droplet ∅ | 3,25 | **1,401** |
| Wire ∅ | 2,32 | 1,00 |

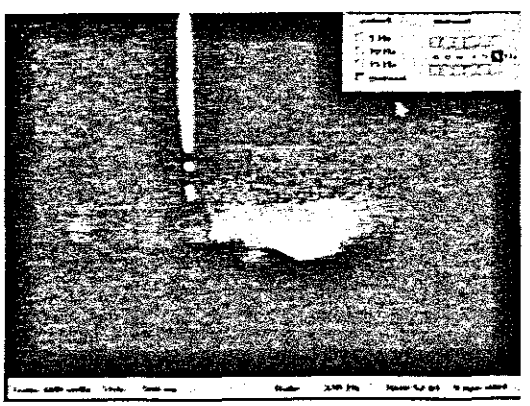

| | Photo | Actual |
|---|---|---|
| Droplet ∅ | 3,30 | **1,435** |
| Wire ∅ | 2,30 | 1,00 |

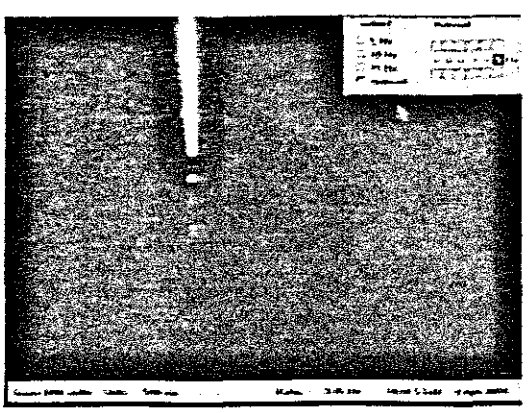

| | Photo | Actual |
|---|---|---|
| Droplet ∅ | -- | -- |
| Wire ∅ | -- | 1,00 |

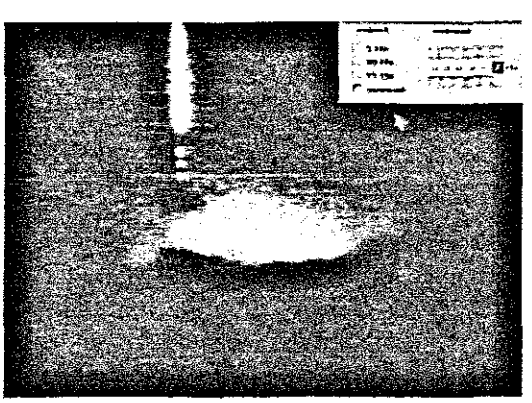

| | Photo | Actual |
|---|---|---|
| Droplet ∅ | 4,90 | **1,630** |
| Wire ∅ | 3,00 | 1,00 |

Welding current **221A**, wire speed **16m/min**

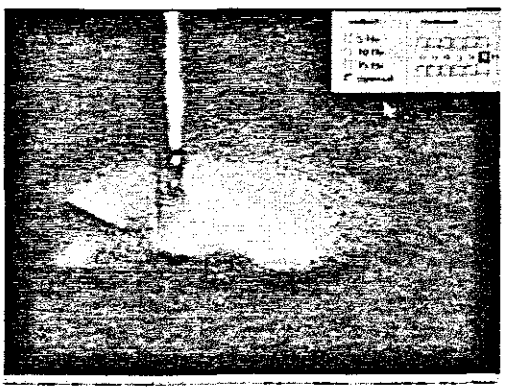

| | Photo | Actual |
|---|---|---|
| Droplet ∅ | 5,10 | **1,244** |
| Wire ∅ | 4,10 | 1,00 |

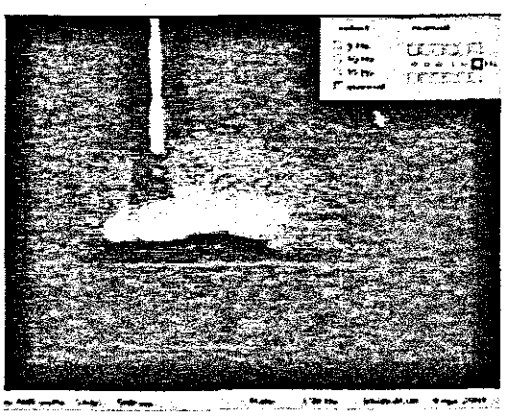

| | Photo | Actual |
|---|---|---|
| Droplet ∅ | 7,30 | **1,46** |
| Wire ∅ | 5,00 | 1,00 |

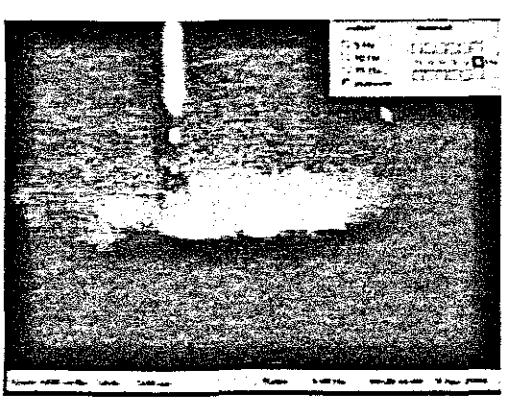

| | Photo | Actual |
|---|---|---|
| Droplet ∅ | 5,20 | **1,156** |
| Wire ∅ | 4,50 | 1,00 |

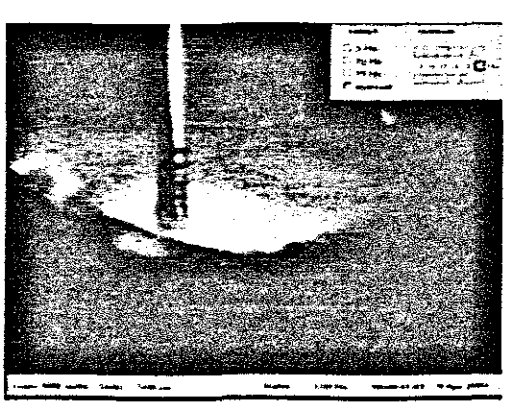

| | Photo | Actual |
|---|---|---|
| Droplet ∅ | 5,00 | **1,163** |
| Wire ∅ | 4,30 | 1,00 |

Welding current **222A**, wire speed **16.5m/min**

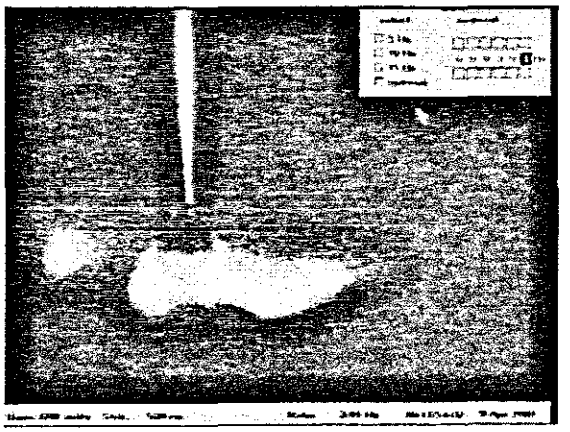

| | Photo | Actual |
|---|---|---|
| Droplet ∅ | 9,20 | **1,095** |
| Wire ∅ | 8,40 | 1,00 |

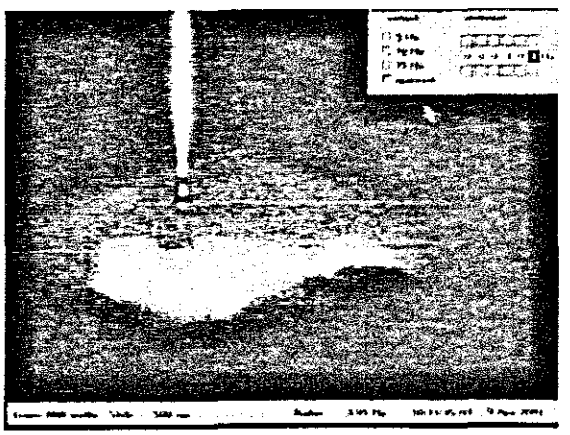

| | Photo | Actual |
|---|---|---|
| Droplet ∅ | 6,60 | **1,015** |
| Wire ∅ | 6,50 | 1,00 |

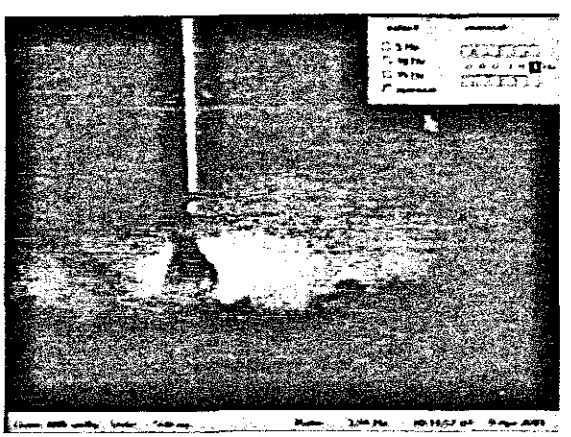

| | Photo | Actual |
|---|---|---|
| Droplet ∅ | 8,30 | **1,239** |
| Wire ∅ | 6,70 | 1,00 |

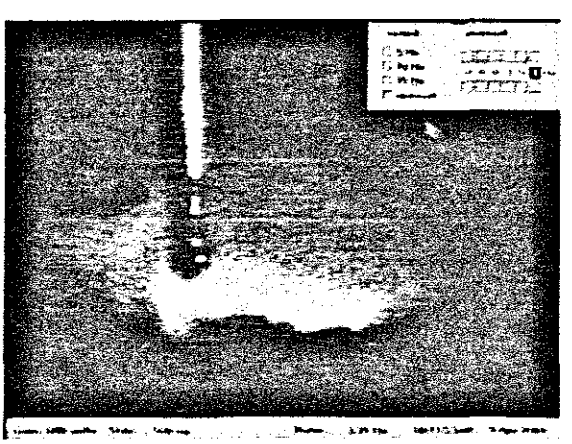

| | Photo | Actual |
|---|---|---|
| Droplet ∅ | 6,80 | **1,133** |
| Wire ∅ | 6,00 | 1,00 |

Welding current **226A**, wire speed **16.7m/min**

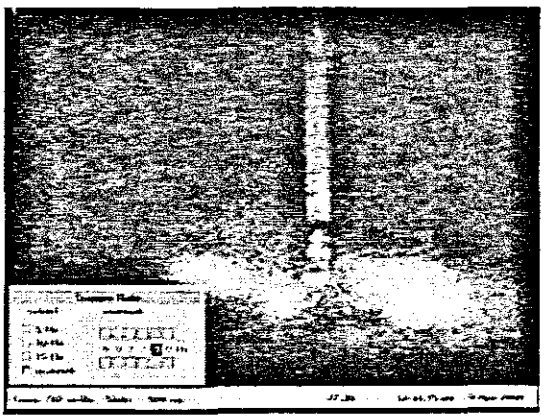

| | Photo | Actual |
|---|---|---|
| Droplet ∅ | 3,00 | **1,00** |
| Wire ∅ | 3,00 | 1,00 |

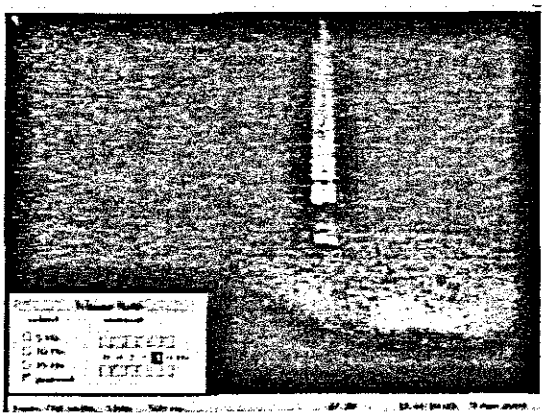

| | Photo | Actual |
|---|---|---|
| Droplet ∅ | 3,01 | **0,997** |
| Wire ∅ | 3,02 | 1,00 |

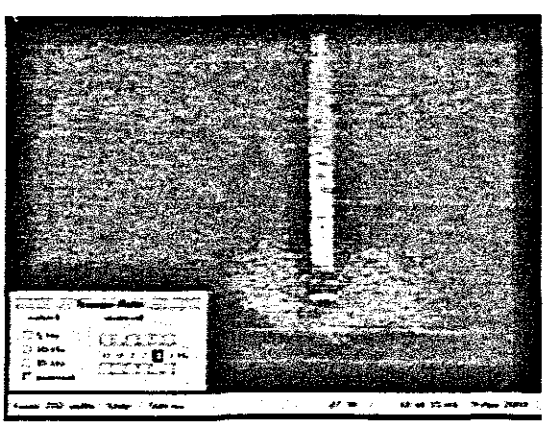

| | Photo | Actual |
|---|---|---|
| Droplet ∅ | 3,01 | **1,003** |
| Wire ∅ | 3,00 | 1,00 |

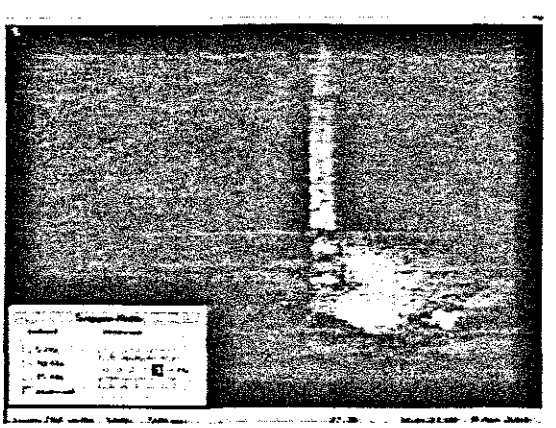

| | Photo | Actual |
|---|---|---|
| Droplet ∅ | 3,01 | **1,00** |
| Wire ∅ | 3,01 | 1,00 |

Welding current **227A**, wire speed **16.8m/min**

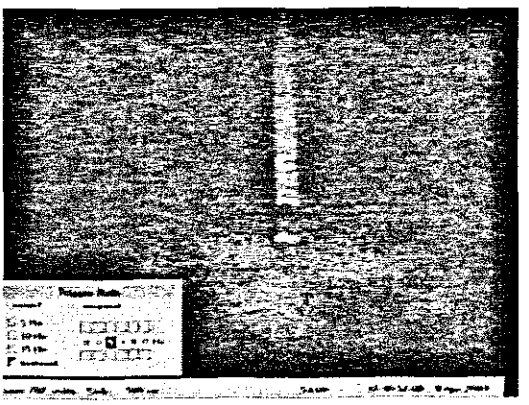

| | Photo | Actual |
|---|---|---|
| Droplet ∅ | 3,00 | **1,00** |
| Wire ∅ | 3,00 | 1,00 |

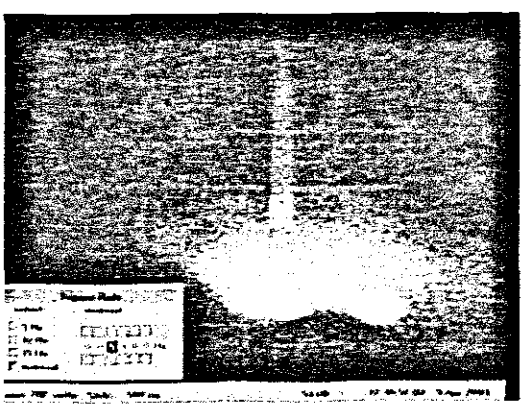

| | Photo | Actual |
|---|---|---|
| Droplet ∅ | 2,80 | **0,933** |
| Wire ∅ | 3,00 | 1,00 |

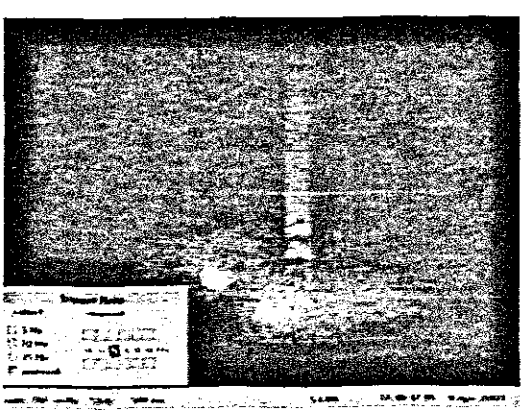

| | Photo | Actual |
|---|---|---|
| Droplet ∅ | 3,01 | **1,00** |
| Wire ∅ | 3,01 | 1,00 |

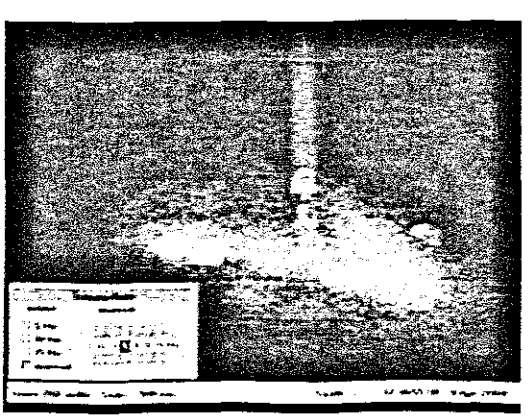

| | Photo | Actual |
|---|---|---|
| Droplet ∅ | 2,88 | **0,960** |
| Wire ∅ | 3,00 | 1,00 |

Welding current **230A**, wire speed **16.9m/min**

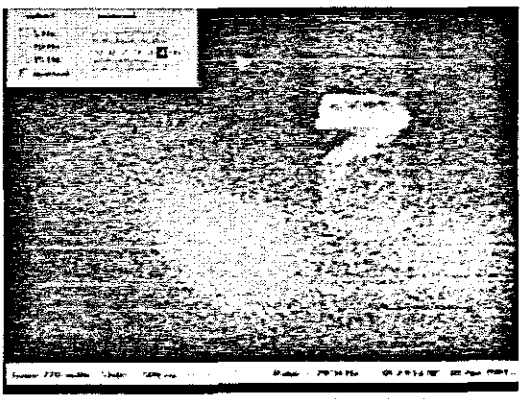

| | Photo | Actual |
|---|---|---|
| Droplet ∅ | 11.00 | **0,917** |
| Wire ∅ | 12,00 | 1,00 |

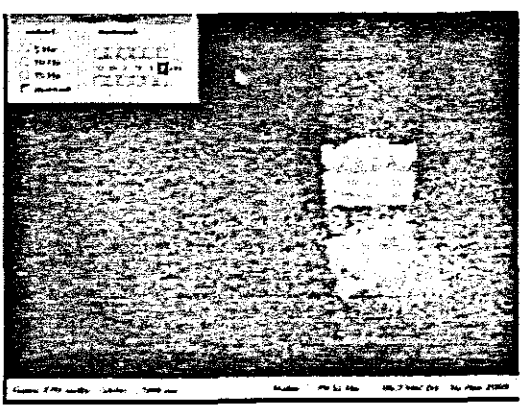

| | Photo | Actual |
|---|---|---|
| Droplet ∅ | 11,40 | **0,983** |
| Wire ∅ | 11,60 | 1,00 |

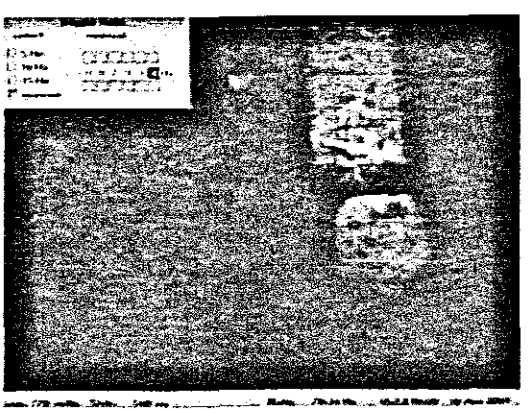

| | Photo | Actual |
|---|---|---|
| Droplet ∅ | 11,20 | **0,974** |
| Wire ∅ | 11,50 | 1,00 |

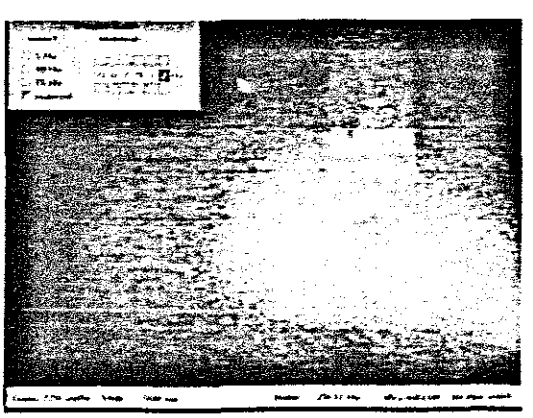

| | Photo | Actual |
|---|---|---|
| Droplet ∅ | 11,20 | **0,949** |
| Wire ∅ | 11,80 | 1,00 |

Welding current **229A**, wire speed **17m/min**

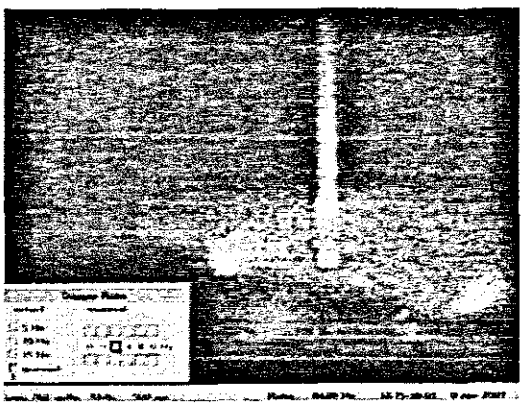

| | Photo | Actual |
|---|---|---|
| Droplet ∅ | 3,20 | **0,914** |
| Wire ∅ | 3,50 | 1,00 |

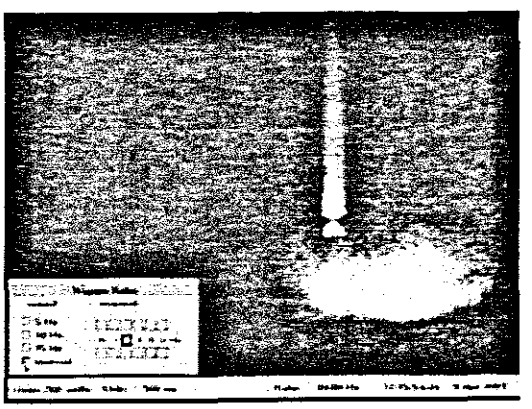

| | Photo | Actual |
|---|---|---|
| Droplet ∅ | 3,00 | **0,857** |
| Wire ∅ | 3,5 | 1,00 |

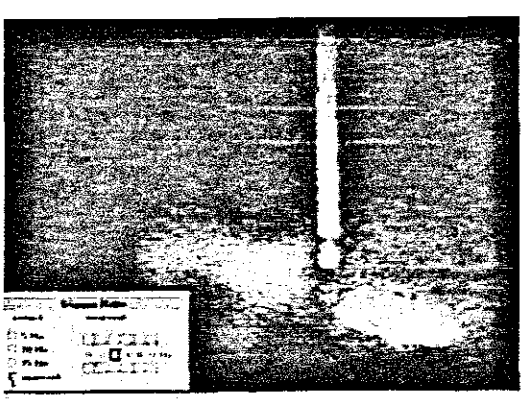

| | Photo | Actual |
|---|---|---|
| Droplet ∅ | 3,00 | **0,882** |
| Wire ∅ | 3,40 | 1,00 |

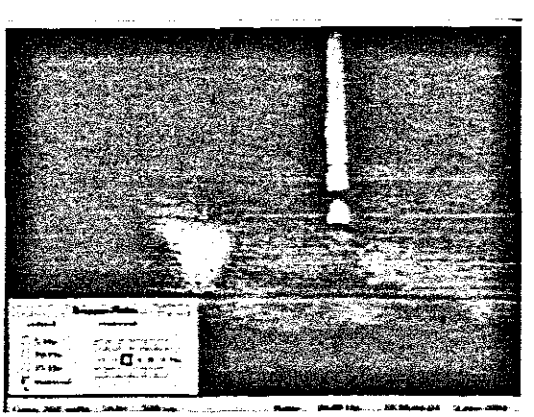

| | Photo | Actual |
|---|---|---|
| Droplet ∅ | 2,90 | **0,828** |
| Wire ∅ | 3,50 | 1,00 |

Welding current **231A**, wire speed **17.5m/min**

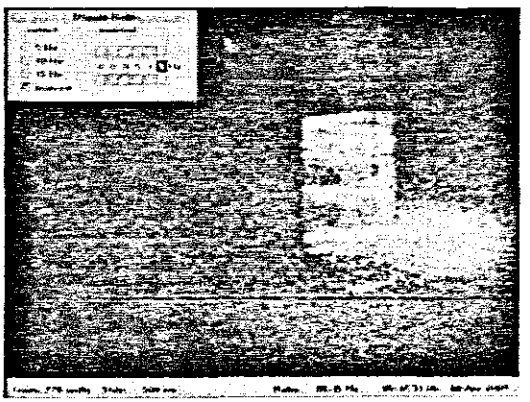

| | Photo | Actual |
|---|---|---|
| Droplet ∅ | 12,20 | **0,897** |
| Wire ∅ | 13,60 | 1,00 |

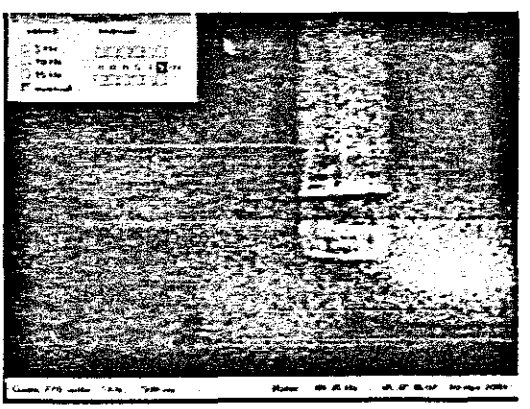

| | Photo | Actual |
|---|---|---|
| Droplet ∅ | 12,00 | **0,882** |
| Wire ∅ | 13,60 | 1,00 |

Welding current **234A**, wire speed **18.5m/min**

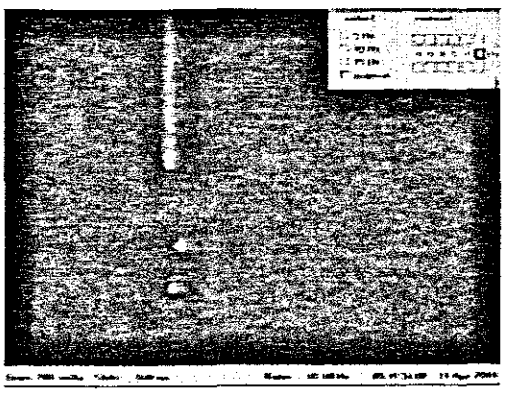

| | Photo | Actual |
|---|---|---|
| Droplet ∅ | 1,30 | **0,65** |
| Wire ∅ | 2,00 | 1,00 |

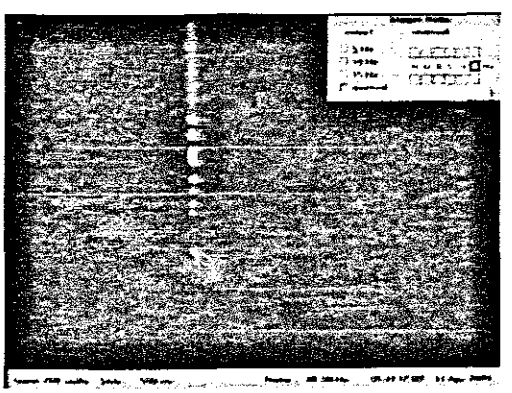

| | Photo | Actual |
|---|---|---|
| Droplet ∅ | 1,31 | **0,619** |
| Wire ∅ | 2,10 | 1,00 |

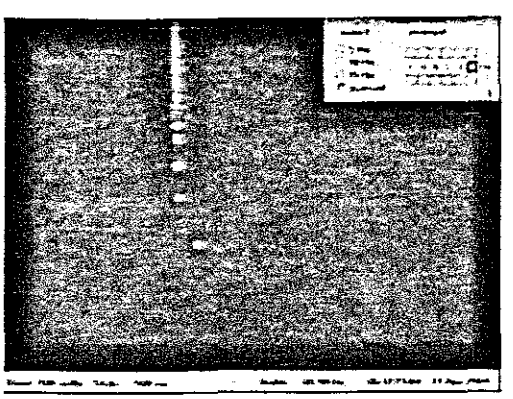

| | Photo | Actual |
|---|---|---|
| Droplet ∅ | 1,00 | **0,435** |
| Wire ∅ | 2,10 | 1,00 |

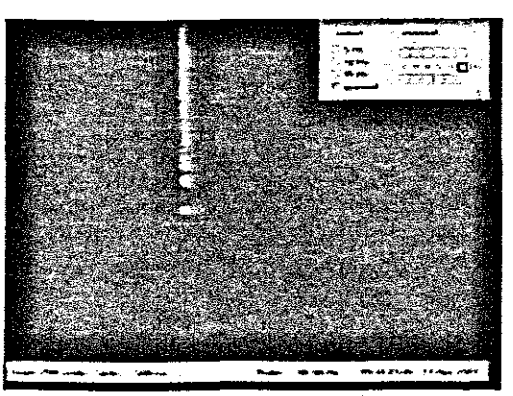

| | Photo | Actual |
|---|---|---|
| Droplet ∅ | 1,31 | **0,565** |
| Wire ∅ | 2,30 | 1,00 |

Welding current **238A**, wire speed **19m/min**

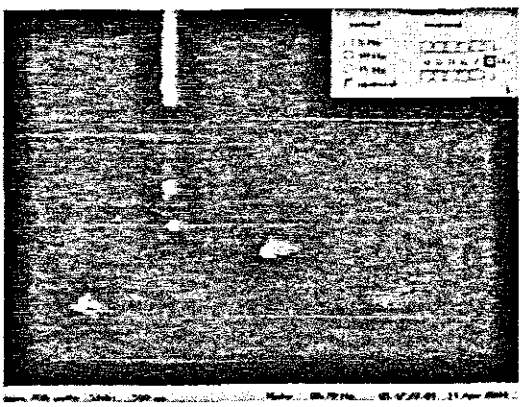

| | Photo | Actual |
|---|---|---|
| Droplet ∅ | 1,01 | **0,668** |
| Wire ∅ | 1,50 | 1,00 |

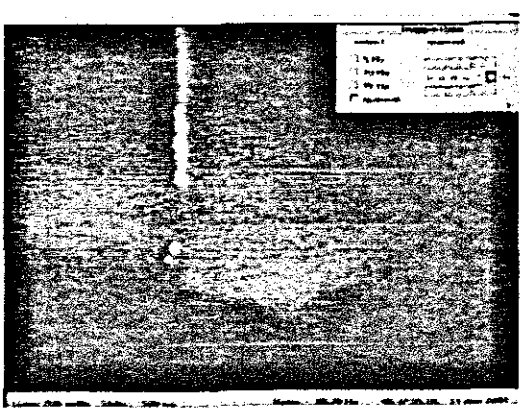

| | Photo | Actual |
|---|---|---|
| Droplet ∅ | 2,50 | **0,862** |
| Wire ∅ | 2,90 | 1,00 |

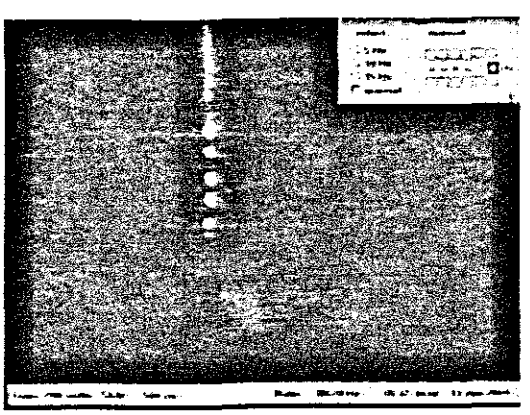

| | Photo | Actual |
|---|---|---|
| Droplet ∅ | 1,50 | **0,75** |
| Wire ∅ | 2,00 | 1,00 |

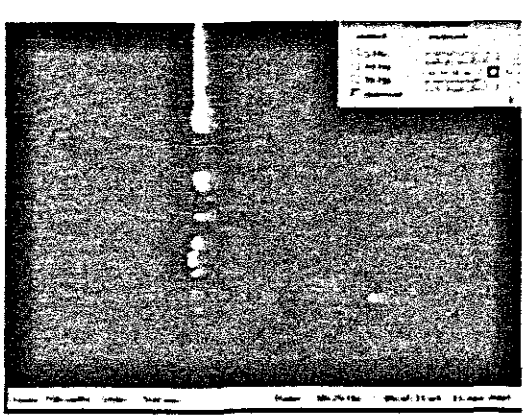

| | Photo | Actual |
|---|---|---|
| Droplet ∅ | 2,00 | **0,645** |
| Wire ∅ | 3,10 | 1,00 |

Welding current **245A**, wire speed **20m/min**

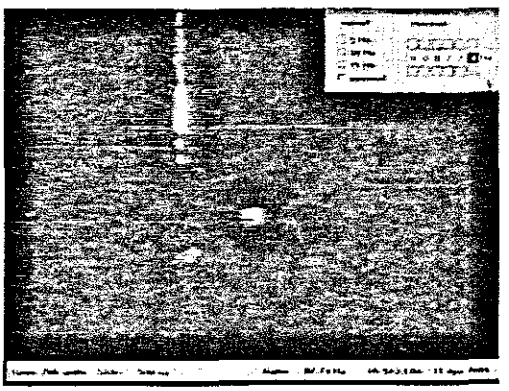

| | Photo | Actual |
|---|---|---|
| Droplet ∅ | 3,00 | **0,75** |
| Wire ∅ | 4,00 | 1,00 |

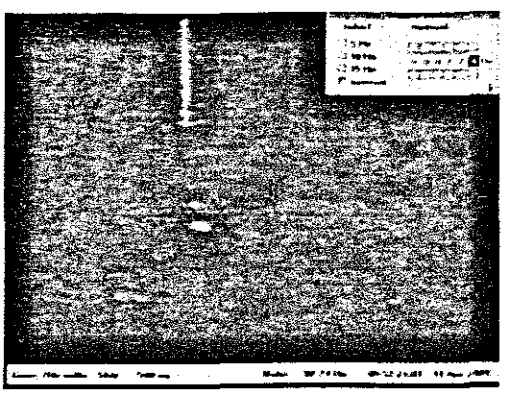

| | Photo | Actual |
|---|---|---|
| Droplet ∅ | 2,20 | **0,733** |
| Wire ∅ | 3,00 | 1,00 |

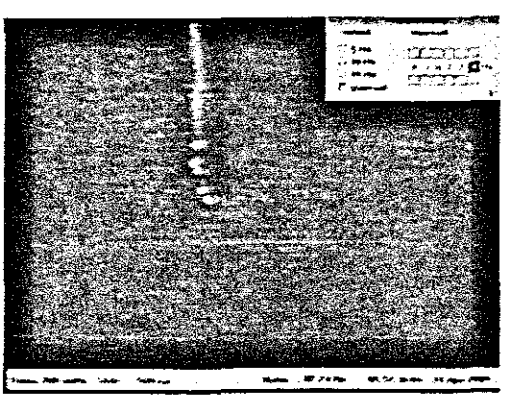

| | Photo | Actual |
|---|---|---|
| Droplet ∅ | 2,30 | **0,719** |
| Wire ∅ | 3,20 | 1,00 |

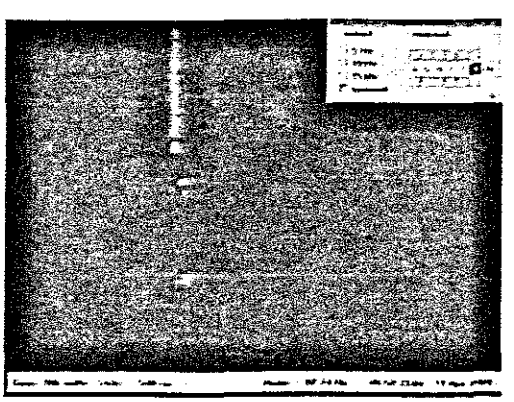

| | Photo | Actual |
|---|---|---|
| Droplet ∅ | 2,20 | **0,688** |
| Wire ∅ | 3,20 | 1,00 |

Welding current **258A**, wire speed **22m/min**

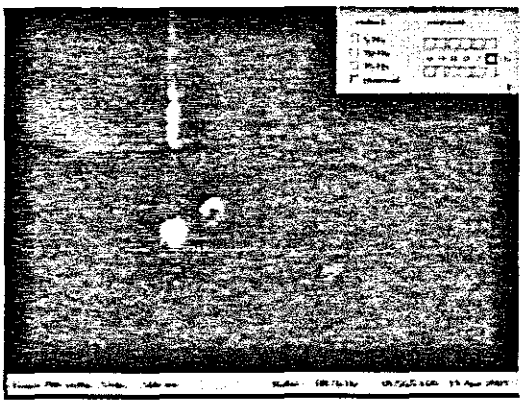

| | Photo | Actual |
|---|---|---|
| Droplet ∅ | 4,41 | **0,730** |
| Wire ∅ | 6,02 | 1,00 |

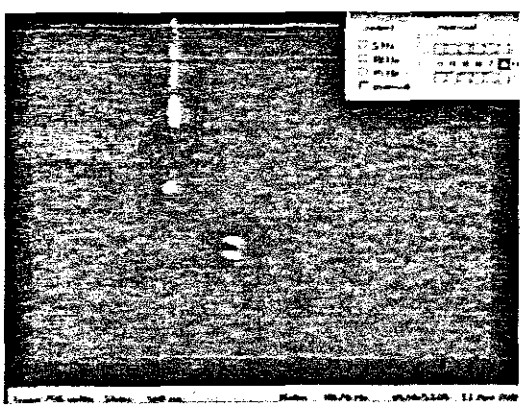

| | Photo | Actual |
|---|---|---|
| Droplet ∅ | 3,00 | **0,714** |
| Wire ∅ | 4,20 | 1,00 |

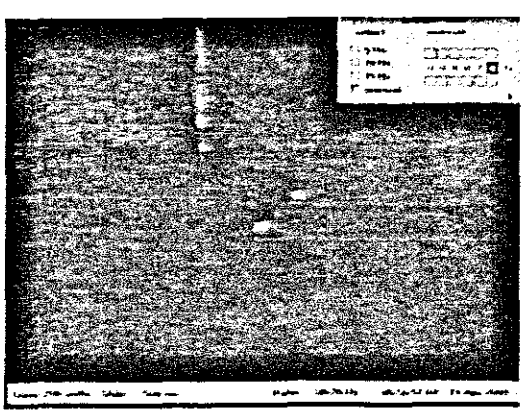

| | Photo | Actual |
|---|---|---|
| Droplet ∅ | 3,00 | **0,750** |
| Wire ∅ | 4,00 | 1,00 |

Welding current **260A**, wire speed **22m/min**

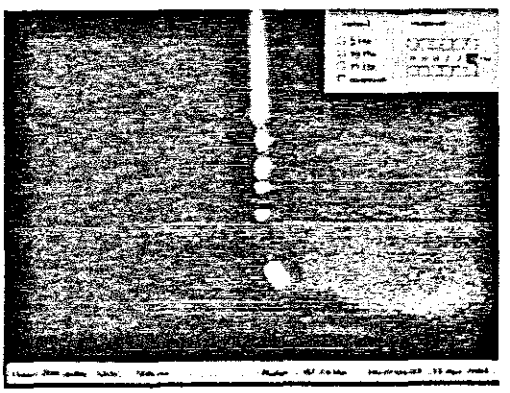

| | Photo | Actual |
|---|---|---|
| Droplet ∅ | 2,51 | **0,718** |
| Wire ∅ | 3,48 | 1,00 |

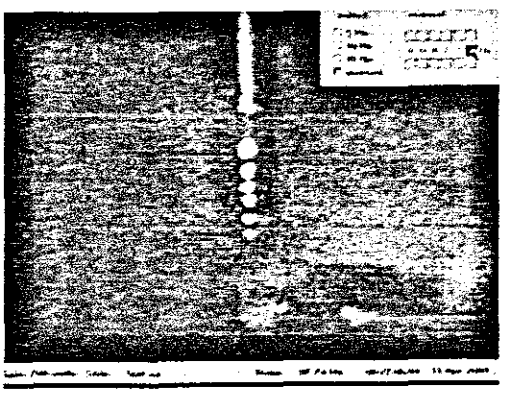

| | Photo | Actual |
|---|---|---|
| Droplet ∅ | 2,00 | **0,719** |
| Wire ∅ | 2,78 | 1,00 |

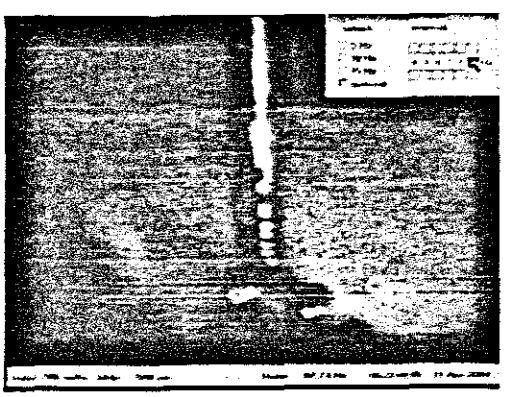

| | Photo | Actual |
|---|---|---|
| Droplet ∅ | 2,30 | **0,767** |
| Wire ∅ | 3,00 | 1,00 |

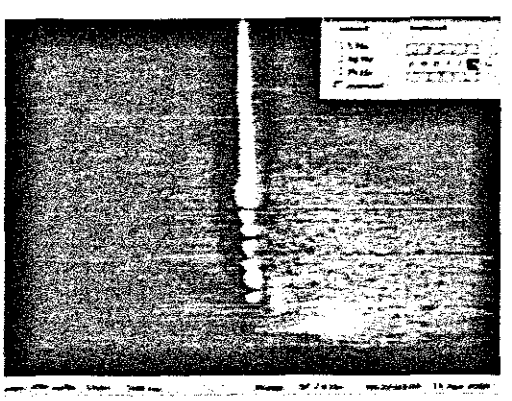

| | Photo | Actual |
|---|---|---|
| Droplet ∅ | 2,21 | **0,710** |
| Wire ∅ | 3,11 | 1,00 |

Welding current **265A**, wire speed **24m/min**

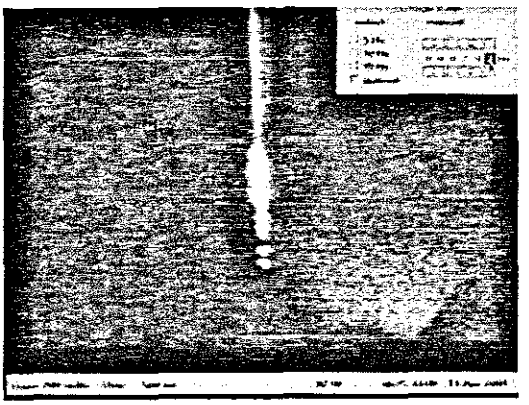

| | Photo | Actual |
|---|---|---|
| Droplet ∅ | 2,00 | **0,667** |
| Wire ∅ | 2,99 | 1,00 |

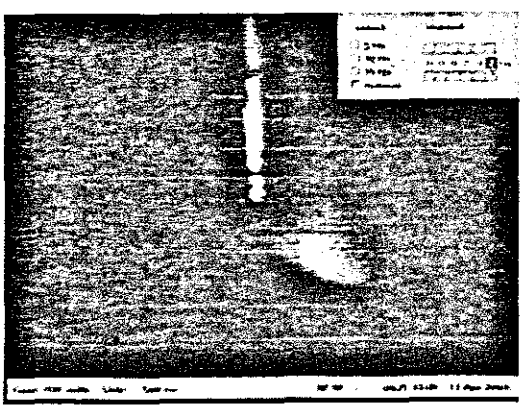

| | Photo | Actual |
|---|---|---|
| Droplet ∅ | 1,80 | **0,581** |
| Wire ∅ | 3,1 | 1,00 |

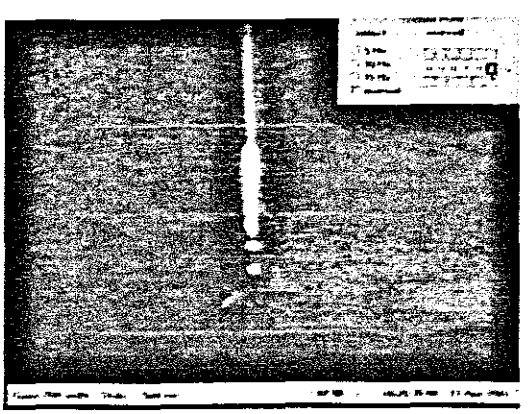

| | Photo | Actual |
|---|---|---|
| Droplet ∅ | 2,40 | **0,674** |
| Wire ∅ | 3,56 | 1,00 |

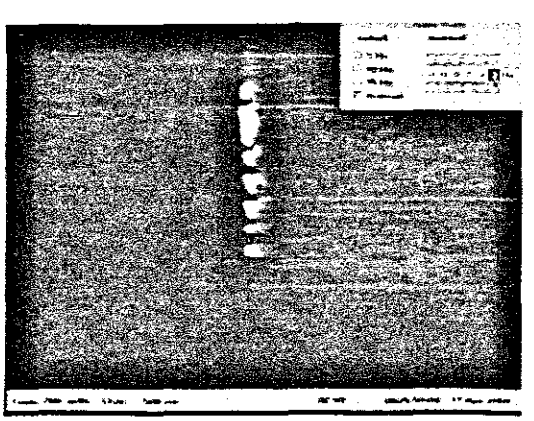

| | Photo | Actual |
|---|---|---|
| Droplet ∅ | 2,00 | **0,692** |
| Wire ∅ | 2,89 | 1,00 |

# Appendix E2

**Laserstrobe Images of MIG Welding with 99%Ar-1%$O_2$ Shielding Gas**

The table below represents the mean droplet diameters obtained from the welding images of a 1mm mild steel electrode with 99%Argon-1%Oxygen shielding. A minimum of 4 images per weld run was used to calculate the mean droplet diameter.

| Weld No. | Wire Feed Rate | Mean droplet diameter |
|---|---|---|
| 1 | 10 | **1.405** |
| 2 | 11 | **1.388** |
| 3 | 11.5 | **1.370** |
| 4 | 12 | **1.301** |
| 5 | 12.5 | **1.225** |
| 6 | 13 | **1.080** |
| 7 | 13.5 | **1.059** |
| 8 | 14 | **1.047** |
| 9 | 14.5 | **1.018** |
| 10 | 15 | **1.040** |
| 11 | 15.5 | **1.037** |
| 12 | 16 | **1.035** |
| 13 | 16.5 | **1.005** |
| 14 | 17 | **1.005** |
| 15 | 17.5 | **1.000** |
| 16 | 18 | **1.003** |
| 17 | 18.5 | **0.993** |
| 18 | 19 | **0.988** |
| 19 | 19.5 | **0.988** |
| 20 | 20 | **0.975** |
| | | |

Welding current **176A**, wire speed **10m/min**

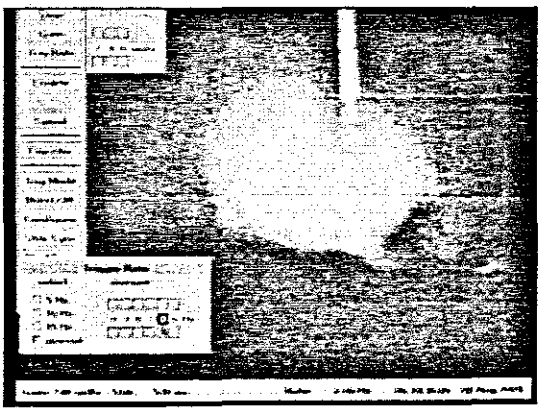

| | Photo | Actual |
|---|---|---|
| Droplet ∅ | 3.60 | **1.20** |
| Wire ∅ | 3.00 | 1,00 |

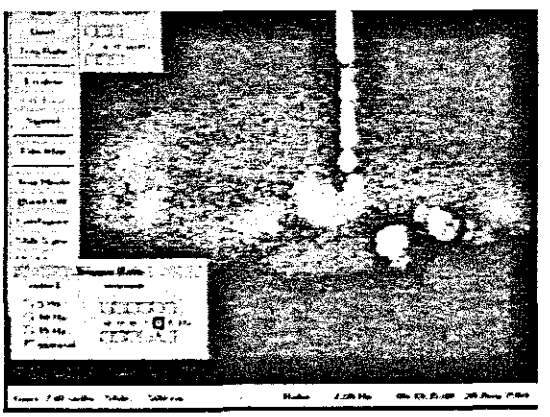

| | Photo | Actual |
|---|---|---|
| Droplet ∅ | 4.82 | **1.60** |
| Wire ∅ | 3.01 | 1,00 |

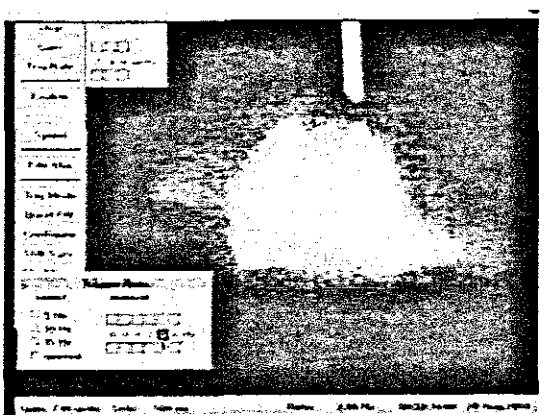

| | Photo | Actual |
|---|---|---|
| Droplet ∅ | 3.62 | **1.25** |
| Wire ∅ | 2.90 | 1,00 |

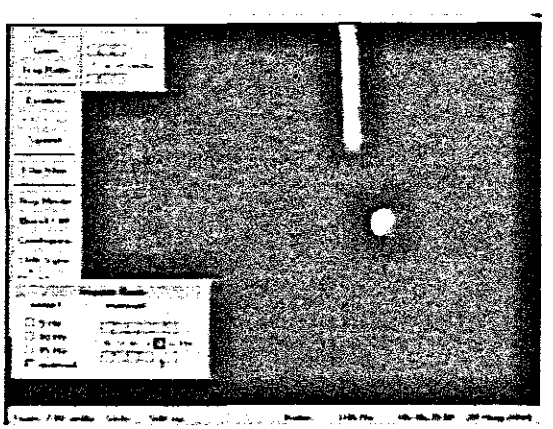

| | Photo | Actual |
|---|---|---|
| Droplet ∅ | 4.34 | **1.57** |
| Wire ∅ | 2.76 | 1,00 |

Welding current **185A**, wire speed **11m/min**

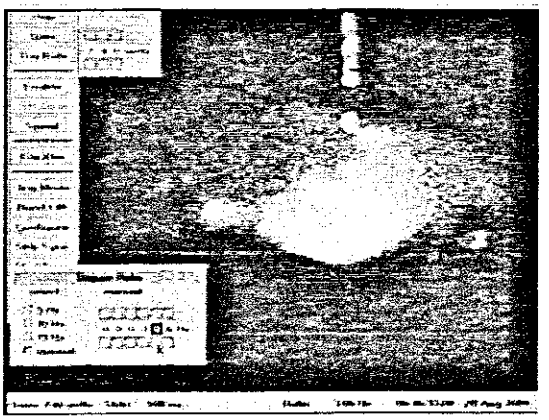

| | Photo | Actual |
|---|---|---|
| Droplet ∅ | 3.83 | **1.462** |
| Wire ∅ | 2.62 | 1,00 |

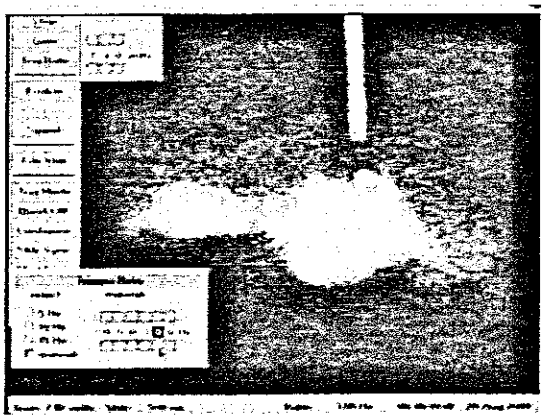

| | Photo | Actual |
|---|---|---|
| Droplet ∅ | 3.25 | **1.31** |
| Wire ∅ | 2.48 | 1,00 |

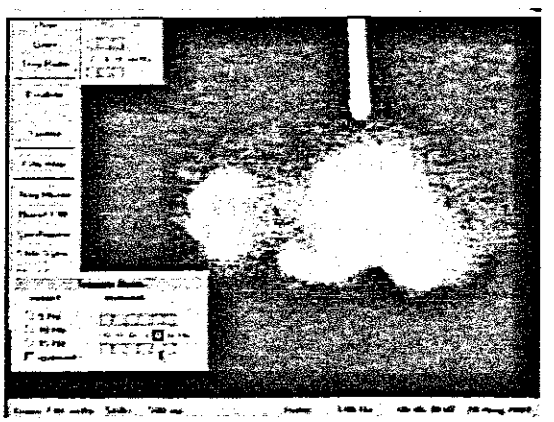

| | Photo | Actual |
|---|---|---|
| Droplet ∅ | 4.12 | **1.36** |
| Wire ∅ | 3.02 | 1,00 |

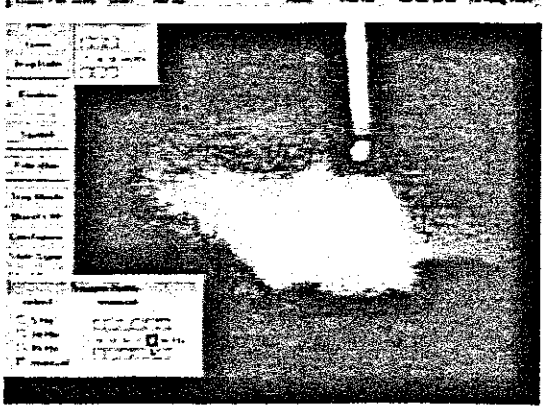

| | Photo | Actual |
|---|---|---|
| Droplet ∅ | 3.86 | **1.420** |
| Wire ∅ | 2.72 | 1,00 |

Welding current **191A**, wire speed **11.5m/min**

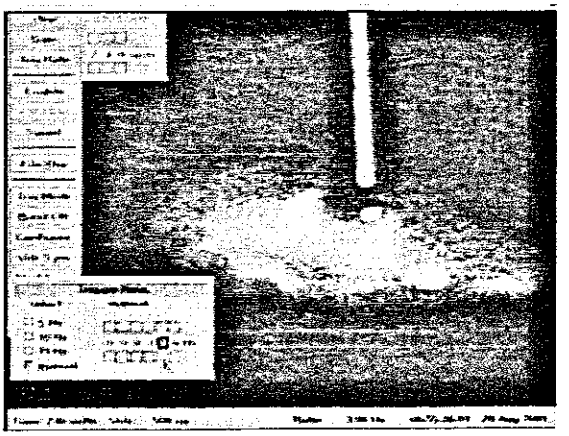

| | Photo | Actual |
|---|---|---|
| Droplet Ø | 3.75 | **1.390** |
| Wire Ø | 2.70 | 1,00 |

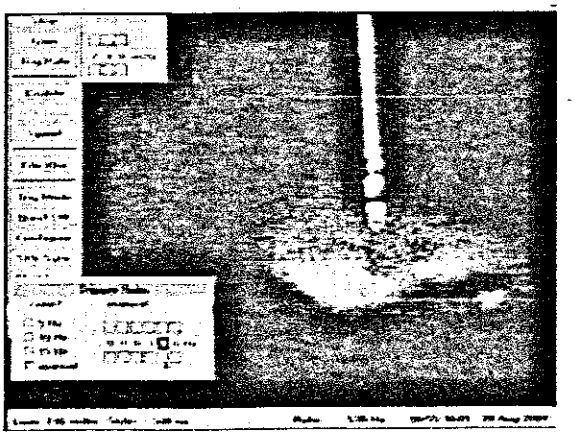

| | Photo | Actual |
|---|---|---|
| Droplet Ø | 3.62 | **1.341** |
| Wire Ø | 2.70 | 1,00 |

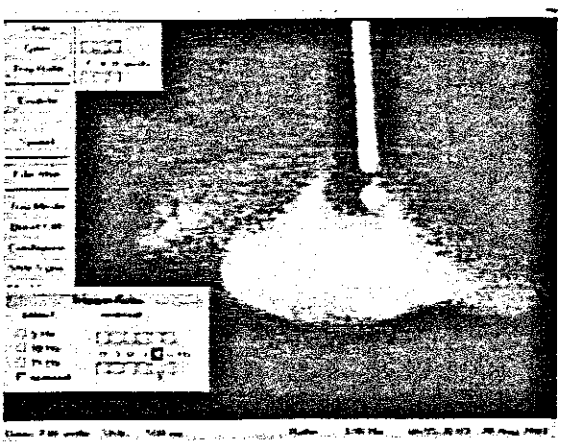

| | Photo | Actual |
|---|---|---|
| Droplet Ø | 4.70 | **1.407** |
| Wire Ø | 3.34 | 1,00 |

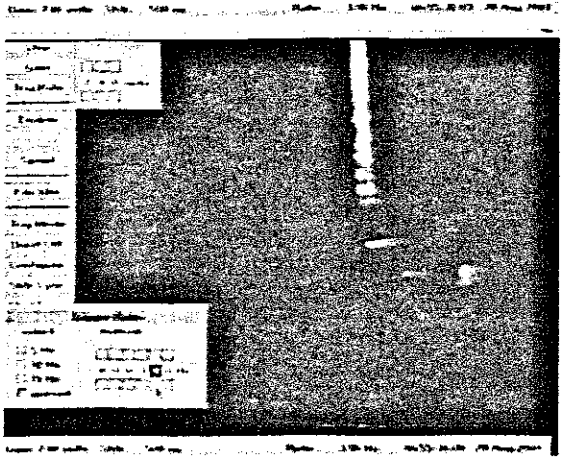

| | Photo | Actual |
|---|---|---|
| Droplet Ø | 3.44 | **1.342** |
| Wire Ø | 2.56 | 1,00 |

Welding current **194A,** wire speed **12m/min**

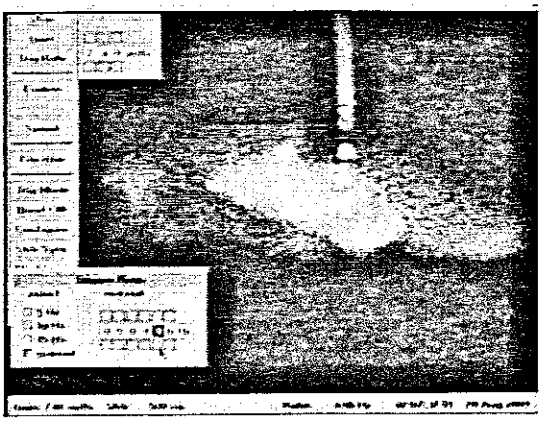

| | Photo | Actual |
|---|---|---|
| Droplet ∅ | 3.12 | **1.20** |
| Wire ∅ | 2.60 | 1,00 |

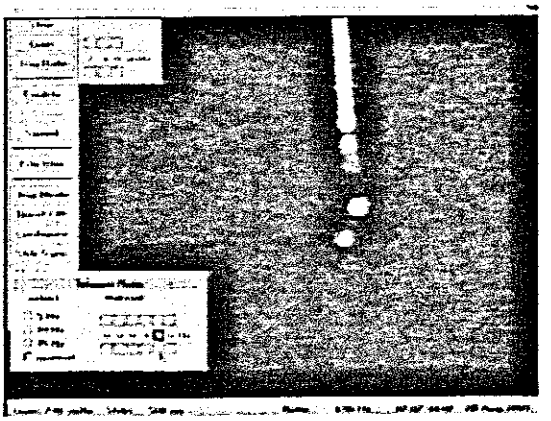

| | Photo | Actual |
|---|---|---|
| Droplet ∅ | 3.20 | **1.07** |
| Wire ∅ | 3.00 | 1,00 |

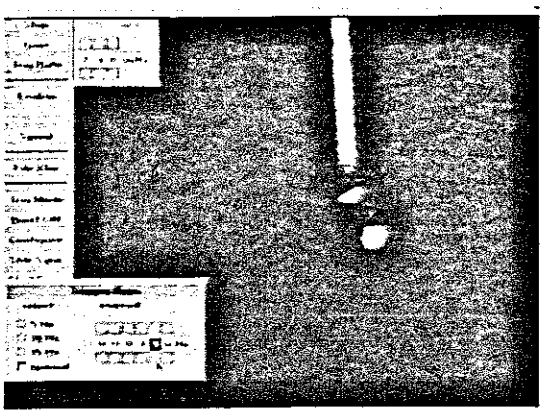

| | Photo | Actual |
|---|---|---|
| Droplet ∅ | 3.62 | **1.21** |
| Wire ∅ | 3.00 | 1,00 |

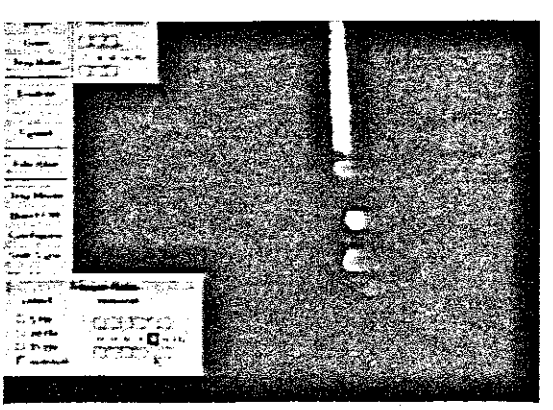

| | Photo | Actual |
|---|---|---|
| Droplet ∅ | 3.20 | **1.23** |
| Wire ∅ | 2.60 | 1,00 |

Welding current **198A**, wire speed **12.5m/min**

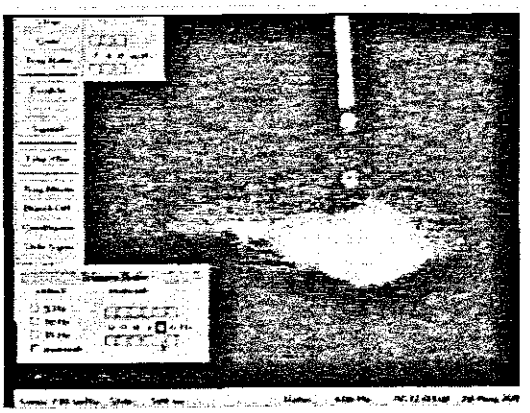

| | Photo | Actual |
|---|---|---|
| Droplet ∅ | 2.88 | **1.17** |
| Wire ∅ | 2.46 | 1,00 |

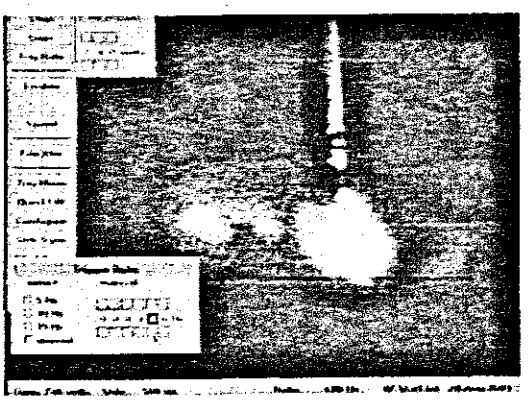

| | Photo | Actual |
|---|---|---|
| Droplet ∅ | 3.00 | **1.18** |
| Wire ∅ | 2.54 | 1,00 |

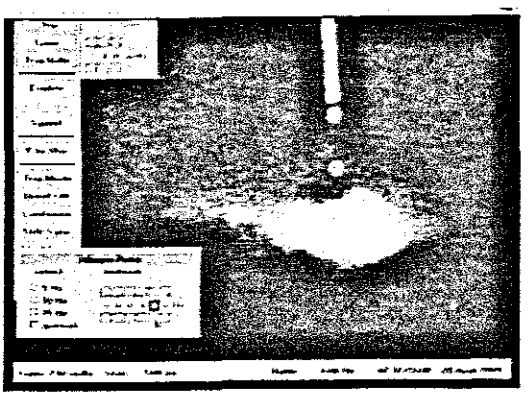

| | Photo | Actual |
|---|---|---|
| Droplet ∅ | 2.44 | **0.99** |
| Wire ∅ | 2.46 | 1,00 |

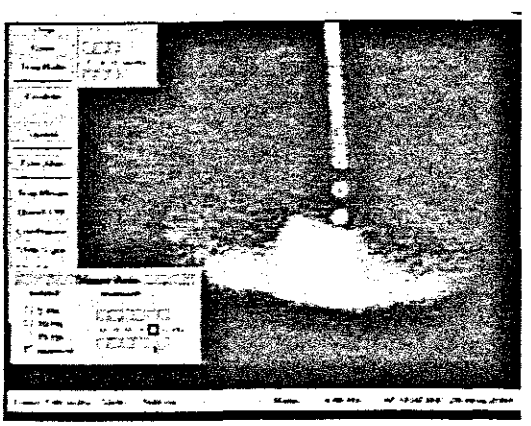

| | Photo | Actual |
|---|---|---|
| Droplet ∅ | 2.68 | **1.16** |
| Wire ∅ | 2.32 | 1,00 |

Welding current **201A**, wire speed **13 m/min**

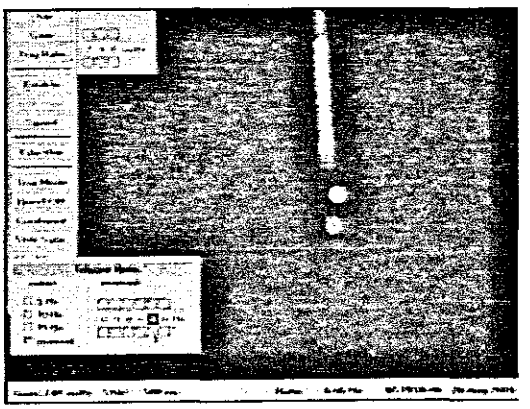

| | Photo | Actual |
|---|---|---|
| Droplet Ø | 2.56 | **1.08** |
| Wire Ø | 2.36 | 1,00 |

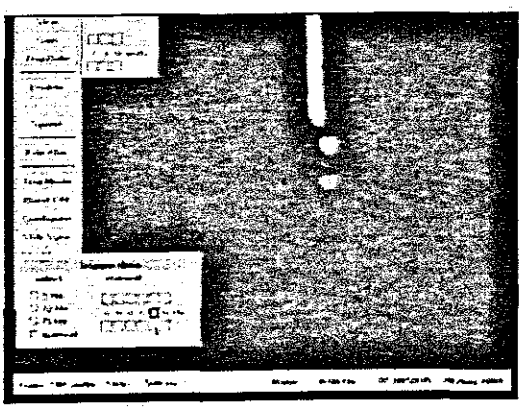

| | Photo | Actual |
|---|---|---|
| Droplet Ø | 2.78 | **1.18** |
| Wire Ø | 2.36 | 1,00 |

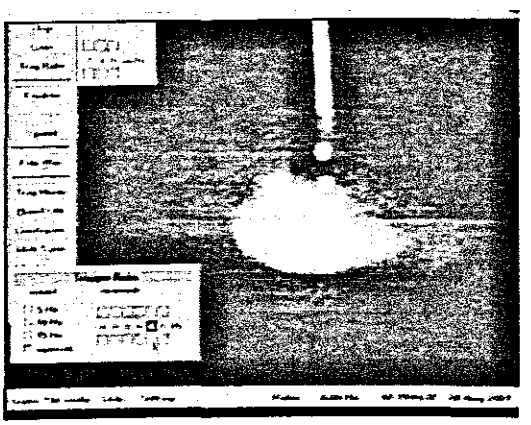

| | Photo | Actual |
|---|---|---|
| Droplet Ø | 2.62 | **1.02** |
| Wire Ø | 2.58 | 1,00 |

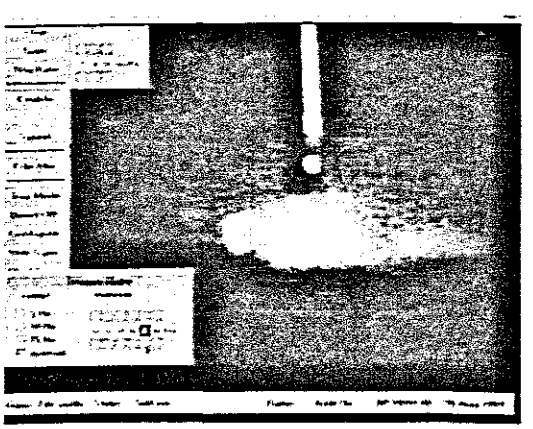

| | Photo | Actual |
|---|---|---|
| Droplet Ø | 2.68 | **1.00** |
| Wire Ø | 2.68 | 1,00 |

Welding current **205A**, wire speed **13,5 m/min**

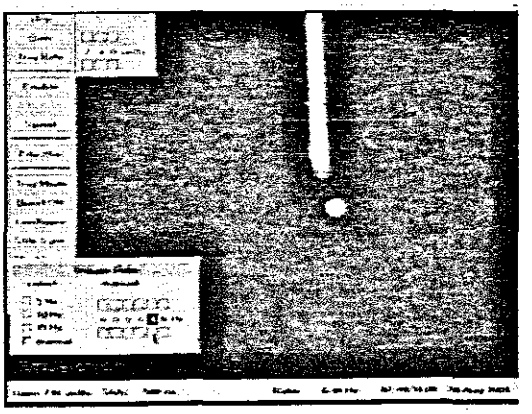

| | Photo | Actual |
|---|---|---|
| Droplet Ø | 3.10 | **1.092** |
| Wire Ø | 2.84 | 1,00 |

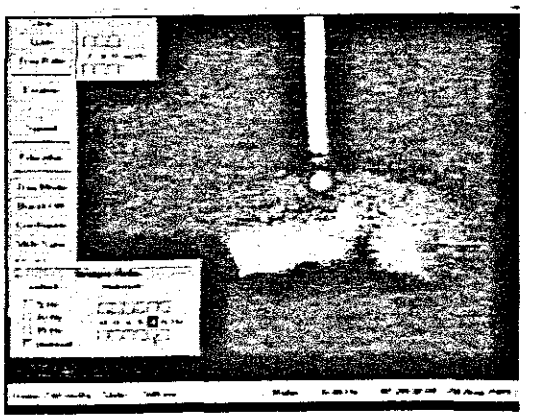

| | Photo | Actual |
|---|---|---|
| Droplet Ø | 3.19 | **1.092** |
| Wire Ø | 2.92 | 1,00 |

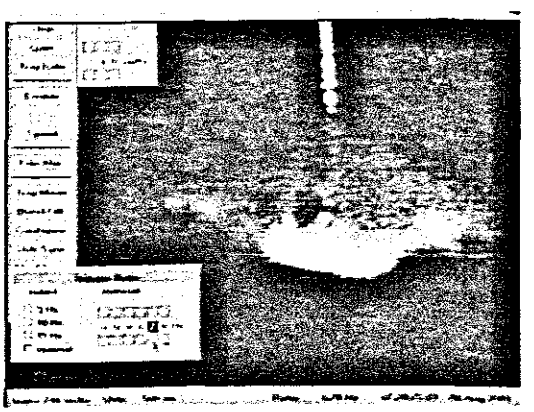

| | Photo | Actual |
|---|---|---|
| Droplet Ø | 2.63 | **1.020** |
| Wire Ø | 2.58 | 1,00 |

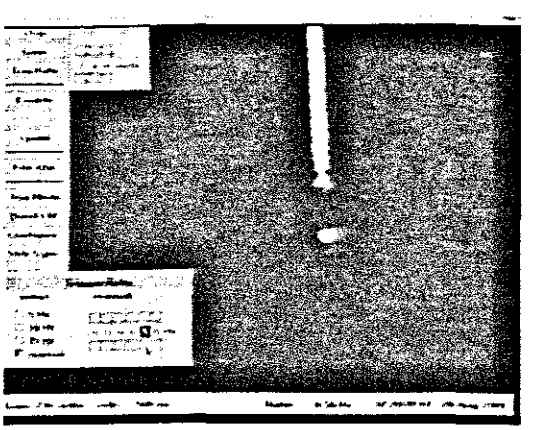

| | Photo | Actual |
|---|---|---|
| Droplet Ø | 2.60 | **1.032** |
| Wire Ø | 2.52 | 1,00 |

Welding current **207A**, wire speed **14 m/min**

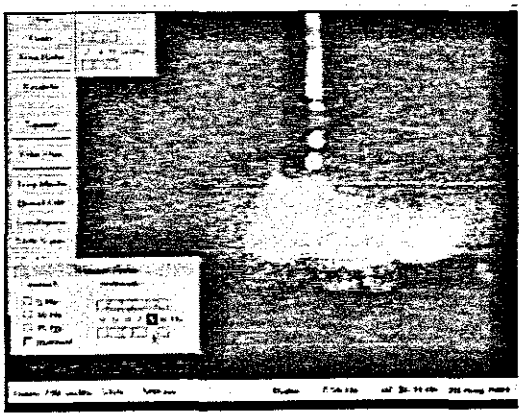

| | Photo | Actual |
|---|---|---|
| Droplet ∅ | 2.98 | **1.190** |
| Wire ∅ | 2.50 | 1,00 |

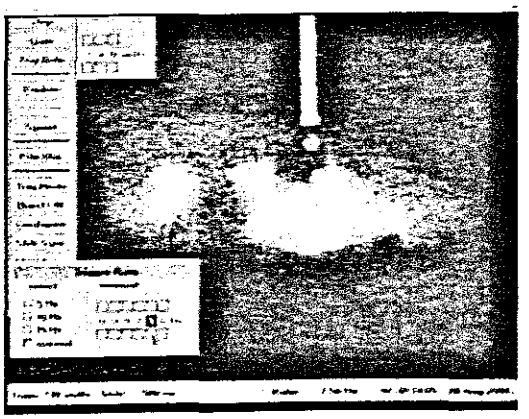

| | Photo | Actual |
|---|---|---|
| Droplet ∅ | 2.58 | **1.00** |
| Wire ∅ | 2.58 | 1,00 |

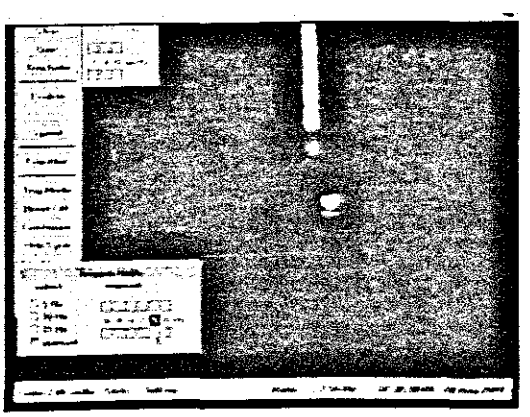

| | Photo | Actual |
|---|---|---|
| Droplet ∅ | 2.41 | **0.948** |
| Wire ∅ | 2.54 | 1,00 |

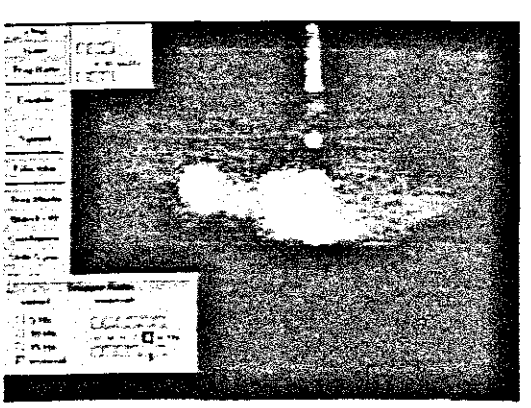

| | Photo | Actual |
|---|---|---|
| Droplet ∅ | 2.78 | **1.050** |
| Wire ∅ | 2.66 | 1,00 |

Welding current **213A**, wire speed **14,5 m/min**

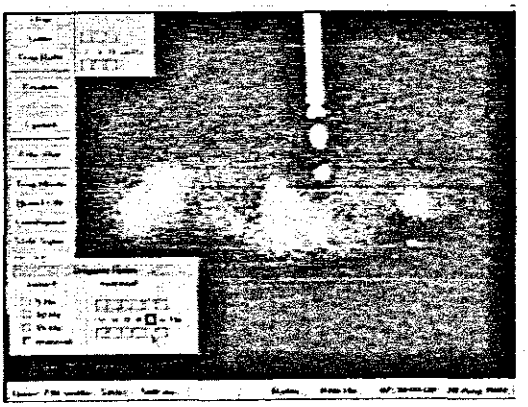

| | Photo | Actual |
|---|---|---|
| Droplet Ø | 2.90 | **1.060** |
| Wire Ø | 2.74 | 1,00 |

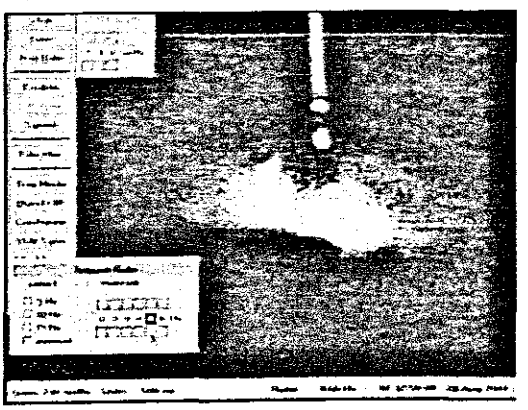

| | Photo | Actual |
|---|---|---|
| Droplet Ø | 2.78 | ***0.983*** |
| Wire Ø | 2.73 | 1,00 |

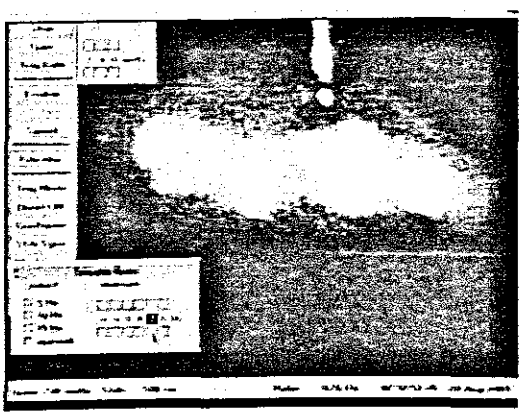

| | Photo | Actual |
|---|---|---|
| Droplet Ø | 2.86 | **1.004** |
| Wire Ø | 2.85 | 1,00 |

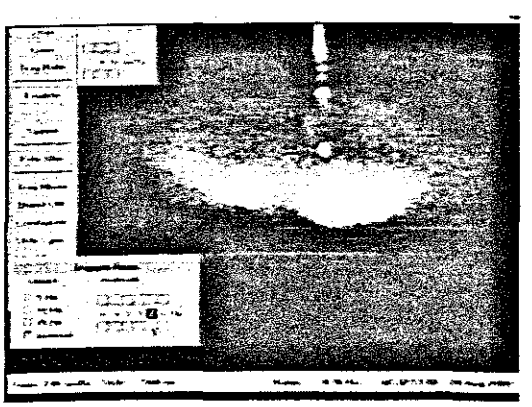

| | Photo | Actual |
|---|---|---|
| Droplet Ø | 2.46 | **1.025** |
| Wire Ø | 2.40 | 1,00 |

Welding current **219A**, wire speed **15 m/min**

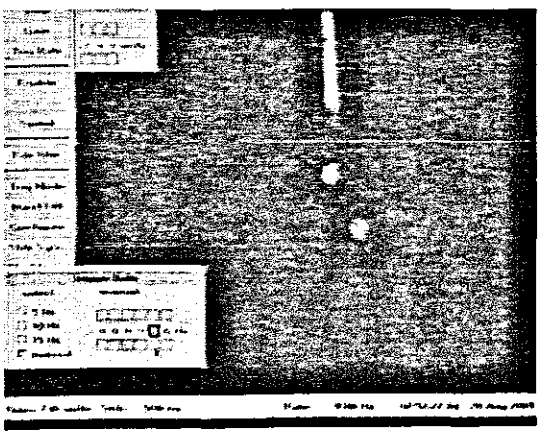

| | Photo | Actual |
|---|---|---|
| Droplet ∅ | 2.68 | **1.08** |
| Wire ∅ | 2.48 | 1,00 |

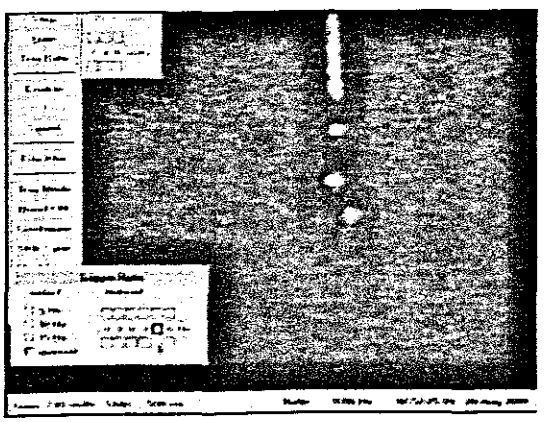

| | Photo | Actual |
|---|---|---|
| Droplet ∅ | 2.72 | **0.944** |
| Wire ∅ | 2.88 | 1,00 |

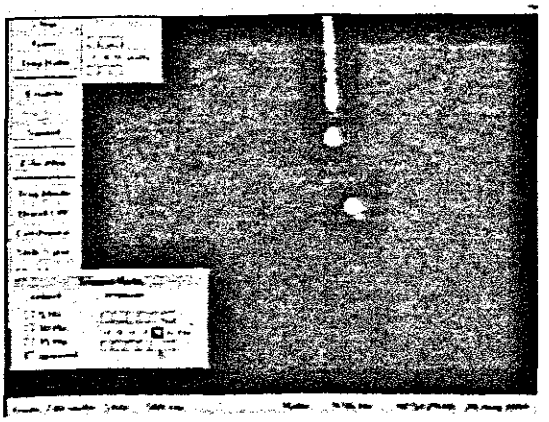

| | Photo | Actual |
|---|---|---|
| Droplet ∅ | 2.66 | **1.090** |
| Wire ∅ | 2.44 | 1,00 |

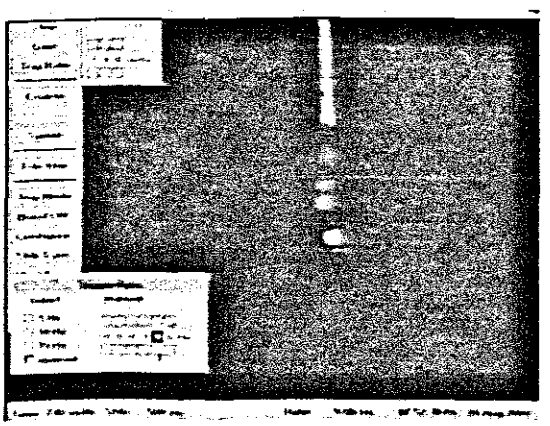

| | Photo | Actual |
|---|---|---|
| Droplet ∅ | 3.16 | **1.046** |
| Wire ∅ | 3.02 | 1,00 |

Welding current **223A**, wire speed **15.5m/min**

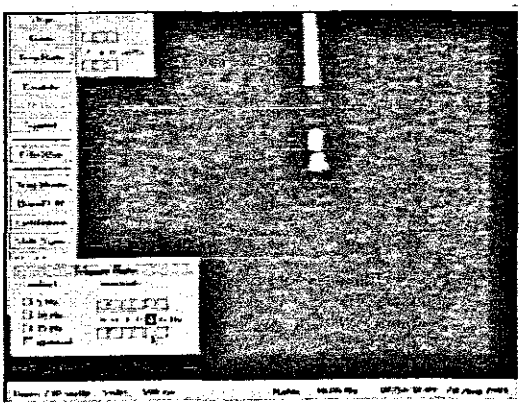

| | Photo | Actual |
|---|---|---|
| Droplet Ø | 2.20 | **1.058** |
| Wire Ø | 2.08 | 1,00 |

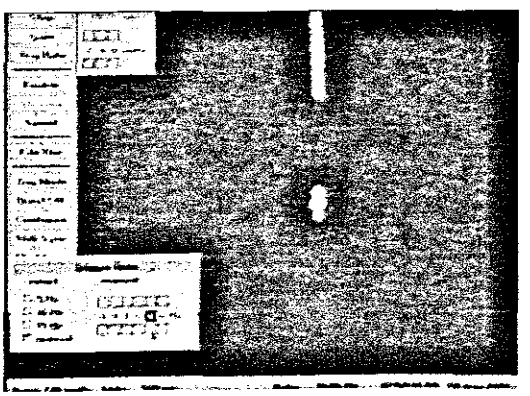

| | Photo | Actual |
|---|---|---|
| Droplet Ø | 2.90 | **0.973** |
| Wire Ø | 2.98 | 1,00 |

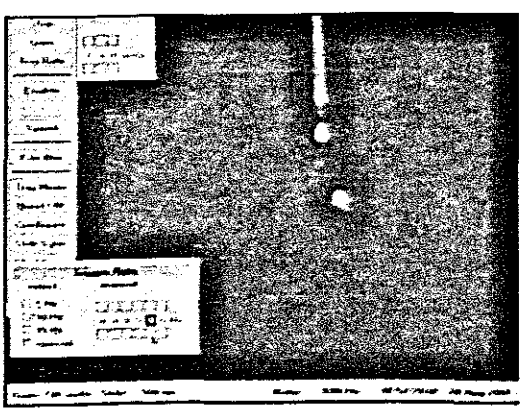

| | Photo | Actual |
|---|---|---|
| Droplet Ø | 2.63 | **1.072** |
| Wire Ø | 2.45 | 1,00 |

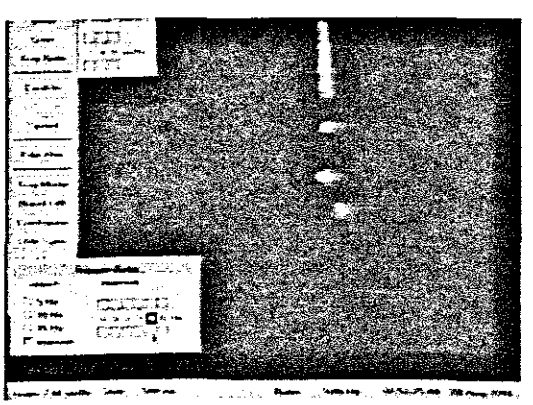

| | Photo | Actual |
|---|---|---|
| Droplet Ø | 2.78 | **1.045** |
| Wire Ø | 2.66 | 1,00 |

Welding current **227A**, wire speed **16m/min**

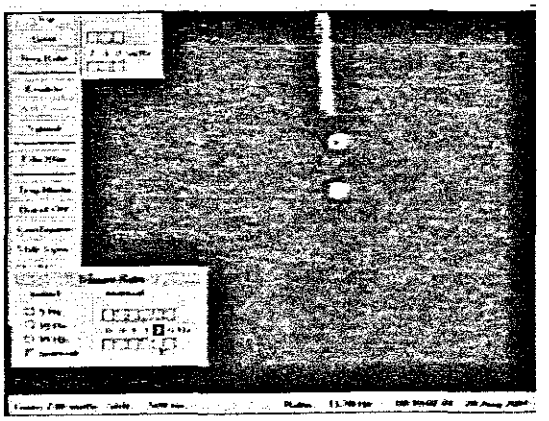

| | Photo | Actual |
|---|---|---|
| Droplet ∅ | 2.76 | **1.091** |
| Wire ∅ | 2.53 | 1,00 |

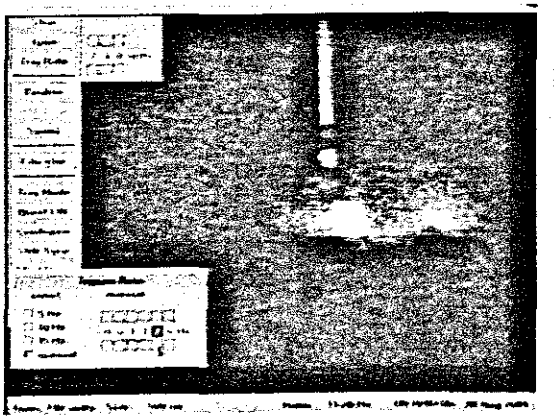

| | Photo | Actual |
|---|---|---|
| Droplet ∅ | 2.37 | **1.088** |
| Wire ∅ | 2.18 | 1,00 |

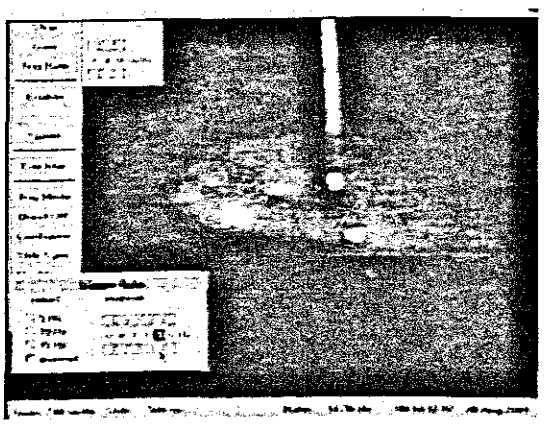

| | Photo | Actual |
|---|---|---|
| Droplet ∅ | 2.48 | **1.008** |
| Wire ∅ | 2.46 | 1,00 |

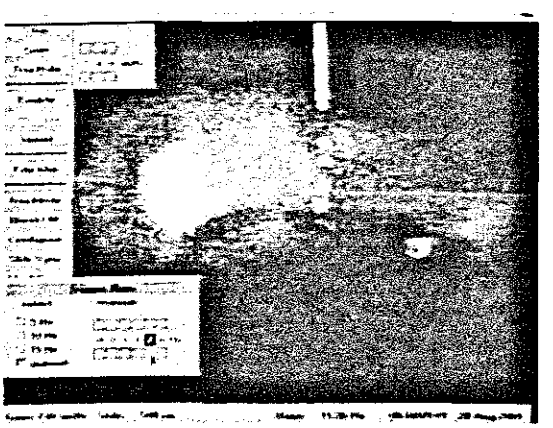

| | Photo | Actual |
|---|---|---|
| Droplet ∅ | 2.46 | **0.953** |
| Wire ∅ | 2.58 | 1,00 |

Welding current **231A**, wire speed **16.5m/min**

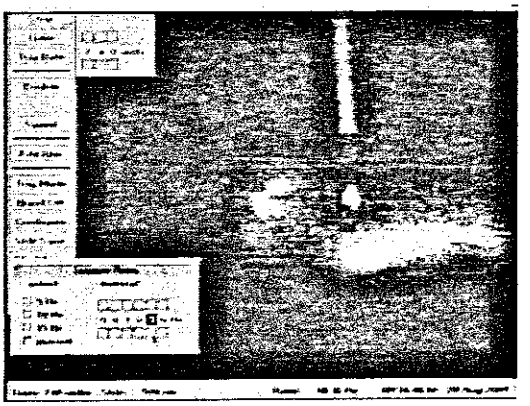

| | Photo | Actual |
|---|---|---|
| Droplet ∅ | 2.48 | **1.01** |
| Wire ∅ | 2.46 | 1,00 |

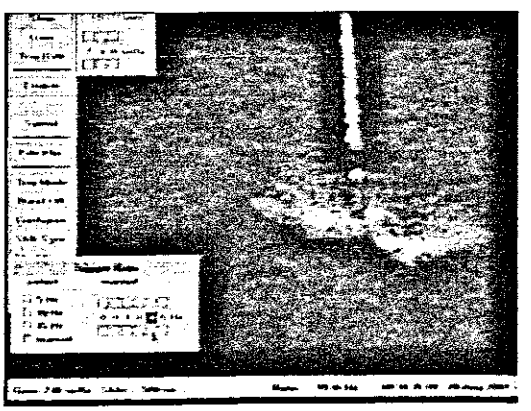

| | Photo | Actual |
|---|---|---|
| Droplet ∅ | 2.00 | **1.00** |
| Wire ∅ | 2.00 | 1,00 |

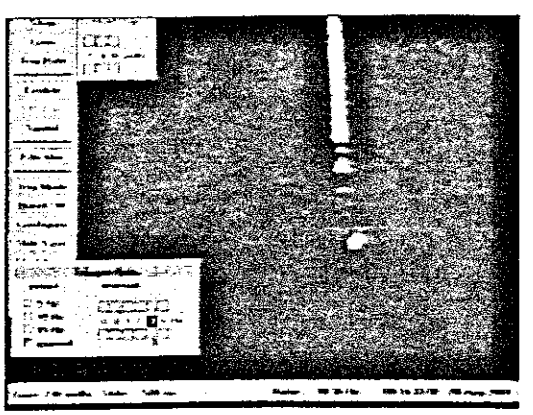

| | Photo | Actual |
|---|---|---|
| Droplet ∅ | 2.66 | **1.00** |
| Wire ∅ | 2.66 | 1,00 |

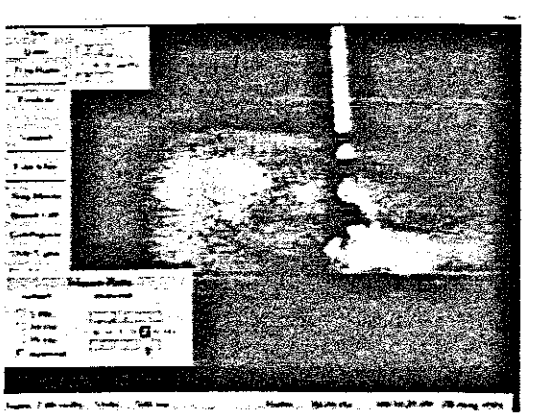

| | Photo | Actual |
|---|---|---|
| Droplet ∅ | 2.42 | **1.00** |
| Wire ∅ | 2.42 | 1,00 |

Welding current **231A**, wire speed **17m/min**

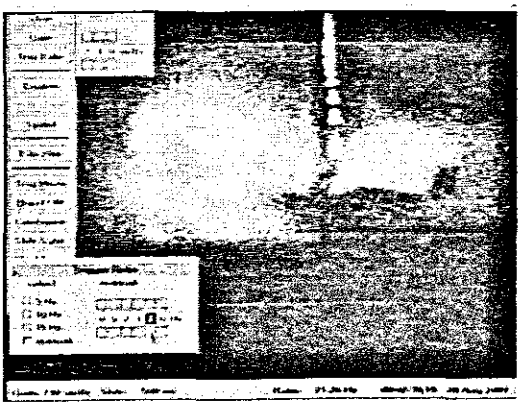

| | Photo | Actual |
|---|---|---|
| Droplet ∅ | 2.02 | **1.01** |
| Wire ∅ | 2.00 | 1,00 |

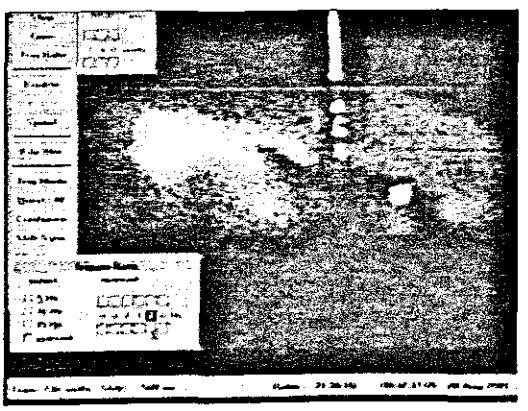

| | Photo | Actual |
|---|---|---|
| Droplet ∅ | 2.02 | **1.00** |
| Wire ∅ | 2.02 | 1,00 |

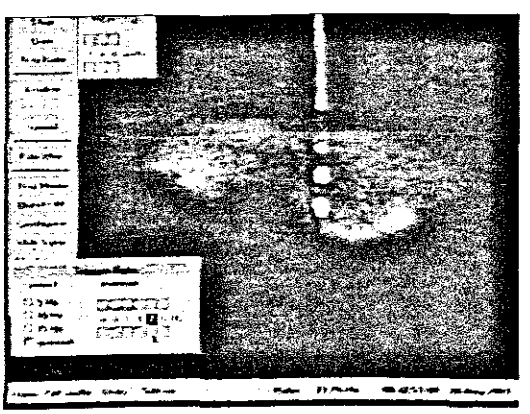

| | Photo | Actual |
|---|---|---|
| Droplet ∅ | 2.02 | **1.02** |
| Wire ∅ | 1.98 | 1,00 |

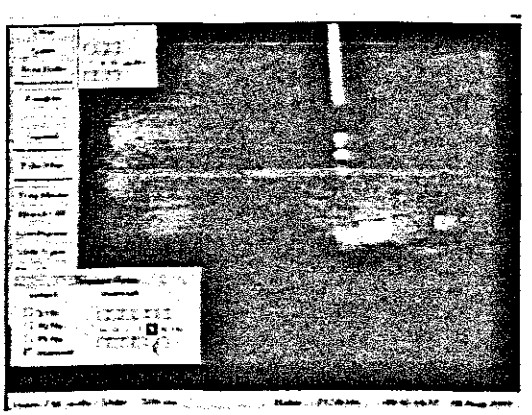

| | Photo | Actual |
|---|---|---|
| Droplet ∅ | 1.98 | **0.99** |
| Wire ∅ | 2.00 | 1,00 |

Welding current **235A**, wire speed **17,5m/min**

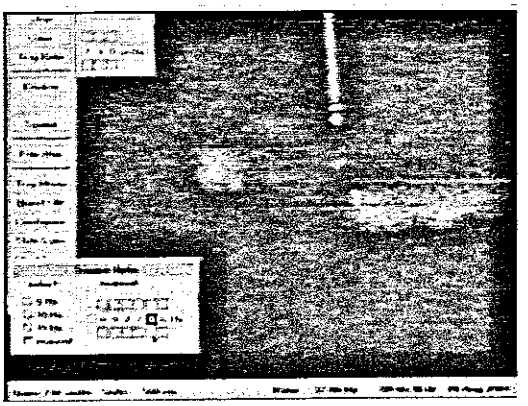

| | Photo | Actual |
|---|---|---|
| Droplet ∅ | 2.00 | **1.01** |
| Wire ∅ | 1.98 | 1,00 |

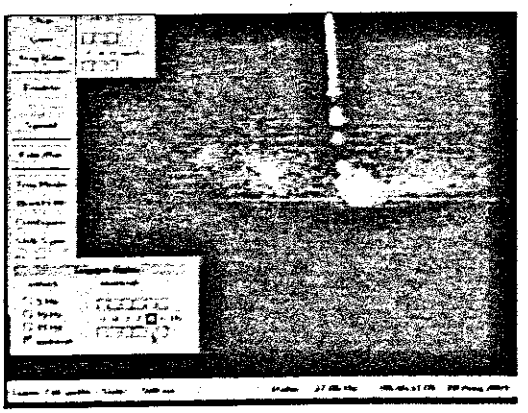

| | Photo | Actual |
|---|---|---|
| Droplet ∅ | 2.00 | **1.00** |
| Wire ∅ | 2.00 | 1,00 |

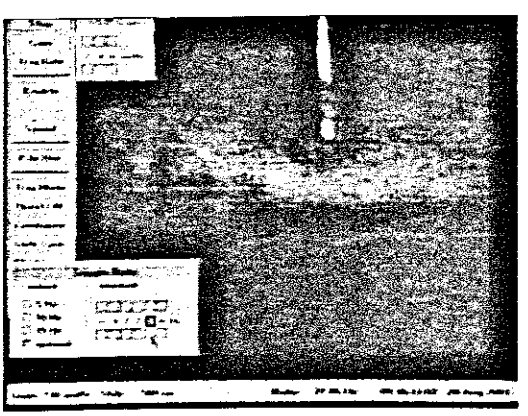

| | Photo | Actual |
|---|---|---|
| Droplet ∅ | 2.02 | **0.99** |
| Wire ∅ | 2.04 | 1,00 |

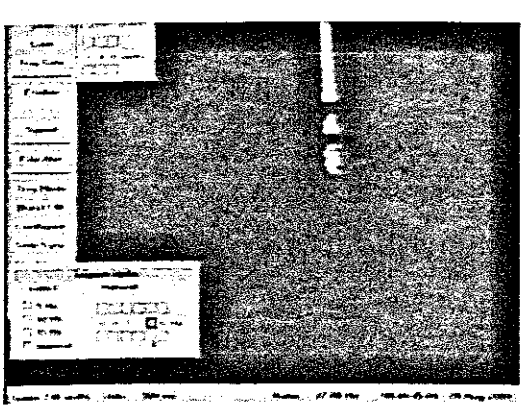

| | Photo | Actual |
|---|---|---|
| Droplet ∅ | 2.00 | **1.00** |
| Wire ∅ | 2.00 | 1,00 |

Welding current **240A**, welding speed **18m/min**

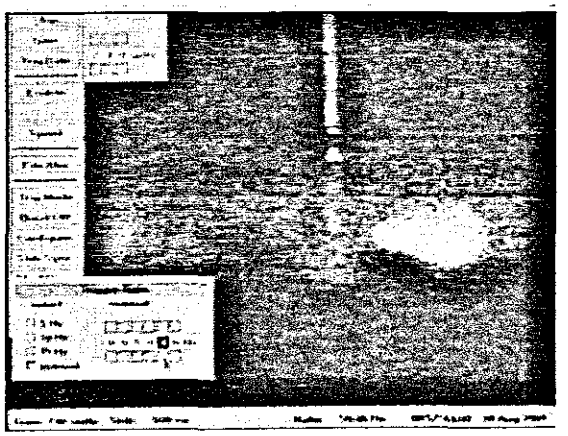

| | Photo | Actual |
|---|---|---|
| Droplet Ø | 2.04 | **1.02** |
| Wire Ø | 2.00 | 1,00 |

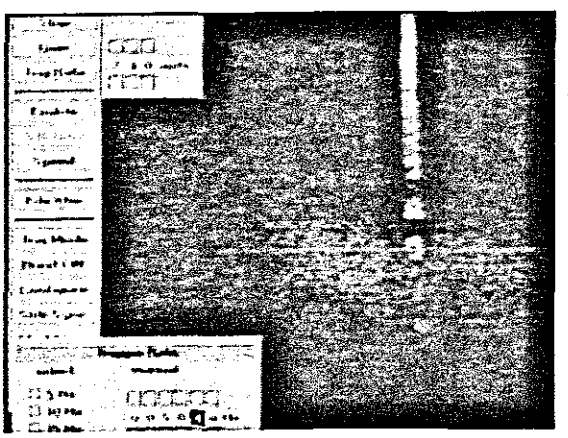

| | Photo | Actual |
|---|---|---|
| Droplet Ø | 2.52 | **1.00** |
| Wire Ø | 2.52 | 1,00 |

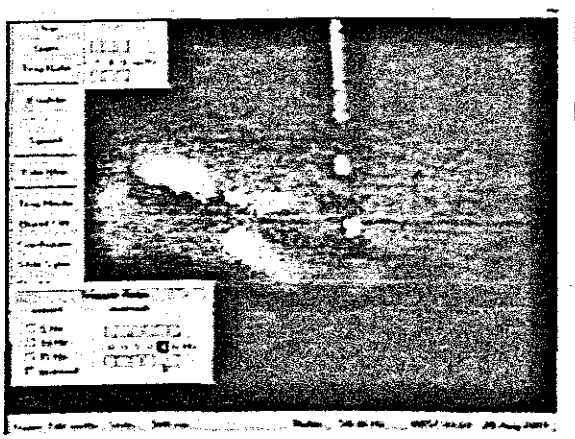

| | Photo | Actual |
|---|---|---|
| Droplet Ø | 2.30 | **1.00** |
| Wire Ø | 2.30 | 1,00 |

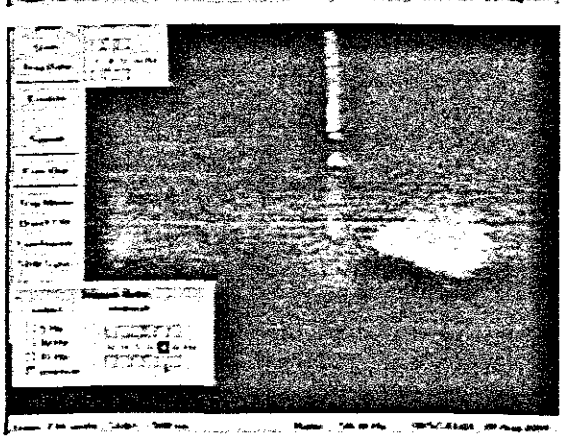

| | Photo | Actual |
|---|---|---|
| Droplet Ø | 2.30 | **0.99** |
| Wire Ø | 2.32 | 1,00 |

Welding current **242A**, wire speed **18,5m/min**

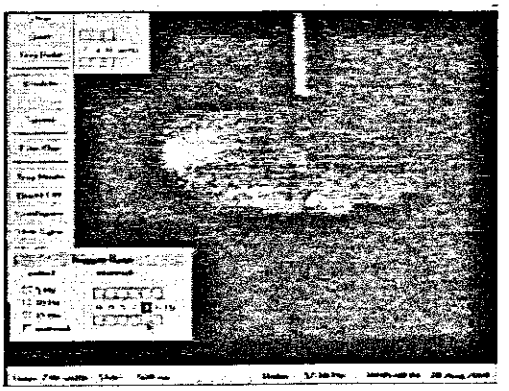

| | Photo | Actual |
|---|---|---|
| Droplet ∅ | 1.90 | **0.99** |
| Wire ∅ | 1.92 | 1,00 |

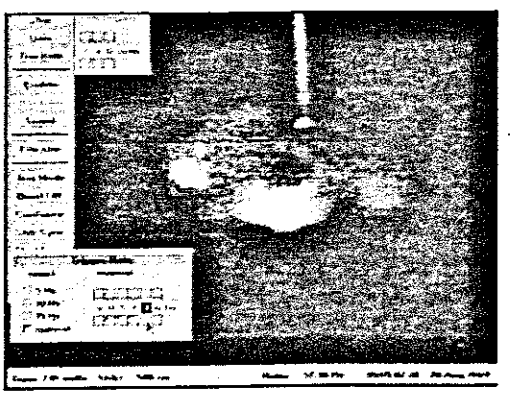

| | Photo | Actual |
|---|---|---|
| Droplet ∅ | 1.88 | **0.99** |
| Wire ∅ | 1.90 | 1,00 |

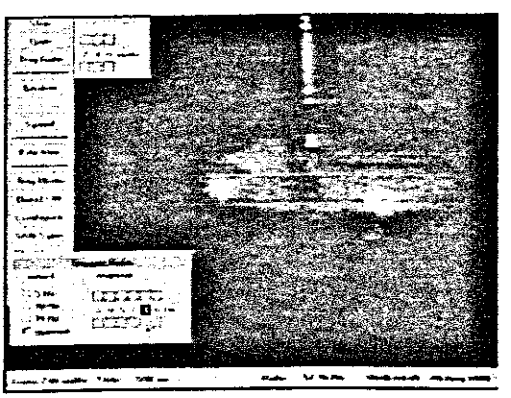

| | Photo | Actual |
|---|---|---|
| Droplet ∅ | 1.78 | **1.00** |
| Wire ∅ | 1.78 | 1,00 |

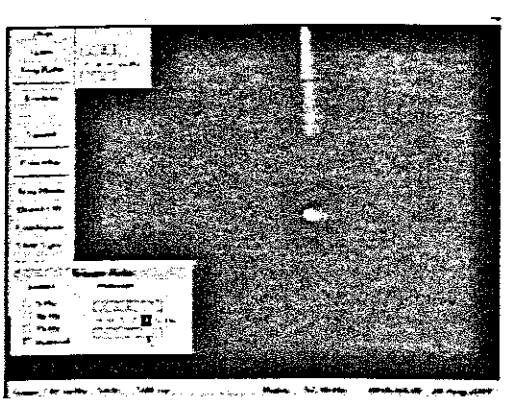

| | Photo | Actual |
|---|---|---|
| Droplet ∅ | 1.78 | **0.99** |
| Wire ∅ | 1.80 | 1.00 |

Welding current **247A**, wire speed **19m/min**

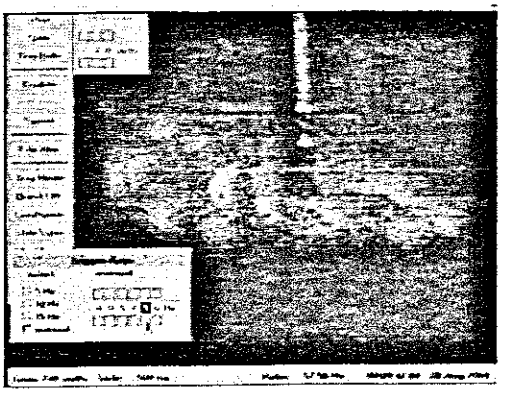

| | Photo | Actual |
|---|---|---|
| Droplet ∅ | 1.82 | **1.00** |
| Wire ∅ | 1.82 | 1,00 |

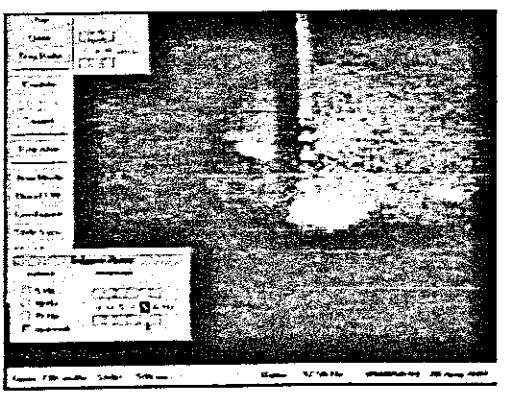

| | Photo | Actual |
|---|---|---|
| Droplet ∅ | 1.78 | **0.99** |
| Wire ∅ | 1.80 | 1,00 |

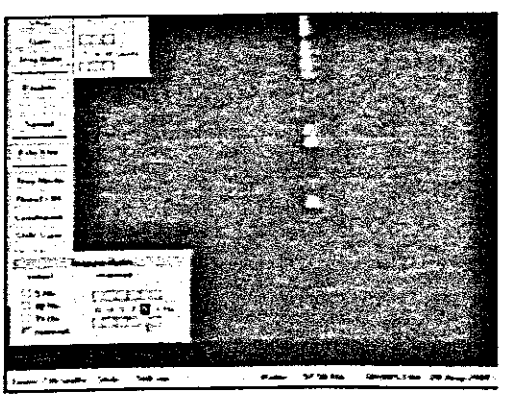

| | Photo | Actual |
|---|---|---|
| Droplet ∅ | 1.78 | **0.99** |
| Wire ∅ | 1.80 | 1,00 |

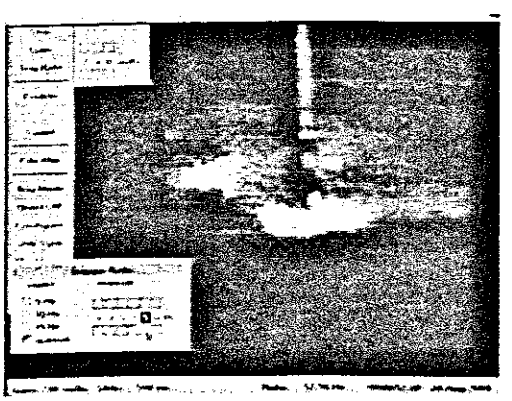

| | Photo | Actual |
|---|---|---|
| Droplet ∅ | 1.94 | **0.97** |
| Wire ∅ | 2.00 | 1,00 |

Welding current **251A**, wire speed **19,5m/min**

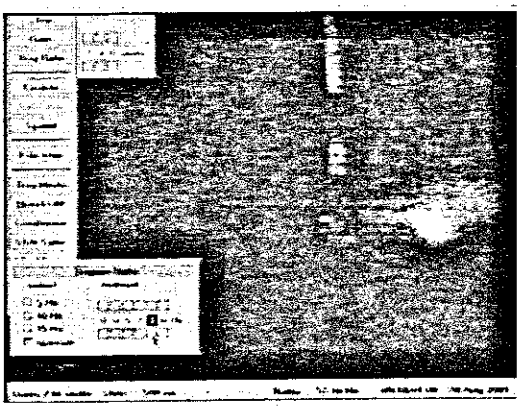

| | Photo | Actual |
|---|---|---|
| Droplet ∅ | 2.06 | **0.98** |
| Wire ∅ | 2.10 | 1,00 |

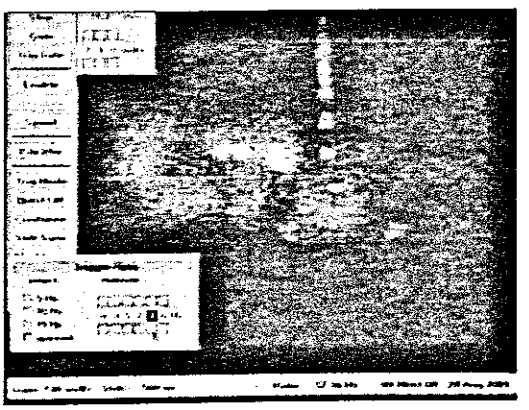

| | Photo | Actual |
|---|---|---|
| Droplet ∅ | 2.10 | **0.99** |
| Wire ∅ | 2.12 | 1,00 |

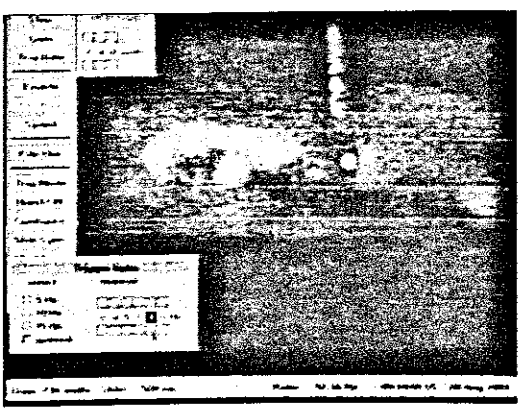

| | Photo | Actual |
|---|---|---|
| Droplet ∅ | 2.08 | **0.99** |
| Wire ∅ | 2.10 | 1,00 |

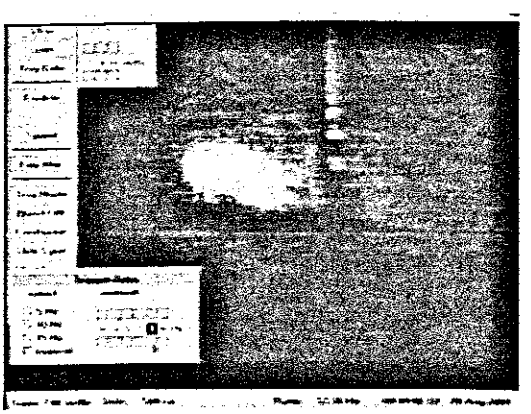

| | Photo | Actual |
|---|---|---|
| Droplet ∅ | 2.08 | **0.99** |
| Wire ∅ | 2.10 | 1,00 |

Welding current **254A**, wire speed **20m/min**

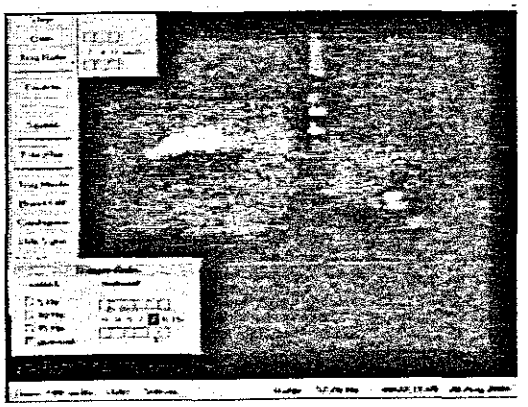

| | Photo | Actual |
|---|---|---|
| Droplet ∅ | 2.10 | **1.00** |
| Wire ∅ | 2.10 | 1,00 |

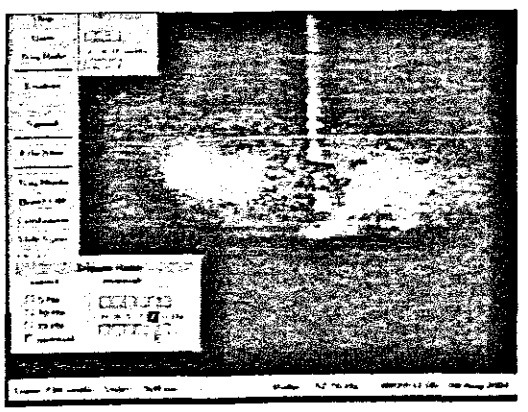

| | Photo | Actual |
|---|---|---|
| Droplet ∅ | 2.06 | ***0.99*** |
| Wire ∅ | 2.08 | 1,00 |

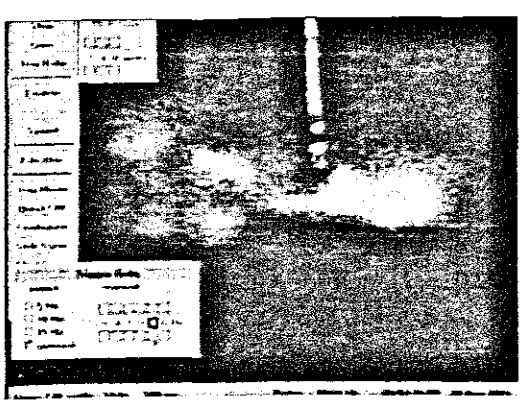

| | Photo | Actual |
|---|---|---|
| Droplet ∅ | 1.96 | **0.98** |
| Wire ∅ | 2.00 | 1,00 |

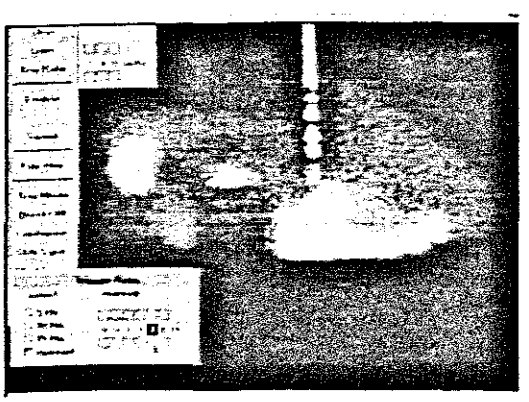

| | Photo | Actual |
|---|---|---|
| Droplet ∅ | 1.98 | **0.93** |
| Wire ∅ | 2.12 | 1,00 |

# Appendix E3

**Laserstrobe Images of MIG Welding with 98%Ar-2%$O_2$ Shielding Gas**

The table below represents the mean droplet diameters obtained from the welding images of a 1mm mild steel electrode with 98%Argon-2%Oxygen shielding. A minimum of 4 images per weld run was used to calculate the mean droplet diameter.

| Weld No. | Wire Feed Rate | Mean droplet diameter |
|---|---|---|
| 1 | 5 | **1.662** |
| 2 | 6 | **1.653** |
| 3 | 7 | **1.670** |
| 4 | 7.5 | **1.645** |
| 5 | 8 | **1.640** |
| 6 | 8.5 | **1.240** |
| 7 | 9 | **1.425** |
| 8 | 10 | **1.500** |
| 9 | 11 | **1.175** |
| 10 | 11.5 | **1.212** |
| 11 | 12 | **1.210** |
| 12 | 12.5 | **1.198** |
| 13 | 13 | **1.154** |
| 14 | 14 | **1.129** |
| 15 | 15 | **1.016** |
| 16 | 16 | **1.075** |
| 17 | 17 | **1.069** |
| 18 | 18 | **0.746** |
| 19 | 19 | **0.870** |
| 20 | 20 | **0.888** |
| 21 | 22 | **0.776** |
| 22 | 24 | **0.772** |

Welding current **132A**, wire speed **6m/min**

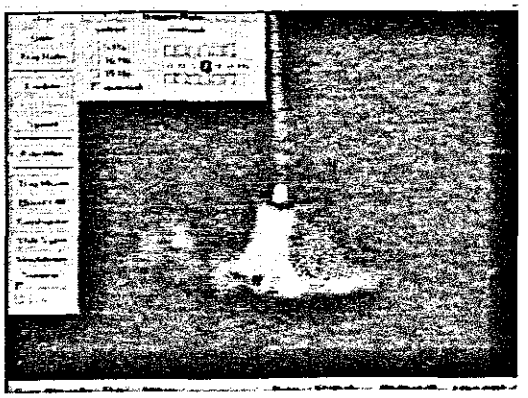

| | Photo | Actual |
|---|---|---|
| Droplet ∅ | 3.35 | **1.667** |
| Wire ∅ | 2.01 | 1.00 |

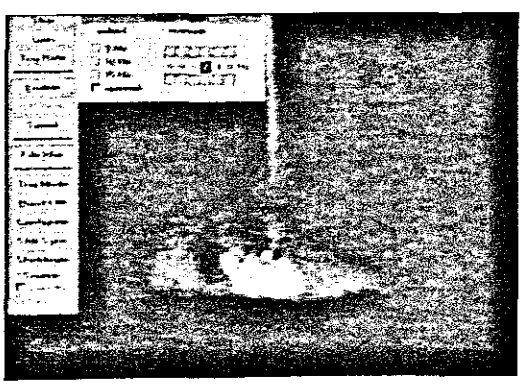

| | Photo | Actual |
|---|---|---|
| Droplet ∅ | 2.70 | **1.607** |
| Wire ∅ | 1.68 | 1.00 |

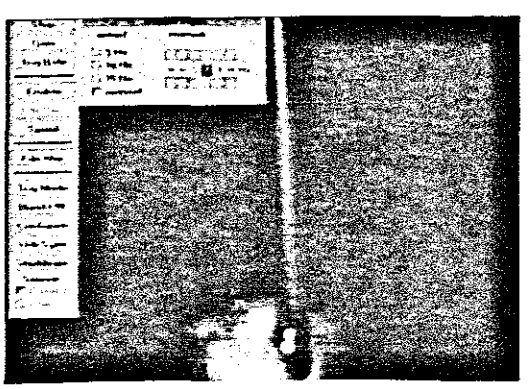

| | Photo | Actual |
|---|---|---|
| Droplet ∅ | 6.60 | **1.670** |
| Wire ∅ | 3.96 | 1.00 |

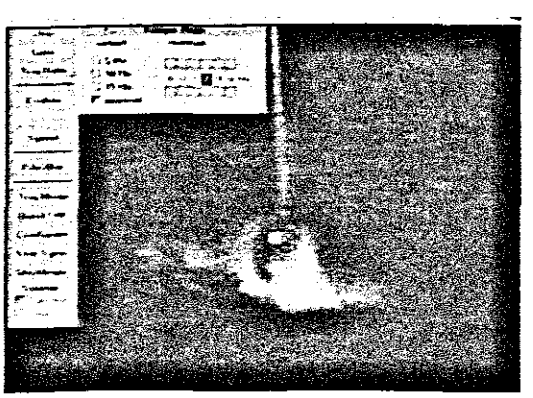

| | Photo | Actual |
|---|---|---|
| Droplet ∅ | 6.68 | **1.665** |
| Wire ∅ | 4.01 | 1.00 |

Welding current **150A**, wire speed **7m/min**

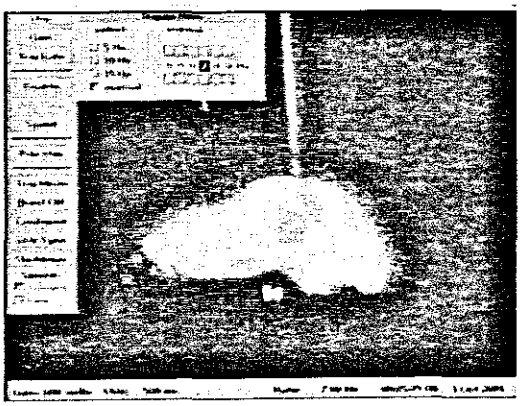

| | Photo | Actual |
|---|---|---|
| Droplet ∅ | 4.68 | **1.665** |
| Wire ∅ | 2.81 | 1.00 |

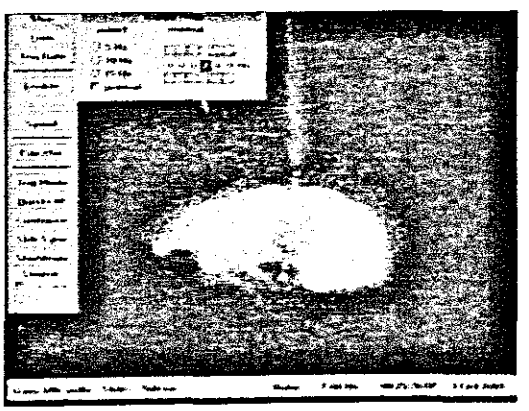

| | Photo | Actual |
|---|---|---|
| Droplet ∅ | 5.82 | **1.668** |
| Wire ∅ | 3.49 | 1.00 |

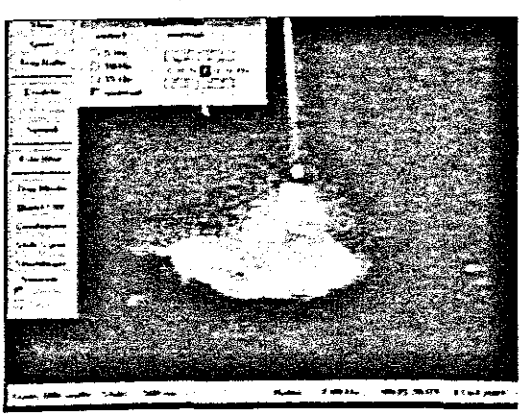

| | Photo | Actual |
|---|---|---|
| Droplet ∅ | 5.20 | **1.677** |
| Wire ∅ | 3.10 | 1.00 |

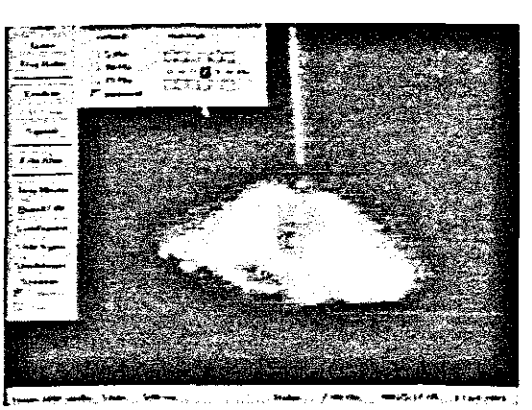

| | Photo | Actual |
|---|---|---|
| Droplet ∅ | 7.88 | **1.670** |
| Wire ∅ | 4.73 | 1.00 |

Welding current **156A**, wire speed **7,5m/min**

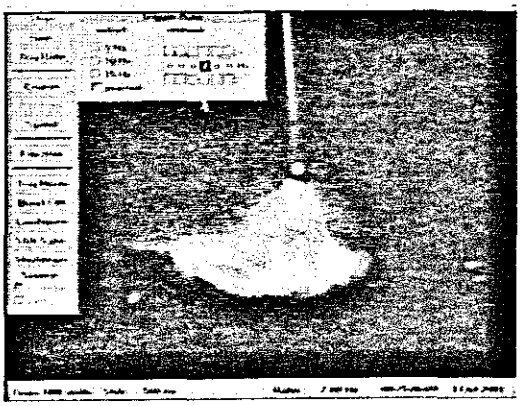

| | Photo | Actual |
|---|---|---|
| Droplet ∅ | 4.62 | **1.644** |
| Wire ∅ | 2.81 | 1.00 |

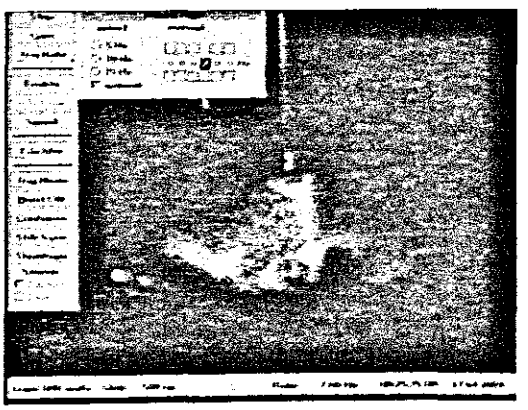

| | Photo | Actual |
|---|---|---|
| Droplet ∅ | 5.08 | **1.643** |
| Wire ∅ | 3.09 | 1.00 |

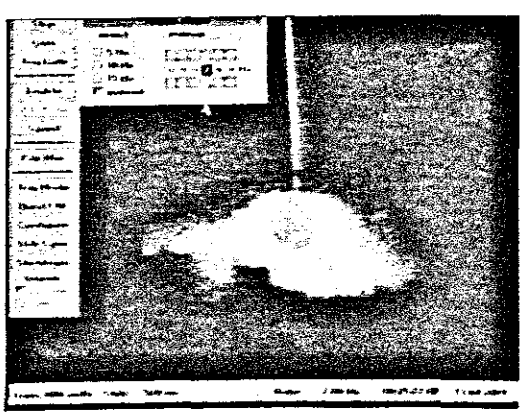

| | Photo | Actual |
|---|---|---|
| Droplet ∅ | 7.22 | **1.648** |
| Wire ∅ | 4.38 | 1.00 |

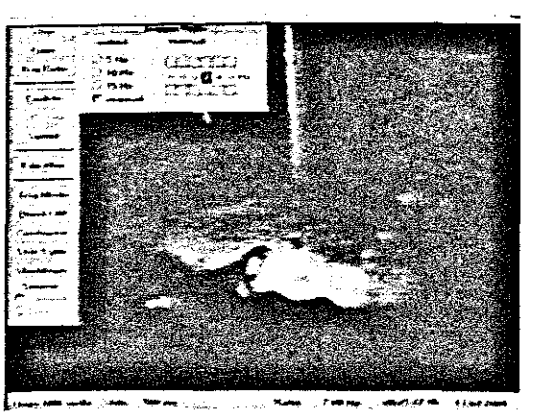

| | Photo | Actual |
|---|---|---|
| Droplet ∅ | 4.08 | **1.645** |
| Wire ∅ | 2.48 | 1.00 |

Welding current **161A**, wire speed **8m/min**

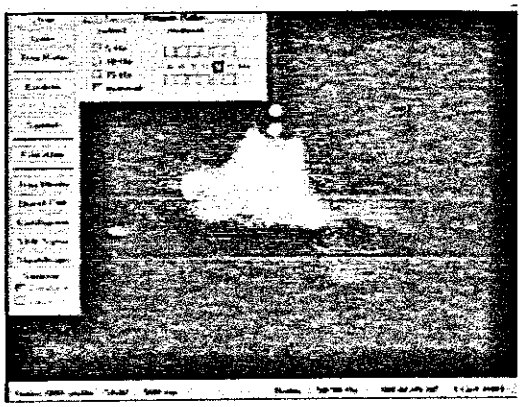

| | Photo | Actual |
|---|---|---|
| Droplet ∅ | 2.98 | **1.637** |
| Wire ∅ | 1.82 | 1.00 |

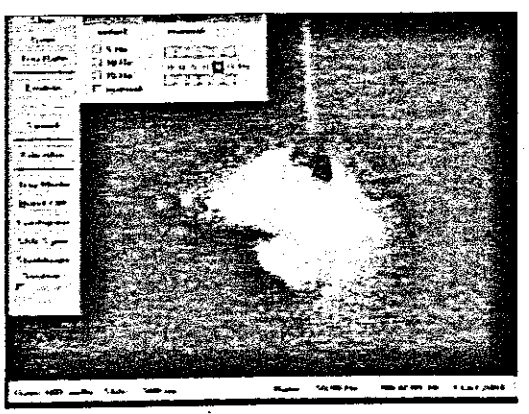

| | Photo | Actual |
|---|---|---|
| Droplet ∅ | 7.72 | **1.639** |
| Wire ∅ | 4.71 | 1.00 |

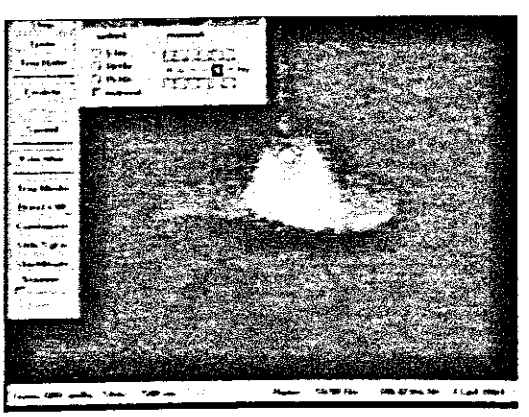

| | Photo | Actual |
|---|---|---|
| Droplet ∅ | 5.98 | **1.638** |
| Wire ∅ | 3.65 | 1.00 |

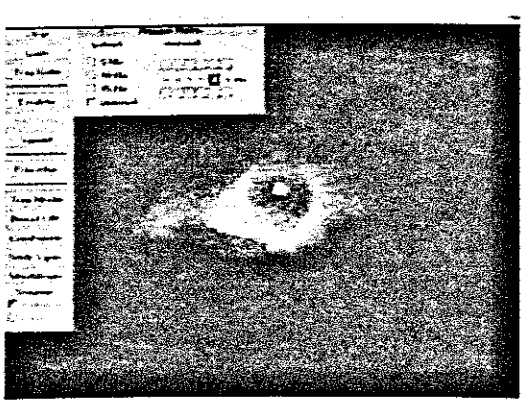

| | Photo | Actual |
|---|---|---|
| Droplet ∅ | 9.22 | **1.646** |
| Wire ∅ | 5.60 | 1.00 |

Welding current **164A**, wire speed **8,5m/min**

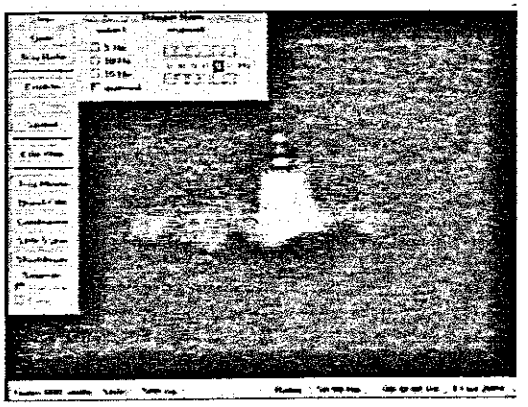

| | Photo | Actual |
|---|---|---|
| Droplet ∅ | 2.42 | **1.210** |
| Wire ∅ | 2.00 | 1.00 |

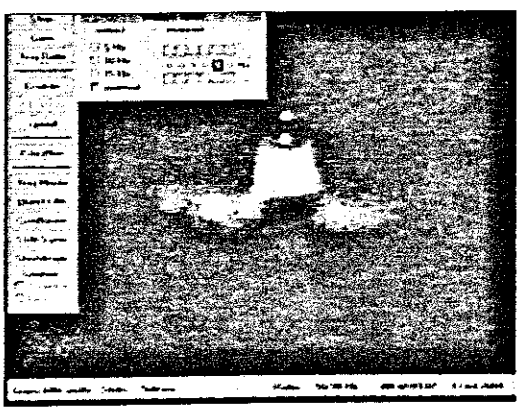

| | Photo | Actual |
|---|---|---|
| Droplet ∅ | 2.22 | **1.220** |
| Wire ∅ | 1.82 | 1.00 |

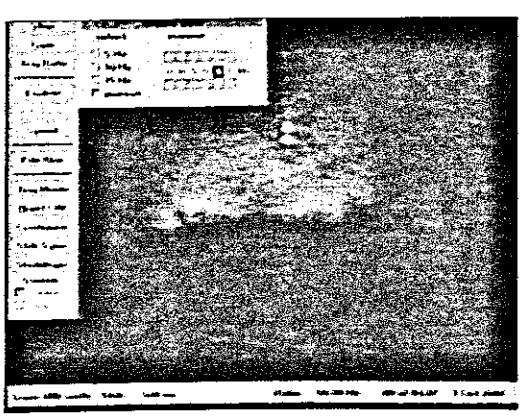

| | Photo | Actual |
|---|---|---|
| Droplet ∅ | 2.15 | **1.280** |
| Wire ∅ | 1.68 | 1.00 |

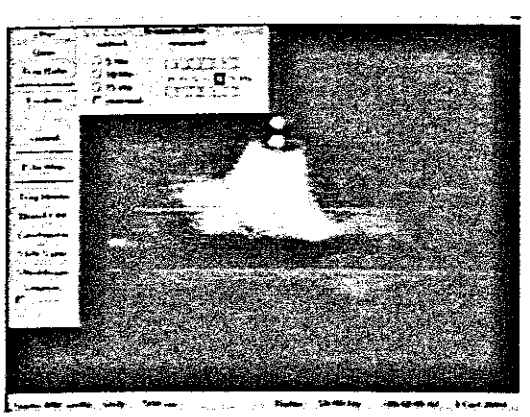

| | Photo | Actual |
|---|---|---|
| Droplet ∅ | 2.30 | **1.250** |
| Wire ∅ | 1.84 | 1.00 |

Welding current **181A**, wire speed **10m/min**

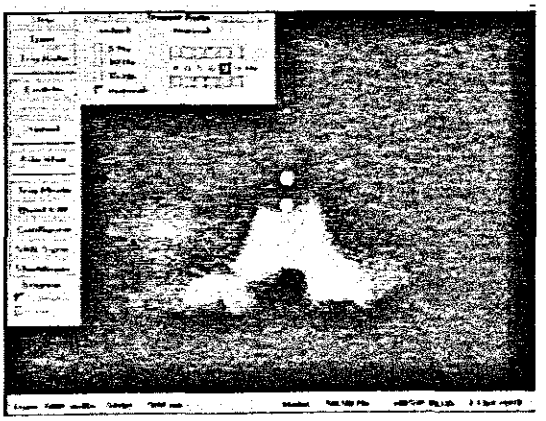

| | Photo | Actual |
|---|---|---|
| Droplet Ø | 2.12 | **1.198** |
| Wire Ø | 1.77 | 1.00 |

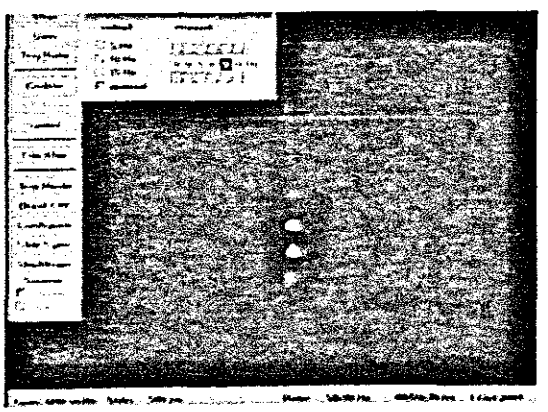

| | Photo | Actual |
|---|---|---|
| Droplet Ø | 2.36 | **1.229** |
| Wire Ø | 1.92 | 1.00 |

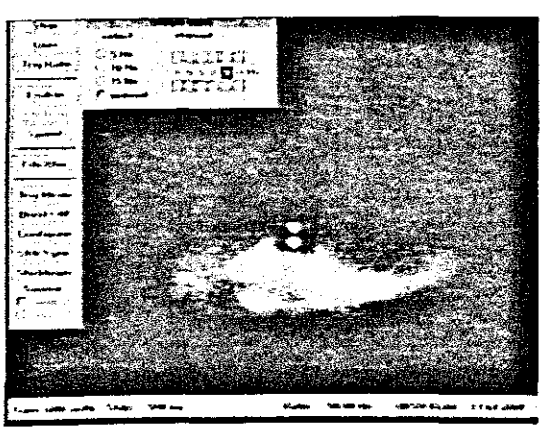

| | Photo | Actual |
|---|---|---|
| Droplet Ø | 2.38 | **1.253** |
| Wire Ø | 1.90 | 1.00 |

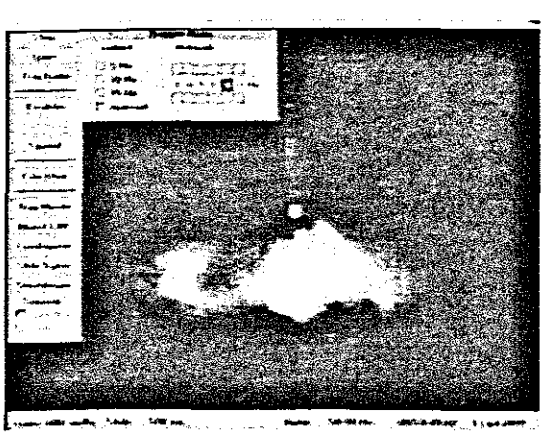

| | Photo | Actual |
|---|---|---|
| Droplet Ø | 2.38 | **1.246** |
| Wire Ø | 1.91 | 1.00 |

Welding current **194A**, wire speed **11m/min**

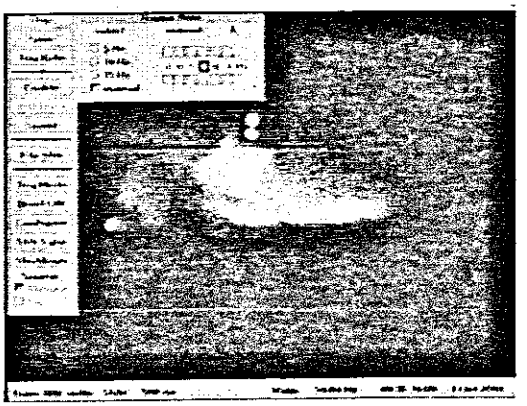

| | Photo | Actual |
|---|---|---|
| Droplet Ø | 2.52 | **1.241** |
| Wire Ø | 2.03 | 1.00 |

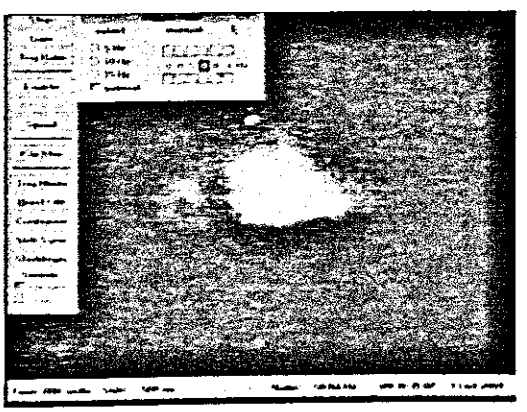

| | Photo | Actual |
|---|---|---|
| Droplet Ø | 2.76 | **1.239** |
| Wire Ø | 2.28 | 1.00 |

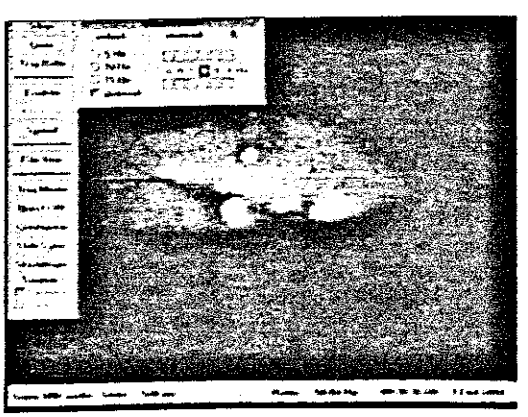

| | Photo | Actual |
|---|---|---|
| Droplet Ø | 4.42 | **1.235** |
| Wire Ø | 3.58 | 1.00 |

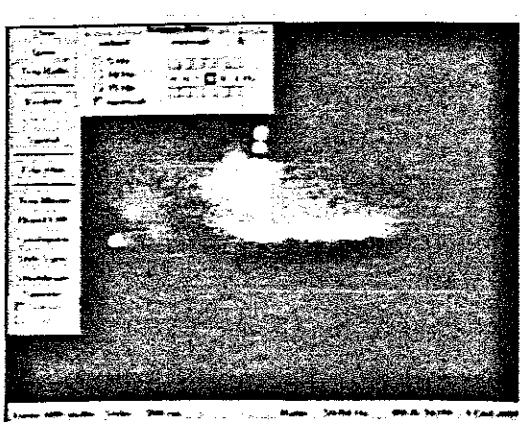

| | Photo | Actual |
|---|---|---|
| Droplet Ø | 2.46 | **1.247** |
| Wire Ø | 1.97 | 1.00 |

Welding current **198A**, wire speed **11,5m/min**

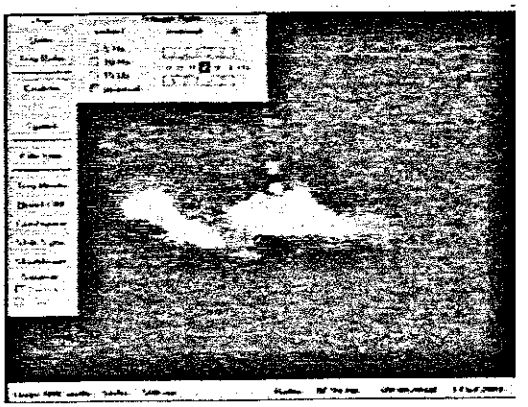

| | Photo | Actual |
|---|---|---|
| Droplet ∅ | 2.68 | **1.240** |
| Wire ∅ | 2.16 | 1.00 |

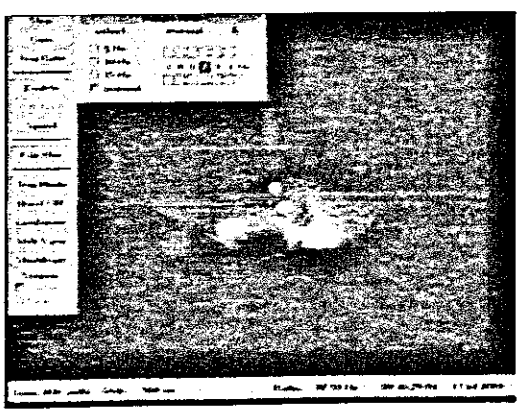

| | Photo | Actual |
|---|---|---|
| Droplet ∅ | 3.00 | **1.201** |
| Wire ∅ | 2.498 | 1.00 |

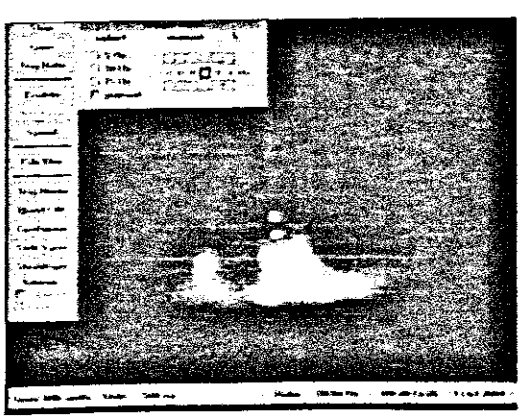

| | Photo | Actual |
|---|---|---|
| Droplet ∅ | 2.26 | **1.215** |
| Wire ∅ | 1.86 | 1.00 |

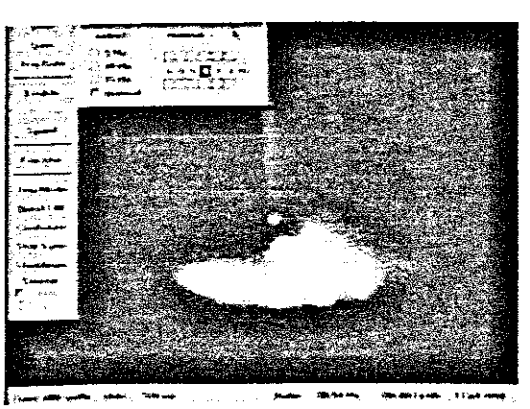

| | Photo | Actual |
|---|---|---|
| Droplet ∅ | 2.50 | **1.190** |
| Wire ∅ | 2.10 | 1.00 |

Welding current **200A**, wire speed **12m/min**

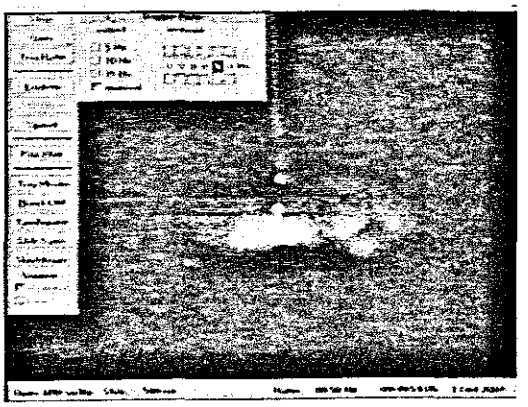

| | Photo | Actual |
|---|---|---|
| Droplet ∅ | 2.58 | **1.211** |
| Wire ∅ | 2.13 | 1.00 |

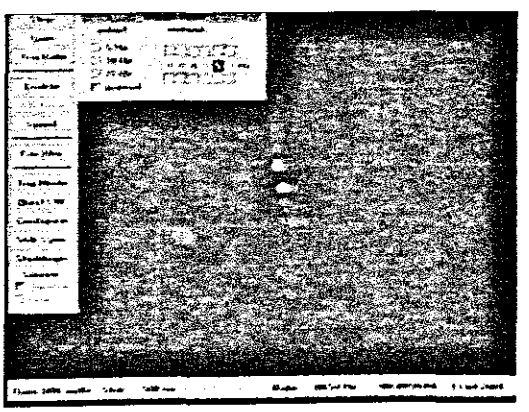

| | Photo | Actual |
|---|---|---|
| Droplet ∅ | 2.60 | **1.209** |
| Wire ∅ | 2.15 | 1.00 |

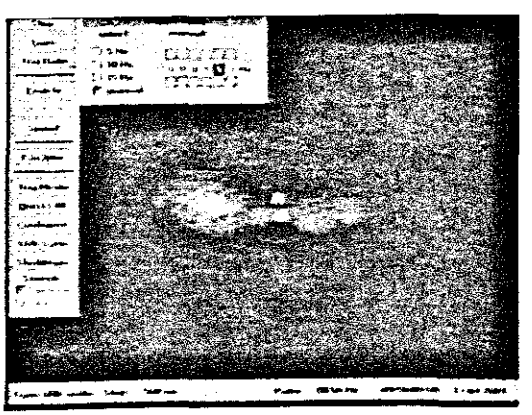

| | Photo | Actual |
|---|---|---|
| Droplet ∅ | 2.72 | **1.208** |
| Wire ∅ | 2.25 | 1.00 |

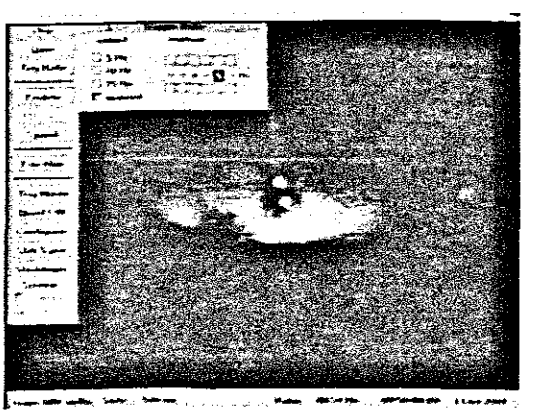

| | Photo | Actual |
|---|---|---|
| Droplet ∅ | 2.76 | **1.2105** |
| Wire ∅ | 2.28 | 1.00 |

Welding current **211A**, wire speed **12,5m/min**

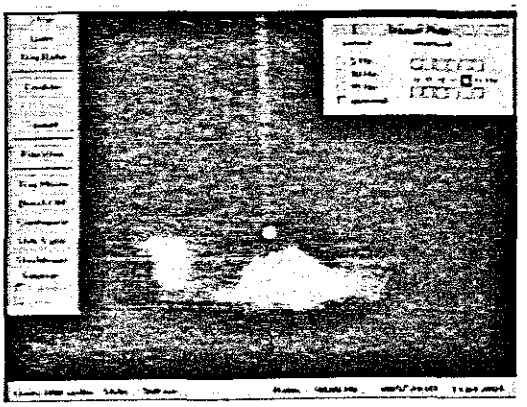

| | Photo | Actual |
|---|---|---|
| Droplet ∅ | 2.28 | **1.086** |
| Wire ∅ | 2.10 | 1.00 |

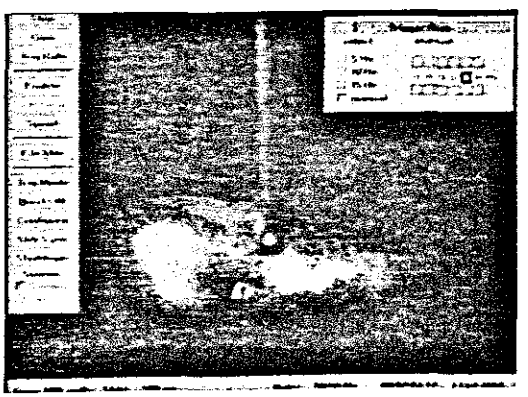

| | Photo | Actual |
|---|---|---|
| Droplet ∅ | 3.54 | **1.200** |
| Wire ∅ | 2.95 | 1.00 |

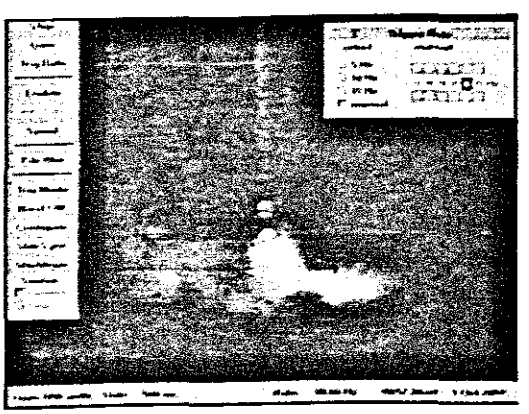

| | Photo | Actual |
|---|---|---|
| Droplet ∅ | 3.12 | **1.333** |
| Wire ∅ | 2.34 | 1.00 |

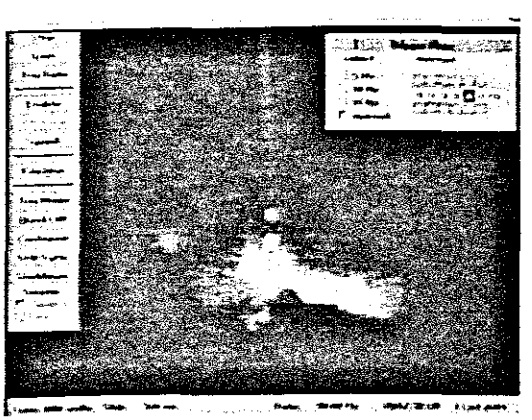

| | Photo | Actual |
|---|---|---|
| Droplet ∅ | 3.00 | **1.172** |
| Wire ∅ | 2.56 | 1.00 |

Welding current **208A**, wire speed **13,0m/min**

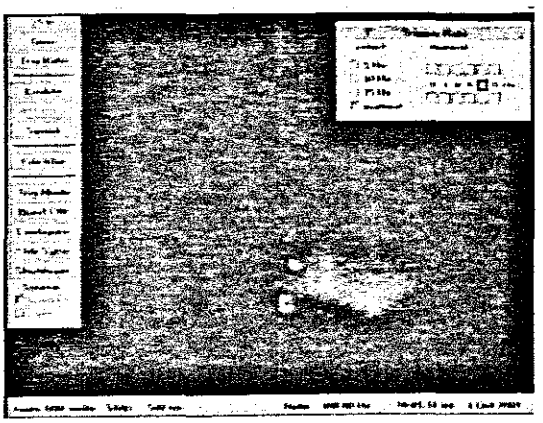

| | Photo | Actual |
|---|---|---|
| Droplet ∅ | 2.72 | **1.133** |
| Wire ∅ | 2.40 | 1.00 |

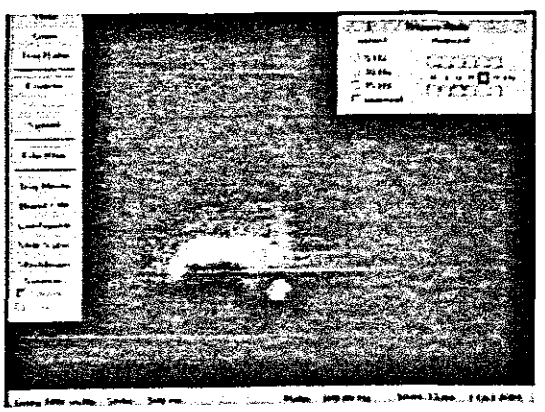

| | Photo | Actual |
|---|---|---|
| Droplet ∅ | 3.32 | **1.149** |
| Wire ∅ | 2.89 | 1.00 |

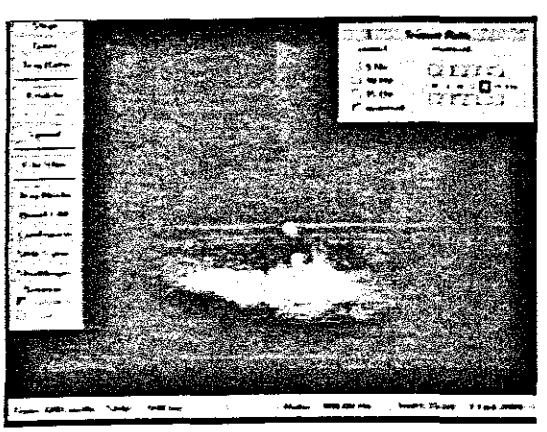

| | Photo | Actual |
|---|---|---|
| Droplet ∅ | 2.82 | **1.156** |
| Wire ∅ | 2.44 | 1.00 |

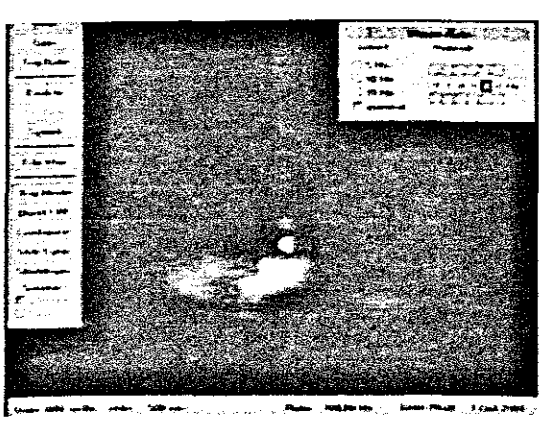

| | Photo | Actual |
|---|---|---|
| Droplet ∅ | 3.08 | **1.176** |
| Wire ∅ | 2.62 | 1.00 |

Welding current **214A**, wire speed **14m/min**

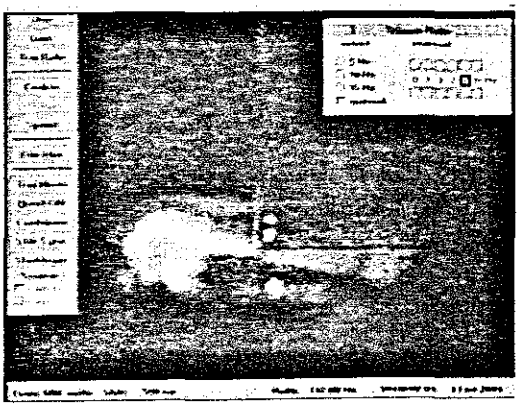

| | Photo | Actual |
|---|---|---|
| Droplet Ø | 3.14 | **1.090** |
| Wire Ø | 2.88 | 1.00 |

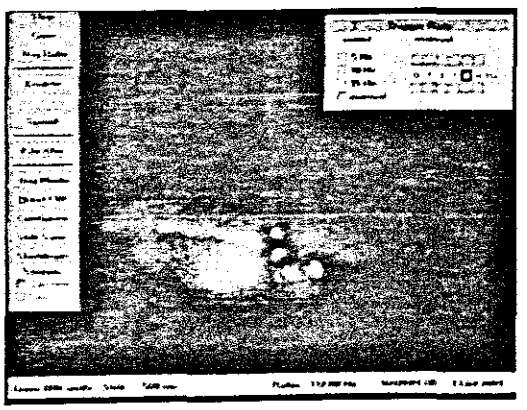

| | Photo | Actual |
|---|---|---|
| Droplet Ø | 3.52 | **1.266** |
| Wire Ø | 2.78 | 1.00 |

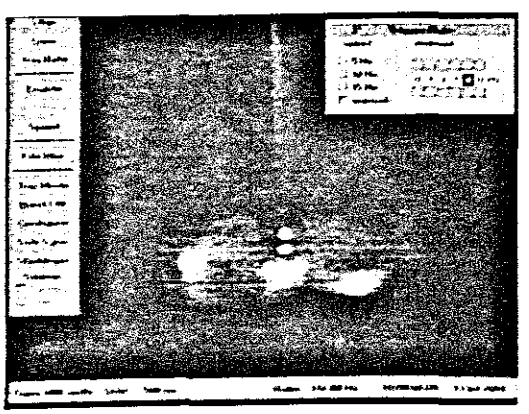

| | Photo | Actual |
|---|---|---|
| Droplet Ø | 2.40 | **1.071** |
| Wire Ø | 2.24 | 1.00 |

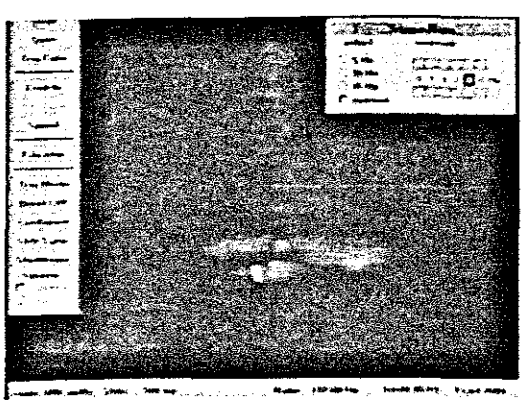

| | Photo | Actual |
|---|---|---|
| Droplet Ø | 3.18 | **1.089** |
| Wire Ø | 2.92 | 1.00 |

Welding current **223A**, wire speed **15m/min**

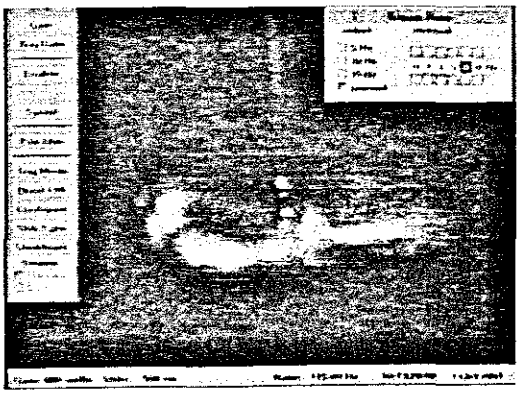

| | Photo | Actual |
|---|---|---|
| Droplet ∅ | 1.16 | **1.000** |
| Wire ∅ | 1.16 | 1.00 |

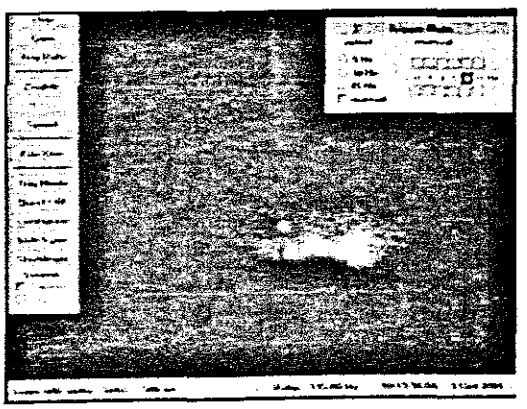

| | Photo | Actual |
|---|---|---|
| Droplet ∅ | 2.18 | **0.995** |
| Wire ∅ | 2.19 | 1.00 |

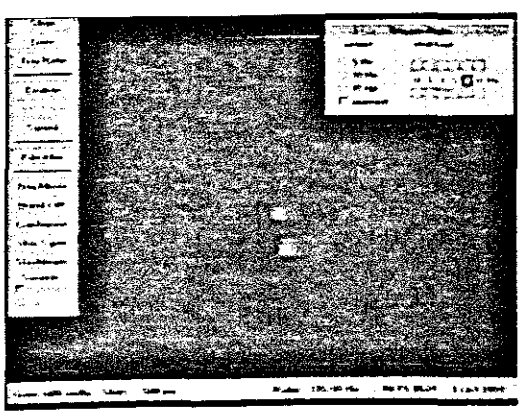

| | Photo | Actual |
|---|---|---|
| Droplet ∅ | 2.12 | **1.060** |
| Wire ∅ | 2.00 | 1.00 |

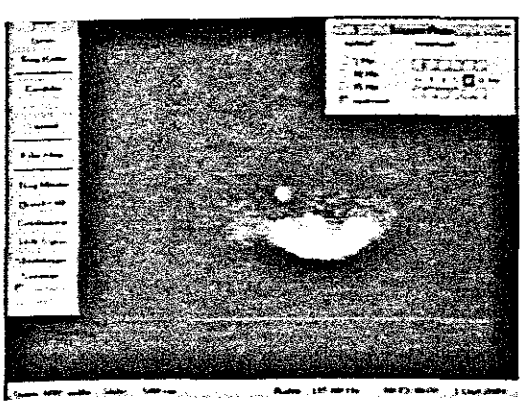

| | Photo | Actual |
|---|---|---|
| Droplet ∅ | 2.10 | **1.010** |
| Wire ∅ | 2.08 | 1.00 |

Welding current **237A**, wire speed **17m/min**

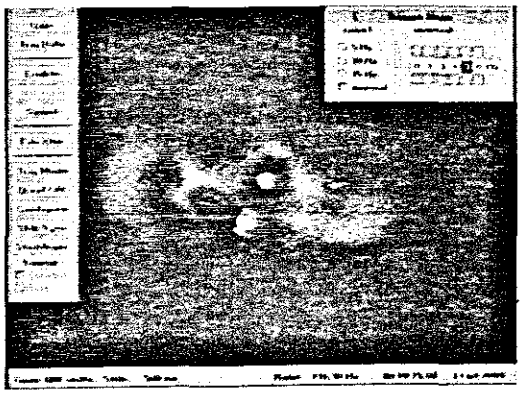

| | Photo | Actual |
|---|---|---|
| Droplet ∅ | 3.82 | **1.230** |
| Wire ∅ | 3.10 | 1.00 |

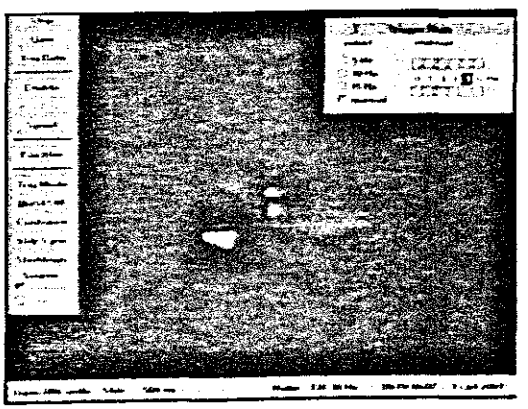

| | Photo | Actual |
|---|---|---|
| Droplet ∅ | 2.08 | **1.010** |
| Wire ∅ | 2.06 | 1.00 |

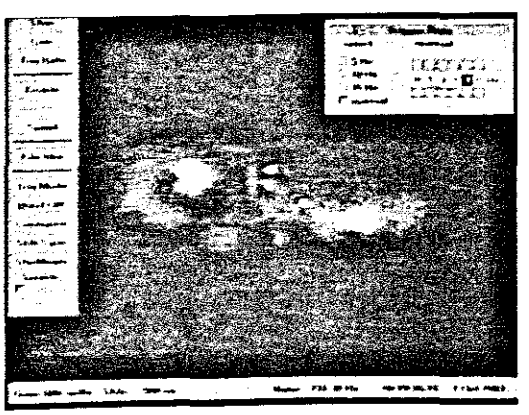

| | Photo | Actual |
|---|---|---|
| Droplet ∅ | 2.40 | **1.034** |
| Wire ∅ | 2.32 | 1.00 |

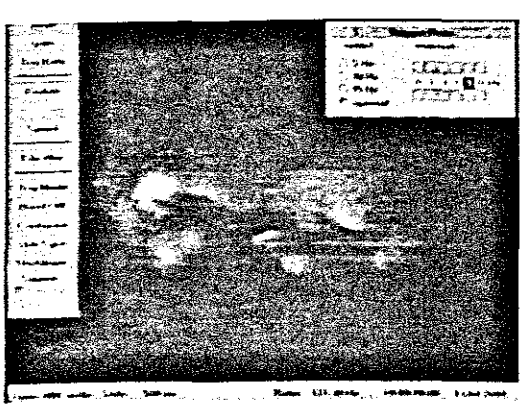

| | Photo | Actual |
|---|---|---|
| Droplet ∅ | 3.46 | **1.000** |
| Wire ∅ | 3.46 | 1.00 |

Welding current **241A**, wire speed **18m/min**

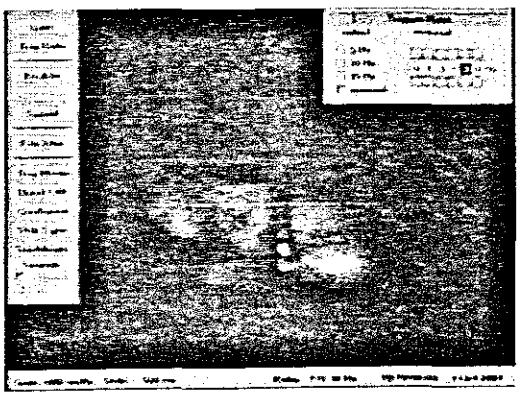

| | Photo | Actual |
|---|---|---|
| Droplet Ø | 1.82 | **0.875** |
| Wire Ø | 2.08 | 1.00 |

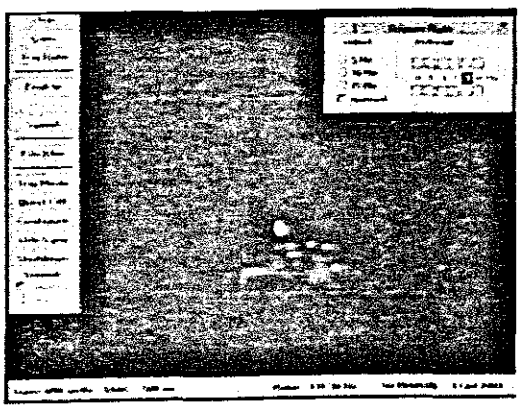

| | Photo | Actual |
|---|---|---|
| Droplet Ø | 1.84 | **0.800** |
| Wire Ø | 2.30 | 1.00 |

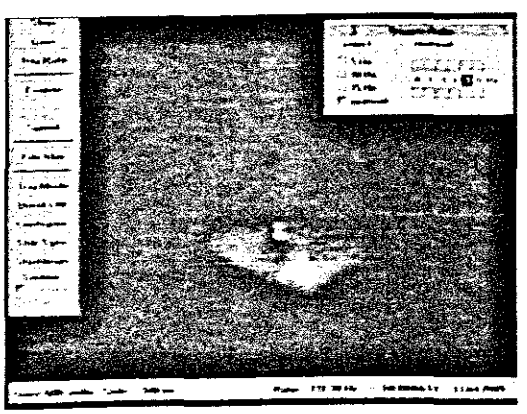

| | Photo | Actual |
|---|---|---|
| Droplet Ø | 2.80 | **1.458** |
| Wire Ø | 1.92 | 1.00 |

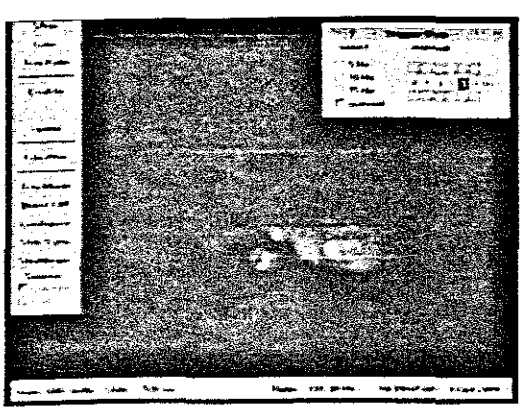

| | Photo | Actual |
|---|---|---|
| Droplet Ø | 3.08 | **1.116** |
| Wire Ø | 2.76 | 1.00 |

Welding current **248A**, wire speed **19m/min**

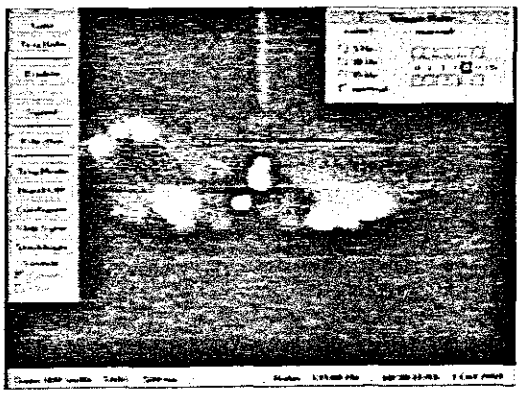

| | Photo | Actual |
|---|---|---|
| Droplet ∅ | 3.14 | **0.872** |
| Wire ∅ | 3.60 | 1.00 |

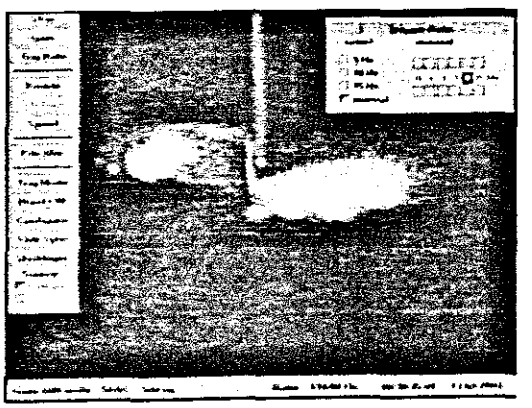

| | Photo | Actual |
|---|---|---|
| Droplet ∅ | 2.12 | **0.991** |
| Wire ∅ | 2.14 | 1.00 |

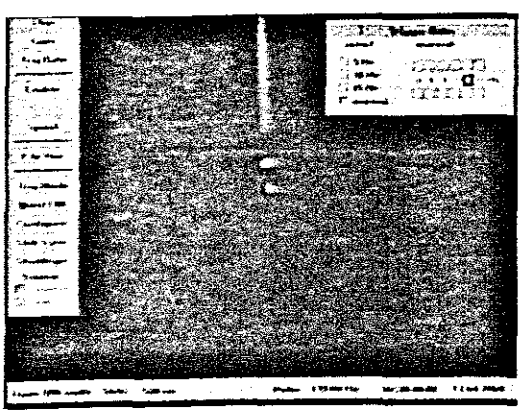

| | Photo | Actual |
|---|---|---|
| Droplet ∅ | 2.44 | **1.061** |
| Wire ∅ | 2.30 | 1.00 |

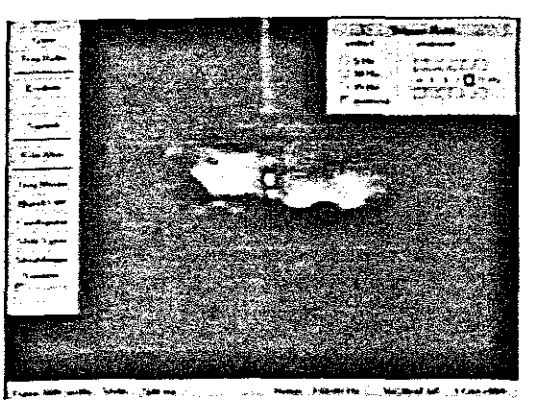

| | Photo | Actual |
|---|---|---|
| Droplet ∅ | 1.88 | **1.093** |
| Wire ∅ | 1.72 | 1.00 |

Welding current **257A**, wire speed **20m/min**

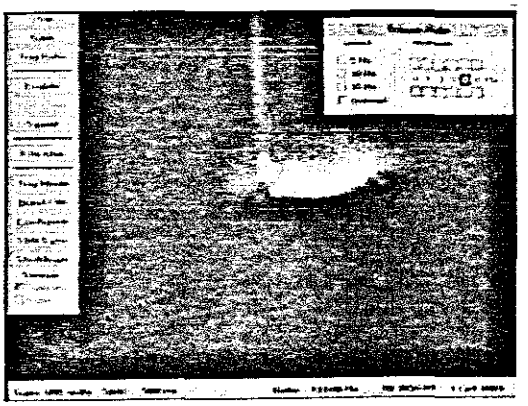

| | Photo | Actual |
|---|---|---|
| Droplet ∅ | 2.12 | **0.779** |
| Wire ∅ | 2.72 | 1.00 |

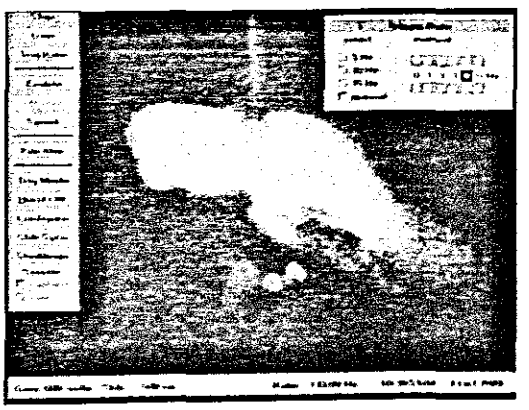

| | Photo | Actual |
|---|---|---|
| Droplet ∅ | 3.10 | **0.901** |
| Wire ∅ | 3.44 | 1.00 |

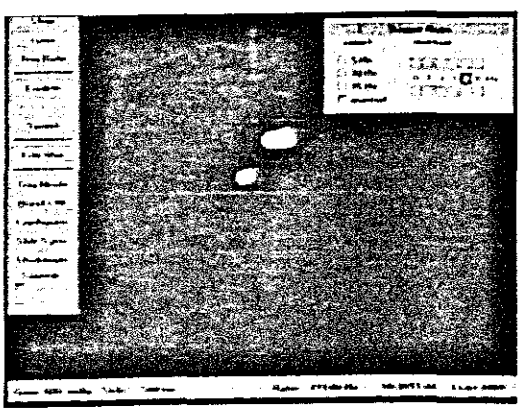

| | Photo | Actual |
|---|---|---|
| Droplet ∅ | 3.08 | **0.911** |
| Wire ∅ | 3.38 | 1.00 |

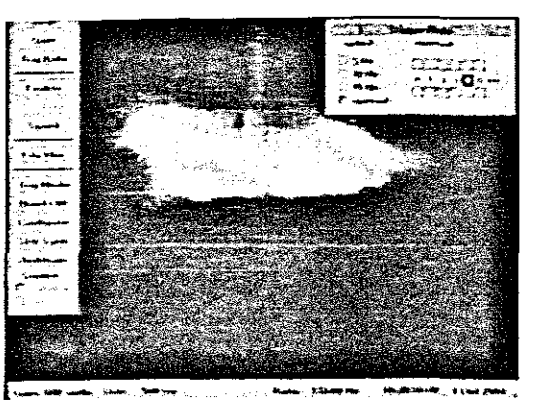

| | Photo | Actual |
|---|---|---|
| Droplet ∅ | 3.02 | **0.962** |
| Wire ∅ | 3.14 | 1.00 |

Welding current **265A**, wire speed **22m/min**

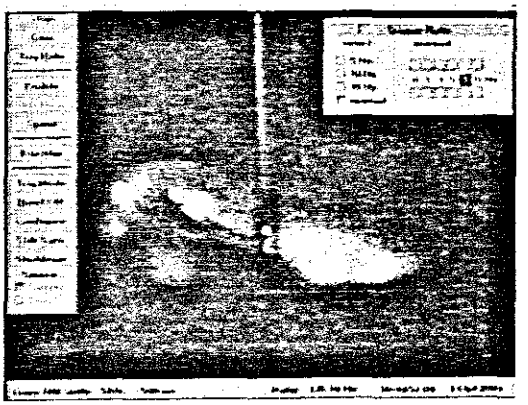

| | Photo | Actual |
|---|---|---|
| Droplet ∅ | 3.02 | **0.770** |
| Wire ∅ | 3.92 | 1.00 |

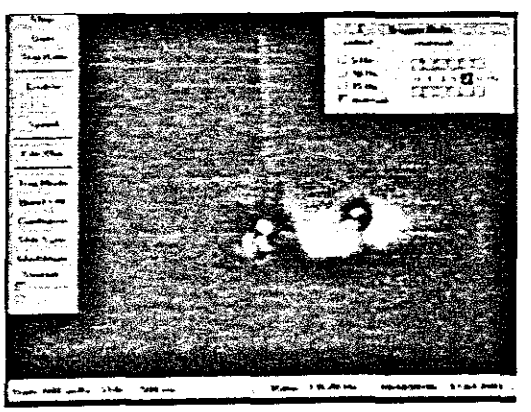

| | Photo | Actual |
|---|---|---|
| Droplet ∅ | 3.04 | **0.779** |
| Wire ∅ | 3.90 | 1.00 |

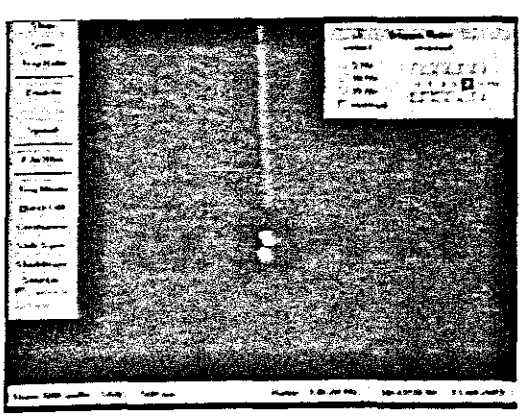

| | Photo | Actual |
|---|---|---|
| Droplet ∅ | 3.14 | **0.789** |
| Wire ∅ | 3.98 | 1.00 |

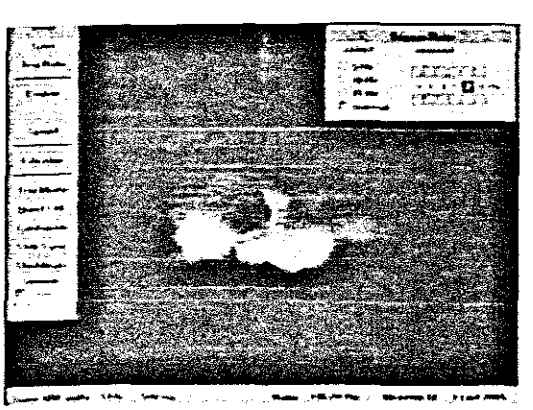

| | Photo | Actual |
|---|---|---|
| Droplet ∅ | 3.00 | **0.765** |
| Wire ∅ | 3.92 | 1.00 |

Welding current **269A**, wire speed **24m/min**

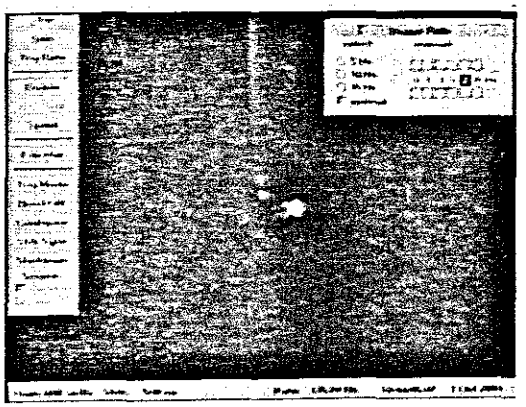

| | Photo | Actual |
|---|---|---|
| Droplet ∅ | 2.98 | **0.797** |
| Wire ∅ | 3.74 | 1.00 |

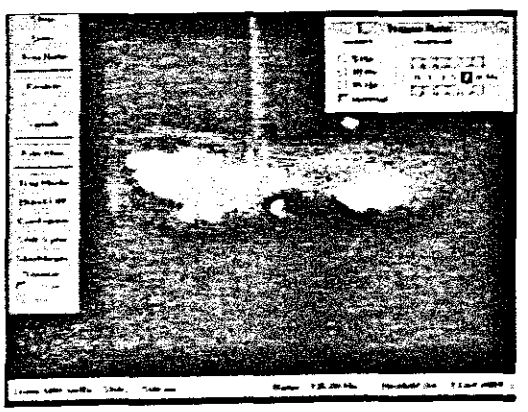

| | Photo | Actual |
|---|---|---|
| Droplet ∅ | 3.06 | **0.761** |
| Wire ∅ | 4.02 | 1.00 |

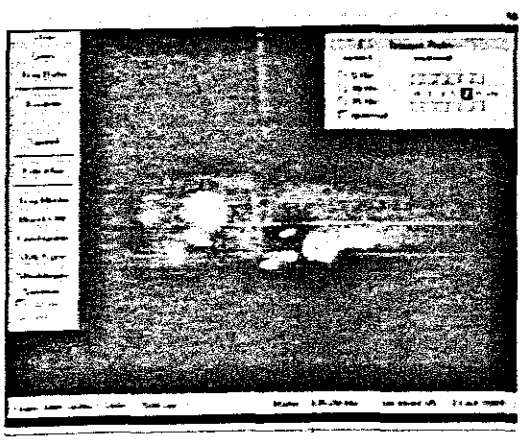

| | Photo | Actual |
|---|---|---|
| Droplet ∅ | 3.00 | **0.758** |
| Wire ∅ | 3.96 | 1.00 |

# Appendix E4

**Laserstrobe Images of GMA/MIG Welding with 98%Ar-2%$CO_2$ Shielding Gas**

The table below represents the average/mean droplet diameters obtained from the welding images of a 1mm mild steel electrode using the abovementioned shielding gas mixture.

| Weld No. | Wire Feed Rate | Mean Droplet diameter |
|---|---|---|
| 1 | 10.0 | **2.402** |
| 2 | 10.5 | **2.370** |
| 3 | 11.0 | **2.325** |
| 4 | 11.5 | **2.249** |
| 5 | 12.0 | **2.197** |
| 6 | 12.5 | **2.150** |
| 7 | 13.0 | **2.010** |
| 8 | 13.5 | **2.001** |
| 9 | 14.0 | **1.948** |
| 10 | 14.5 | **1.849** |
| 11 | 15.0 | **1.752** |
| 12 | 15.5 | **1.750** |
| 13 | 16.0 | **1.741** |
| 14 | 16.5 | **1.660** |
| 15 | 17.0 | **1.550** |
| 16 | 17.5 | **1.501** |
| 17 | 18.0 | **1.455** |
| 18 | 18.5 | **1.500** |
| 19 | 19.0 | **1.405** |
| 20 | 19.5 | **1.351** |
| 21 | 20.0 | **1.259** |
| 22 | 20.5 | **1.250** |
| 23 | 21.0 | **1.105** |
| 24 | 22.0 | **1.075** |
| 25 | 23.0 | **0.998** |
| 26 | 24.0 | **0.980** |

Welding current **197A**, wire speed **10m/min**

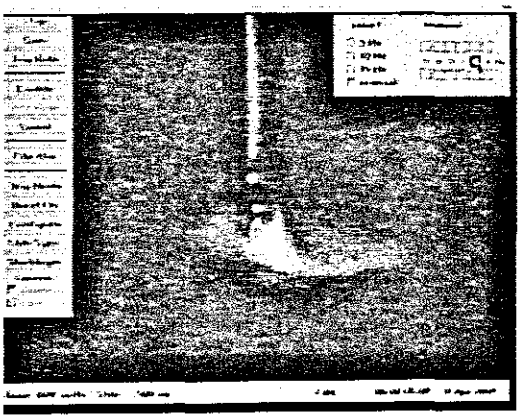

| | Photo | Actual |
|---|---|---|
| Droplet ∅ | 7.44 | **2.400** |
| Wire ∅ | 3,10 | 1,00 |

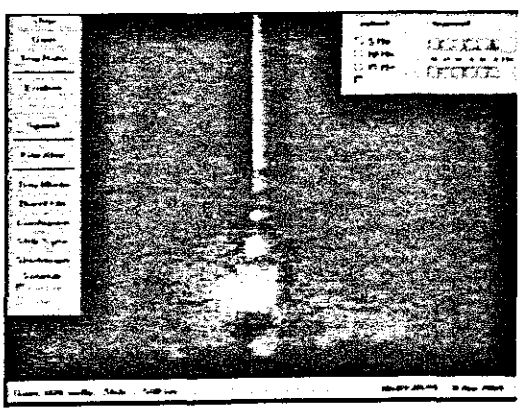

| | Photo | Actual |
|---|---|---|
| Droplet ∅ | 6.94 | **2.401** |
| Wire ∅ | 2,89 | 1,00 |

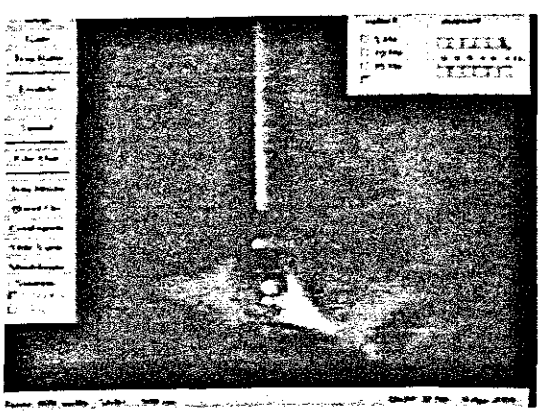

| | Photo | Actual |
|---|---|---|
| Droplet ∅ | 7.71 | **2,41** |
| Wire ∅ | 3,20 | 1,00 |

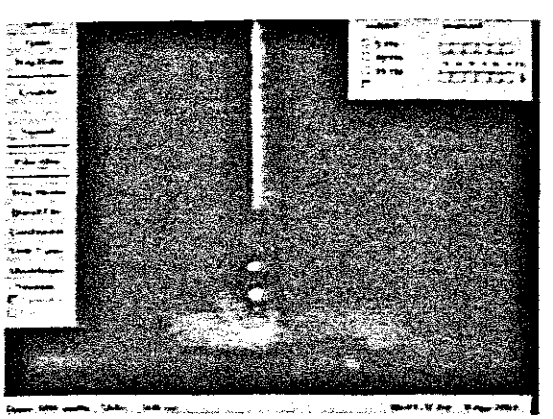

| | Photo | Actual |
|---|---|---|
| Droplet ∅ | 6.75 | **2.397** |
| Wire ∅ | 2,81 | 1,00 |

Welding current **199A**, wire speed **10.5m/min**

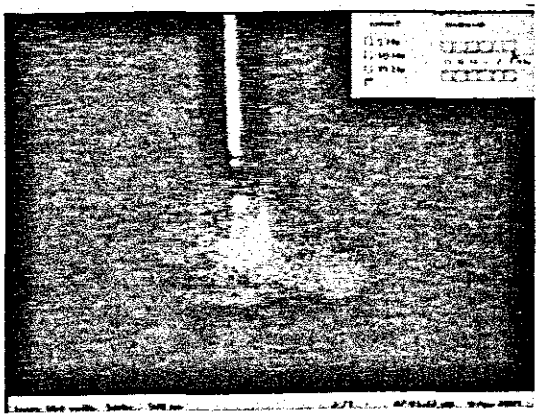

| | Photo | Actual |
|---|---|---|
| Droplet ∅ | 9.99 | **2.70** |
| Wire ∅ | 3,70 | 1,00 |

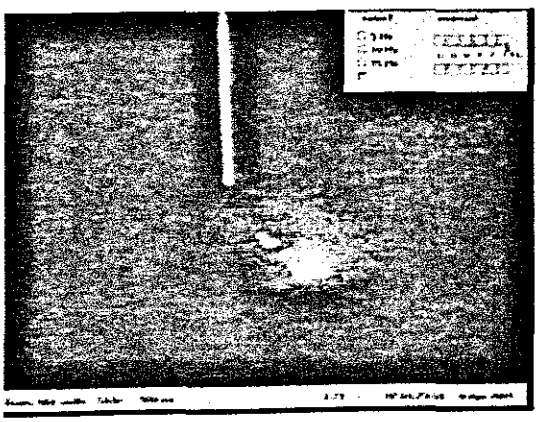

| | Photo | Actual |
|---|---|---|
| Droplet ∅ | 10.28 | **2.705** |
| Wire ∅ | 3,80 | 1,00 |

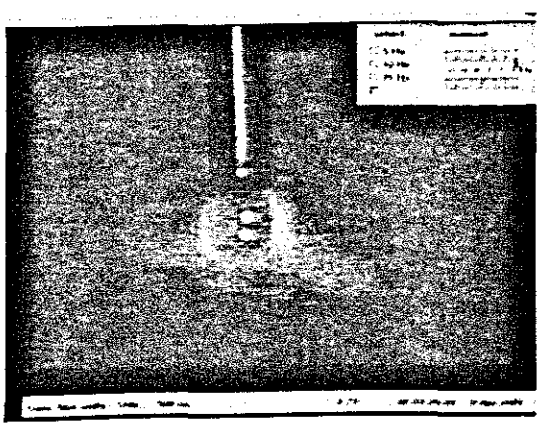

| | Photo | Actual |
|---|---|---|
| Droplet ∅ | 10.38 | **2.668** |
| Wire ∅ | 3,89 | 1,00 |

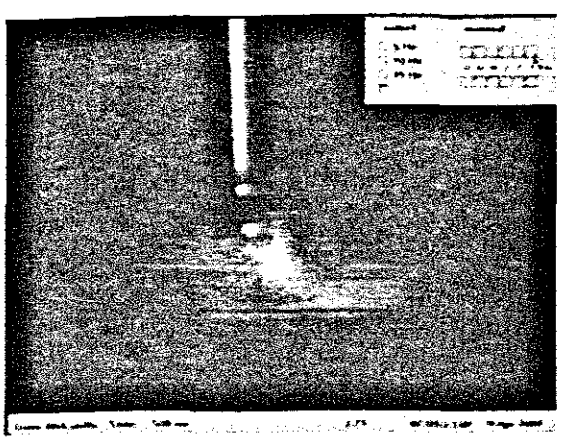

| | Photo | Actual |
|---|---|---|
| Droplet ∅ | 9.40 | **2.687** |
| Wire ∅ | 3,50 | 1,00 |

Welding current **205A**, wire speed **11m/min**

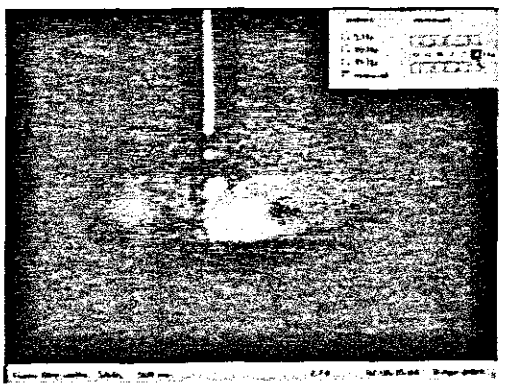

| | Photo | Actual |
|---|---|---|
| Droplet ∅ | 8.09 | **2.688** |
| Wire ∅ | 3,01 | 1,00 |

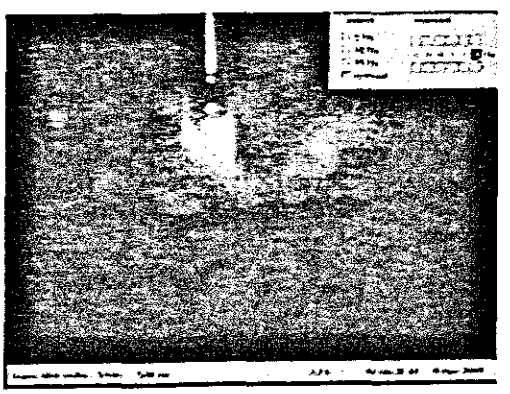

| | Photo | Actual |
|---|---|---|
| Droplet ∅ | 8.55 | **2.697** |
| Wire ∅ | 3,17 | 1,00 |

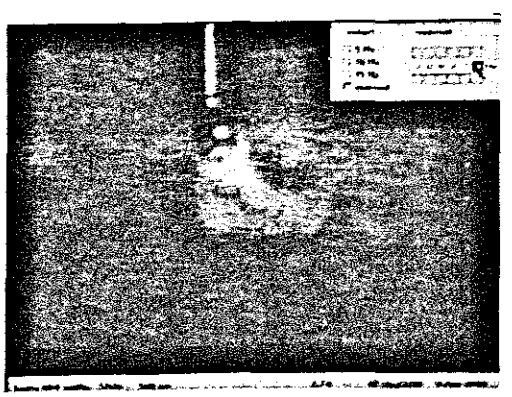

| | Photo | Actual |
|---|---|---|
| Droplet ∅ | 8.53 | **2.708** |
| Wire ∅ | 3,15 | 1,00 |

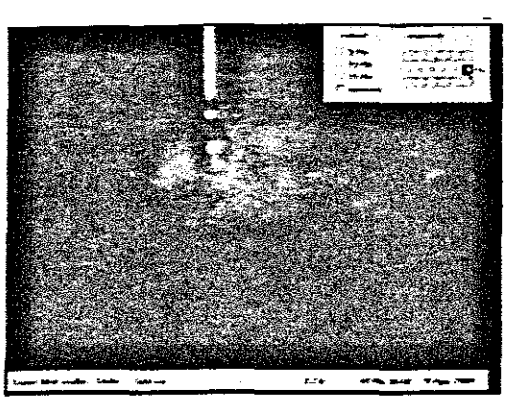

| | Photo | Actual |
|---|---|---|
| Droplet ∅ | 8.40 | **2.667** |
| Wire ∅ | 3,15 | 1,00 |

Welding current **226A**, wire speed **15m/min**

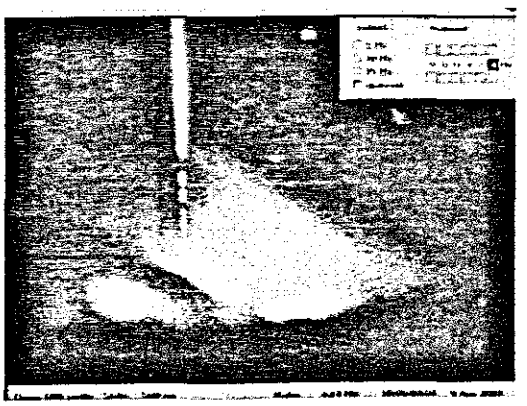

| | Photo | Actual |
|---|---|---|
| Droplet ∅ | 5,28 | **1,760** |
| Wire ∅ | 3,00 | 1,00 |

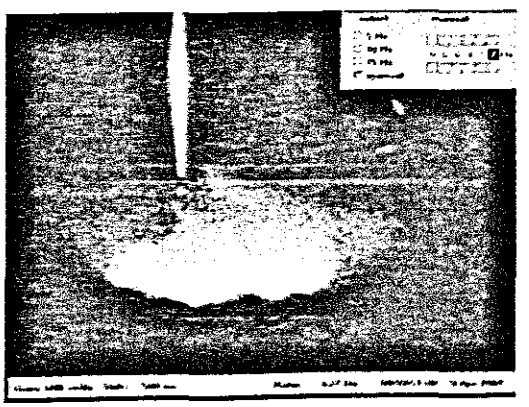

| | Photo | Actual |
|---|---|---|
| Droplet ∅ | 5,23 | **1,755** |
| Wire ∅ | 2,98 | 1,00 |

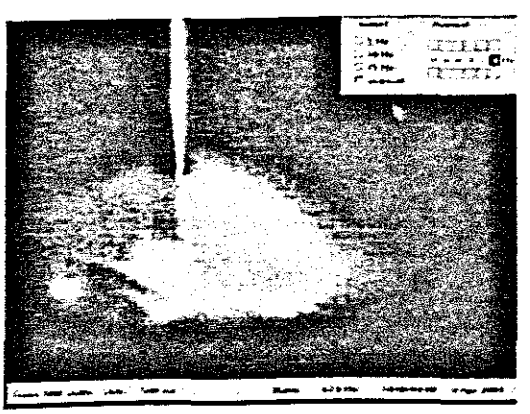

| | Photo | Actual |
|---|---|---|
| Droplet ∅ | 5,25 | **1,749** |
| Wire ∅ | 3,00 | 1,00 |

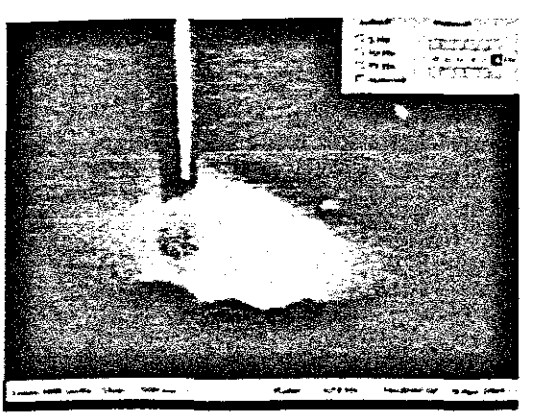

| | Photo | Actual |
|---|---|---|
| Droplet ∅ | 7,50 | **1,744** |
| Wire ∅ | 4,50 | 1,00 |

Welding current **230A**, wire speed **15.5m/min**

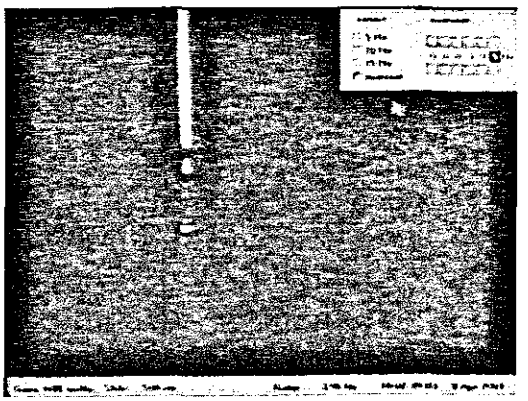

| | Photo | Actual |
|---|---|---|
| Droplet ∅ | 4,11 | **1,749** |
| Wire ∅ | 2,35 | 1,00 |

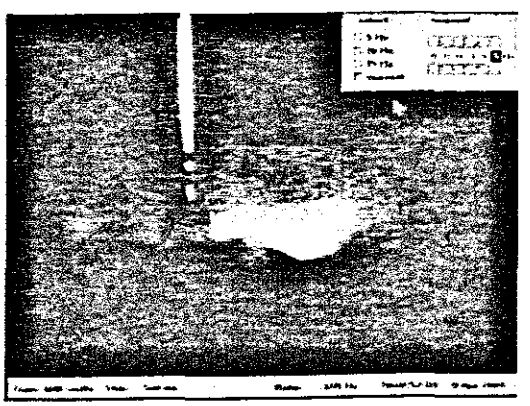

| | Photo | Actual |
|---|---|---|
| Droplet ∅ | 4,20 | **1,750** |
| Wire ∅ | 2,40 | 1,00 |

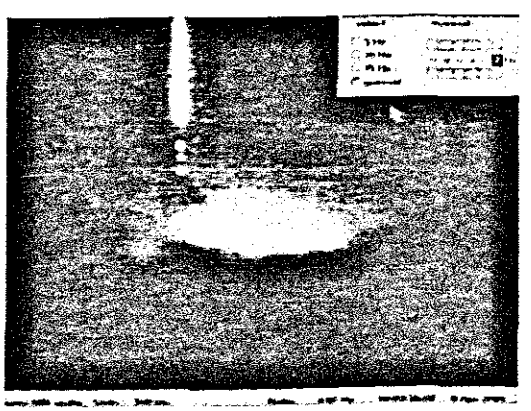

| | Photo | Actual |
|---|---|---|
| Droplet ∅ | 5,34 | **1,751** |
| Wire ∅ | 3,05 | 1,00 |

Welding current **272A**, wire speed **23m/min**

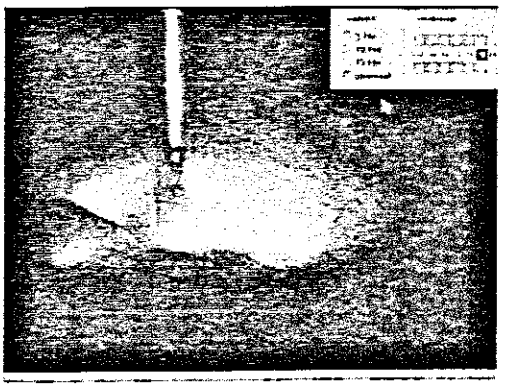

| | Photo | Actual |
|---|---|---|
| Droplet ∅ | 4.18 | **1,045** |
| Wire ∅ | 4,00 | 1,00 |

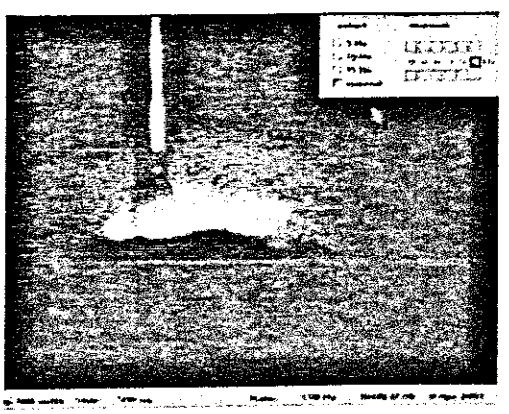

| | Photo | Actual |
|---|---|---|
| Droplet ∅ | 5,24 | **1,046** |
| Wire ∅ | 5,01 | 1,00 |

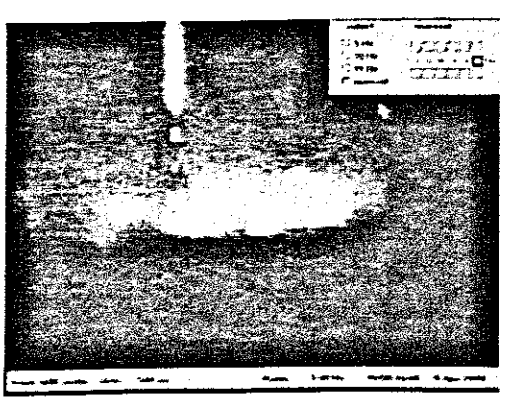

| | Photo | Actual |
|---|---|---|
| Droplet ∅ | 5,20 | **0,901** |
| Wire ∅ | 5,77 | 1,00 |

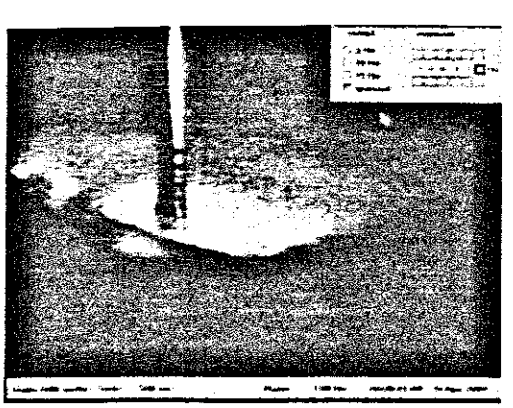

| | Photo | Actual |
|---|---|---|
| Droplet ∅ | 4,30 | **1,00** |
| Wire ∅ | 4,30 | 1,00 |

Welding current **275A**, wire speed **24m/min**

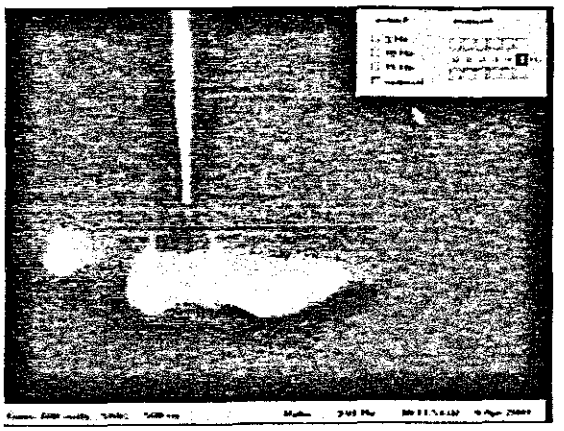

| | Photo | Actual |
|---|---|---|
| Droplet ∅ | 8,72 | **1,090** |
| Wire ∅ | 8,00 | 1,00 |

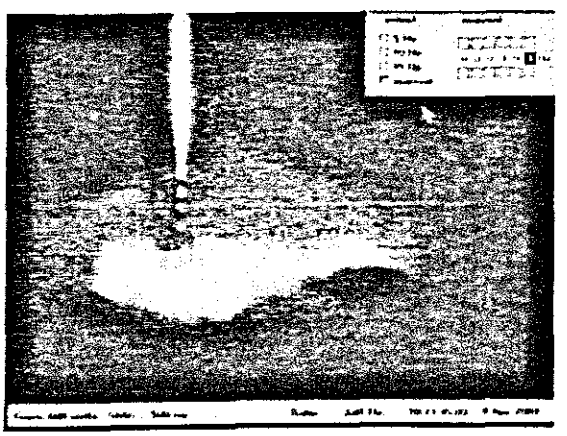

| | Photo | Actual |
|---|---|---|
| Droplet ∅ | 5.83 | **0,870** |
| Wire ∅ | 6,70 | 1,00 |

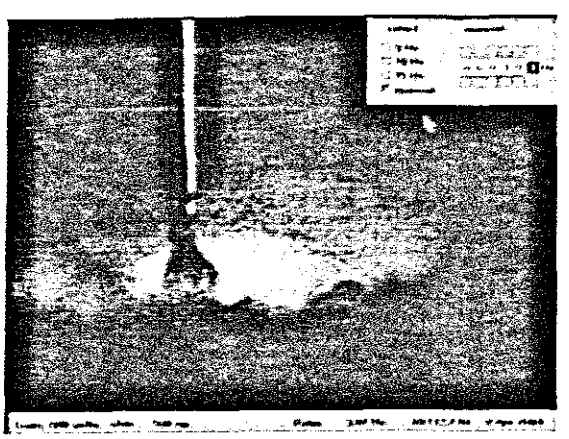

| | Photo | Actual |
|---|---|---|
| Droplet ∅ | 8,30 | **0,977** |
| Wire ∅ | 6,70 | 1,00 |

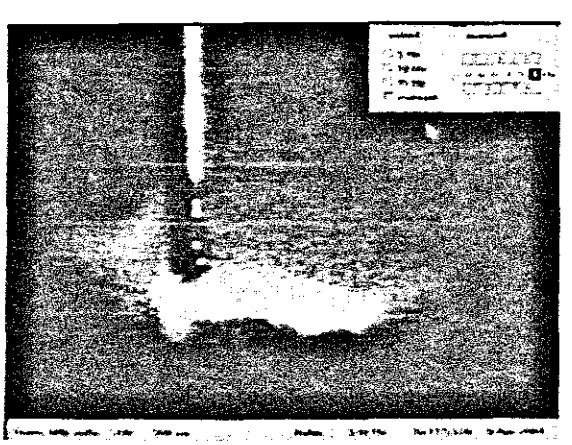

| | Photo | Actual |
|---|---|---|
| Droplet ∅ | 6,80 | **0,983** |
| Wire ∅ | 6,00 | 1,00 |